Combinations of costimulatory antibody-ligand fusion proteins for targeted cancer immunotherapy

Von der Fakultät Energie-, Verfahrens- und Biotechnik der Universität Stuttgart zur Erlangung der Würde eines Doktors der Naturwissenschaften (Dr. rer. nat.) genehmigte Abhandlung

Vorgelegt von

Nora Hornig

aus Hannover

Hauptberichter: Prof. Dr. Roland E. Kontermann

Mitberichter: Prof. Dr. Klaus Pfizenmaier

Tag der mündlichen Prüfung: 14.10.2013

Institut für Zellbiologie und Immunologie

Universität Stuttgart

2013

I hereby declare that I performed the present thesis independently without further help or other materials than stated.

Nora Hornig

Lübeck, June 18th, 2013

“Eigentlich bin ich ganz anders, nur komme ich so selten dazu.”

Ödön von Horváth

Table of Contents

Index of Figures

Index of Tables

Abbreviations

°C	degree celsius
α	anti
µ	micro- (x10^{-6})
aa	amino acid
ABD	albumin-binding domain
AEs	adverse events
amp	ampicillin
APC	antigen presenting cell
AUC	area under the curve
BiTE	bispecific T cell engager
B-NHL	B cell Non-Hodgkin's lymphoma
bp	base pairs
BTLA	B- and T-lymphocyte attenuator
CD	cluster of differentiation (surface antigen)
CEA	carcinoembryonic antigen
CFSE	carboxyfluorescein diacetate succinimidyl ester
CRD	cysteine rich domain
CTL	cytotoxic T lymphocyte
CTLA-4	Cytotoxic T Lymphocyte Antigen-4
Da	Dalton, molecular mass
DC	dendritic cell
DMSO	dimethyl sulfoxide
DNA	deoxyribonucleic acid
dNTP	deoxyribonucleoside triphosphate
EC_{50}	half maximal effective concentration
ECD	extracellular domain
EDG	endoglin
EDTA	ethylenediaminetetraacetate
ELISA	enzyme linked immunosorbent assay
Fab	fragment antigen binding
FAP	Fibroblast Activation Protein
FBS	fetal bovine serum
Fc	fragment crystallizable
FDA	Food and Drug Administration
FITC	fluorescein isothiocyanate
g	gram
GITR(L)	Glucocorticoid-induced TNF-related protein (ligand)
glc	glucose
GrB	granzyme B
h	hour
His-tag	hexahistidyl-tag
HPLC	high pressure liquid chromatography
HRP	horse radish peroxidase
hu	human
HVEM	Herpes virus entry mediator
l	liter
ICOS(L)	Inducible T cell costimulator (ligand)
Ig	Immunoglobulin
IgBD	Immunoglobulin-binding domain B
IL	Interleukin
IMAC	immobilized metal affinity chromatography
i.p.	intraperitoneal
i.v.	intravenous

k	kilo- ($x10^3$)
LIGHT	Lymphotoxin-like, exhibits inducible expression, and competes with HSV glycoprotein D for HVEM, a receptor expressed by T lymphocytes
m	milli- ($x10^{-3}$)
mAb	monoclonal antibody
MHC	major histocompatibility complex
MFI	mean fluorescence intensity
min	minute
Mm	molecular mass
mo	mouse
MWCO	molecular weight cut-off
n	nano- ($x10^{-9}$)
NF-κB	nuclear factor-kappa B
Ni-NTA	Ni^{2+}-nitrilo-triacetic acid
OD	optical density
p	pico- (10^{-12})
PAA	polyacrylamide
PBMC	peripheral blood mononuclear cell
PBS	phosphate buffered saline
PCR	polymerase chain reaction
PD-(L)1	programmed cell death protein (ligand) 1
PE	R-phycoerythrin
PEG	polyethylene glycol
PerCP	peridinin chlorophyll crotein
PK	pharmacokinetics
PKB	protein kinase B
r	recombinant
RT	room temperature
s.c.	subcutaneous
scFv	single-chain fragment variable
SDS-PAGE	sodium dodecyl sulfate polyacrylamide gel electrophoresis
SEC	size exclusion chromatography
SF	superfamily
$t_{1/2}\alpha$	initial half-life
$t_{1/2}\beta$	terminal half-life
TAA	tumor associated antigen
T_{eff}	effector T cell
TMB	tetra-methylbenzidine
TNC	tenascin C
TNF(R/L)	Tumor necrosis factor (receptor/ligand)
TRADD	TNFR associated death domain
TRAF	TNFR associated factor
T_{reg}	regulatory T cell
Tris	tris-(hydroxymethyl) aminomethane
V_H, V_L	variable domains of the heavy (H) and light (L) chain of an antibody
wt	wildtype

Summary

Combinatorial strategies are of emerging interest in cancer immunotherapy. Costimulation by individual members of the Ig- or TNF-superfamily have already revealed promising antitumor potential, thus prompting the exploration of their synergistic abilities in combinatorial approaches. Here, in order to avoid systemic side effects, costimulation was restricted to the tumor site by pursuing a targeted strategy with antibody-ligand fusion proteins composed of tumor antigen-directed antibodies and the extracellular domain of the costimulatory ligands B7 or 4-1BBL, respectively. Costimulatory activity was assessed in an experimental model system where tumor cells coexpressed the antigens fibroblast activation protein (FAP) and endoglin (EDG) and initial MHC-independent T cell activation and tumor-targeting was mediated by a bispecific antibody (scDbFAPxCD3). Combined costimulation with B7- and 4-1BBL-fusion proteins (B7-DbFAP, scFvEDG-4-1BBL) was shown to be superior to the individual effects in terms of cytokine release (IL-2/IFN-γ), proliferation and activation marker expression (CD25), leading to a T cell population with enhanced levels of an activation-experienced memory phenotype and with a higher capability for target cell killing. Furthermore, the model system was adapted for a time-shift costimulation setting. Here, enhanced T cell proliferation and granzyme B expression as well as reduced levels of PD-1 expression demonstrated the benefit of B7.1- and 4-1BBL-costimulation-assisted restimulation. Consequently, the antitumor activity of this combinatorial setting was confirmed in vivo in a lung metastasis mouse model. Finally, the combinatorial spectrum was expanded by the generation and subsequent incorporation of antibody-fusion proteins comprising the extracellular domains of the TNF-superfamily ligands Ox40L, LIGHT or GITRL. Here, advantages of combined costimulation with either B7.1- or 4-1BBL- fusion proteins were shown in terms of T cell proliferation and IFN-γ release.

In summary, combinatorial approaches with tumor-directed costimulatory ligands in form of antibody-ligand fusion proteins were shown to be feasible, revealing a great potential for the modulation and enhancement of a T cell response. Thus, they appear to be a promising strategy in cancer immunotherapy that should be considered for further investigation.

Zusammenfassung

Im Rahmen der Tumorimmuntherapie gewinnen kombinatorische Strategien zunehmend an Bedeutung. Da für Kostimulation durch einzelne Mitgliedern der Ig- oder TNF-Superfamilie bereits ein vielversprechendes antitumorales Potential nachgewiesen werden konnte, sollten in dieser Arbeit auch deren synergistische Fähigkeiten in kombinatorischen Ansätzen ausgetestet werden. Um hierbei systemische Nebenwirkungen zu vermeiden, wurde die Kostimulation mittels einer „Targeting-Strategie“ auf den Tumor begrenzt. Dafür wurden Antikörper-Ligand-Fusionsproteine eingesetzt, die aus einer Tumorantigen-spezifischen Antikörperkomponente und der extrazellulären Domäne kostimulatorischer Liganden (B7 oder 4-1BBL) bestanden. Für die Untersuchung der kostimulatorischen Aktivität der Fusionsproteine wurde ein experimentelles Setting etabliert, in dem Tumorzellen die Antigene Fibroblast Activation Protein (FAP) und Endoglin (EDG) koexprimierten und die initiale, MHC-unabhängige T-Zell-Aktivierung und das Tumor-Targeting über einen bispezifischen Antikörper (scDbFAPxCD3) erfolgte. Der kombinierte Einsatz von B7- und 4-1BBL-Fusionsproteinen war der Kostimulation mit nur einem Fusionsprotein deutlich überlegen, was für Zytokinausschüttung (IL-2, IFN-γ), Proliferation und Aktivitätsmarker-Expression (CD25) gezeigt werden konnte. Zudem führte die Kombination zu einer T-Zell-Population, die sowohl einen größeren Anteil eines aktivierungserfahrenen Gedächtnis-Phenotyps als auch ein höheres Potential für das Töten der Targetzellen aufwies. Das Modellsystem wurde auch hinsichtlich einer zeitversetzten Kostimulation analysiert. Hierbei erwies sich die gemeinsame Kostimulation mit B7.1- und 4-1BBL-Fusionsproteinen während der scDb-Restimulationsphase als das vorteilhafteste Setting, bei dem sowohl eine verstärkte T-Zell-Proliferation und Granzym B-Expression, als auch eine erniedrigte PD-1-Expression zu beobachten war. Die antitumorale Wirksamkeit dieses Settings wurde auch in vivo in einem Lungenmetastasen-Mausmodell bestätigt. Darüber hinaus wurde das kombinatorische Spektrum durch neue Fusionsproteine, bestehend aus der extrazellulären Domäne der TNF-Superfamilie-Liganden Ox40L, LIGHT und GITRL, erweitert. Dabei konnten die Vorteile einer kombinierten Kostimulation mit B7.1- als auch mit 4-BBL-Fusionsproteinen in Bezug auf T-Zell-Proliferation und IFN-γ-Ausschüttung nachgewiesen werden.

In dieser Arbeit wurde die Einsetzbarkeit und das Potential kombinatorischer Ansätze bestehend aus tumor-gerichteten kostimulatorischen Liganden in Form von Antikörper-Fusionsproteinen gezeigt. Für die Krebsimmuntherapie erscheinen sie als eine vielversprechende Strategie, die weiter verfolgt werden sollte.

1 - Introduction

1.1 - Costimulatory approaches in cancer immunotherapy

Since the discovery of the first costimulatory receptor-ligand pair CD28 and B7.1 more than 25 years ago[1,2], tremendous progress has been made in the field of T cell costimulation. In addition to the identification of a broad range of new members (receptors as well as ligands), also the importance of costimulation for the development of a potent T cell response has been acknowledged[3,4]. Accordingly, costimulatory approaches have extensively been incorporated into immunotherapeutic studies facing cancer[5,6]. Especially promising are agonistic monoclonal antibodies (mAbs) directed against costimulatory receptors since they have shown to be able to enhance the antitumor potential of T cells[7]. Although in the case of a superagonistic antibody against CD28 (TGN1412) severe systemic toxicity has been observed in a phase 1 clinical trial[8], the overall concept has shown to be effective and currently, several antibodies are in clinical trials (Table 1) [9].

Table 1: Antagonist antibodies for inhibitory receptors and agonist antibodies for costimulatory receptors in clinical trials against cancer.

Target	Agent	Company	Indication	Stage of Development
Inhibitory pathway antagonists				
CTLA-4	Ipilimumab (CTLA-4 Mab)	Bristol-Myers Squibb	Melanoma	FDA approved
			Multiple cancers	Phase 1–3
	Tremilimumab (CTLA-4 Mab)	MedImmune	TBD[b]	
PD-1/PD-L1	MDX1106 (PD-1 Mab)	Bristol-Myers Squibb	Melanoma, lung, kidney	Phase 1–3
	MK3475 (PD-1 Mab)	Merck	Multiple cancers	Phase 1
	CT-011[a] (PD-1)	CureTech	Multiple cancers	Phase 1 / 2
Costimulatory pathway agonists				
CD137	BMS663513 (CD137 Mab)	Bristol-Myers Squibb	TBD[b]	
CD40	CP-870893 (CD40 Mab)	Pfizer	Pancreas cancer	Phase 1
OX40	Anti-OX40 Mab	AgonOX	Multiple cancers	Phase 1 / 2
CD127	CDX-1127 (CD27 Mab)	Celldex	Multiple cancers	Phase 1

[a]Antibody not yet validated for target specificity.

[b]Antibody previously tested in melanoma patients; plans to re-initiate clinical testing after a hiatus.
(FDA: U.S. Food and Drug Administration)

Source: Pardoll, D. & Drake, C. Immunotherapy earns its spot in the ranks of cancer therapy. The Journal of Experimental Medicine 209, 201–9 (2012).

Moreover, also antagonistic antibodies against inhibitory receptors have been developed, which function via counteracting the inhibitory effect on the T cell response (Table 1)[7]. In 2011,

Ipilimumab (developed by Medarex/Bristol-Myers Squibb), a fully humanized monoclonal antibody directed against the inhibitory receptor CTLA-4, has been approved by the FDA for the therapy of late-stage melanoma patients[5]. Besides the artificial costimulation mediated via an antibody, also the physiological ligands can be incorporated into therapeutic applications[10]. Accordingly, costimulatory ligand-Fc fusion proteins have been developed and their enhancement of the antitumor immune response could be shown[11,12]. However, these approaches still bear the risk of systemic toxicity, since several different cell types are known to express Fc receptors. To avoid unspecific side effects, costimulatory ligands have to be restricted to the tumor site. Using viral transduction techniques, several studies introduced costimulatory ligand expression on tumor cells, thus revealing an enhanced antitumor immune response[6]. As an alternative to genetic approaches, targeting of costimulatory ligands to the tumor site can also be achieved by their subsequent fusion to antibody moieties directed against antigens specifically expressed on tumors. So far, several studies revealed an antitumor effect of costimulatory antibody-ligand fusion proteins in combination with a primary stimulus, hence rendering this approach promising for cancer immunotherapy[13–15].

1.2 - Costimulation of T cells

According to the concept of the “two signal model”, T cells require a primary stimulation via the T cell receptor (TCR) and a secondary signal via a costimulatory receptor (e.g. CD28) to become fully activated[16]. Physiologically, T cells receive these signals via the interaction with antigen presenting cells (APCs), namely dendritic cells (DCs), macrophages and B cells. In the absence of a costimulatory signal, the T cell attains an anergic state, in which it is incapable of eliciting an immune response to a presented antigen or it may even lead to apoptosis of the cell[17]. On the contrary, when the first stimulus is lacking, no biological effect can be observed[16]. Thus, only when the T cell receives both signals, an efficient immune response can be generated accompanied by clonal expansion, differentiation into effector T cells (T_{eff}) and subsequent exertion of effector functions. In this manner, cytotoxic T_{eff} can directly kill antigen-expressing tumor cells either via the induction of apoptosis through the expression of FasL, or via the directed release of cytotoxic granules containing perforin and granzymes[18].

In the last two decades, a broad variety of costimulatory molecules, as well as several inhibitory receptor-ligand pairs have been discovered, which can collectively be termed cosignaling molecules (Fig. 1)[19]. The latter can be divided into two major classes: The Immunoglobulin (Ig)- and the Tumor Necrosis Factor (TNF)-superfamily (SF) with the most prominent member pair, CD28-B7, belonging to the former one[16,20].

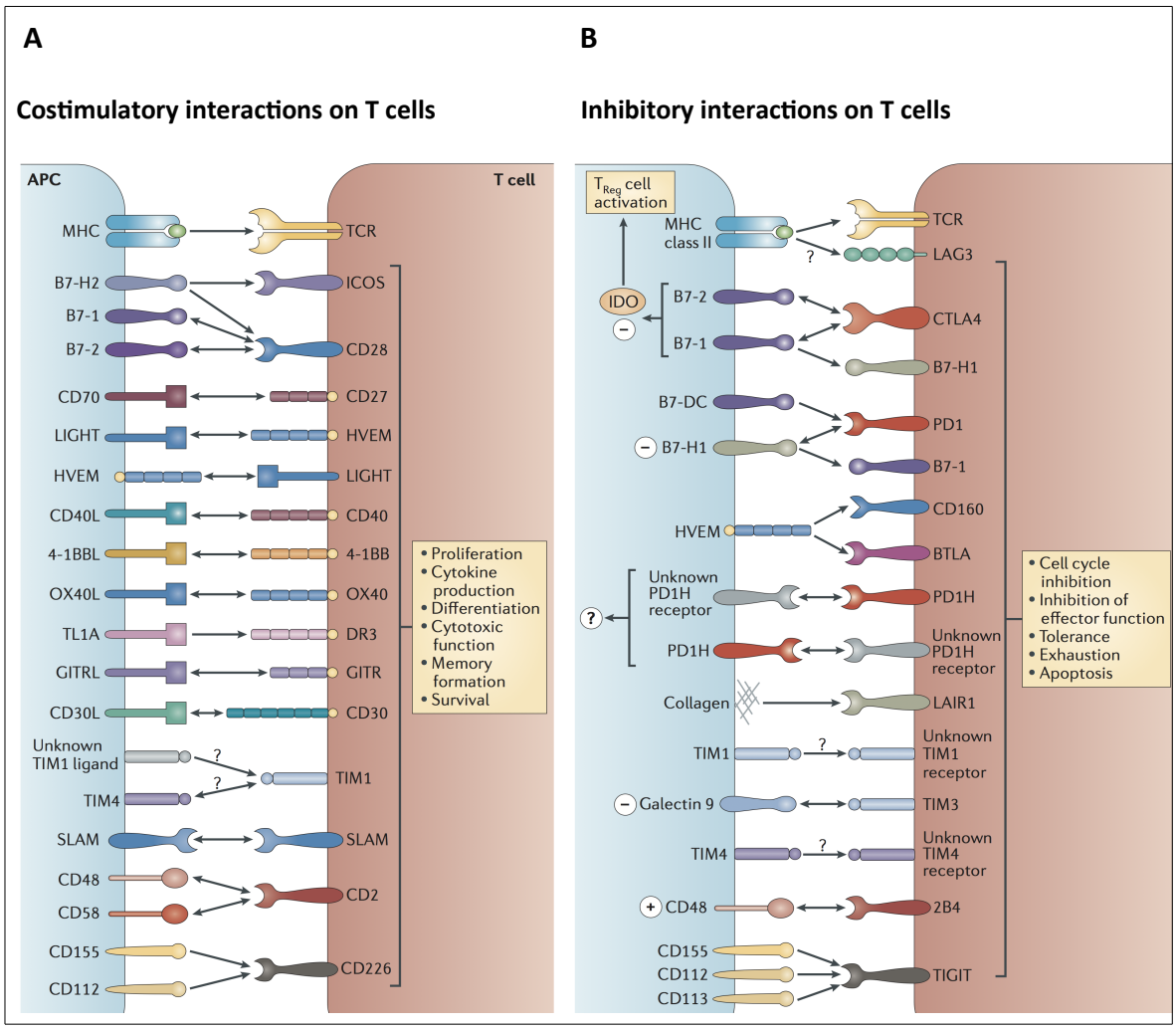

Source: Chen, L. & Flies, D. B. Molecular mechanisms of T cell co-stimulation and co-inhibition. Nature Reviews Immunology 13, 227–242 (2013).

Fig. 1: Costimulatory and inhibitory interactions in T cells. A) Schematic representation of ligands and receptors of the Ig- and TNF-superfamily in the immunological synapse that play a role in the activation, modulation and inhibition of a T cell response. Costimulatory molecules deliver positive signals to T cells following their engagement by ligands or receptors on an antigen presenting cell (APC) leading to T cell proliferation, cytokine production, differentiation and development of effector functions. B) Negative signals are delivered to T cells by inhibitory molecules resulting in the subsequent inhibition of the cell cycle and effector functions and finally in apoptosis. Several cosignaling interactions are bidirectional (bidirectional arrows).

1.2.1 - Ig-superfamily

The Ig-superfamily comprises a wide variety of cosignaling members and still new ones are being discovered. Based on structural differences, the members can be further subdivided into receptors belonging to the CD28 family and ligands belonging to the B7 family. Besides its most prominent receptor, CD28, the CD28 family consists of Cytotoxic T lymphocyte-Associated Antigen 4 (CTLA-4, CD152), Inducible T Cell Costimulator (ICOS, CD278), Programmed Cell Death protein 1 (PD-1, CD279) and B- and T-Lymphocyte Attenuator (BTLA, CD272). For the B7 family, the ligands B7.1 (CD80), B7.2 (CD86), ICOSL (CD275, B7-H2), PD-L1 (CD274, B7-H1), PD-L2 (CD273, B7-DC), B7-H3 (CD276) and B7-H4 can be named[3].

The B7.1/B7.2-CD28/CTLA-4 network represents the best-characterized T cell costimulatory pathway that is crucial in T cell activation and tolerance. Both receptors, CD28 and CTLA-4, exist as disulfide linked homodimers of Ig variable (IgV) domains sharing 30 % sequence identity[21]. The activating receptor CD28 is constitutively expressed on T cells and binding of either B7.1 or B7.2 in combination with TCR-mediated stimulation leads to the activation of naïve T cells which is predominately characterized by IL-2 release and proliferation[16]. In contrast, the inhibitory receptor CTLA-4, which is predominately localized in intracellular perforin-containing secretary granules, can only be detected on the surface following the activation of naïve T cells, whereas it is constitutively expressed on regulatory T cells[22]. Since CTLA-4 has a higher affinity to B7.1 and B7.2 than CD28, its upregulation results in a rapid attenuation or termination of the T cell response[23].

B7.1 and B7.2 are both type I transmembrane proteins with a membrane distal IgV and a membrane proximal Ig constant (IgC) domain sharing 25 % sequence identity[24]. They have a molecular mass of 60-70 kDa and are highly glycosylated (8 potential N-glycosylation sites)[25,26]. Although interacting with the same receptors and being structurally homologous molecules, B7.1 and B7.2 also exhibit some distinct features: While B7.2 is constitutively expressed at low levels on APCs, B7.1 expression is only detectable following their activation[16]. Furthermore, B7.2 binds to its receptors with approx. 10–100-fold lower affinity than B7.1[27]. In addition to their different affinities for the two receptors, B7.1 and B7.2 also display different cell surface oligomeric states with B7.2 existing as a monomer, while B7.1 is present as a mixed population predominantly composed of noncovalent dimers and a lower proportion of monomers[24]. It is

assumed that the distinct oligomeric states of B7.2 and B7.1 allow the formation of qualitatively different complexes with the monovalent CD28 or bivalent CTLA-4 which might have an impact on signaling in the immunological synapse (IS)[28]. Thus, a sophisticated system has been developed in order to control T cell immunity.

Nevertheless, the finding that in the absence of CD28-B7 signaling immune responses are not totally nullified[29] suggests that other costimulatory molecules can at least partially compensate for their lack. One such molecule is ICOS, which is structurally and functionally related to CD28, although it is not expressed on naïve T cells[16]. ICOS expression is rapidly induced upon T cell activation and can be enhanced by CD28 signaling[16]. ICOSL is the only known ligand for ICOS[30], being expressed constitutively at low levels on APCs, including B cells and macrophages and being upregulated following T cell activation on T cells, B cells and monocytes[16]. Furthermore, ICOSL can also be detected on fibroblasts and epithelial cells after inflammatory signals in peripheral sites[16]. In analogy to the B7 ligands with which ICOSL shares 20 % sequence homology, it is a type I transmembrane glycoprotein (6 potential N-glycosylation sites) additionally containing a free cysteine residue in its extracellular IgC domain[31]. Despite its binding to ICOS, ICOSL can also interact with CD28 and CTLA-4[32]. According to their expression profile, the ICOSL-ICOS interaction predominately regulates the activity of recently activated and effector T cells, whereas especially the production of IL-10 can be named[33,34]. Using knockout mice, it was shown that both the B7-CD28 and the ICOSL-ICOS costimulatory pathways are required for an immune response, although defects in one of the costimulatory pathways can at least partially be compensated[35,36].

Another pathway belonging to the Ig-superfamily is the PD-1-PD-L1 interaction which seem to be mainly involved in the downregulation of T cell responses[16]. PD-1 is a 55 kDa type I transmembrane receptor that lacks the relevant motif for binding to B7-1 and B7-2. Its wide expression on activated but not naïve $CD4^+$ and $CD8^+$ T cells, B cells and myeloid cells in contrast to the restricted expression of CTLA-4 and CD28 suggests a broader role in immune regulation, mainly concerning peripheral tolerance[37]. PD-1 solely binds to PD-L1 and PD-L2, and the PD-1 ligands do not bind to additional CD28 superfamily members[16]. Upon ligating its receptor, PD-L1 has been reported to decrease TCR-mediated proliferation and cytokine production[38]. In contrast to normal tissues, which show minimal surface expression of PD-L1 protein, the latter

was found to be abundantly expressed on many murine and human cancers and could be further up-regulated upon IFN-γ stimulation[38]. Thus, PD-L1 might play an important role in tumor immune evasion[39]. However, some other reports identified costimulatory functions of these ligands possibly mediated via an unidentified receptor different from PD-1[38]. Since several interactions and interferences are known between the different Ig-family member pathways, it is assumed that the overall outcome resulting from costimulatory and inhibitory signals will depend on the relative expression of the individual molecules[6].

So far, a broad variety of approaches incorporating members of the Ig-SF have been described supporting their applicability for cancer immunotherapy[6]. Despite the already mentioned mAb against CD28 and CTLA-4, an antagonist mAb against PD-1 has been developed and has shown to display anti-tumor activity[6]. Currently, three humanized anti-PD-1 antibodies (CT-011, MDX-1106 and MK3475) and a second antibody against CTLA-4 (Tremelimumab) are in clinical testing (1.1, Table 1)[9]. Besides mAbs, it could be shown that the introduction of B7.1 on tumor cells led to $CD8^+$ T cell-mediated rejection in several in vivo models, as well as the generation of a memory response capable of protecting the mice against rechallenge with the wildtype tumor[40]. Other studies provided costimulation by fusing B7.1 or B7.2 to tumor targeting antibody moieties or to an Fc portion, thus revealing strong costimulatory effect for the fusion proteins[41,42]. In the case of the ICOS-ICOSL interaction, its direct involvement in tumor rejection has not been shown so far. Nevertheless, a recent study revealed that the ICOS-ICOSL pathway is required for the optimal therapeutic benefit of Ipilimumab[43].

1.2.2 - TNF-superfamily

With regard to 19 ligands and 29 receptors, the TNF-SF comprises a wide variety of different costimulatory molecules[4]. Therefore, in this study the focus lays on the most promising ones for cancer immunotherapy, the ligand-receptor pairs 4-1BBL (CD137L) - 4-1BB (CD137, TNFRSF9), Ox40L (CD252) - Ox40 (CD134, TNFRSF4), LIGHT (Lymphotoxin-like, exhibits inducible expression, and competes with HSV glycoprotein D for HVEM, a receptor expressed by T lymphocytes, CD258) - HVEM (Herpes virus entry mediator, CD270, TNFRSF14) and GITRL (Glucocorticoid-induced TNF-related ligand) - GITR (Glucocorticoid-induced TNF-related protein, CD357, TNFRSF18)[4]. Both TNF ligands (TNFL) and receptors (TNFR) share common characteristics among each other: The receptors are type I transmembrane proteins comprising

several extracellular cysteine-rich domains (CRDs, typically consist of pseudo-repeats of six cysteines that form three disulfide bridges) and exist either as monomers or as self-assembled oligomers forming trimeric signaling complexes when interacting with their ligand, respectively[20,44]. Each costimulatory TNFR binds TNFR-associated factors (TRAFs) that function as adaptor proteins for kinases. Notably, TRAF2, which is used by all TNFR molecules, links to several common signaling pathways, including JUN N-terminal kinase (JNK), the AP1 (FOS/JUN) transcriptional complex, NF-κB, phosphatidylinositol 3-kinase (PI3K) and protein kinase B (PKB, also known as AKT), thus mediating cell survival, cytokine production and proliferation[20].

TNFL are type II transmembrane proteins sharing a TNF homology domain (THD) in the carboxyl terminus and are composed of β-strands and loops in a "jelly roll" topology[45]. The THD is responsible for ligand trimerization as well as binding to the CRDs of TNFRs[44]. The majority of the TNF ligands contain potential N-glycosylation sites (LIGHT: 1, Ox40L 4: GITRL: 2, mouse 4-1BBL: 3), except human 4-1BBL. 4-1BBL and Ox40L are not constitutively expressed by resting or immature APCs, but are induced 24 h to several days after activation, largely coinciding with the expression peak level of their receptors on T cells[20]. In contrast, GITRL is constitutively expressed by APCs at low levels, transiently upregulated due to Toll-like receptor (TLR) stimulation and finally downregulated by 24h[46]. Expression of LIGHT is upregulated with activation of T cells, monocytes and NK cells and can also be found on immature but not on mature DC. Furthermore, LIGHT has even been shown to enhance HVEM downregulation[47].

In terms of cancer immunotherapy, promising in vivo results were obtained with agonist mAbs directed against 4-1BB[48], Ox40[49,50] and GITR (DTA-1)[51]. For the latter, it could be shown that the rejection of several murine syngeneic tumors was induced through an IFN-γ dependent mechanism by promoting the activation of effector T cells and altering of the intratumor ratio of regulatory T cells and effector T cells[6]. Currently, a fully humanized mAb against 4-1BB (BMS-666513)[52] and a murine mAb against Ox40 (ClinicalTrials.gov Identifier: NCT01416844) are in clinical trials (1.1, Table 1) and a phase I study of a humanized Fc-disabled (aglycosylated), GITR-specific agonist antibody (TRX518) is recruiting participants (unresectable stage III or IV melanoma)[9,53]. Besides mAbs, several studies approached the expression of costimulatory ligands within the tumor in order to achieve an anti-tumor immune response. Accordingly, it could be shown that the introduction of either 4-1BBL[54] or GITRL[55,56] on tumor cells revealed an

improvement in tumor burden. In the case of LIGHT, its property to serve both as a costimulatory ligand for T cells as well as stromal cell activator inducing chemokine production and lymphoid recruitment renders it attractive for approaches facing cancer[6]. Hence, the introduction of LIGHT into tumor cells via gene transfer induced antigen-specific cytolytic T cell response and therapeutic immunity against established tumors[57]. Other studies successfully provided costimulation by fusing costimulatory ligands to tumor targeting antibody moieties or to an Fc portion, as it could be revealed for GITRL[15,58], Ox40[59,60] and 4-1BB[14,61].

1.2.3 - Costimulation of T cell subsets

Today, it is known that costimulatory molecules not only play a role during T cell activation, but also be required during all phases of T cell responses, such as differentiation, development of effector functions and survival[19]. In naïve T cells, CD28 is the major costimulatory receptor leading to the activation of naïve T cells in the presence of TCR-mediated signaling[62]. Besides CD28, also a limited number of receptors of the TNF-SF are known to be expressed on naïve T cells as well, namely HVEM[63] and to a lesser extent CD27[64] (Fig. 2), which have been shown to be involved in the process of T cell priming (transition from a quiescent to an activated state). Although it is assumed that alternative costimulatory molecules such as CD2 seem to at least partially compensate in the case of a CD28 deficiency[65,66], it may not be the case for CD27, since the latter was shown to be unable to initiate cell cycling in the absence of CD28 costimulation[64]. For HVEM, it has not been addressed yet.

In effector T cells, HVEM is temporarily downregulated, while other costimulatory receptors of the TNFR-SF become upregulated and play a substantial role in the regulation of effector T cell responses[20](Fig. 2). In particular, 4-1BB, Ox40, CD30, CD27 and GITR have been described to promote the expansion and survival of effector T cells[20,67]. Furthermore, also a member of the B7-family, ICOS, has been shown to positively regulate the survival of activated effector T cells[68]. Later on during the course of effector T cell development, HVEM is upregulated again on on the cell surface of both $CD4^+$ and $CD8^+$ effector T cells and regulates effector functions either via ligation of LIGHT (costimulatory effect) or via BTLA and CD160 (inhibitory effect)[63]. Since the expression of LIGHT is decreased on activated APCs, it alleviates the costimulatory potential of HVEM, thus rendering it more susceptible to the inhibitory actions of BTLA and CD160[69]. In addition to the expression of BTLA and CD160, also other inhibitory receptors, such as CTLA-4,

PD-1, Lymphocyte Activation Gene 3 protein (LAG3, CD223) and T Cell Immunoglobulin Domain and Mucin Domain 3 (TIM-3) are upregulated during the effector T cell phase, thus limiting both $CD4^+$ and $CD8^+$ effector T cell responses[19]. Hence, it is assumed, that the overall balance of costimulatory and inhibitory signals determines the qualitative and quantitative outcome of the effector T cell response and subsequently also the size and quality of the memory T cell pool[19].

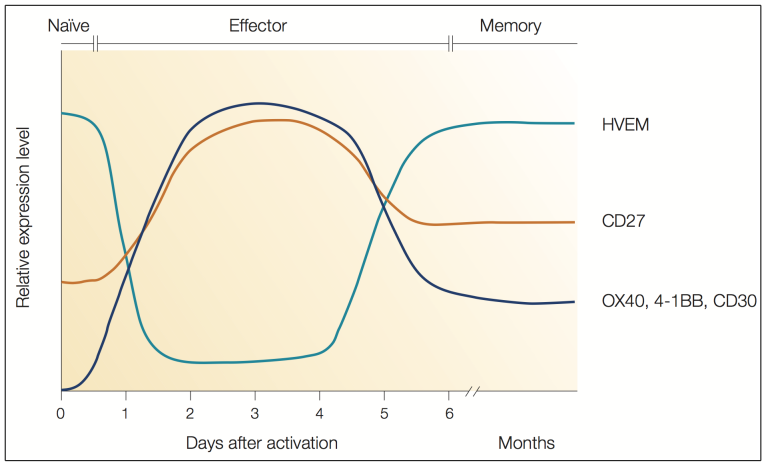

Source: Croft, M. Costimulatory Members of the TNFR Family: Keys to Effective T-Cell Immunity? Nature Reviews. Immunology 3, 609–620 (2003).

Fig. 2: Generalized time course model of the expression of costimulatory TNFR-family members. After the activation of naïve T cells the transition to effector and memory T cell stages is accompanied by the up- or downregulation of the expression of receptors belonging to the TNFR-family. While HVEM is constitutively expressed by naïve T cells, it is downregulated after T cell activation and re-expressed during the memory phase. In contrast, Ox40, 4-1BB and CD30 are not expressed by naïve T cells, but become upregulated during the effector phase of the T cell and are also expressed at lower levels on the memory T cell population. CD27 shows a similar expression pattern to Ox40, 4-1BB and CD30, but it is constitutively expressed on naïve T cells (at lower levels than HVEM).

In addition to their role during the effector T cell phase, TNFR-SF members are also crucial for the memory T cell population[20]. Individual as well as collective effects have been shown for 4-1BB, Ox40, CD30 and CD27 in promoting memory T cell responses as well as initiating memory T cell expansion in response to secondary challenge[19,20]. Furthermore, CD28 plays a role as well within the memory T cell population, mainly via promoting its survival and via promoting secondary responses of $CD4^+$ and $CD8^+$ memory T cells to viral infections[70]. Similarly, ICOS has also been shown to be important, since its deficiency results in a reduced memory T cell compartment and in defective memory T cell reactivation[71]. In contrast, in exhausted T cells, which are characterized by greatly reduced proliferative capacity and effector functions, multiple inhibitory receptors such as PD-1, CTLA-4, BTLA, CD160, TIM3 and LAG3 are

upregulated, thus correlating with the degree of T cell unresponsiveness[72]. Nevertheless, it was found out that exhaustion can be rescued by costimulatory signals, as it was recently shown for an agonist mAb against 4-1BB in combination with IL-7 in a model of chronic T cell infection with lymphocytic choriomeningitis[73].

Besides the T cell subsets described so far, costimulatory and inhibitory molecules are also known to be essential for the development and function of regulatory T cells (T_{regs})[74]. While CD28 is required for both the generation in the thymus as well as for the maintenance of T_{regs} in the periphery, ICOS promotes their proliferation, survival and maintenance[74]. Furthermore, also several members of the TNF-SF are involved in costimulation of regulatory T cells as well. The most prominent one is GITR, which is expressed in very high levels on unstimulated T_{regs} and promotes their suppressive activity along with HVEM and CD30[19]. In contrast, it has been shown that 4-1BB, Ox40 and DR3 (TNFRSF25) reduce the suppressive activity of T_{regs}, while they simultaneously promote their expansion[19]. Furthermore, also several inhibitory receptors including CTLA-4, PD-1 and LAG3 are expressed on the surface of regulatory T cells and it is assumed that they negatively regulate conventional T cells in an indirect, cell-extrinsic manner[19,74]. Finally, costimulatory molecules are also required for $CD4^+$ T helper cell differentiation and their respective subset functions[19]. Besides ICOS, TIM1 and TIM4 as well as the TNFR-SF members CD27, HVEM, DR3 and Ox40 have been shown to play an important role in this T cell subpopulation and future studies might reveal more defined functions for them[19].

1.2.4 - A new understanding of costimulation

With a growing knowledge of costimulation it has become apparent, that the classical “two signal model” needs to be revised in order to describe the complex mechanisms involved in the process of T cell costimulation[75]. Hence, it is now understood that costimulatory signals do not only provide an “on or off” switch but rather represent a complex network of receptor–ligand interactions that qualitatively and quantitatively influence immune responses, thus affecting both T cells and APCs[19]. Therefore, in order to better describe the costimulatory process, the “tidal model of costimulation” has been proposed previously by Zhu et al[75]. It is based on the finding, that the expression of many costimulatory and inhibitory molecules on T cells is induced following activation and that most changes in the cell surface expression occur in an overlapping manner during T cell proliferation and differentiation[19]. In addition, it is assumed,

that cell surface interactions and subsequent intracellular signaling are continuously varied in response to dynamic environmental conditions. According to the tidal model, the T cell activation process resembles an incoming tide with a great variety of costimulatory receptors "pulling" the T cell into functional responsiveness. At peak tide, inhibitory receptors become upregulated on the T cell surface so that the functional outcome of the T cell response depends on the opposing "forces" of costimulatory and inhibitory receptors. Finally, during receding tide, the expression of inhibitory receptors dominates the expression of costimulatory receptors, thus leading to the termination of the T cell response[19].

In order to improve the understanding of the diverse costimulatory interactions, efforts have been made to reveal their regulatory mechanisms. Several levels of regulation are found to be involved in T cell costimulation, among them e.g. the modulation of cell surface expression of cosignaling molecules as well as differential expression patterns of receptor-ligand pairs (as in the case of the reciprocal expression pattern of HVEM and LIGHT[63]. In most cases, cell surface expression is regulated on the transcriptional and post-transcriptional level[19], whereas an additional mechanism has been discovered recently: The expression of B7.1 and B7.2 on APCs can be downregulated through trans-endocytosis by CTLA-4. In this manner, CTLA-4 captures its ligands from opposing cells, thus preventing their interaction with CD28[76]. Another regulatory mechanism was revealed by the finding that several costimulatory or coinhibitory molecules can interact with more than one ligand or receptor, resulting in multiple functions for a single cosignaling molecule[19]. Furthermore, for some molecules, the interaction can even occur through more than one binding site. A prominent example for this mechanism is HVEM, since it has been shown to bind to LIGHT (costimulatory signal) as well as to BTLA and CD160 (inhibitory signal)[69]. In total, 14 different molecular interactions have been described for the HVEM pathway so far[69]. Moreover, since CD28 and CTLA-4 use a different binding motif for their interaction with ICOSL than with B7.1 and B7.2 (MYPPPY), it is assumed that CD28 and CTLA-4 can bind either B7.1 or B7.2, while simultaneously interacting with ICOSL through a second binding site[32] (Fig. 3). Finally, it has been shown for B7.1 that it can also interact with PD-L1[77]. Since the B7.1 – PD-L1 interface overlaps with the B7.1 – CTLA-4/CD28 and PD-L1 – PD-1 interfaces[77], CD28, CTLA-4 and PD-L1 seem to compete for binding to B7.1, while it is assumed that the latter competes with PD-1 for binding to PD-L1[19]. The B7.1 – PD-L1 interaction is also an

example for bidirectional co-signaling, which is as well widely distributed among the cosignaling molecules of both the Ig- and the TNF-SF[77–79] (Fig. 1, indicated via bidirectional arrows). Thereby, intracellular signals can be transduced through both molecules upon binding. In the case of the B7.1-PD-L1 interaction, an inhibitory signal can be transduced into the T cell either via B7.1 or PD-1, depending on the respective molecule expressed on the surface of the T cell[77].

Thus, costimulation is a far more complex process than originally thought. Hence, in order to approach costimulatory members for cancer immunotherapy, it is crucial to understand the fundamental mechanisms of T cell costimulation and inhibition and subsequently take them into account.

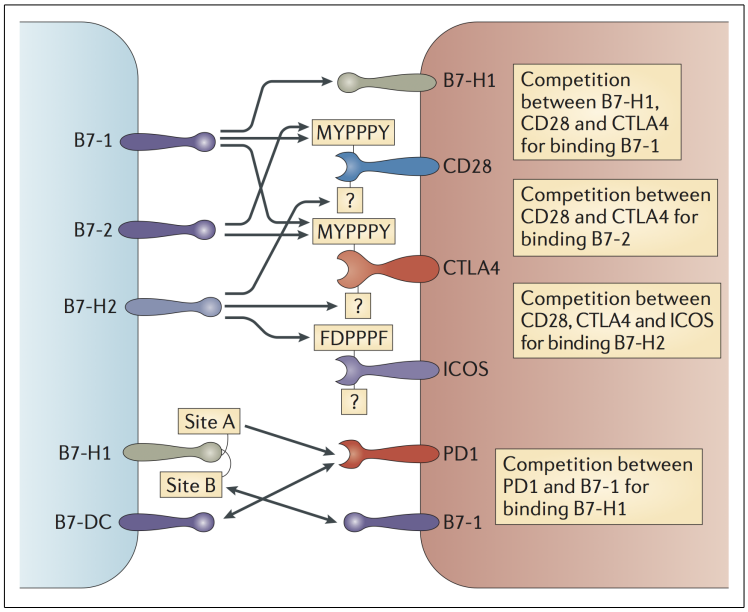

Source: Chen, L. & Flies, D. B. Molecular mechanisms of T cell co-stimulation and co-inhibition. Nature Reviews Immunology 13, 227–242 (2013).

Fig. 3: Cosignaling interactions through multiple interfaces. Despite CD28 and CTLA-4, also PD-L1 (B7-H1) interacts with B7.1. Similarly, CD28 and CTLA-4 compete for binding to B7.2, while CD28, CTLA-4 and ICOS have a competition for ICOSL (B7-H2)-binding. Since B7.1 and B7.2 bind to a different binding site on CD28 and CTLA-4 than ICOSL, it is assumed that the receptors can act simultaneously with both B7.1/B7.2 and ICOSL. Finally, B7.1 also competes with PD-1 for binding to PD-L1, since the binding sites (Site A and Site B) are partially overlapping.

1.3 - Recombinant antibody formats for cancer immunotherapy

1.3.1 - Costimulatory antibody-ligand fusion proteins

In order to restrict costimulatory ligands to the tumor site and to present them in a membrane-bound state, they can be fused to antibodies targeting tumor associated antigens[80]. Besides whole immunoglobulins (Ig), also the Fc part of an antibody or antigen-binding fragments can be used[81]. While the large size of whole Ig molecules and the presence of a Fc region can be advantageous in terms of pharmacokinetics, these characteristics are also limiting the suitability of an antibody for cancer immunotherapy due to poor tissue penetration and Fc-mediated side effects (e.g. cytokine release syndrome, thrombocytopenia, leukopenia). Therefore, antigen-binding fragments have shown to be advantageous[82].

The smallest antigen-binding fragments which are also the building units for the most commonly used recombinant antibody formats are single-chain fragment variables (scFvs) (Fig. 4)[83]. The latter consist of the variable regions of the heavy (V_H) and the light (V_L) chain of an antibody fused via a short linker (V_H-V_L or V_L-V_H), thus forming a small and functional monospecific antigen-binding moiety. The linker thereby is usually comprised of 15 amino acids in order to allow correct folding of the two domains[83]. When the linker length is reduced (5-10 aa), the V_H-V_L domains on the same chain can not assemble anymore and therefore the domains are forced to pair with their complementary domains on a second chain, thus forming a diabody (Db) with two functional antigen binding sites[84]. By using scFvs derived from two different antibodies (antibody A and B), a bispecific diabody with either the structure V_HA-V_LB and V_HB-V_LA (V_H-V_L configuration) or V_LA-V_HB and V_LB-V_HA (V_L-V_H configuration) can be achieved[84]. Furthermore, the two diabody units can also be combined on one chain via an additional linker of 15-20 aa resulting in a monomeric, bispecific molecule with a diabody-like structure (single-chain Db (scDb))[83]. Another scFv-based format is represented by the tandem scFv (taFv), where two scFvs (with different antigen-binding sites) are connected by an additional short linker (V_HA-V_LA-linker-V_HB-V_LB), so that each scFv moiety forms a separate unit[85].

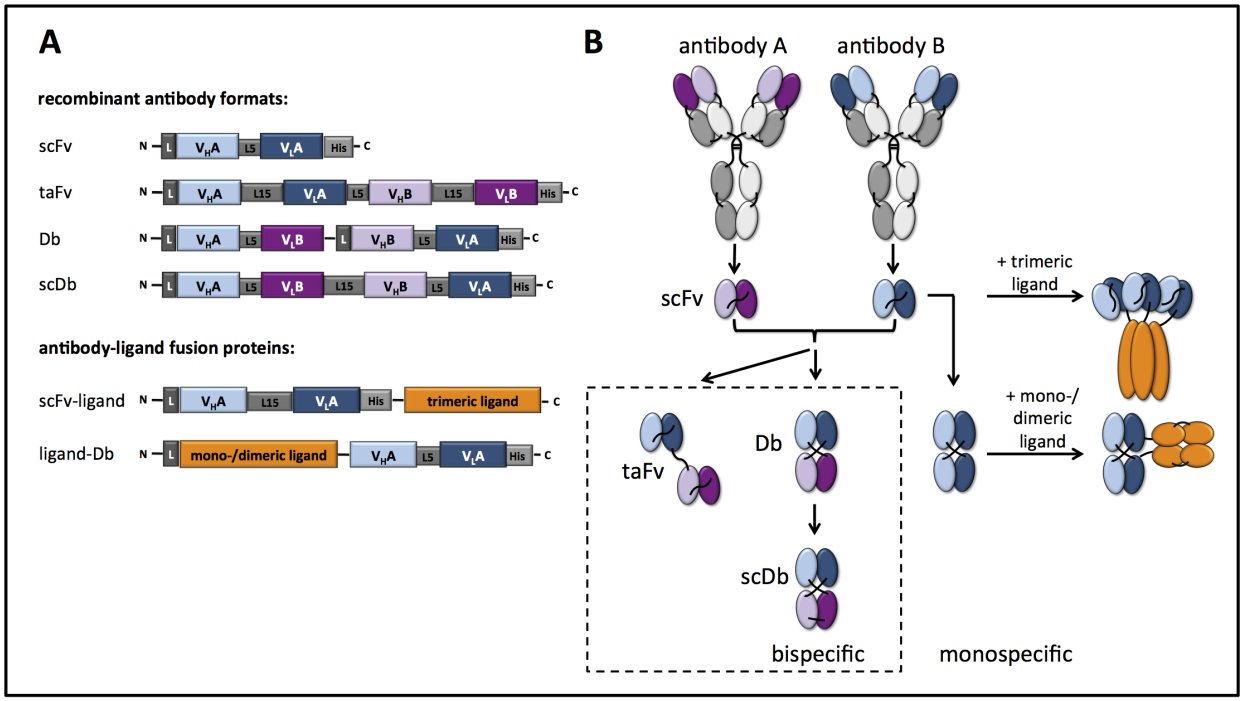

Fig. 4: Schematic representation of sequences and structures of various recombinant antibody formats and antibody-ligand fusion proteins. A) Domain and linker arrangements in single-chain Fv fragments (scFv), tandem scFv molecules (taFv), diabodies (Db), single-chain diabodies (scDb) and antibody-ligand fusion proteins (scFv-ligand, ligand-Db) (V_H: variable domain of a heavy chain, V_L: variable domain of a light chain, His: His-tag, L: leader, L5/12/15: linker). B) Structural scheme of two whole IgG molecules (specificities A and B) and recombinant antibody formats derived thereof. Two scFv molecules of either the same or a different specificity are the building blocks for either mono- or bispecific Db, scDb or taFv moieties. Genetic fusion of a trimeric ligand to a scFv leads to a homotrimeric assembly, while fusion of a mono- or dimeric ligand to a Db results in a homodimeric assembly of the respective antibody-ligand fusion protein.

So far, a variety of different antibody fusion proteins have been described incorporating immune activators, such as cytokines (IL-2, IL-15, IFN-γ), chemokines (LEC (CCL16)) or costimulatory ligands (B7.1, 4-1BBL)[80,81,86]. In these approaches, the immune activators can be fused either at the amino- (N-terminal) or carboxy-terminus (C-terminal) of the antibody depending on both the structure of the immune activating molecule and the antibody moiety in order to conserve their biological activity[87]. Furthermore, the size and valency of the fusion proteins is directly influenced by the respective antibody format as well as the composition of the immune activating molecule[81]. For example, fusion of a scFv to a monomeric molecule results in a fusion protein binding monovalently to the antigen and the respective receptor, while fusion of a scFv to a homotrimeric molecule reveals a trivalent scFv assembly (Fig. 4)[81]. Accordingly, for the homotrimeric ligands of the TNF superfamily several studies already described the generation of functional, homotrimeric fusion proteins (scFv-TNF) with three antigen-binding sites and three ligand moieties[14,88,89]. Moreover, also a scFv fusion protein with

a member of the Ig-SF (B7.2) has been generated and shown to be functional in terms of both antibody-mediated tumor targeting and costimulatory activity[42]. However, it could be shown in our group that a B7.2-scFvCEA fusion protein displayed a lower costimulatory activity than a Db-based fusion protein (B7.2-DbCEA) (unpublished data), which was probably due to insufficient cross-linking of CD28 in the case of monomeric B7.2-scFv. Accordingly, it was assumed that dimeric B7.2 resulting from the fusion to the diabody format facilitates efficient clustering of CD28 leading to stronger costimulatory effects on the T cell response[90]. Thus, in this study, ligands of the B7-family were incorporated into Db fusion proteins, while members of the TNF-SF were fused to scFv moieties. Since costimulatory approaches focus by definition on the promotion and modulation of a T cell response without being capable to initiate it themselves, their efficacy relies essentially on an appropriate tumor-directed first signal. Artificially, such a signal can be provided by bispecific antibodies (1.3.2).

1.3.2 - The concept of bispecific antibodies

Physiologically, T cells receive activating signals via their T cell receptor (TCR) interacting with a cognate antigen-loaded Major Histocompatibility Complex (MHC) on APCs. In this manner, only the T cell clone which is directed against the respective antigen becomes activated (monoclonal T cell activation)[91]. However, T cells can also be activated artificially by triggering them through the non-variable T cell co-receptor signal transduction complex CD3 which is associated with the TCR[92]. In this manner, any existing T cell clone can be activated, irrespective of the antigen specificity of the individual T cell or even the expression of a MHC molecule (polyclonal T cell activation)[93]. Especially suitable for this purpose have shown to be bispecific antibodies since they combine T cell activation with a redirection to the tumor site by simultaneously binding to CD3 on the T cell and an antigen on the tumor cell[83]. Although the feasibility and functionality of the bispecific antibody concept has been confirmed in several studies using a broad range of different recombinant formats, tumor antigens and effectors[83], most studies with anti-CD3 bispecific antibodies have shown that T cells need a second stimulus, such as a mAb directed against CD28 or a B7-fusion protein, to efficiently lyse target cells[94,95]. In contrast, ‘‘bispecific T cell engager’’ antibodies (BiTE), which are tandem scFvs (taFv) directed against CD3 and a tumor-associated antigen, were shown to be able to induce a costimulation-independent T cell response[96] and currently, three BiTE antibodies (MT103, MT110, MT111) are in clinical trials[97].

Nevertheless, there is evidence, that BiTE molecules might also benefit from additional costimulation[98].

1.4 - Targets in cancer therapy

Due to the diversity of tumors, more than 2000 different tumor antigens have been identified so far[99]. Despite the variety of categories proposed for their classification according to their origin or function, tumor antigens can be roughly classified into two categories: Tumor specific antigens are solely expressed on tumors, whereas tumor associated antigens (TAA) can also be found on normal tissue, but are mostly over-expressed on tumors. In detail, TAA often bear mutations, show differences in splicing or glycosylation patterns or are expressed during embryogenesis and not on adult tissues. Besides tumor cells, a solid tumor is also composed of tumor vasculature and tumor stroma and is embedded in a so-called tumor microenvironment that further includes the extracellular matrix (ECM), diffusible growth factors, cytokines and inflammatory cells (lymphocytes, macrophages, mast cells)[100]. Based on this knowledge, the understanding of a tumor as a more or less homogeneous isolated “structure” changed towards seeing it as a complex network of diverse interactions, thus leading to the incorporation of the tumor microenvironment into cancer targeting strategies. Since the tumor stroma comprises most of the tumor mass in many carcinomas and its destruction causes loss of structural as well as other beneficial support, it is especially attractive as a target[101]. Fibroblasts are the predominant cells found in the stroma and are responsible for ECM alterations promoting tumor cell invasion and metastasis, tumor angiogenesis and availability of growth factors and cytokines[102].

Fibroblast activation protein α (FAPα)

One tumor associated antigen applied in this study is Fibroblast activation protein α (FAPα). Although its expression is normally restricted to wound healing and fetal mesenchymal tissues, it is highly overexpressed on cancer associated fibroblasts (CAFs) in the stroma of about 90 % of all human epithelial cancers such as breast, lung and colorectal cancers[103].

FAPα is a 170 kDa non-covalently linked homodimer of N-glycosylated 97 kDa subunits that belongs to the serine protease family (S9b peptidase family)[104]. As a member of this family,

FAPα degrades gelatin I and type I collagen of the extracellular matrix due to its dipeptidyl peptidase and collagenolytic activity[105]. Monomeric FAPα contains a large C- terminal extracellular domain comprising the active site (triad) and six potential N-glycosylation sites[104]. It has been shown that the enzymatic activity of FAPα is regulated by N-glycosylation and dimerization of the two monomers into a functional homodimer, since the non-glycosylated 95 kDa monomers have been shown to lack any detectable post-prolyl and gelatinase activity[106]. The degradative activity of FAPα suggests its suitable role in the remodeling of tumor tissue, by means of tumor invasion and metastasis[107]. The fact that FAP was also shown to be directly involved in tumor promotion, revealing increases in tumor incidence, growth and microvessel density[103], renders it even more into a promising tumor target. Its suitability in terms of selectivity and specificity was shown by tumor imaging with an antibody directed against FAP, where the antibody bound specifically to the tumor sites without apparent side effects[108]. The applied antibody was sibrotuzumab, a humanized version of the first antibody directed against FAPα (mAb F19), which was also tested in clinical phase I and limited phase II trials[108,109]. Furthermore, the therapeutic effect of FAP-targeting could be shown in several in vitro studies leading to a subsequent inhibition of tumor growth[110,111].

So far, various FAPα-specific antibodies have been isolated by phage display technology, amongst them the antibody fragments scFv mo33 and mo36[112–114]. The latter were generated by Brocks and coworkers and were the source for two of the antibody constructs applied in this study, namely scDb33CD3 and B7.2-Db36[112]. Although both antibodies are directed against two different FAP epitopes, the latter seem to partially overlap or at least be adjacent since for higher concentrations, a competitive effect could be observed[89]. Furthermore, both antibodies are cross-reactive for both human and mouse FAP which share 89 % amino acid sequence homology[115]. In 2001, the first recombinant bispecific antibody directed against FAP and CD3 on T cells was generated in a taFv format, and its functionality and the feasibility of the approach was shown via the recruitment of cytotoxic T cells and subsequent target cell killing[116]. However, the antibodies against FAP (OS4) and CD3 (TR66) were different from the ones applied for the bispecific antibody scDb33CD3 (FAP (33), CD3 (UCHT-1)[117]) in this work.

Endoglin (EDG)

The second model antigen applied in this study is endoglin (CD105), whose expression is mainly restricted to vascular endothelial and stromal cells, while it is weakly detectable on activated monocytes, macrophages, erythroid precursors and fibroblasts[118]. Since EDG is highly upregulated in actively proliferating endothelial cells, such as those in the neoplasm, it has been suggested as an appropriate marker for tumor-related angiogenesis and neovascularization[119]. Accordingly, till now, it is used as the gold standard for measuring tumor microvessel density[120].

Human endoglin is an 180 kDa homodimeric, disulfide-linked, type I transmembrane protein that functions as an accessory receptor for transforming growth factor beta (TGF-β)[118]. The latter is a pleiotropic cytokine involved in the regulation of cellular proliferation, differentiation, migration and adhesion[121]. Endoglin consists of a large N-terminal extracellular domain, a hydrophobic transmembrane domain, and a short intracellular domain[122]. In detail, the extracellular domain comprises an Arg-Gly-Asp (RGD) tripeptide, four N-linked glycosylation sites and a region of O-linked glycosylation[123]. Two different endoglin isoforms are described in literature, namely L and S, differing in tissue distribution, phosphorylation degree and length of their intracellular domains[124]. A high amino acid sequence homology was observed among human and murine endoglin (75 %, transmembrane and cytoplasmatic domains showing 95 % identity) with major differences in the extracellular domain[118]. CD105 is essential for angiogenesis and its potential use as a diagnostic, prognostic and therapeutic agent has been described in several studies[125]. Initial support for the therapeutic potential of endoglin arose from in vitro studies showing anti-endoglin mAbs being able to induce apoptosis in HUVECs[126]. Consequently, studies with recombinant bispecific antibodies followed in which the recruitment of cytotoxic T cells was analyzed in vitro[127]. In vivo, anti-endoglin mAb have been shown to inhibit tumor growth and metastasis in immunocompromised as well as in immunocompetent mice, and the inhibition was based on either the destruction of tumor vasculature or the inhibition of tumor angiogenesis[118]. Currently, TRC105, a therapeutic monoclonal antibody against endoglin, is tested in clinical trials: A phase I study with patients suffering from advanced solid tumors could evidence its safety profile and clinical activity, thus supporting

ongoing phase Ib and phase II studies with advanced prostate, ovarian, breast, bladder, and hepatocellular cancer[120].

The anti-human EDG antibody applied in this study is based on the scFv fragment A5, which was isolated from a fully synthetic scFv library via phage display[128]. Since then, several studies revealed the functionality of the antibody[89,127,129]. Since scFvA5 is not cross-reactive against mouse EDG, for the in vivo experiments a mouse-specific antibody (scFvmE12) was applied, which was also isolated from a phage display library[130].

1.5 - Therapeutic potential of combinatorial costimulatory approaches

Besides all the efforts being made with approaches focusing on only one costimulatory molecule at a time, it has become more and more apparent that combinatorial approaches might be more effective than monotherapeutic ones[7]. Accordingly, several studies revealed an enhanced antitumor activity for a mAb directed against either a costimulatory (e.g. 4-1BB, Ox40, GITR) or an inhibitory receptor (e.g. CTLA-4) when it was combined with cancer vaccines, radiotherapy, chemotherapy or cytokines (Fig. 5)[7,10]. With increasing knowledge of the differential effects of each costimulatory molecule and the diverse interactions within the costimulatory network, studies also started to address multiple costimulatory molecules instead of a single one[131,132]. Promising candidates thereby were e.g. CD28 and 4-1BB, since they have differential expression profiles and are known to exert their costimulatory potential on different T cell subsets (1.2.3). Accordingly, the combined expression of B7 and 4-1BBL on tumor cells showed a synergistic effect in eliciting an antitumor response in mouse models, with increased CTL activity and long-term tumor immunity[54,133,134]. Importantly, also dual costimulation of TNFR family members has been approached (Fig. 5): The combination of mAbs against 4-1BB and Ox40 revealed strong cooperative effects in boosting $CD8^+$ T cell effector functions and antitumor immunity in various mouse studies and an even synergistic enhancement of $CD8^+$ T cell expansion could be observed[135]. Furthermore, also the combined application of agonists for 4-1BB and CD40 was shown to be beneficial in mediating $CD8^+$ T cell responses although the effect was lower compared to addressing 4-1BB and Ox40[136].

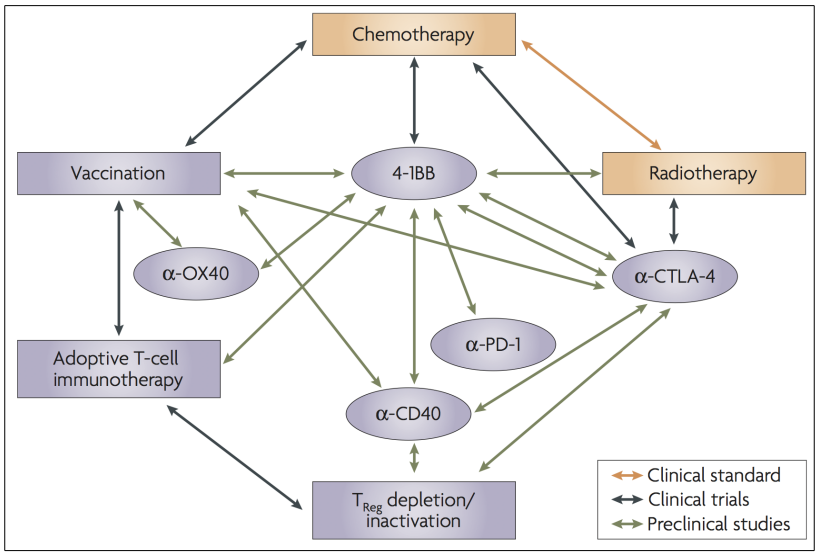

Source: Melero, I., Hervas-Stubbs, S., Glennie, M., Pardoll, D. M. & Chen, L. Immunostimulatory monoclonal antibodies for cancer therapy. Nature Reviews. Cancer 7, 95–106 (2007).

Fig. 5: Combinatorial strategies involving immunostimulatory mAbs for cancer therapy. An overview of combinatorial therapeutic approaches with immunostimulatory monoclonal antibodies (mAbs) for cancer in clinical and preclinical development. The status of each treatment or each combination (bidirectional arrows) is referred to by a color code (α: anti, T_{reg}: regulatory T cells).

Another example for an effective combination therapy involving three mAbs ("trimAb") directed against members of the TNF-SF was demonstrated by Uno et al[137]. Here, the induction of tumor-cell apoptosis by an agonistic mAb to DR5 (death receptor 5) in combination with T cell activation mediated by two mAbs directed against 4-1BB and CD40 elicited $CD8^+$ T cell-dependent eradication of pre-established tumors in mice. Importantly, the therapeutic effect for treatment with anti-DR5 in combination with either anti-4-1BB or anti-CD40 was substantially less effective than the combination of both. Besides, also approaches were described focusing on simultaneous stimulation of a costimulatory receptor while blocking of an inhibitory one (Fig. 5). For the combination of anti-4-1BB mAb with either anti-CTLA-4[138] or anti-PD-1[139], a synergistic effect could be observed. Furthermore, since it has been revealed that the ICOS-ICOSL pathway is necessary for the optimal therapeutic effect of anti-CTLA-4, the receptor-ligand interaction is implicated as a target for future combinatorial strategies in order to improve the efficacy of anti-CTLA-4 therapy[43]. In addition, a clinical trial is currently recruiting participants for investigating the therapeutic benefits of combined stimulation via mAbs directed against Ox40 and CTLA-4 (Ipilimumab).

Although the combinatorial studies described above revealed very promising results for the use of immunostimulatory mAb in cancer immunotherapy so far, still some challenging obstacles remain to be overcome. Very often, the application of immunostimulatory mAbs is associated with immune-related adverse events (AEs), involving the skin, gastrointestinal apparatus, liver and endocrine system and which are most likely be due to the mAb-mediated hyperstimulation of the immune system[140]. Furthermore, it has been observed that activated, effector T cells which successfully reached the tumor, were subsequently rendered nonresponsive due to the suppressive milieu within the tumor microenvironment[141]. In order to circumvent these barriers, the physiological costimulatory ligands could be used in a tumor-targeted manner as it is approached with costimulatory antibody-ligand fusion proteins in this work. In this manner, hyperstimulation of the immune system could be prevented and T cells would receive costimulation within the tumor, thus countering the suppressive activities.

1.6 - Purpose of the study

Combinatorial approaches involving members of the costimulatory network are an emerging strategy in cancer immunotherapy. In this work, combinations of costimulatory antibody-ligand fusion proteins ought to be analyzed for their synergistic abilities to promote the generation of a potent, tumor-directed T cell response in the presence of a first signal-mediating bispecific antibody. Therefore, a model system ought to be established consisting of target cells coexpressing two different tumor antigens (FAP and EDG) and T cells. The bispecific antibody (scDbFAPxCD3) and the costimulatory fusion proteins are combined in this setting via targeting either the same or a different antigen, thus achieving a fully tumor-targeted approach. In this model system, the combinatorial potential of B7 (B7-DbFAP)- and 4-1BBL (scFvEDG-4-1BBL)-fusion proteins ought to be analyzed for its effect on T cell activation, phenotype and effector functions. Furthermore, also the influence of costimulation on the T cell response in a restimulation context ought to be approached. Moreover, the spectrum of costimulatory fusion proteins ought to be expanded by the generation of antibody-ligand fusion proteins comprising other members of the TNF-superfamily (Ox40L, LIGHT and GITRL), thus allowing for further combinatorial possibilities.

2 - Material and Methods

2.1 - Material

2.1.1 - Instruments and special implements

Instruments

Balances	Feinwaage Basic [Sartorius AG, Göttingen, Germany] 440-39N and 440-33N [Kern, Balingen, Germany]
Blotter	Trans-Blot SD Semi-dry transfer cell [Bio-Rad, Munich, Germany]
Centrifuges	Eppendorf 5804R [Eppendorf, Hamburg, Germany] J2-MC, rotors: JA10, 14, 20 [Beckman Coulter, Krefeld, Germany] Avanti-J301, rotors: JA10, 14, 30.5 [Beckman Coulter, Krefeld, Germany] CR 422 [Jouan, Rennes, France] GR4i [Jouan, Rennes, France]
Electrophoresis system/ Power supply	Mini-PROTEAN®3 Cell Electrophoresis System [Bio-Rad, Munich, Germany] Ready Agarose Precast Gel Electrophoresis System [Bio-Rad, Munich, Germany] Power Pac Basic and HC [Bio-Rad, Munich, Germany]
Film developing machine	Curix60 [Agfa, Cologne, Germany]
Flow cytometer	Cytomics FC 500, argon-ion laser (488 nm) [Beckman Coulter, Krefeld, Germany]
Gel documentation	Transilluminator, Gel documentation system Felix [Biostep, Jahnsdorf, Germany]
Heat block	HBT-1-131 [HLC–Haep Labor Consult, Bovenden, Germany]
HPLC system	Waters HPLC-System [Millipore, Billerica, USA] Chromatography Software Clarify Lite v.2.4.1.65
Incubator for bacteria	Infors HAT Multitron 2 [Infors Ag, Basel, Switzerland]
Incubator for cell culture	NuAire™ US Autoflow Model Nr. 4850-E [Plymouth, UK]
Laminar flow cabinet	Variolab Mobilien W90, [Waldner-Laboreinrichtungen, Wangen, Germany]
Magnetic stirrer	MR 3001K 800W [Heidolph Instruments, Nürnberg, Germany]
Microplate reader	Tecan infinite M200 [Tecan, Crailsheim, Germany]
Microscope	Olympus CKX41SF [Olympus, Tokyo, Japan]
PCR cycler	RoboCycler 96 [Stratagene, La Jolla, USA]
Spectrophotometer	Nanodrop® ND-1000 [pEQLab Biotechnology, Erlangen, Germany] Eppendorf BioPhotometer plus [Eppendorf, Hamburg, Germany]
Vortex mixer	Sky Line [Elmi Ltd., Riga, Latvia]

Special implements

Cryobox	filled with isopropanol for eukaryotic cell freezing [Nalgene, Rochester, USA]
Hemocytometer	Neubauer improved (PlanOprik, Elsoff, Germany)
Dialysis chamber	Slide-A-Lyzer®Dialysis Cassettes: Prod.no 66380, 0.5 – 3 ml Capacity, cut off (MWCO) 10,000 [Thermo Scientific, Rockford, USA]
ELISA plates	MICROLON 96-well high binding capacity [Greiner Bio-One, Frickenhausen, Germany]
FACS tubes	FACS tubes PS, 5ml [Greiner Bio-One, Frickenhausen, Germany]
HPLC columns	BioSep-SEC-S2000 [Phenomenex, Aschaffenburg, Germany] TSK-GEL G3000SW$_{XL}$ [Tosoh Bioscience, Stuttgart, Germany]
IMAC affinity matrix	Ni-NTA-Agarose [Qiagen, Hilden, Germany]
LD columns	[Miltenyi Biotec, Bergisch Gladbach, Germany]
MACS separator	[Miltenyi Biotec, Bergisch Gladbach, Germany]
Microtiter plates	Microtiter plate Cellstar® 96-well (F-, U-, V-bottom) [Greiner Bio-One, Frickenhausen, Germany]
MS columns	[Miltenyi Biotec, Bergisch Gladbach, Germany]
Nitrocellulose membrane	BioTrace NT Pure Nitrocellulose Blotting Membrane [Pall Life Sciences Pensacola, USA]
Gradient gel (SDS-PAGE)	NuPAGE® 4-12 % Bis-Tris Gel [Life technologies, Carlsbad, USA]
Pre-separation filter (30 µm]	[Miltenyi Biotec, Bergisch Gladbach, Germany]
Pasteur pipettes	[Hirschmann Laborgeräte, Eberstadt, Germany]
Plastic pipettes	Costar® [Corning Incorporated, New York, USA]
Polycarbonate filter membrane	Armatis (pore diameter: 50 nm; diameter: 19 mm) Liposofast [Avestin, Ottawa, Canada]
Sterile filter	cut-off 0.2 µm (FP30/0.2 CA-S) and cut-off 0.45 µm (FP30/0.45 CA-S), cellulose acetate, non-pyrogenic [Schleicher & Schuell, Brentford, UK]
Tissue culture flasks and dishes	T_{175} CellStar®, 175 cm^2 [Greiner Bio-One, Kremsmünster, Austria] Nunc®Triple Flasks, 500 cm^2 [Thermo Scientific, Ulm, Germany]
Whatman filter paper	3 mm, 46 x 57 cm Chromatography Paper [GE Healthcare, Munich, Germany]
X-ray film	CEA, RP NEW, Medical X-Ray Screen [CEA AB, Strangnas, Sweden]

2.1.2 - Software, homepages

Clone Manager Professional 7.0	[Scientific & Educational Software, Cary, USA]
FlowJo Version 8.8.6	[Tree star, Ashland, USA]
GraphPad Prism 5	[GraphPad Software, La Jolla, USA]

NCBI BLAST	[http://blast.ncbi.nlm.nih.gov/Blast.cgi]
NCBI PubMed	[http://www.ncbi.nlm.nih.gov/pubmed]

2.1.3 - Chemicals

All chemicals were purchased in p.a. quality by Merck [Darmstadt, Germany], Roche [Basel, Switzerland], Roth [Karlsruhe, Germany], Sigma-Aldrich [Taufkirchen, Germany] or VWR International (Fontenay-sous-Bois, France) unless otherwise stated.

2.1.4 - Solutions, reagents, media and supplements

Solutions and reagents

BD GolgiStop™	Protein transport inhibitor (containing monensin) [BD Biosciences, Heidelberg, Germany]
Blotting buffer	20 % methanol, 192 mM glycine, 25 mM Tris, pH 8.3
Bradford solution	Bio-Rad Protein Assay [Bio-Rad, Munich, Germany]
Coomassie solution	80 mg Coomassie Brilliant Blue (CBB) G-250, (Serva Blau GC. I.42655, Fa. Serva Feinbiochemica, Heidelberg, Germany), in 1l ddH_2O, 35 mM HCl
DNA loading buffer, 5x	1 ml 50x TAE buffer, 2.5 ml glycerol, 0.02 % (w/v) bromophenol blue, ad 10 ml ddH_2O
ECL reagent Solution A	0.1 M Tris, 1.25 mM luminol sodium salt in H_2O, pH 8.6
ECL reagent Solution B	0.11 % (w/v) p-coumaric acid in DMSO
Eosin	0.4 % eosin, 10 % FBS, 0.02 % NaN_3 in PBS
Fekete's solution	580 ml 95% ethanol, 200 ml H_2O, 80 ml 37 % formaldehyde solution, 40 ml glacial acetic acid, ad 1 l
Ficoll	LSM 1077 Lymphocyte Separation Medium [PAA Laboratories, Pasching, Austria]
IMAC Na-phosphate buffer, 5x (low salt)	250 mM Na-phosphate (37.38 g $Na_2HPO_4 \cdot 2H_2O$ + 6.24 g $NaH_2PO_4 \cdot 2H_2O$), 1.25 M NaCl, pH 7.5, ad 1 l H_2O
Lipofectamine™ 2000	Cat.no. 11668-019 [Life technologies™ Gibco, Carlsbad, USA]
Lysis buffer for mammalian cells	100 mM NaH_2PO_4, 10 mM Tris, 8 M urea
MPBS	2 % (w/v) skim milk powder in PBS
MPBST	5 % (w/v) skim milk powder in PBST
MTT	5 g/L MTT in ddH_2O (Thiazol Blue Tetrazolium Bromide, approx. 98 % TLC)
MTT lysis-buffer	15 % SDS (w/v) in Dimethylformamide/H_2O (1:1) with 80 % acetic

	acid, pH 4.5 - 5
PBA	2 % FCS, 0.2% NaN_3 in sterile PBS
PBS	2.67 mM KCl, 1.47 mM KH_2PO_4, 137.93 mM NaCl, 8.06 mM $Na_2HPO_4 \cdot 7H_2O$, pH 7.5
PBST	0.1 % Tween20 in PBS
SDS loading buffer, 5 x	non-reducing: 30 % (v/v) glycerol, 3 % (w/v) SDS, 2 µg/ml bromophenol blue in 62.5 mM Tris-HCl, pH 6.8 reducing loading buffer: 5 % (v/v) β-mercaptoethanol
SDS running buffer, 10 x	1.92 M glycine, 0.25 M Tris, 1 % SDS, pH 8.3
TAE buffer, 50 x	2 M Tris, 0.95 M glacial acetic acid, 50 mM EDTA in H_2O, pH 8
TMB substrate	100 µl TMB (100 mg/ml stock in DMSO), 2 µl 30 % H_2O_2, 10 ml Na-acetate buffer, pH 6 (100mM)

Media and supplements

Bacterial culture

Ampicillin	100 mg/ml [Roth, Karlsruhe, Germany]
LB medium, 1x	1 % peptone, 0.5 % yeast extract, 0.5 % NaCl in H_2O
$LB_{amp, glc}$ agar plates	LB medium, 1.5 % (w/v) agar, autoclave, after cooling-down: 100 µg/ml ampicillin, 1 % (w/v) glucose

Mammalian cell culture

FBS	FBS Standard Quality, EU approved, Cat #A15-101, Lot #A10106-1033 [PAA Laboratories, Pasching, Austria] heat inactivated at 56°C for 30 minutes
Geneticin® (G418)	100 mg/ml in PBS [Life technologies™ Gibco, Carlsbad, USA]]
Opti-MEM I	Reduced serum medium [Life technologies™ Gibco, Carlsbad, USA]
Penicillin/Streptomycin (P/S), 100x	10^4 U/ml / 10^4 µg/ml [Life technologies™ Gibco, Carlsbad, USA]
RPMI 1640	supplemented with L-Glutamine [Life technologies™ Gibco, Carlsbad, USA]
Trypsin/EDTA 10x	0.5 % Trypsin, 5.3 mM EDTA, diluted to 1x in PBS [Life technologies™ Gibco, Carlsbad, USA]
Zeocin™	100 mg/ml [Life technologies™ Invitrogen, Carlsbad, USA]

2.1.5 - Bacterial strain E. coli TG1

Genotype: supE thi-1 Δ(lac-proAB) Δ(mcrB-hsdSM)5 (rK– mK –) [F' traD36 proAB lacIqZΔM15] [Stratagene, La Jolla, USA]

2.1.6 - Cell lines

Cell line	Origin	Stably transfected	Culture	Media [RPMI 1640]	Selection
B16-FAP	Mouse melanoma	Human FAP	Adherent	5 % FCS	Zeocin [200 µg/ml]
HEK293	Human embryonic kidney	/	Adherent	5 % FCS	/
HT1080 wt	Human fibrosarcoma	/	Adherent	5 % FCS	/
HT1080 #33	Human fibrosarcoma	Human FAP	Adherent	5 % FCS	G418 [200 µg/ml]
PBMC	Human buffy coats	/	Non-adherent	10 % FCS	/

2.1.7 - Antibodies

Antibodies	Isotype	Dilution	Company
Human IgG (10 mg/ml)	Human IgG	1:50 (flow cytometry)	Sigma [Saint Louis, USA]
α-CD86-HRP	Mouse IgG1	1:333 (ELISA)	ImmunoTools [Friesoythe, Germany]
His-Probe-HRP [sc-8036 HRP]	/	1:1000 (Western Blot) 1:2000 (ELISA)	Santa Cruz Biotechnology [Santa Cruz USA]
α-huIgG-Fc-HRP	/	1:4000 (ELISA)	Sigma-Aldrich [Taufkirchen, Germany]
α-$(His)_6$-Tag-FITC	Mouse IgG1, κ	1:500 (flow cytometry)	Dianova [Hamburg, Germany]
α-His–PE	Mouse IgG1	1:50 (flow cytometry)	Miltenyi Biotech [Bergisch Gladbach, Germany]
α-huCD3-FITC	Mouse IgG2a	1:20 (flow cytometry)	ImmunoTools [Friesoythe, Germany]
α-huCD3-PE	Mouse IgG1	1:20 (flow cytometry)	ImmunoTools [Friesoythe, Germany]
α-huCD3-PE	Mouse IgG1	1:50 (flow cytometry)	BioLegend [San Diego, USA]
α-huCD3-PerCP	Mouse IgG1, κ	1:50 (flow cytometry)	BioLegend [San Diego, USA]
α-huCD4-PE	Mouse IgG1	1:20 (flow cytometry)	ImmunoTools [Friesoythe, Germany]
α-huCD8-PE	Mouse IgG1, κ	1:50 (flow cytometry)	BioLegend [San Diego, USA]
α-huCD8-PerCP	Mouse IgG1, κ	1:50 (flow cytometry)	BioLegend [San Diego, USA]
α-huCD25-FITC	Mouse IgG1	1:20 (flow cytometry)	ImmunoTools [Friesoythe, Germany]
α-huCD45RO-FITC	Mouse IgG2a	1:20 (flow cytometry)	ImmunoTools [Friesoythe, Germany]

α-huCD45RA-PE	Mouse IgG2b	1:20 (flow cytometry)	ImmunoTools [Friesoythe, Germany]
α-huCD27-PerCP	Mouse IgG1, κ	1:50 (flow cytometry)	BioLegend [San Diego, USA]
α-huCD62L-FITC	Mouse IgG1	1:20 (flow cytometry)	ImmunoTools [Friesoythe, Germany]
α-huFOXP3-Alexa Fluor® 488/CD25-PE/CD4-PerCP antibody cocktail	Mouse IgG1, κ	1:10 (flow cytometry)	One step staining human Treg Flow™ kit [BioLegend; San Diego, USA]
α-huCD279-FITC	Mouse IgG1, κ	1:50 (flow cytometry)	BioLegend [San Diego, USA]
α-huCD152-PE	Mouse IgG1, κ	1:50 (flow cytometry)	BioLegend [San Diego, USA]
α-huGranzyme B-PE	Mouse IgG1	1:20 (flow cytometry)	ImmunoTools [Friesoythe, Germany]
α-huCD107a-FITC	Mouse IgG1	1:50 (flow cytometry)	Santa Cruz Biotechnology [Santa Cruz, USA]
Isotype control IgG1-FITC	/	1:20 (flow cytometry)	ImmunoTools [Friesoythe, Germany]
Isotype control IgG1-PE	/	1:20 (flow cytometry)	ImmunoTools [Friesoythe, Germany]
Isotype control IgG1, κ-PE	/	1:50 (flow cytometry) 1:50 (flow cytometry)	BioLegend [San Diego, USA]
Isotype control IgG1, κ-PerCP	/	1:50 (flow cytometry)	BioLegend [San Diego, USA]
Isotype control IgG2a-FITC	/	1:50 (flow cytometry)	ImmunoTools [Friesoythe, Germany]
Isotype control IgG2b-PE	/	1:50 (flow cytometry)	ImmunoTools [Friesoythe, Germany]
Isotype control IgG1-Alexa Fluor® 488/CD25-PE/CD4-PerCP antibody cocktail	/	1:10 (flow cytometry)	One step staining human Treg Flow™ kit [BioLegend; San Diego, USA]

2.1.8 - Enzymes

Alkaline Phosphatase	1 U/µl, AP Calf Intestinal [Promega, Madison, USA]
DNA Polymerase REDTaq ReadyMix™	0.06 U/µl [Sigma-Aldrich, Taufkirchen, Germany]
PNGase F	1 U/µl, N-Glycosidase F [Roche, Mannheim, Germany]
Restriction enzymes	NotI, SfiI 10 U /µl [Fermentas, Burlington, USA]
Taq DNA-Polymerase	1 U/µl, [Fermentas, Burlington, USA]
T4 DNA ligase	5 U/µl, [Fermentas, Burlington, USA]

2.1.9 - Kits, marker, receptors

Kits

CellTrace™ CFSE Cell Proliferation Kit #11131D	[Life technologies™, Invitrogen, Carlsbad, USA]
DuoSet Human IL-2 # DY202	[R&D Systems, Minneapolis, USA]
DuoSet Human IFN-γ # DY285	[R&D Systems, Minneapolis, USA]
MycoAlert®Mycoplasma Detection Kit	[Lonza Cologne GmbH, Cologne, Germany]
Naïve $CD8^+$ T Cell Isolation Kit human	[Miltenyi Biotec, Bergisch Gladbach, Germany]
NucleoBond® Xtra Midi	[Macherey-Nagel, Düren, Germany]
NucleoSpin® Gel and PCR Clean-up	[Macherey-Nagel, Düren, Germany]
QIAprep® Spin Miniprep Kit	[Qiagen, Hilden, Germany]
REDTaq ReadyMix PCR Reaction Mix (1 U/ml)	[Sigma-Aldrich, St. Louis, USA]
One Step Staining Human T_{reg} Flow™ Kit (FOXP3 Alexa Fluor® 488/CD25 PE/CD4 PerCP) #320121	[BioLegend, San Diego, USA]

Marker

Gene Ruler™ DNA Ladder Mix ready-to- use	[Fermentas, Burlington, USA]
Page Ruler™ Prestained Protein Ladder	[Fermentas, Burlington, USA]
Page Ruler™ Prestained Protein Ladder Plus	[Fermentas, Burlington, USA]
Spectra™ Multicolor Broad Range Protein Ladder	[Fermentas, Burlington, USA]

Recombinant proteins

rhCTLA-4/Fc	recombinant human CTLA-4/Fc chimera #325-CT/CF [R&D Systems, Minneapolis, USA]
rh4-1BB/Fc	recombinant human 4-1BB/Fc chimera #838-4B [R&D Systems, Minneapolis, USA]
rmCD28/Fc	recombinant mouse CD28/Fc chimera #483-CD [R&D Systems, Minneapolis, USA]
rm4-1BB/Fc	recombinant mouse 4-1BB/Fc chimera #937-4B [R&D Systems, Minneapolis, USA]

2.1.10 - Primer

All primers were purchased from Thermo Fisher Scientific [Ulm, Germany]. An overhang within the primer sequence is shown in lowercases, while a restriction site is underlined.

Primer for the generation of scFv36-Ox40L

BamHI-Ox40L-back (42 bp):
5' cgc gga tcc cag GTA TCA CAT CGG TAT CCT CGA ATT CAA AGT 3'

Ox40L-XbaI-for (31 bp):
5' GGT GAA TTC TGT GTC CTT TAA TCT AGA CTAG 3'

Primer for the generation of scFv36-GITRL or scFv36-TNC-GITRL

BamHI-GITRL-back (30 bp):
5' cgc gga tcc CAA TTA GAG ACT GCT AAG GAG 3'

BamHI-TNC-back (30 bp):
5' cgc gga tcc GCC TGT GGC TGT GCG GCT GCC 3'

GITRL-XbaI-for (34 bp):
5' GCA AAT CCC CAA TTC ATC TCC TAA TCT AGA CTAG 3'

Primer for screening or sequencing

pET-Seq1 (Nr. 89) (19 bp):
5' TAA TAC GAC TCA CTA TAG G 3'

pSec-Seq2 (Nr. 91) (18 bp):
5' TAG AAG GCA CAG TCG AGG 3'

2.1.11 - Vectors

pAB1 (3342 bp)	vector for prokaryotic protein expression in E.coli TG1 [derived from pUC19][6]
pSecTagA (5166 bp)	vector for eukaryotic protein expression [from Invitrogen, Carlsbad, USA]
B7.1 GeneArt vector	GeneArt® vector containing the extracellular domain of B7.1 [Life technologies™, Invitrogen, Carlsbad, USA]
ICOSL GeneArt vector	GeneArt® vector containing the extracellular domain of ICOSL [Life technologies™, Invitrogen, Carlsbad, USA]

For vector maps and sequences see appendix.

2.2 - Methods

2.2.1 - Cloning

2.2.1.1 - Cloning strategies for costimulatory antibody-ligand fusion proteins

B7.1-Db36 and ICOSL-Db36

For the generation of B7.1-Db36 and ICOSL-Db36, the B7.2 domain in B7.2-Db36 was replaced by the extracellular domain of either B7.1 (aa 35-242) or ICOSL (aa 19-256). The DNA sequences of the latter were codon-optimized for the expression in HEK293 cells and synthesized by GeneArt® [Life technologiesTM, Invitrogen, Carlsbad, USA]. Therefore, pSecTagAHis B7.2-Db36 and the GeneArt® vectors were cut with SfiI and XhoI.

scFv36-Ox40L, scFv36-GITRL, scFv36-TNC-GITRL

For the generation of scFv36-GITRL and scFv36-TNC-GITRL, the sequences encoding for the extracellular domain of GITRL (aa 72-199) or TNC-GITRL were amplified from GITRL-Flag-TNC-pCR3 (provided from H. Wajant) using the same reverse primer (GITRL-XbaI-for) but different forward primers (BamHI-GITRL-back and BamHI-TNC-back). After restriction digestion with BamHI and XbaI, GITRL or TNC-GITRL were inserted into pSecTagAHis scFv36-1BBL, thereby replacing 4-1BBL.

ScFv36-Ox40L (extracellular domain of Ox40L: aa 51-183) was cloned analogous to scFv36-(TNC-)GITRL using the primer pair BamHI-Ox40L-back and Ox40L-XbaI-for.

scFvA5-Ox40L, scFvA5-LIGHT, scFvA5-TNC-GITRL

For the generation of scFvA5-Ox40L and scFvA5-LIGHT in pSecTagAHis, the scFv36 antibody moiety was replaced by scFvA5 via SfiI and NotI. For the generation of pSecTagAHis scFvA5-TNC-GITRL, the scFv36 moiety in pSecTagAHis scFv36-TNC-GITRL was replaced by scFvA5 via SfiI and NotI as well, but since NotI also has a restriction site between the TNC and the GITRL domain, a 3 fragment ligation had to be performed (GITRL backbone vector, TNC-domain and scFvA5 insert).

2.2.1.2 - Polymerase chain reaction (PCR)

Polymerase chain reaction was used for the amplification of DNA fragments and for the introduction of restriction sites for subsequent cloning.

PCR reaction mix:

Template DNA	10 ng
Taq DNA Polymerase (1 U/µl)	1.25 µl
Primer (each 10 pmol/µl)	1 µl
Desoxyribonucleotides (each dNTP 50 mM, 200 mM total)	2.5 µl
Taq buffer 10x (+$(NH_4)_2SO_4$)	5 µl
$MgCl_2$ (25 mM)	4 µl
ddH_2O	ad 50 µl

The following PCR program was used for amplification, with varying elongation times (1 min per kb, according to the size of the expected DNA fragment) and annealing temperatures (according to the melting temperatures of the respective primers):

	pre-cycle	denaturation	annealing	elongation	post-cycle
duration [min]	5	1	1	1-2.5	5
temperature [°C]	94	94	50-55	72	72
cycles [#]	1	30			1

2.2.1.3 - Agarose gel electrophoresis and DNA gel extraction

Analysis and purification of DNA fragments (PCR products or digested DNA) was performed using horizontal agarose gel electrophoresis. Therefore, DNA samples, mixed with DNA loading buffer, were separated on a 1 % agarose gel containing 1 µg/ml ethidium bromide in TAE buffer (80 V, 45 min). Relevant DNA bands were excised under UV light and purified via the NucleoSpin® Gel and PCR Clean-up kit according to the manufacturers instructions. DNA was eluted from the column using 30 µl H_2O.

2.2.1.4 - Restriction digestion

For the digestion of DNA, either 10 µg vector DNA or the total amount of DNA extracted from an agarose gel (2.2.1.3) were applied. Depending on the respective restriction enzymes, the

corresponding buffer and conditions (incubation time, temperature) had to be chosen according to the manufacturers instructions. If buffer exchange was required, DNA was isolated previously via a kit [NucleoSpin® Gel and PCR Clean-up]. After the restriction digestion, vector and insert fragments were separated by agarose gel electrophoresis and isolated as indicated in 2.2.1.3.

DNA	10 µg (plasmid) or DNA extracted from agarose gel
10x buffer	5 µl
Restriction enzyme	20 U
ddH_2O	ad 50 µl

In order to avoid religation, vector DNA was dephosphorylated after the digestion. Therefore, 1 U Shrimp Alkaline Phosphatase (SAP) was added for 1 h at 37°C.

2.2.1.5 - Ligation

Ligation of linearized, dephosphorylated vector and insert was carried out at a molar ratio of 1:3 to 1:5 for 1 h at RT. As controls, a preparation with the vector alone and a preparation without vector and insert were included.

Vector DNA	x µl (100 ng)
Insert DNA	x µl
T 4 DNA ligase buffer (10x)	2 µl
T4 DNA ligase	5 U
ddH_20	ad 20 µl

2.2.1.6 - Preparation of chemical competent E.coli TG1 cells

For the preparation of chemical competent E.coli TG1 cells, 50 ml LB medium supplemented with 1 % glucose were inoculated with 1 ml of an o/n culture of TG1 cells. Bacterial culture was grown to an OD_{600} of 0.5 - 0.6 at 37°C before cells were chilled on ice for 15 min and were harvested by centrifugation (2500 x g, 5 min, 4°C). The pellet was resuspended in 50 ml ice-cold $CaCl_2$ (100 mM) and incubated on ice for 30 min before centrifugation. Cells were resuspended in 10 ml pre-chilled $CaCl_2$ (50 mM) and 20 % glycerol, aliquoted and were frozen at -80°C until transformation.

For the determination of the transformation efficiency, which was defined as “colony forming units” / µg DNA, a defined amount of plasmid DNA (10ng) was transformed into 100 µl competent cells.

2.2.1.7 - Transformation of E. coli TG1

For the transformation of the ligation product into E.coli cells, 100 µl of chemical competent TG1 cells were thawed on ice, mixed with 10 µl ligation and were chilled for 15 min. After a heat shock (water bath, 42°C, 2 min), cells were chilled again for 1 min followed by the addition of 1 ml LB medium. Cells were incubated for 1 h at 37°C (shaker) before they were harvested (15,700 g, 1 min), plated on $LB_{Amp, Glc}$ plates and incubated o/n at 37°C.

2.2.1.8 - Screening of colonies

To analyze whether the vector containing the respective insert was taken up by the chemical competent TG1 cells, a PCR screening of colonies from the $LB_{Amp, Glc}$ plate was performed using the REDTaq ReadyMix. Therefore, colonies were “picked” with the tip of a pipette and were both applied to a PCR tube and additionally plated on a master plate o/n (37°C). For the PCR, primer were chosen for the amplification of a sequence within the insert. The PCR product was analyzed on an agarose gel and positive clones were identified via their correct size. Plasmid DNA was prepared as indicated in 2.2.1.9 and the identity was confirmed by control digestion with appropriate restriction enzymes. In order to revise correctness of the DNA sequence and to exclude mutations, plasmid DNA was sequenced (GATC Biotech AG, Constance, Germany). For sequence analysis and alignments, the Clone Manager program and the Blast algorithm were applied.

2.2.1.9 - Plasmid DNA isolation (Midi, Mini)

For plasmid DNA isolation, a Midi (NucleoBond® Xtra Midi) or a Mini (QIAprep® Spin Miniprep) kit was used according to the manufacturers instructions. As starting material, an o/n culture (LB medium supplemented with 1 % glucose and 100 µg/ml ampicillin) was used (Midi: 100 ml, Mini: 5 ml). The latter was centrifuged (4967 g, 15 min, 4°C, J2-MC, rotor JA14) in order to harvest the cells for the isolation procedure. After the isolation, DNA was air dried and the pellet was dissolved in ddH_2O (MIDI: 100 µl, MINI: 30 µl) and stored at -20°C.

2.2.1.10 - Photometric determination of DNA concentration

The absorbance was measured at 260 nm (OD_{260}) and the DNA concentration (c) was calculated according to the following formula:

c_{DNA} [µg/µl] = OD_{260} · dilution factor · 0.05

2.2.2 - Mammalian cell culture techniques

2.2.2.1 - Cell cultivation

Cultivation of mammalian cells was performed in a humidified incubator (60 % rel. humidity) at 37°C with 5 % CO_2 atmosphere. Adherent cells were cultivated in tissue culture flasks filled with 20 ml of the respective culture medium and were split every 2-3 days. For detachment Trypsin/EDTA was used. For the quantification of viable cells, an hemacytometer and eosin staining was used. For storage, cells from 80 % confluent tissue culture flasks were resuspended in 90 % FBS + 10 % DMSO, aliquoted into cryovials and were gradually frozen to -80°C in a cryobox filled with isopropanol. For long term storage, cells were stored in liquid nitrogen (-196°C). In order to thaw cells, a cryovial was quickly incubated in a water bath (37°C) before the addition of 5 ml culture medium. After centrifugation (5 min, 616 g), cells were resuspended in culture medium and transferred to a cell culture flask.

2.2.2.2 - Transfection (transient, stable)

Transient transfection

In order to test the expression of recently cloned constructs in HEK293 cells, they were first of all transfected transiently. Therefore, $1 \cdot 10^6$ cells per well were seeded in a 6-well plate and incubated o/n. The next day, supernatant was discarded and 1.33 ml Opti-MEM were added. In parallel, 166 µl Opti-MEM were incubated with either 6.66 µl Lipofectamine (preparation A), or 2.66 µg plasmid DNA (preparation B) for 5 min before the two preparations were gently mixed. After 20 min of incubation at RT, the transfection mix was added to the HEK293 cells and the 6-well plate was stored o/n in the incubator. The next morning, medium was replaced by fresh Opti-MEM (supplemented with P/S), and supernatant was collected after 3 days in order to analyze protein expression via Western blot.

Stable transfection

Transfection was performed as indicated above. Medium was not changed until 24 h post transfection, when HEK293 cells were carefully detached from the 6-well (without Trypsin/EDTA) and transferred to a cell culture flask in 10 ml RPMI + 5 % FCS. For selection of stable transfectants, 300 µg/ml zeocin was added. Medium supplemented with zeocin was exchanged 1-2 times a week until zeocin resistant colonies started to appear after 3-5 weeks. In order to achieve a confluent cell layer, colonies were carefully detached and resuspended. When cells achieved 80 % confluence, one half of the cells were cryopreserved and the other half was expanded for protein production (2.2.3.1). Here, zeocin concentration was lowered to 50 µg/ml.

2.2.2.3 - Isolation of human Peripheral Blood Mononuclear Cells (PBMC)

Starting material for the isolation of human PBMC were buffy coats from healthy anonymous donors provided by a hospital (Katharinenhospital, Stuttgart, Germany). Buffy coats are a leukocyte concentrate that results as a byproduct during the manufacturing of red cell and platelet concentrate from a whole blood donation. The leukocyte concentrate was stored at RT and the isolation procedure was performed at RT as well.

The buffy coat (approx. 80 ml), was diluted in RPMI medium to a total volume of 240 ml. 10 ml Ficoll was carefully overlaid with 30 ml buffy coat dilution followed by a centrifugation step in order to separate erythrocytes and granulocytes from PBMC (796 g, 20 min, RT, without brake). Afterwards, the interphase (containing the PBMC) was collected and transferred to a new tube. Cells were diluted in RPMI to a total volume of 40 ml, followed by a second centrifugation step (644 g, 15 min, with brake). Supernatant was discarded and cells were resuspended in 40 ml RPMI and centrifuged at 199 g (10 min, with brake) in order to remove residual platelets. In the last step, PBMC were pooled and absolute cell number was determined (approximately 1.8-3.6·10^8). PBMC were either frozen at 10-20·10^6 cells per vial (according to the freezing conditions described in 2.2.2.1, using pre-chilled reagents) until their usage or incubated at a density of 10-15 ·10^6 cells per Ø 10 cm culture dish o/n at 37°C.

2.2.2.4 - Protein production in HEK293 cells

For eukaryotic protein production, stable transfected HEK293 cells were expanded in T_{175} or Triple flasks (500 cm^2). At 90 % cell confluency, RPMI medium was replaced by Opti-MEM + P/S (25 ml per T_{175}, 100 ml per triple flask) and supernatant collected twice a week until cells started to detach (2-6 weeks). The collected supernatant was immediately centrifuged in order to remove residual cells and was then stored at 4°C until protein purification.

2.2.2.5 - Isolation of naïve $CD8^+$ T cells

The isolation of naïve $CD8^+$ T cells was performed in a two-step procedure according to the manufacturers instructions [Naïve $CD8^+$ T Cell Isolation Kit human, Miltenyi Biotec, Bergisch Gladbach, Germany]. As starting material, fresh PBMC were used, which were isolated from buffy coat the day before (2.2.2.3). Since the percentage of naïve $CD8^+$ T cells within the overall PBMC population is approx. 5 % (personal communication with Miltenyi Biotec, Bergisch Gladbach, Germany), high amounts of PBMC from one buffy coat ($1.5\text{-}3 \cdot 10^8$) were applied for the isolation. Naïve $CD8^+$ T cells were obtained with a purity of 89 – 95 % and an average yield of approx. 60 %.

2.2.3 - Protein production and purification

2.2.3.1 - Ammonium sulphate precipitation of proteins

In order to precipitate proteins from cell culture supernatants, ammonium sulfate was slowly applied up to a saturation of 60 % (390 g/l, 4°C, under stirring). After further 30 min of stirring, the solution was centrifuged (12,613 g, 30 min, 4°C, J2-MC, rotor JA14) and the pellet was resuspended in 10 ml PBS.

2.2.3.2 - Protein purification by Immobilized Metal Affinity Chromatography (IMAC)

Since the entire collection of antibodies described in this work contains a His-tag, they could all be purified via IMAC, using immobilized Ni^{2+}-nitrilo-triacetic acid (Ni-NTA) agarose beads.

Semi-batch purification

1 ml Ni-NTA agarose beads were equilibrated with PBS (3-fold washing step with 1 ml PBS) before they were applied to the resuspended protein pellet (2.2.3.1) and incubated o/n under rotation (4°C). The next day, the protein-Ni-NTA suspension was filled into a column and flow through was collected and unbound proteins were washed away with 10-20 ml IMAC washing buffer. Elution of bound proteins was performed with IMAC elution buffer in 4-6 500 µl fractions. The washing and elution procedure was thereby monitored via a qualitative Bradford assay (10 µl of eluate were applied to 90 µl of 1x Bradford reagent), with a blue color indicating the presence of protein. Elution factions with similar protein content were pooled and dialyzed against 2 l PBS o/n (4°C). Finally, purified proteins were filtered sterile and the concentration was photometrically determined.

2.2.3.3 - Photometric determination of protein concentration

Protein concentration (c) was determined photometrically by measuring the absorbance at 280 nm (OD_{280}) using the Nanodrop [pEQLab Biotechnology, Erlangen, Germany]:

$$c[mg/ml] = M[mol/l] \cdot M_m[g/mol] = \frac{OD_{280}}{\epsilon} \cdot M_m$$

$$\epsilon = (number_{Trp} \cdot 5540) + (number_{Tyr} \cdot 1480)$$

(M: molarity, Mm: molecular mass, ε: molar extinction coefficient, Trp: tryptophan, Tyr: tyrosin)

2.2.4 - Biochemical characterization

2.2.4.1 - SDS-PAGE and Western Blot analysis

SDS-Polyacrylamide Gel Electrophoresis (SDS-PAGE)

Protein samples (2-3 µg) were mixed with reducing SDS loading buffer and were denaturated (95°C, 5 min). Polyacrylamide (PAA) gels were run at 40 mA/gel for approx. 1 h and were then heated 3 times in ddH_2O (microwave, 800 W, 1 min). For staining, the gel was heated in Coomassie and was then incubated for 2-24 h under shaking (RT). For destaining of the background color, the gel was repeatedly heated in ddH_2O and was incubated o/n under shaking.

	Running gel (12 %)	Stacking gel (5 %)
ddH_2O	4.9 ml	4.1 ml
30 % acrylamide mix	6 ml	1 ml
1.5 M Tris, pH 8.8	3.8 ml	-
1.0 M Tris, pH 6.8	-	750 µl
10 % SDS	150 µl	60 µl
10 % APS	150 µl	60 µl
TEMED	6 µl	6 µl

Western Blot

In order to confirm the identities of the purified proteins, Western Blot analysis was performed: Therefore, the proteins separated on the PAA gel were blotted onto a nitrocellulose membrane (110 mA, 12 V constant, 45 min) in a semidry procedure according to the manufacturers instructions [Bio-Rad Laboratories GmbH, Munich, Germany].

After the protein transfer, the membrane was blocked in MPBST for 1 h (shaker, RT) before incubation with an HRP-conjugated anti-His-tag antibody (1:1000 dilution in MPBST, o/n, 4°C). The next day, the blot was washed (3 times with PBST, 1-fold with PBS) before it was developed. After a 2 minutes incubation step with ECL substrate solution in the dark (5 ml Solution A + 500 µl Solution B + 1.5 µl H_2O_2 (30 %)), the blot was exposed to a light-sensitive film (approx. 2 minutes). The latter was then developed in a film processor (Curix 60, Agfa).

2.2.4.2 - Deglycosylation of proteins

5 µg of protein were boiled (95°C, 5 min) before addition of 1.5 U PNGase F (N-Glycosidase F) in a total volume of 25 µl (PBS). Protein deglycosylation was performed at 37°C o/n and was visualized by SDS-PAGE analysis.

2.2.4.3 - Size Exclusion chromatography by High Performance Liquid Chromatography (HPLC)

Analytical gel filtration was performed to determine the oligomerization state of the recombinant proteins under native conditions. Therefore, 25-30 µl of a protein sample (0.2 – 1 mg/ml) were loaded on a HPLC column (either BioSep-SEC-S2000 at a flow rate of 0.5 ml/min or TSK-GEL G3000SWXL) with PBS as mobile phase. As standard proteins, thyroglobulin (670 kDa),

β-Amylase (200 kDa), gamma globulin (158 kDa), bovine serum albumin (67 kDa), ovalbumin (44 kDa), carbonic anhydrase (29 kDa), myoglobin (17 kDa) and vitamin B-12 (1.4 kDa) were used. The sizes of the recombinant proteins were obtained by interpolation of the standard curve fit (retention times vs. molecular masses) in GraphPad Prism.

2.2.4.4 - Binding analysis

Tumor antigen-specific binding of the recombinant antibodies was analyzed via flow cytometry. Therefore, $0.5 \cdot 10^6$ target cells/well were incubated with the respective recombinant antibody (scDb33CD3, B7.2-DbFAP, scFvA5-4-1BBL, scDb33211, B7.1-Db36 and scFvmE12-m4-1BBL: 10 µg/ml; scFv36-GITRL, -TNC-GITRL, -LIGHT, scFvA5-Ox40L, -TNC-GITRL and -LIGHT: 300 nM; B7.1-Db36, ICOSL-Db36: 100-0.1 nM, 3-fold serial dilution) in 100 µl PBA in a 96-well plate (V-shaped bottom) (2h, 4°C). Subsequently, cells were washed 3 times with PBA (150 µl, 616 g, 5 min, RT) before addition of a directly-labeled His-tag specific detection antibody (α-His-FITC (1:500) or α-His-PE (1:50 dilution), 2 h, 4°C). After a 3-fold washing step, cells were resuspended in 500 µl PBA, transferred to FACS tubes and analyzed via flow cytometer. Obtained data were analyzed using the program FlowJo Version 8.8.6.

2.2.4.5 - Enzyme Linked Immunosorbent Assay (ELISA)

The ligand-receptor binding ability of the costimulatory antibody-ligand fusion proteins was determined via ELISA. Therefore, recombinant antibodies (B7.1-Db36: 180-2.1 nM, 3-fold serial dilution; scFvmE12-m4-1BBL: 300-0.3 nM, 3-fold serial dilution; scFvA5-h4-1BBL: 100 nM) were titrated on a ELISA plate (in PBS, 100 µl/well) and coated o/n at 4°C. The next day, remaining binding sites were blocked with 400 µl MPBS (2 h, RT) followed by a washing step (3-fold with PBST, 1-fold with PBS). Subsequently, the respective recombinant receptor/Fc fusion proteins were applied (diluted in MPBS, 100 µg/ml, 100 µl/well) and incubated for 1 h at RT. As a blank, coated wells with the detection antibody in the absence of the recombinant receptor/Fc fusion protein were used. After a washing step, 100 µl/well HRP-conjugated anti-h Fc-specific detection antibody was added (1:1000 dilution in MPBS), incubated for 1 h at RT and was then washed away. For the development of the ELISA, 100 µl/well TMB substrate solution was applied. The color reaction was stopped by 50 µl/well H_2SO_4 and absorption at 450 nm was determined in a Tecan reader.

2.2.5 - Functional studies (in vitro)

2.2.5.1 - Setting for the cell-based assays

Isochronic combinatorial setting

The costimulatory potential of the antibody-ligand fusion proteins was analyzed in terms of T cell activation, proliferation, differentiation and cytotoxicity by coculturing target cells with human PBMC or isolated naïve $CD8^+$ T cells. For all assays, RPMI medium supplemented with 10 % FCS was used. Target cells (HT1080 #33) were seeded at a density of $2 \cdot 10^4$ cells per well in 96-well F-bottom plates. PBMC were thawed and cultivated o/n at a density of $10\text{-}15 \cdot 10^6$ cells in Ø 10 cm cell culture dishes to allow adherence of monocytes. For enhanced removal of monocytes, PBMC could also be transferred to a fresh cell culture dish after 2 hours. The next day, target cell supernatant was discarded and 50 µl of medium was applied, followed by 100 µl of the respective recombinant proteins. The latter were prediluted previously in a 96-well plate (V-bottom). For the calculation of the concentrations, the molecular mass of the multimers was used instead of the monomers (e.g.: scFvA5-4-1BBL: trimer, B7.2-Db36: dimer) and the control antibodies were adjusted accordingly (e.g. 3-fold concentration of scFvA5 in the case of scFvA5-4-1BBL). The plate was incubated for 1 hour at RT to ensure antigen-binding to the target cells before addition of $2 \cdot 10^5$ PBMC per well (total volume per well: 200 µl). The assay was incubated up to 7 days depending on the readout, respectively, and on day 3 and 5 50 µl fresh media was applied to each well in order to compensate for vaporization as well as nutrient consumption. As readouts, cytokine release and proliferation were chosen. For the latter, the dye combinations FITC, PE, PerCP or CFSE, PE, PerCP were used.

Time-shift combinatorial setting

Target cells (HT1080 #33) were seeded at a density of $2 \cdot 10^4$ cells per well in 96-well F-bottom plates. The next day, cells were incubated with scDb (33 pM) for 1 h, before washing (2-fold with 150 µl medium) and the addition of PBMC ($2 \cdot 10^5$/well). After 3 days of coculture, stimulated PBMC were transferred to a 96-well plate (V-shaped bottom) and washed (3 times with 150 µl medium) before they were restimulated on a fresh plate of HT1080 #33 previously incubated with scDb as indicated above. Costimulation was provided by the incubation with B7.1-Db (10 nM) and scFv-4-1BBL (10 nM) for 1 h before the addition of PBMC. Therefore, they

were added together either in combination with scDb-mediated initial or final stimulation. Alternatively, B7.1-Db was administered together with scDb on day 0, followed by the administration of scFv-4-1BBL together with scDb on day 3. PBMC, which were only stimulated on day 0 without restimulation on day 3, were washed and transferred to a fresh plate of target cells on day 3 where they were incubated in the absence of antibody-ligand fusion proteins for 4 additional days. On day 7, PBMC were harvested and T cell proliferation and expression of granzyme B, CTLA-4 and PD-1 was analyzed by flow cytometry. Block shift correction was applied to the data.

2.2.5.2 - Cytokine release

Concentrations of IL-2 and IFN-γ were determined by sandwich ELISA (kit IL-2: DuoSet Human IL-2 # DY202, kit IFN-γ: DuoSet Human IFN-γ # DY285, R&D Systems, Minneapolis, USA) according to the manufacturers instructions. Cell-free supernatant was collected after 48 h and stored at -20°C. For the ELISA, supernatant was diluted 3-5-fold (IL-2) or 30-100-fold (IFN-γ).

Blocking with recombinant receptor

In order to revise that the costimulatory effect of the antibody-ligand fusion proteins was due to its ligand part, the ligand-receptor interaction was blocked by incubation with 5-fold excess of the corresponding recombinant receptor-Fc (CTLA-4-Fc/ 4-1BB-Fc). Therefore, target cells were incubated for 1 hour with the scDb and antibody-ligand fusion proteins, followed by an incubation step with the recombinant receptor-Fc proteins (1 h) before addition of PBMC. After 48 h, cytokine release levels (IL-2, IFN-γ) were determined.

2.2.5.3 - Proliferation

For the analysis of T cell divisions in response to stimulation, PBMC were CFSE-labeled prior to their use in the assay. Therefore, PBMC were resuspended in prewarmed PBS supplemented with 0.1 % BSA at a concentration of $1 \cdot 10^6$ cells/mL before addition of CFSE (working concentration: 625 nM, stock solution: 5 mM in DMSO). After 10 minutes incubation (37°C), staining was quenched by the 2-fold volume of ice-cold culture medium without FBS (5 min, chilled), followed by a 3-fold washing step with prewarmed medium. Finally, absolute cell numbers were determined and PBMC were applied to the target cells previously incubated with

the respective antibody constructs. After 7 days, cells in the supernatant were collected and transferred to a V-bottom 96-well plate. After a centrifugation step, PBMC were resuspended in PBA and transferred to FACS tubes for analysis. In order to analyze proliferation of T cells or T cell subsets, additional staining was performed: Therefore, to avoid unspecific antibody binding, cells were preincubated with human IgG (100 pM) for 10 min at 4°C, followed by the respective fluorochrome-conjugated antibodies (α-CD3-PerCP, α-CD8-PE/α-CD4-PE; 45 min, 4°C). Cells were washed three times with PBA before analysis in the flow cytometer. For evaluation, the percentage of proliferating T cells or its $CD4^+/CD8^+$ subpopulations was determined.

2.2.5.4 - Analysis of differentiation and cell surface marker expression

T cells were also analyzed for subsequent changes in subpopulations after 7 days of stimulation. For the analysis of memory, naïve and regulatory T cells as well as the surface expression of CD25, CTLA-4 and PD-1 PBMC were used as effector cells. In order to analyze differentiation into central memory or effector memory T cells, naïve $CD8^+$ T cells were chosen.

Analyzed T cell population/cell surface marker	fluorochrome-conjugated antibodies
Activated ($CD4^+/CD8^+$) T cells	α-CD3-PerCP, α-CD4-PE, α-CD25-FITC α-CD3-PerCP, α-CD8-PE, α-CD25-FITC
Memory/naïve T cells	α-CD3-PerCP, α-CD45RA-PE, α-CD45RO-FITC
Central memory (T_{CM})/ effector memory (T_{EM}) T cells	α-CD27-PerCP, α-CD45RA-PE, α-CD62L-FITC
CTLA-4^+ ($CD8^+/CD8^-$) T cells	α-CD3-FITC, α-CD8-PerCP, α-CTLA-4-PE
PD-1^+ ($CD8^+/CD8^-$) T cells	α-CD3-PerCP, α-CD8-PE, α-PD-1-FITC
Regulatory T cells (T_{regs})	α-hFoxP3-AlexaFluor® 488, α-CD25-PE, α-CD4-PerCP

Regulatory T cells

T_{regs} were identified after 7 days by the markers CD4, CD25 and Foxp3, using the antibodies provided by the One Step Staining Human Treg FlowTM Kit (BioLegend, San Diego, USA). In brief, cells were fixed and permeabilized according to the manufacturers instructions (the procedure was adjusted to a 96-well plate (V-bottom) with a total volume of 150 µl). After a washing step (150 µl PBA/well), anti-hFoxP3-Alexa Fluor® 488/CD25-PE/CD4-PerCP antibody cocktail was applied (10 µl/well) for 1 h at 4°C.

2.2.5.5 - Granzyme B

Expression of granzyme B (GrB) was analyzed after 7 days. Therefore, cells were fixed and permeabilized in analogy to the regulatory T cells using the same kit (2.2.5.4). For subsequent staining, cells were incubated with anti-CD3-FITC, anti-CD8-PerCP and anti-GrB-PE for 1 h at 4°C.

2.2.5.6 - CD107a

Freshly isolated naïve $CD8^+$ T cells were prestimulated according to the setting described for PBMC (2.2.5.1, Isochronic combinatorial setting) with titrating scDb (32-2 pM) in the presence or absence of costimulatory antibody-ligand fusion proteins (10 nM). After 7 days, T cells were collected, washed twice with medium and triggered for degranulation: Therefore, T cells, resuspended in 100 µl medium in the presence of 1.4 µl monensin and 5 µl α-CD107a-FITC, were applied to a fresh plate with HT1080 #33 cells (seeded the day before, $2 \cdot 10^5$/well), previously incubated with 1 nM scDb (1 h, 3-fold washing step). After 6 h, T cells were transferred to a 96-well plate (V-shaped bottom), centrifuged and were resuspended in PBA for staining with α-CD3-PE (1 h, 4°C) before analysis of T cell degranulation via flow cytometry.

2.2.5.7 - Target cell killing assays (MTT)

The cytotoxic potential of prestimulated T cells was assessed in terms of target cell killing. To ensure sufficient cell numbers for restimulation, prestimulation was carried out in a 6-well plate (conversion factor 96- to 6-well: 1:32). Therefore, target cells (HT1080 #33 seeded at a density of $6.4 \cdot 10^5$ cells per 6-well the previous day) were incubated with either scDb (16 or 20 pM) alone or in combination with the respective costimulatory antibody-ligand fusion protein (10 nM) for 1 h before addition of $6.4 \cdot 10^6$ PBMC. After 7 days, PBMC were collected, washed twice with medium and absolute cell numbers were determined. Subsequently, PBMC were transferred to a fresh 96-well plate of target cells ($2 \cdot 10^4$ cells/well) which had been seeded the day before. PBMC were added at an E : T ratio of either 12:1 ($1.2 \cdot 10^5$ PBMC : $1 \cdot 10^4$ HT1080 #33) or 5:1 ($1 \cdot 10^5$ PBMC : $2 \cdot 10^4$ HT1080 #33). Retargeting of T cells to tumor cells was achieved by titrating scDb (12-0.05 pM, 3-fold serial dilution or 20-0.63 pM, 2-fold serial dilution) and incubation for 6 h. Next, PBMC were thoroughly removed. The plate was washed 3 times with

150 µl medium/well before addition of 100 µl medium and 10 µl MTT were added per well and the plate was incubated on a shaker for 2 h at 37°C) before the addition of 100 µl MTT lysis buffer. Cells were lysed o/n at RT and the released formazan was quantified via photometric measurement (595 nm, reference wavelength: 660 nm, Tecan reader). For the analysis of the data, OD values were normalized. Here, target cells without PBMC were defined as 100 % living cells, while medium without target cells was 0 % of living cells.

2.2.5.8 - Block shift correction

In order to compensate for the daily variability of both effector and target cells in assays, a block shift correction was performed on the basis of the following formula:

$$X'_n = X_n - (Y_n - \overline{Y})$$

(X'_n is the corrected value of X from the experiment n, Y is the average of the X values from all experiments performed and Y_n is the average of the duplicate values of X from experiment n.)

2.2.5.9 - Ligand activity in soluble and cross-linked form

The costimulatory activity of the antibody-ligand fusion proteins in coated or soluble form was analyzed in a target cell-free assay. Therefore, ELISA plates were coated with scDb33CD3 (1, 3, 10 nM) +/- 50 nM antibody-ligand fusion protein o/n at 4°C. The next day, after blocking with FBS (100 µl/well, 2h, RT) CFSE-labeled PBMC ($2 \cdot 10^5$ cells/well) +/- 50 nM antibody-ligand fusion protein were added. Proliferation was measured after 4 days via flow cytometry.

2.2.6 - Functional studies (in vivo)

All experimental animal studies complied with federal guidelines and were conducted according to protocols approved by the university and state authorities.

2.2.6.1 - Pharmacokinetic studies

Groups of 3 to 4 female C57BL/6JRj mice received intravenous injections of 100 µl 0.5 nmol antibody-ligand fusion protein (B7.2-Db36 or scFvmE12-m4-1BBL) per mouse. Blood samples were taken at different time intervals (3, 30, 60 min, 2, 6 and 24 h) from the tail. Mice were sacrificed by exposure to carbon dioxide after collection of the last blood sample. After

incubation of the blood samples on ice (1 h), clotted blood was centrifuged at 10,000 x g for 10 min at 4 °C. Serum samples were stored at -20°C until serum concentration of the fusion proteins was determined via ELISA (for a general ELISA procedure description, see 2.2.4.5).

For the quantification of scFvmE12-m4-1BBL, mEDG (3 µg/mL) and for B7.2-Db36 an α-B7.2 antibody (3 µg/mL) was coated o/n (4°C). After blocking with MPBS, serum samples were applied in 2 different dilutions (1:20 and 1:100 in MPBS), while for a standard curve, purified fusion protein was titrated (serial 1:4 dilution, 9 steps, starting from 100 nM). Bound protein was detected via HRP-conjugated His-tag–specific antibody. Subsequently, the serum concentration of the respective fusion protein was determined by interpolating the corresponding standard curve. Furthermore, in order to enable a comparative analysis between the pharmacokinetics of both fusion proteins, the data were normalized by setting the 3 min value to 100 %. Pharmacokinetic parameters were calculated via Microsoft Office Excel: for the initial half-life ($t_{1/2}\alpha$), the first 3 time points and for the terminal half-life ($t_{1/2}\beta$) the last 3 time points were used, while the area under the curve (AUC) was determined for the overall time interval up to 24 hours.

2.2.6.2 - B16-FAP lung metastasis model

Treatment with scDb332C11 in combination with 2 costimulatory settings

Groups of 6 female C57BL/6JRj mice (3 month) were injected i.v. with $0.85 \cdot 10^6$ B16-FAP cells/animal. Treatment was applied i.p. on day 1,2,3 and day 10, 11 and 12 with either scDb alone (4 nM or 0.4 nM) or in combination with consecutive costimulation (day 1, 2, 3: B7.1-Db36 (0.2 nM), day 10, 11, 12: scFvmE12-m4-1BBL (0.2 nM)) or late simultaneous costimulation (day 1, 2, 3: PBS, day 10, 11, 12: B7.1-Db36 (0.2 nM) + scFvmE12-m4-1BBL (0.2 nM)). As control groups, mice were treated according to the 2 costimulatory settings in the absence of scDb. On day 21, mice were sacrificed and lungs were removed, fixed in formaldehyde and metastases counted.

3 - Results

3.1 - Combination of a bispecific antibody with B7- and 4-1BBL-antibody fusion proteins

3.1.1 - The combinatorial setting

In this work, a combinatorial setting consisting of two costimulatory antibody-ligand fusion proteins in the presence of a bispecific antibody was established. The target cell line HT1080 #33 coexpresses the two antigens FAP and EDG. The bispecific antibody (scDb33CD3) activates and retargets T cells by simultaneously binding to FAP (mo33) on the target cell and to CD3 on the T cell. Stimulation of T cells is further supported by two antibody-ligand fusion proteins, which present their ligands to the corresponding costimulatory receptors on the retargeted T cell by binding to their respective antigen on the target cell. Here, the fusion proteins B7.2-DbFAP (homodimer) and scFvEDG-4-1BBL (homotrimer) were chosen each of which had previously been shown to be suitable for the combination with scDb33CD3, resulting in an enhancement of the scDb-mediated signal[88,89]. In detail, B7.2-DbFAP consists of the extracellular domain of B7.2 fused to a diabody moiety directed against FAP (mo36), while the scFvEDG-4-1BBL fusion protein is comprised of a scFv targeting EDG (A5) which is fused to the extracellular domain of 4-1BBL. Hence, the following model system was applied (Fig. 6). Here, B7.2-Db36 and scDb both target FAP, although their antibody moieties are different, recognizing close or partially overlapping epitopes (mo33 and mo36[112]). To allow optimal ligand presentation, scFvA5-4-1BBL binds to the second antigen, EDG. For the analysis of the combinatorial approach, the activation (cytokine release, proliferation, activation marker expression) and the cytotoxic potential of T cells (target cell lysis, expression of cytotoxicity markers) as well as T cell differentiation (generation of effector/memory phenotype) was monitored.

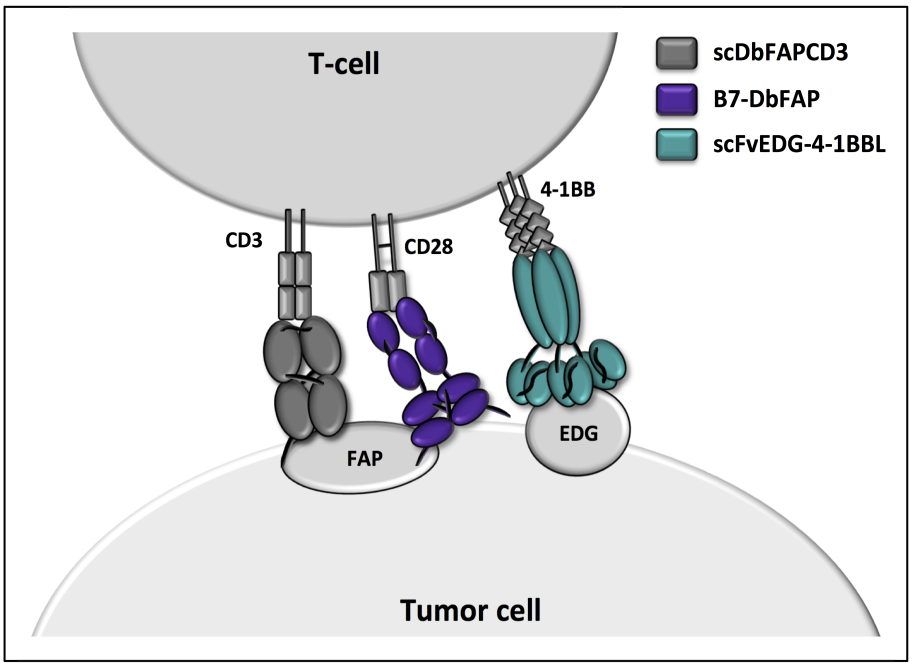

Fig. 6: Concept of the combinatorial model system. The bispecific antibody in the scDb format (scDbFAPCD3) retargets T cells to tumor cells by simultaneous binding to fibroblast activation protein (FAP) on the tumor cell and CD3 on the effector cell. Stimulation of T cells is further supported by the antibody-ligand fusion proteins B7.2-DbFAP (homodimer) and scFvEDG-4-1BBL (homotrimer), which bind through their antibody moieties to either FAP or endoglin (EDG) on the target cell, thus presenting their ligands to the corresponding costimulatory receptors (CD28 and 4-1BB) on the retargeted T cell.

3.1.2 - Biochemical and functional properties of the recombinant proteins

The recombinant proteins were produced and their biochemical and functional properties reconfirmed (Fig. 7). Accordingly, yields of approximately 10 mg/l (scDb33CD3), 0.4 mg/l (B7.2-Db36) and 5 mg/l (scFvA5-4-1BBL) were obtained. Analysis of the purified proteins by SDS-PAGE (Fig. 7A) and Western blot (Fig. 7B) under reducing (R) or non-reducing (NR) conditions revealed single bands of approximately 57 and 49 kDa for scDb33CD3 and scFvA5-4-1BBL, corresponding to the calculated molecular mass of the monomers of 54 and 47 kDa. B7.2-Db36 showed a higher and diffuse band of approximately 98 kDa, which was due to the high glycosylation status of B7.2 (8 potential N-glycosylation sites), since deglycosylation shifted the band towards a lower molecular mass of approximately 57 kDa, which was in correspondence with the calculated molecular mass of 53.8 kDa (data not shown). Size exclusion chromatography revealed a major defined peak for all three constructs in their native state, suggesting mainly homogenous populations (Fig. 7C). Correlation of the peak retention times to a set of standard proteins led to an apparent molecular mass of approx. 163 kDa for scFvA5-4-1BBL, which is in

accordance with the existence as a trimer (141 kDa). B7.2-Db36 showed an even lower retention time than scFvA5-4-1BBL, leading to an apparent molecular mass of approx. 293 kDa which stands in contrast to its calculated molecular mass of 107,6 kDa (homodimer). The strong glycosylation might account here for a retention pattern that differs from that predicted by the globular standard proteins. The peak of the scDb33CD3 suggested a lower molecular mass than the calculated 53.8 kDa. Nevertheless, similar results have been obtained by analyzing other scDb in the laboratory, pointing to a particular chromatographic behaviour of this antibody format. Furthermore, the functionality of the antibody moieties was analyzed by flow cytometry (Fig. 7D). Strong binding of scDb33CD3, B7.2-Db36 and scFvA5-4-1BBL to the FAP- and EDG-positive cell line HT1080 #33 but not to the respective control cell lines HT1080 wt (FAP^-, EDG^+) or HEK293 (FAP^-, EDG^-) could be observed. In addition, binding of scDb33CD3 to PBMC was shown.

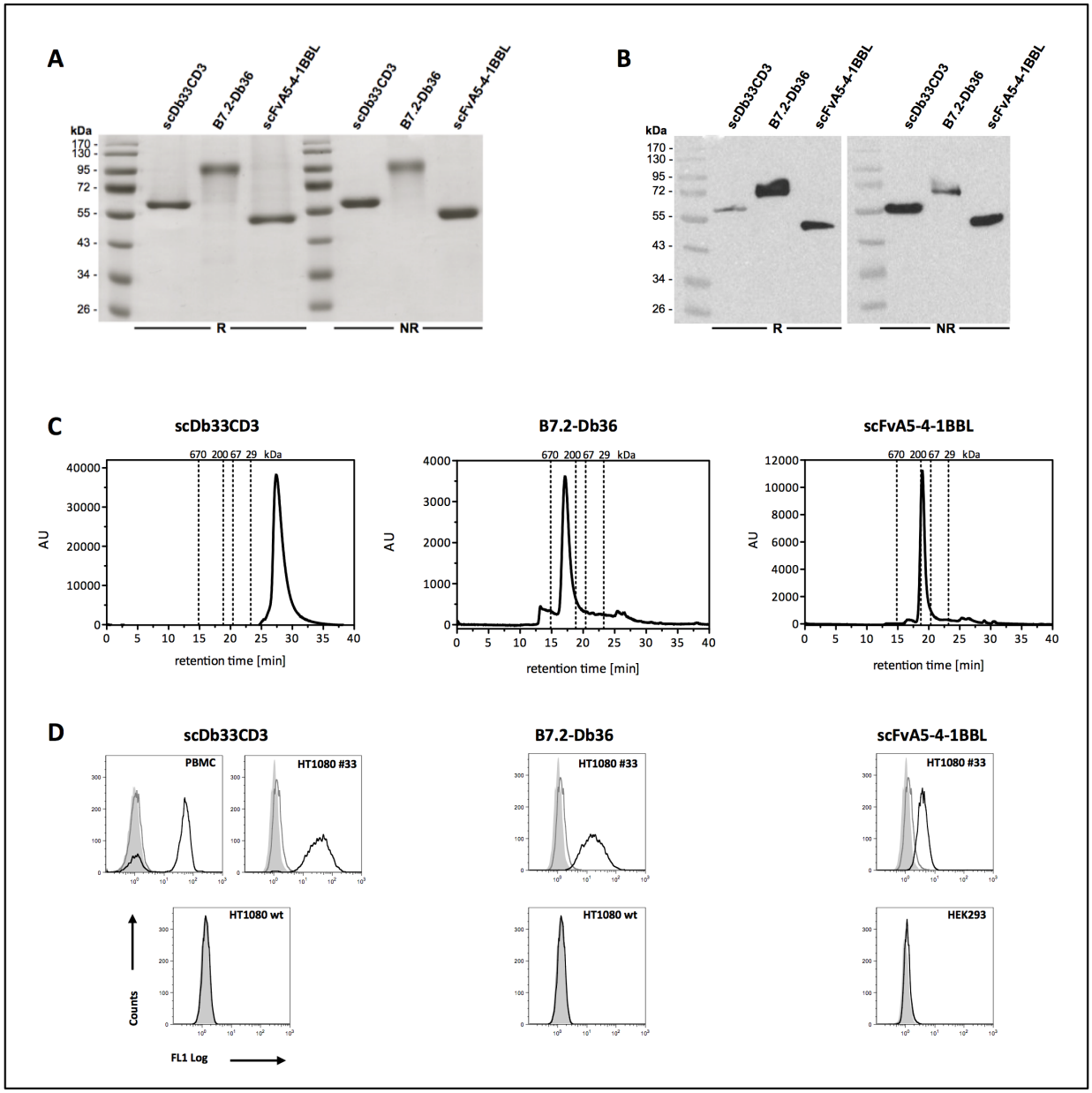

Fig. 7: Biochemical characterization and antibody binding of scDb33CD3, B7.2-Db36 and scFvA5-4-1BBL. IMAC-purified proteins were analyzed by (A) SDS-PAGE (12 %, 2 µg/lane, Coomassie staining) or by (B) Western blot (1 µg/lane, anti-His-HRP detection antibody) under reducing (R) or non-reducing (NR) conditions. (C) HPLC analysis of the recombinant proteins (7 µg protein, BioSep-SEC-2000 column, PBS as mobile phase, peak positions of standard proteins are indicated). (D) Specific binding of the recombinant antibodies to antigen-positive cells analyzed via flow cytometry. HT1080 #33 (FAP^+, EDG^+), HT1080 wt (FAP^-, EDG^+), HEK293 (FAP^-, EDG^-) or PBMC ($CD3^+$) were incubated with 10 µg/ml protein. Bound constructs were detected via a FITC-conjugated anti-His-tag antibody (gray filled: cells, dark gray line: detection antibody only, black line: construct with detection antibody).

The costimulatory potential of the individual fusion proteins was confirmed in a cell-based in vitro assay. Therefore, B7.2-Db36 (Fig. 8A, B) or scFvA5-4-1BBL (Fig. 8C, D) were titrated (90-0.3 nM) and incubated in the presence of a suboptimal concentration (10 pM) of scDb33CD3 on FAP- and EDG-positive target cells (HT1080 #33) before the addition of PBMC as effector cells.

After 2 days, activation of PBMC was measured by cytokine release (IL-2 and IFN-γ). Both B7.2-Db36 and scFvA5-4-1BBL significantly enhanced the scDb-mediated effect in a concentration-dependent manner for both IL-2 and IFN-γ release. In concordance with the concept of costimulation, the effect of the costimulatory ligands was depending on the first stimulus and in its absence, no cytokine release could be observed. As controls, the antibody moieties without the ligands were also applied in combination with the scDb33CD3 and, as expected, showed no enhancement in cytokine release. In the case of the Db36, a decrease in cytokine release could be observed for higher concentrations, which was most likely due to a partial competition in antigen-binding. Consequently, it can be assumed that competition for FAP binding also takes place between B7.2-Db36 and scDb33CD3, lowering the first signal. Here, the strong costimulatory potential of B7.2-Db was able to rescue and even enhance cytokine release at concentrations where the scDb-induced first signal was almost not detectable any more. In contrast, the combination of the scDb33CD3 with scFvA5 targeting different antigens, showed no indication of competition. Ligand specificity of the costimulatory antibody-ligand fusion proteins was shown by blocking the ligand-receptor interaction between the fusion protein and PBMC with the respective recombinant receptors (CTLA-4-Fc/4-1BB-Fc) (Fig. 8E, F).

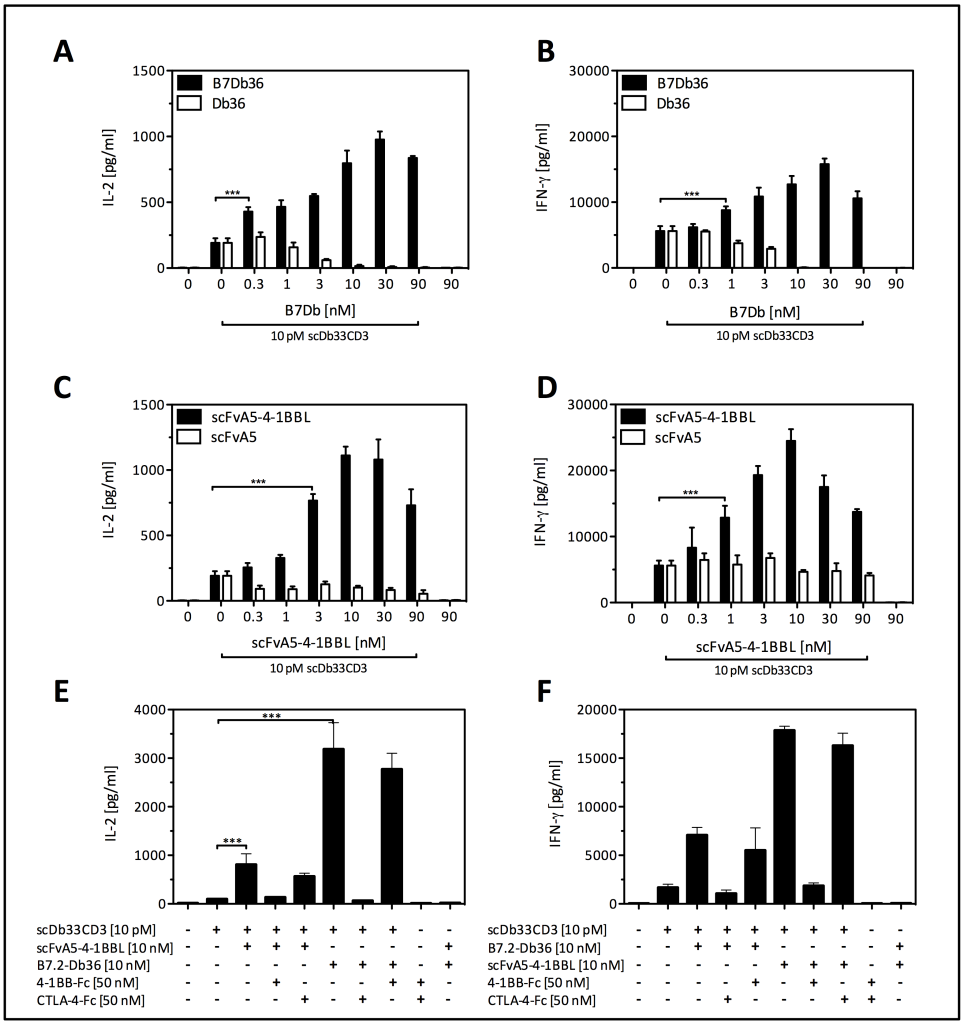

Fig. 8: Costimulatory activity and ligand specificity of B7.2-Db36 and scFvA5-4-1BBL analyzed by cytokine release. HT1080 #33 cells (FAP^+, EDG^+) were incubated for 1 h with scDb33CD3 (10 pM) and the antibody-ligand fusion proteins before the addition of PBMC. B7.2-Db36 (A, B) or scFvA5-4-1BBL (C, D) were either titrated (90-0.3 nM) (A-D) or applied at a constant concentration (10 nM) (E, F). Costimulatory ligand-receptor interactions were blocked by incubation with 5-fold excess of the corresponding recombinant receptor-Fc (CTLA-4-Fc/ 4-1BB-Fc). After 48 h, IL-2 (A, C, E) or IFN-γ (B, D, F) levels were determined via sandwich ELISA. [n=3, block shift correction, mean ± SD, One-way ANOVA, Tukey post test, *** $p < 0.0001$]

Costimulatory activity of B7.2-Db and scFv-4-1BBL in coated or soluble form

In order to assess the costimulatory potential of B7.2-Db and scFv-4-1BBL in a non-targeted, soluble form, scDb33CD3 (1, 3, 10 nM) was coated on an ELISA plate and the costimulatory fusion proteins (50 nM) were applied either in solution (non-targeted form) or were coated together with the scDb.

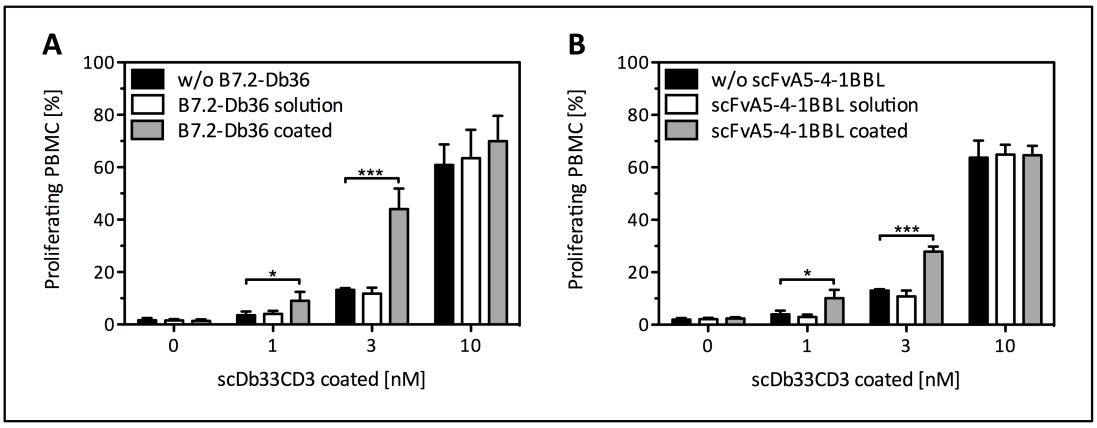

Fig. 9: Costimulatory activity of B7.2-Db36 and scFvA5-4-1BBL in coated or soluble form analyzed by proliferation of PBMC. Coated scDb33CD3 (ELISA plate) was titrated in the presence of 50 nM B7.2-Db36 (A) or scFvA5-4-1BBL (B) in coated or soluble form. Proliferation of CFSE-labeled PBMC was measured after 4 days by flow cytometry. [n=3, mean ± SD, One-way ANOVA, Tukey post test, * $p < 0.05$, *** $p < 0.0001$]

Cross-linked presentation of either B7.2-Db or scFv-4-1BBL in their coated form strongly enhanced scDb-mediated proliferation of PBMC, whereas their soluble form remained inactive (Fig. 9). Thus, it could be assumed, that in the cell-based setting described in this work, the costimulatory activity of the fusion proteins depends on the antibody-mediated cell surface presentation of the costimulatory ligands.

3.1.3 - Combined costimulation with B7.2-Db and scFv-4-1BBL

3.1.3.1 - Cytokine release assays

In the previous experiments the individual costimulatory activity of B7.2-Db and scFv-4-1BBL was reconfirmed. In the following, the simultaneous application of both costimulatory fusion proteins ought to be analyzed in the combinatorial setting (Fig. 6). Therefore, a concentration was chosen (10 nM), at which both fusion proteins individually showed a distinct costimulatory effect.

In addition to the costimulatory enhancement of the scDb-mediated T cell activation by either B7.2-Db or scFv-4-1BBL, the signal of each costimulatory fusion protein could be significantly (*** $p < 0.0001$) enhanced by the combined application of both at the same time, which was shown for either IL-2 or IFN-γ release (Fig. 10).

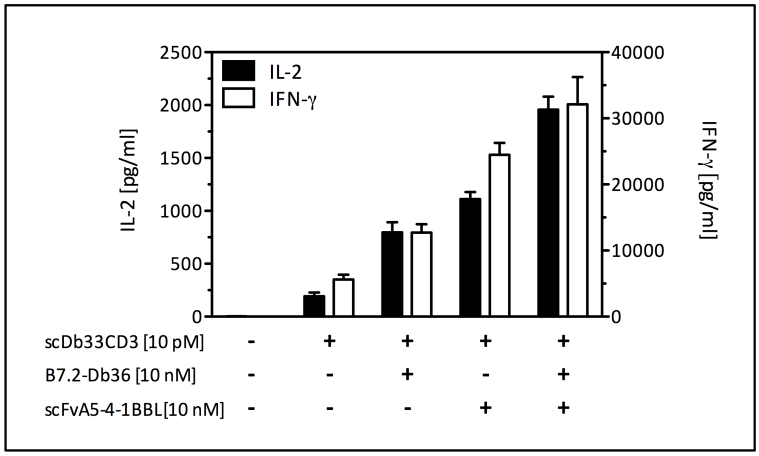

Fig. 10: Combined costimulation with B7.2-Db36 and scFvA5-4-1BBL analyzed by cytokine release. ScDb33CD3 (10 pM) was applied either with one of the costimulatory antibody-ligand fusion proteins (10 nM) or the combination of both to HT1080 #33 cells (FAP^+, EDG^+) and incubated for 1 hour before addition of PBMC. After 48 h, IL-2 or IFN-γ levels were determined via sandwich ELISA. [n=3, block shift correction, mean ± SD]

Thus, it could be concluded, that in the applied cell-based setting, simultaneous targeting of the two costimulatory fusion proteins in combination with the scDb is feasible and effective.

3.1.3.2 - T cell proliferation and differentiation studies

The combinatorial approach was further analyzed in terms of T cell proliferation. Therefore, the recombinant fusion proteins (10 nM) were incubated on HT1080 #33 cells in the presence of a suboptimal scDb concentration (2 pM) followed by the addition of CFSE-labeled PBMC. After 7 days, proliferation of T cells or $CD4^+$ and $CD8^+$ T cell subpopulations was analyzed by flow cytometry.

In analogy to the cytokine release results, stimulation with the scDb alone could be significantly (*** $p < 0.0001$) enhanced by either B7.2-Db or scFv-4-1BBL and the combination of both costimulatory fusion proteins led to a further, significant (*** $p < 0.0001$) increase in the amount of proliferating T cells (Error: Reference source not foundA). As expected, in the absence of the scDb, B7.2-Db or scFv-4-1BBL did not induce proliferation at all.

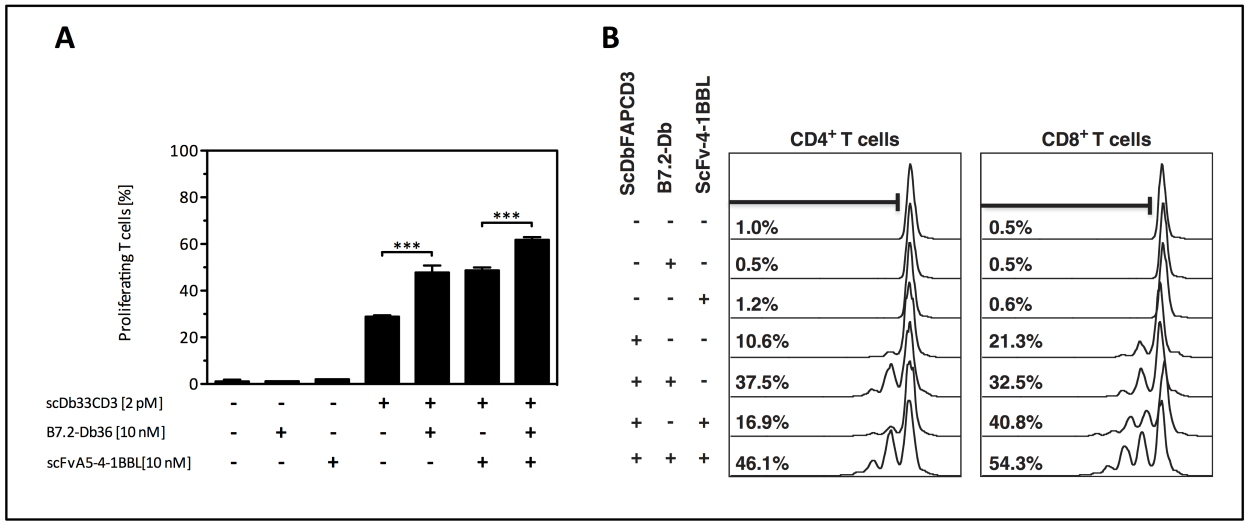

Fig. 11: Combined costimulation with B7.2-Db36 and scFvA5-4-1BBL analyzed for T cell proliferation by flow cytometry. HT1080 #33 cells (FAP^+, EDG^+) were incubated for 1 h with the indicated construct combinations before addition of CFSE-labeled PBMC. After 7 days, proliferation of T cells (A) or $CD4^+$ and $CD8^+$ T cell subsets (B) was analyzed by flow cytometry (anti-CD3-PerCP, anti-CD4-PE/anti-CD8-PE). [(A) n=3, block shift correction, mean ± SD, One-way ANOVA, Tukey post test, *** $p < 0.0001$; (B) a representative experiment out of five with different donors is shown]

The proliferation analysis of $CD4^+$ and $CD8^+$ T cell subsets revealed a significant (*** $p < 0.0001$) responsiveness of both subpopulations to either one of the two costimulatory fusion proteins, but with slight preferences: A higher percentage of $CD4^+$ proliferating T cells in response to costimulation with B7.2-Db (38 %) could be detected compared to costimulation with scFv-4-1BBL (17 %). In contrast, $CD8^+$ T cells seemed to respond slightly stronger to costimulation with scFv-4-1BBL (41 %) than to B7.2-Db (33 %) (Error: Reference source not foundB). However, in the overall T cell response, the different susceptibilities of the T cell subsets towards both ligands compensated each other, leading to a similar outcome for the costimulation with either B7.2-Db (48 %) or scFv-4-1BBL (49 %).

A similar pattern was obtained when T cell expression of the activation marker CD25 was analyzed. ScDb-mediated stimulation led to an upregulation of CD25 expression on T cells (54 %), that could be enhanced to a similar extent by costimulation with either B7.2-Db (70 %) or scFv-4-1BBL (71 %) (Fig. 12A). A further, significant increase was achieved by the combined application of both costimulatory fusion proteins (81 %). In the absence of scDb, B7.2-Db and scFv-4-1BBL did not enhance the expression of CD25 compared to its expression level on unstimulated T cells (10 %).

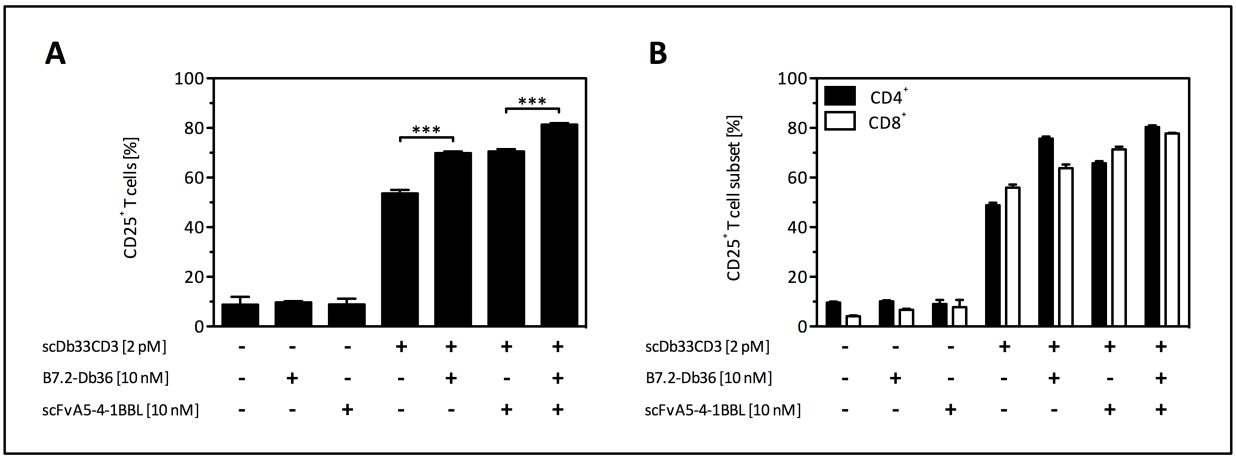

Fig. 12: Combined costimulation with B7.2-Db36 and scFvA5-4-1BBL analyzed for T cell activation by flow cytometry. HT1080 #33 were incubated for 1 h with the indicated construct combinations before addition of PBMC. After 7 days, activation of T cells (A) or $CD4^+$ and $CD8^+$ T cell subpopulations (B) was analyzed by flow cytometry (anti-CD3-PerCP, anti-CD4-PE/anti-CD8-PE, anti-CD25-FITC). [n=3, block shift correction, mean ± SD, One-way ANOVA, Tukey post test, *** $p < 0.0001$]

Furthermore, also the $CD4^+$ and $CD8^+$ T cell subpopulations were analyzed for their CD25 expression, and as expected, both subpopulations significantly (*** $p < 0.0001$) responded to costimulation with either one of the two fusion proteins in the presence of a scDb-induced primary signal (Fig. 12B). In analogy to the proliferation experiments, slight ligand-preferences could be observed: $CD4^+$ T cells seemed to express higher levels of CD25 when costimulated with B7.2-Db (76 %) compared to costimulation with scFv-4-1BBL (66 %), whereas the contrary effect was observed for the $CD8^+$ T cell subset which expressed higher CD25 levels when costimulated with scFv-4-1BBL (71 %) than with B7.2-Db (64 %).

In addition to the expression of the activation marker CD25, the effect of the combinatorial approach was also analyzed in terms of T cell differentiation. Therefore, the composition of naïve and activation-experienced T cells was monitored using the opposing expression profiles of CD45RA and CD45RO (naïve T cells: $CD45RA^+$, $CD45RO^-$, activation-experienced T cells (memory phenotype): $CD45RA^-$, $CD45RO^+$). Stimulation with the scDb (2 pM) alone led to an increase in the percentage of memory T cell phenotype accompanied by a decrease in naïve T cell phenotype (increase and decrease of 17 %, respectively). Costimulation with either B7.2-Db or scFv-4-1BBL (10 nM) enhanced the effect, whereas the strongest effect could be observed for combined costimulation (15 % increase in memory T cell and 10 % decrease in naïve T cell phenotype compared to the effect of the scDb alone) (Fig. 13).

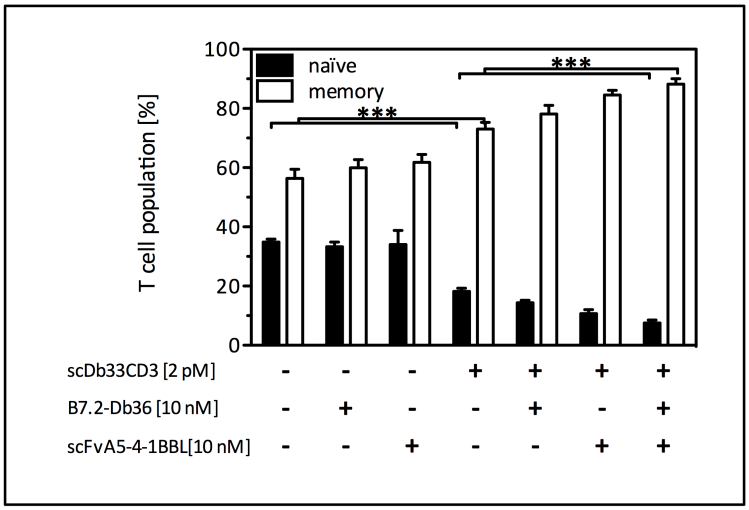

Fig. 13: Combined costimulation with B7.2-Db36 and scFvA5-4-1BBL analyzed for a T cell memory phenotype by flow cytometry. HT1080 #33 cells (FAP^+, EDG^+) were incubated for 1 h with the indicated construct combinations before addition of PBMC. After 7 days, T cell phenotype was analyzed by flow cytometry using memory and naïve T cell phenotype specific staining (naïve: $CD3^+$, $CD45RA^+$, $CD45RO^-$; memory: $CD3^+$, $CD45RA^-$, $CD45RO^+$; anti-CD3-PerCP, anti-CD45RA-PE, anti-CD45RO-FITC). [n=3, mean ± SD, One-way ANOVA, Tukey post test, *** $p < 0.0001$]

Furthermore, the effect of combined costimulation with B7.2-Db and scFv-4-1BBL was also analyzed on the regulatory T cell subset (T_{regs}) which was characterized by the expression of CD4, CD25 and the intracellular transcription factor Foxp3. Stimulation with the scDb (2 pM) alone led to an 8 % increase in T_{regs} within the $CD4^+$ T cell population, whereas neither costimulation with B7.2-Db nor scFv-4-1BBL (10 nM) alone led to a further increase. Only the combined costimulation with both fusion proteins slightly further enhanced the percentage of T_{regs} within the $CD4^+$ T cell population (4 % increase compared to the effect of the scDb alone) (Fig. 14). Thus, the costimulatory support of the effect induced by the bispecific antibody seems rather limited.

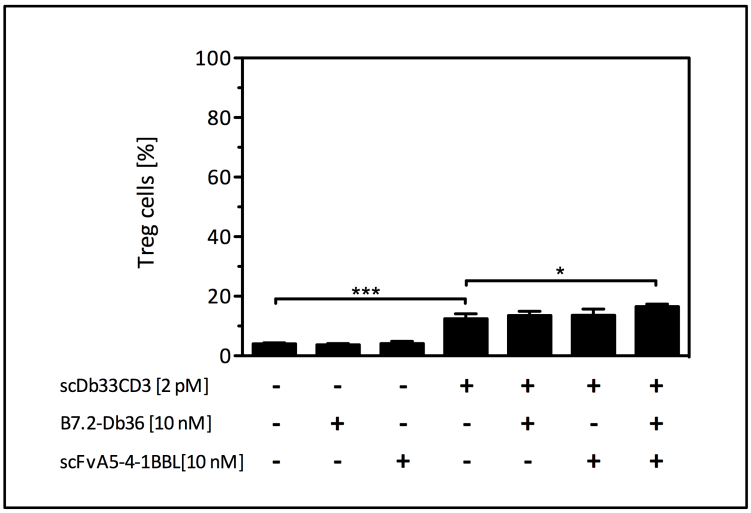

Fig. 14: Combined costimulation with B7.2-Db36 and scFvA5-4-1BBL analyzed for a regulatory T cell (T_{regs}) phenotype by flow cytometry. HT1080 #33 (FAP^+, EDG^+) were incubated for 1 h with the indicated construct combinations before addition of PBMC. After 7 days, PBMC were fixed and permeabilised and T cell phenotype was analyzed by flow cytometry using T_{regs}-specific staining (anti-CD4-PerCP, anti-CD25-PE, anti-Foxp3-Alexa Fluor 488). [n=3, mean ± SD, One-way ANOVA, Tukey post test, * $p < 0.05$, *** $p < 0.0001$]

3.1.4 - Antibody-ligand fusion proteins with other costimulatory members of the Ig-superfamily

In order to extend the ligand spectrum for the established cell-based in vitro setting, two novel antibody-ligand fusion proteins were generated. The latter consisted of a FAP-targeting diabody (Db36) linked to a member of the Immunoglobulin-superfamily, namely B7.1 (CD86) or Inducible T Cell Costimulator Ligand (ICOSL) (Fig. 15).

3.1.4.1 - Generation, expression and biochemical characterization

For the generation of B7.1-Db36 and ICOSL-Db36, the B7.2 moiety in the B7.2-Db36 sequence was replaced by the sequence coding for the extracellular domain of either B7.1 or ICOSL. The recombinant proteins were expressed and produced in HEK293 cells stably transfected with the pSecTagAHis vector encoding the appropriate sequences. For purification, the proteins were precipitated from the supernatant and purified via Ni-NTA IMAC with yields of approx. 2.7 mg/l (B7.1-Db36) and 7 mg/l (ICOSL-Db36).

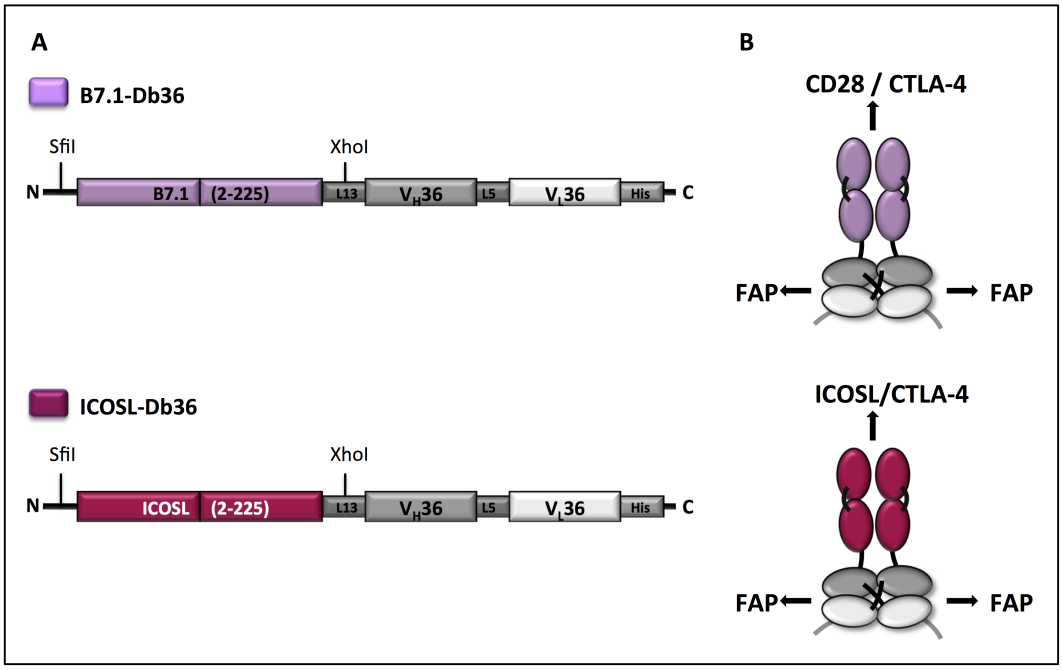

Fig. 15: Schematic representation of B7.1-Db36 and ICOSL-Db36. (A) Arrangement of the extracellular domain of B7.1 or ICOSL and the variable domains of the heavy (V_H) and the light chain (V_L) specific for FAP (L5, L13: linker; His: His-tag). (B) Structural scheme of B7.2-Db36 and ICOSL-Db36, which are dimerized due to the antibody part (linker: black lines, His-tag: grey lines). Antigen and receptor binding sites are indicated with arrows.

Analysis of the purified proteins by SDS-PAGE and Western blot under reducing conditions revealed single bands of approx. 78 and 87 kDa for B7.1-Db36 and ICOSL-Db36, respectively (Fig. 16). The bands were diffuse and higher than the calculated molecular masses of the fusion proteins (B7.1-Db36: 52.6 kDa, ICOSL-Db36: 55.2 kDa) due to the high glycosylation status of B7.1 and ICOSL (8 and 6 potential N-glycosylation sites, respectively).

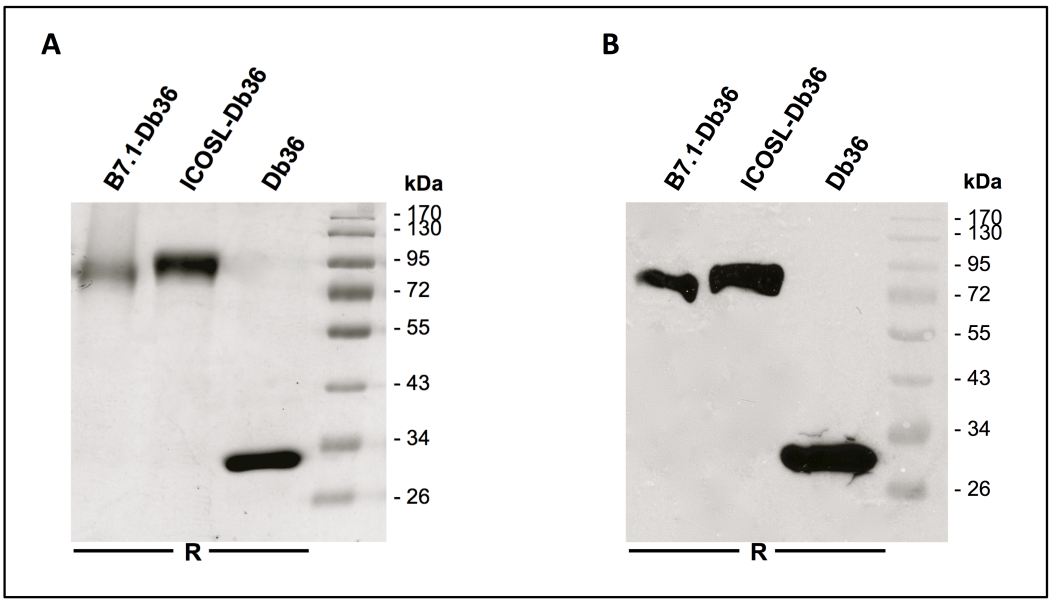

Fig. 16: SDS-PAGE and Western blot of B7.1-Db36 and ICOSL-Db36. IMAC purified B7.1-Db36, ICOSL-Db36 and Db36 were analyzed by SDS-PAGE (A) (12 %, 3 µg/lane, Coomassie staining) or by Western blot (B) (1.5 µg/lane, anti-His-HRP detection antibody) under reducing conditions (R).

Deglycosylation with N-glycosidase F shifted the protein bands towards a lower molecular mass of approx. 61 and 57 kDa for B7.1-Db36 (double band) and 66 kDa for ICOSL-Db36 which was more in correspondence with their calculated molecular masses (Fig. 17).

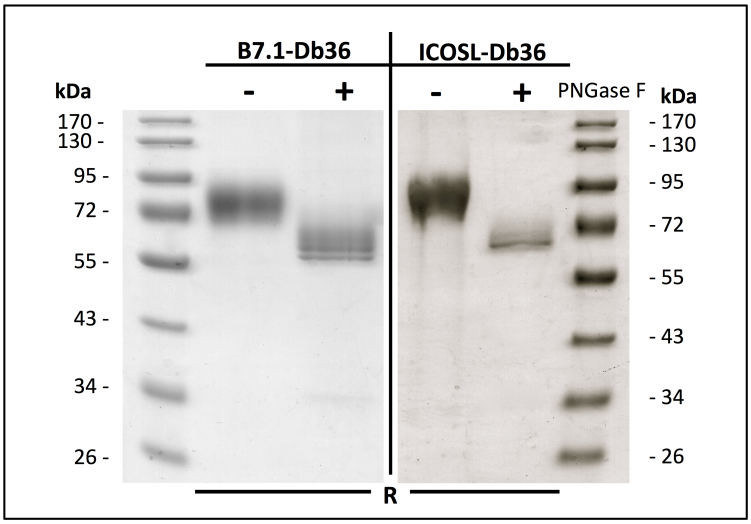

Fig. 17: Deglycosylation of B7.1-Db36 and ICOSL-Db36 analyzed in SDS-PAGE. 3 µg protein (B7.1-Db36, ICOSL-Db36) was digested with the N-glycosidase PNGase F and was compared to untreated protein under reducing conditions (R) (12 %, 3 µg/lane, Coomassie staining).

Furthermore, size exclusion chromatography revealed a defined main peak for both B7.1-Db and ICOSL-Db (Fig. 18). The correlation of the retention times of the main peaks to a set of standard proteins of known molecular masses revealed molecular masses of 235 kDa for B7.1-

Db36 and 274 kDa for ICOSL-Db36. The difference between the apparent molecular masses and the calculated ones (B7.1-Db36: 105.2 kDa, ICOSL-Db36: 110.4 kDa) might be related to strong glycosylation, thus altering their performance compared to the globular standard proteins.

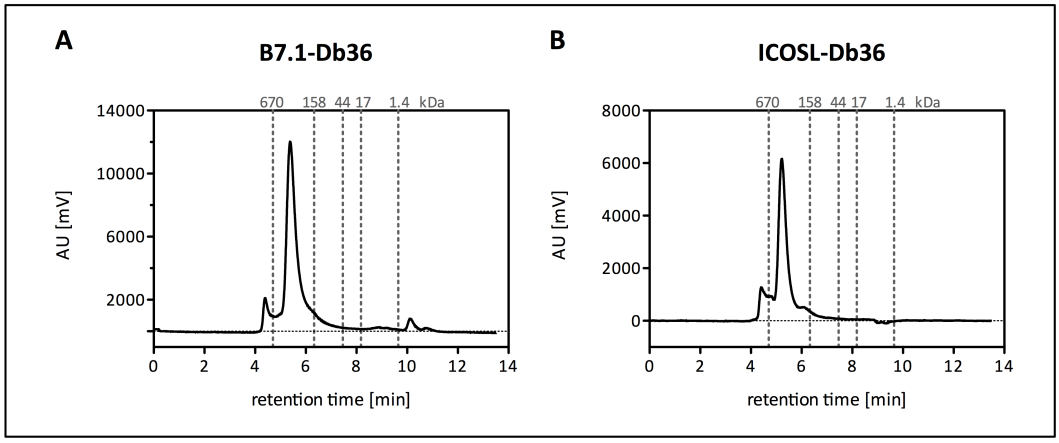

Fig. 18: HPLC analysis of B7.1-Db36 and ICOSL-Db36. 15 µg (A) B7.1-Db36 or (B) ICOSL-Db36 were loaded on a TSK-GEL G3000SW$_{XL}$ column with PBS as mobile phase. Peak positions of standard proteins are indicated.

3.1.4.2 - Binding studies

Antigen-specific binding of B7.1-Db36 and ICOSL-Db36 was analyzed by flow cytometry. Therefore, the two fusion proteins and the control Db36 were incubated on FAP-positive HT1080 #33 or FAP-negative HT1080 wt cells and, as expected, binding was only observed to the antigen-positive cell line (Fig. 19A). Binding of the proteins was compared by titrating them on the target cells: ICOSL-Db36 had a higher functional affinity towards FAP (EC_{50}: 2.3 ± 0.2 nM) than B7.1-Db36 (EC_{50}: 5.2 ± 0.3 nM), whereas both fusion proteins showed impaired binding compared to the Db36 (EC_{50}: 0.2 ± 0.004 nM) (Fig. 19B).

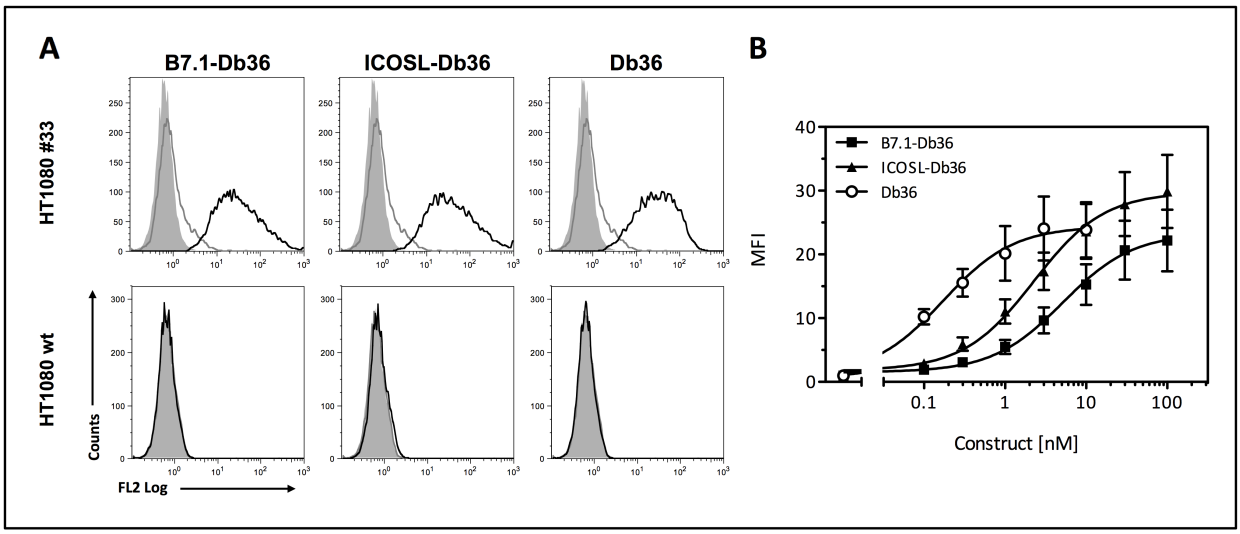

Fig. 19: Qualitative and quantitative analysis of B7.1-Db36 and ICOSL-Db36-specific binding to FAP-positive cells analyzed by flow cytometry. (A) HT1080 #33 (FAP^+EDG^+) or HT1080 wt (FAP^-EDG^+) cells were incubated with B7.1-Db36, ICOSL-Db36 (100 nM) or control Db36 (3 nM). Bound constructs were detected via a PE-conjugated anti-His-tag antibody (gray filled: cells, dark grey line: detection antibody, black line: construct with detection antibody). (B) For binding affinity analysis, constructs were titrated on HT1080 #33 cells with EC_{50} values of 5.2 ± 0.3 nM (B7.1-Db36), 2.3 ± 0.2 nM (ICOSL-Db36) and 0.2 ± 0.004 nM (Db36). [n=3, mean ± SD, column statistics]

3.1.4.3 - Costimulatory activity

In order to show the functionality of the extracellular domains of B7.1 and ICOSL, B7.1-Db and ICOSL-Db were analyzed in an immobilized, i.e. coated, form. Therefore, titrating concentrations of scDb (1, 3, 10 nM) were coated in an ELISA plate in the presence of the fusion proteins (50 nM) in either coated or soluble from. Costimulation with the immobilized form of either ICOSL-Db36 or B7.1-Db36 significantly enhanced scDb-mediated PBMC proliferation (Fig. 20A, B). The effect was greatest for 3 nM scDb revealing a 9- (ICOSL-Db) to 11-fold (B7.1-Db) enhancement of the scDb-induced signal. In solution, both ligands were mainly inactive, although for ICOSL a slight costimulatory activity could be observed for 10 nM scDb. As a negative control, the antibody moiety Db36 was also applied in the presence of the scDb and as expected, did not show any costimulatory activity at all (Fig. 20C).

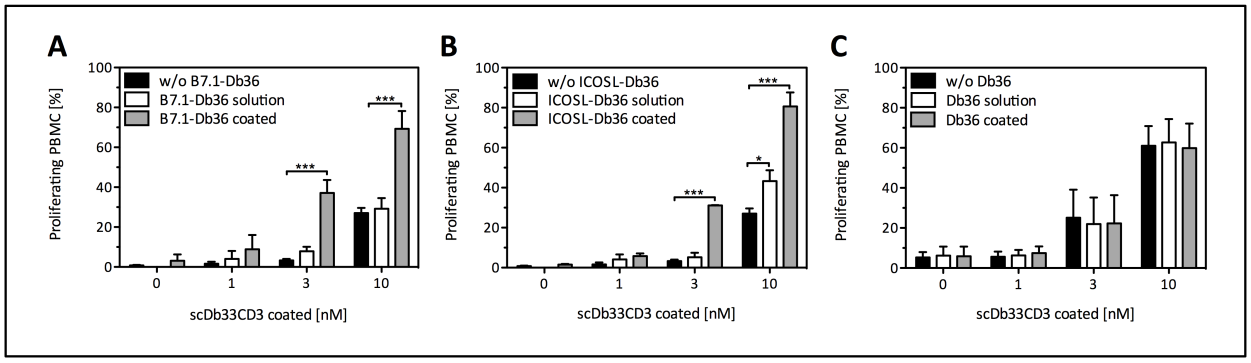

Fig. 20: Costimulatory activity of B7.1-Db36 and ICOSL-Db36 in coated or soluble form analyzed by proliferation of PBMC via flow cytometry. Coated scDb33CD3 (ELISA plate) was titrated in the presence of (A) B7.1-Db36, (B) ICOSL-Db36 or (C) control Db36 (50 nM each) in coated or soluble form. Proliferation of CFSE-labeled PBMC was measured after 4 days by flow cytometry. [n=3, mean ± SD, One-way ANOVA, Tukey post test, * $p < 0.05$, *** $p < 0.0001$]

Subsequently, the costimulatory potential of the two fusion proteins was also analyzed in a cell-based assay. Therefore, B7.1-Db36 and ICOSL-Db36 were titrated (90-0.3 nM) and incubated on HT1080 #33 at a constant, suboptimal scDb concentration (10 pM) before addition of PBMC. As can be seen from Fig. 21, B7.1-Db36 strongly enhanced scDb-mediated T cell activation in a concentration-dependent manner and showed the strongest effect in the concentration range of 10–30 nM with a 19-21-fold increased IL-2 signal compared to the scDb alone. In contrast, no costimulatory activity was detected for ICOSL-Db36 in the cell-based setting, neither for cytokine release (IL-2, IFN-γ) nor proliferation (data not shown). Thus, its application for further experiments was excluded.

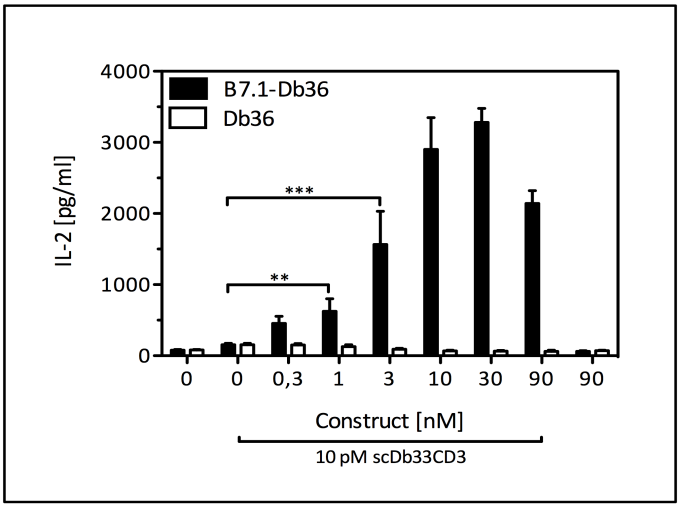

Fig. 21: Costimulatory activity of B7.1-Db36 analyzed by cytokine release. B7.1-Db36 or control Db36 were titrated and incubated on HT1080 #33 (FAP^+, EDG^+) in the presence of 10 pM scDb33CD3 for 1 hour before addition of PBMC. After 48 h, IL-2 levels were determined via sandwich ELISA. [n=4, block shift correction, mean ± SD, One-way ANOVA, Tukey post test, ** $p < 0.01$, *** $p < 0.0001$]

3.1.4.4 - Comparative analysis of B7.2-Db and B7.1-Db

In order to compare the costimulatory activity of B7.1-Db36 to the primary fusion protein B7.2-Db36, both fusion proteins were titrated (90-0.3 nM) in the presence of a suboptimal concentration of scDb (10 pM) on FAP-positive target cells (HT1080 #33) before the addition of PBMC. After 2 days, T cell activation was measured via IL-2 release. At 10 nM, B7.1-Db36 led to a 3-fold higher IL-2 release than B7.2-Db36 (B7.1-Db36: 10.7-fold increase of scDb-mediated signal, B7.2-Db36: 3.5-fold) (Fig. 22).

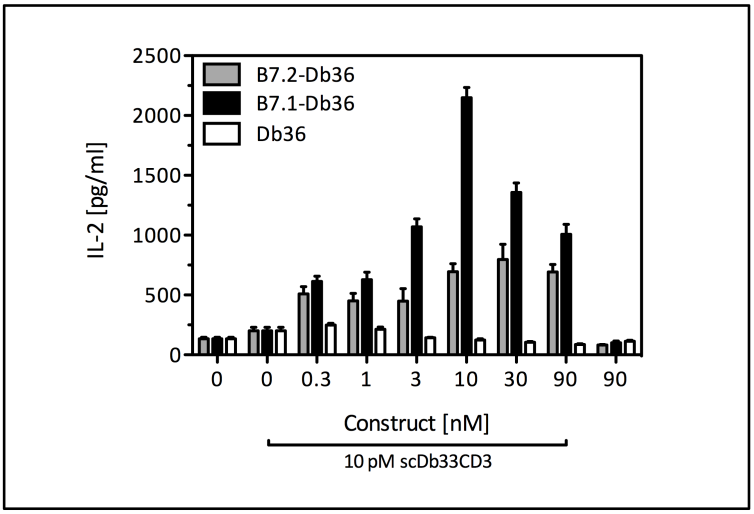

Fig. 22: Costimulatory activity of B7.2- and B7.1-Db36 analyzed by cytokine release. B7.2-Db36, B7.1-Db36 or control Db36 were titrated and incubated on HT1080 #33 (FAP^+, EDG^+) in the presence of 10 pM scDb33CD3 for 1 hour before addition of PBMC. After 48 h, IL-2 levels were determined via sandwich ELISA. [n=2, block shift correction, mean ± SD]

Furthermore, the activity of the fusion proteins was also compared in terms of their potential to increase T cell cytotoxicity, thus enhancing scDb-mediated target cell killing. Therefore, PBMC were prestimulated with scDb (16 pM) alone or in combination with either B7.1-Db or B7.2-Db (10 nM each). After 7 days, prestimulated PBMC were harvested and retargeted by the bispecific antibody to tumor cells at an effector to target cell ratio of 12:1. After six hours, PBMC were washed away and target cell viability was measured by a MTT assay. As can be seen from Fig. 23, costimulation with either one of the two B7-Db fusion proteins during the scDb-mediated prestimulation phase increased the cytotoxic potential of the T cells. Consequently, enhanced target cell killing (up to 37 %) could be achieved in the subsequent cytotoxicity assay. Here, only at low scDb concentrations (0.15 pM), costimulation by B7.1-Db showed to be slightly more effective than by B7.2-Db (Fig. 23B).

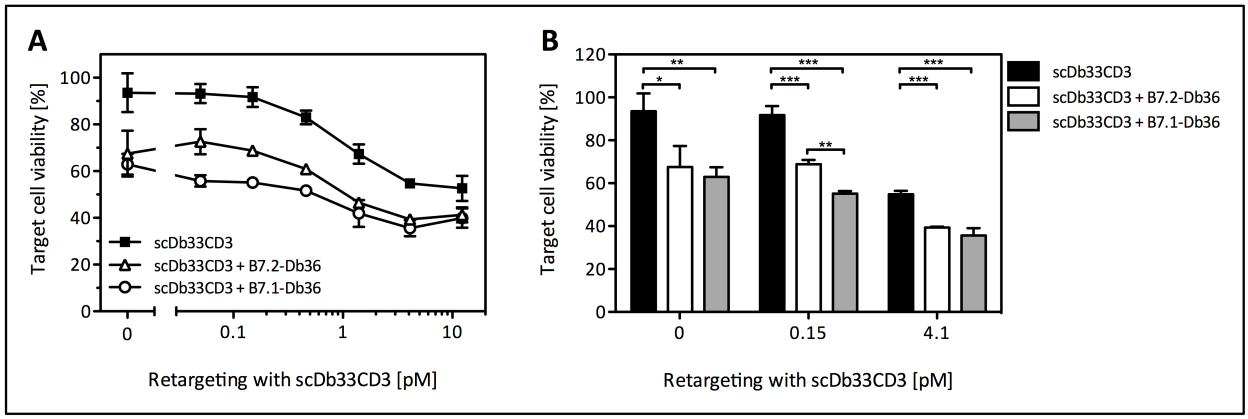

Fig. 23: Tumor target cell killing with B7.2- or B7.1-Db36-prestimulated PBMC was analyzed by MTT assay. HT1080 #33 were incubated in a 6-Well plate for 1 h with scDb (16 pM) alone or in combination with either B7.2-Db36 or B7.1-Db36 (10 nM each) before addition of PBMC. After 7 days of stimulation, PBMC were collected, counted and retargeted with scDb titrated on HT1080 #33 (E:T ratio of 12:1). After 6h, PBMC were washed away and target cell viability was determined via MTT assay. [n=3, mean ± SD, One-way ANOVA, Tukey post test, * $p < 0.05$, ** $p < 0.01$, *** $p < 0.001$]

In addition to its superior costimulatory activity, B7.1-Db36 also displayed a 6.7-fold higher purification yield than B7.2-Db36 (2.7 mg/l vs. 0.4 mg/l) and was shown to be stable at -20°C, while B7.2-Db showed loss of activity after 2-3 month. Taking these findings into account, B7.1-Db36 was chosen for the further experiments.

3.1.5 - Combined costimulation with B7.1-Db and scFv-4-1BBL

3.1.5.1 - Cytotoxicity assays with prestimulated PBMC

In order to analyze the effect of combined costimulation by B7.1-Db36 and scFvA5-4-1BBL on T cell cytotoxicity, PBMC were prestimulated with scDb (20 pM) alone, in combination with either B7.1-Db or scFv-4-1BBL or the combination of both (10 nM each). After 7 days, prestimulated PBMC were harvested and retargeted with scDb titrated on target cells at an effector to target cell ratio of 5:1. After six hours, PBMC were washed away and target cell viability was measured by a MTT assay.

Greatest differences between the differentially prestimulated PBMC populations could be observed for retargeting with lower scDb concentrations (0.6 pM, Fig. 24B): Here, scFv-4-1BBL-mediated costimulation significantly enhanced the percentage of target cell killing mediated by the scDb alone, whereas the effect was even stronger for B7.1-Db. Combined costimulation by B7.1-Db and scFv-4-1BBL led to a slightly further enhancement in target cell killing, although the

effect was not significant in comparison to costimulation with B7.1-Db alone. At higher scDb concentrations (10 pM), all prestimulated PBMC populations showed maximal target cell killing (10-20 % target cell viability) (Fig. 24A). Furthermore, the potential of prestimulation on the cytotoxic capacity of the T cells was demonstrated by the inability of non-prestimulated T cells to induce target cell killing within the applied concentration range of the scDb.

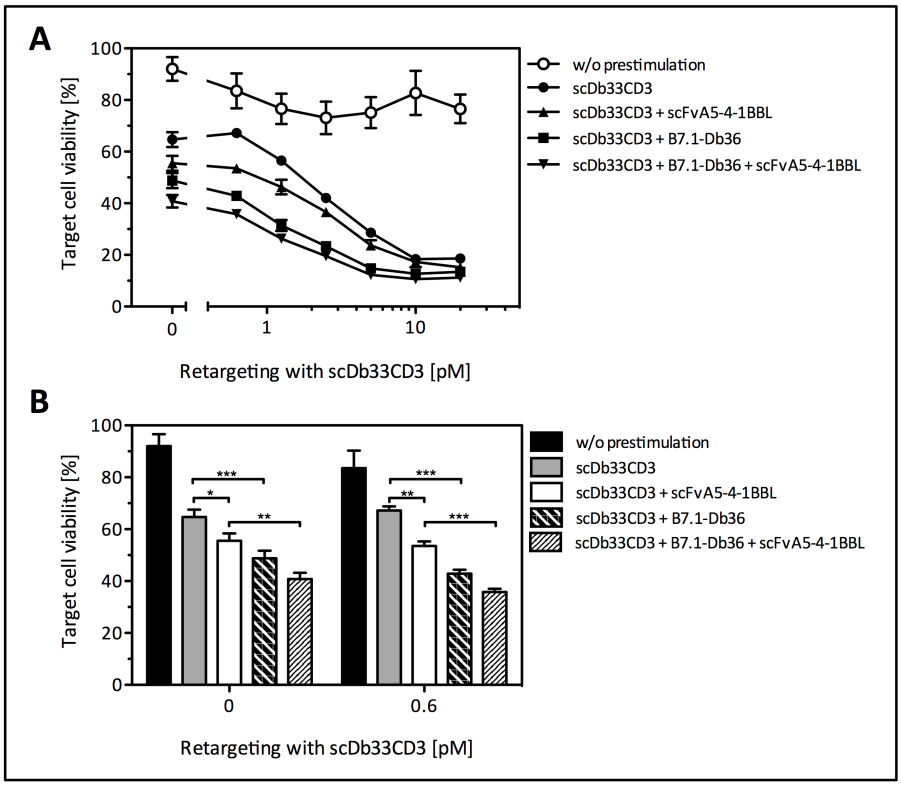

Fig. 24: Tumor target cell killing with B7.1-Db36 and scFvA5-4-1BBL prestimulated PBMC was analyzed by MTT assay. HT1080 #33 were incubated in a 6-Well for 1 h with the indicated construct combinations (scDb: 20 pM, B7.1-Db/scFv-4-1BBL: 10 nM) before addition of PBMC. After 7 days of stimulation, PBMC were collected, counted and retargeted with scDb titrated on HT1080 #33 (E:T ratio of 5:1). After 6h, PBMC were washed away and target cell viability was determined via an MTT assay. [n=3, mean ± SD, One-way ANOVA, Tukey post test, * $p < 0.05$, ** $p < 0.01$, *** $p < 0.001$]

In addition, first attempts were also made in analyzing the expression of the cytotoxicity marker granzyme B (GrB) on T cells and their $CD8^+$ and $CD8^-$ subsets within the prestimulated PBMC population (via flow cytometry). GrB is a serine protease which is synthesized and stored in cytotoxic granules along with other granzymes and perforin during differentiation into effector T cells. Upon restimulation of the cells, the content of the granules is rapidly released towards the target cell, leading to target cell entry of the granzymes possibly through perforin pores and apoptosis induction through activation of intracellular caspases[142].

Although stimulation with the scDb (20 pM) alone showed only a little effect, costimulation with either scFv-4-1BBL or B7.1-Db (10 nM) strongly enhanced scDb-induced PBMC expansion (1.5-fold, 1.6-fold) and the combination of both led to a further increase in absolute cell numbers (1.8-fold, Fig. 25A).

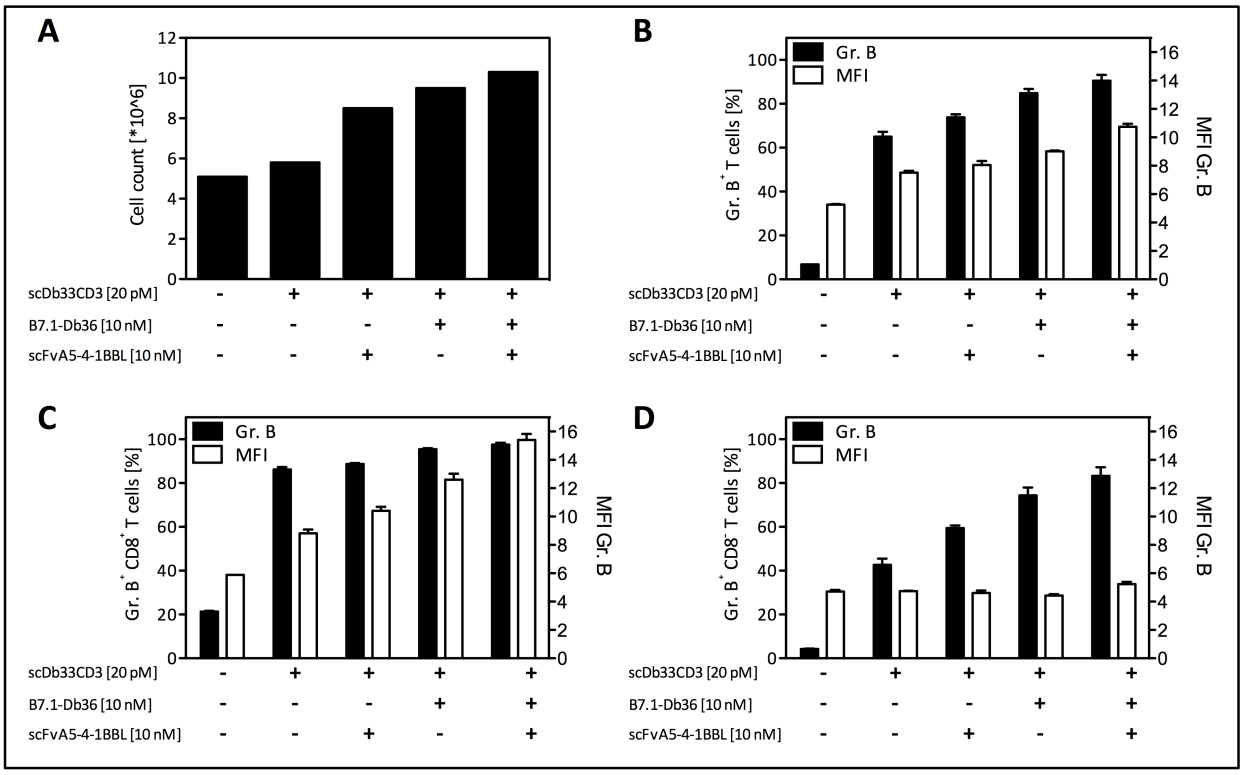

Fig. 25: PBMC expansion and T cell granzyme B (GrB) expression and intensity after 7 days of stimulation was analyzed by cell count and flow cytometry. HT1080 #33 were incubated for 1 h with the indicated construct combinations before addition of PBMC. After 7 days, absolute cell numbers were calculated from cell count (A) and GrB expression and intensity (MFI = mean fluorescence intensity) of T cells (B) or $CD8^+$ (C) and $CD8^-$ (D) subsets was analyzed by flow cytometry using specific staining (anti-CD3-FITC, anti-CD8-PerCP, anti-Gr. B-PE). [n=1, mean ± SD]

Despite its minor effect on T cell expansion, scDb-mediated prestimulation strongly upregulated intracellular GrB expression in T cells (65 %, Fig. 25B). Individual costimulation with either scFv-4-1BBL (74 %) or B7.1-Db (85 %) further enhanced GrB expression and an even slightly further increase could be detected for the combined application of both fusion proteins (91 %). A similar pattern could be observed for the $CD8^+$ and $CD8^-$ T cell subpopulations (Fig. 25C, D), whereas the signal level was much higher for $CD8^+$ T cells. In addition, the $CD8^+$ T cell subset also showed the highest values for the mean fluorescence intensity (MFI) of GrB expression following the pattern observed for the percentage of GrB^+ T cells. Since the MFI is a parameter for the amount of marker expression, it can be assumed, that within $CD8^+$ T cells, costimulation resulted not only in higher percentages of GrB positive cells but also in higher amounts of

intracellular GrB expression. This effect was not observed for the $CD8^-$ T cell subset, in which the MFI remained at the same level throughout the different stimulations, although the amount of GrB^+ cells increased with costimulation.

Thus, using cytotoxicity assays and first GrB expression studies it could be shown, that costimulation during the prestimulation phase enhances the target cell killing capacity of T cells, where, as expected, the $CD8^+$ subpopulation was addressed in particular.

3.1.6 - Expansion, cytotoxicity and differentiation studies with naïve $CD8^+$ T cells

The costimulatory effect of the fusion proteins on T cell cytotoxicity also ought to be analyzed in terms of a defined $CD8^+$ T cell population, namely naïve $CD8^+$ T cells. Therefore, the surface expression of CD107a, a marker for the degranulation of T cells, was monitored. In detail, CD107a is present in the membrane of cytotoxic granules and becomes exposed onto the cell surface following activation-induced degranulation, which is a prerequisite for the cytolysis of target cells. When CD107a is exposed on the cell surface, it can be detected via an antibody and measured by flow cytometry[143]. Freshly isolated naïve $CD8^+$ T cells were prestimulated with scDb (2, 4, 16, 32 pM) alone or together with scFv-4-1BBL (10 nM) for 7 days before they were triggered with scDb (1 nM) on a new plate of HT1080 #33 cells. After six hours, CD107a expression was measured.

Costimulation with scFv-4-1BBL strongly enhanced the percentage of degranulating $CD107a^+$ T cells (approx. 4-fold) at low and high scDb concentrations, whereas the effect of the scDb alone was very low (Fig. 26B, C). These data correlated with the proliferative capacity of the naïve $CD8^+$ T cells, since costimulation with scFv-4-1BBL significantly enhanced their proliferation leading to a 2.2-2.5-fold increase of scDb-mediated T cell expansion, whereas the effect of the scDb alone was very little (Fig. 26A).

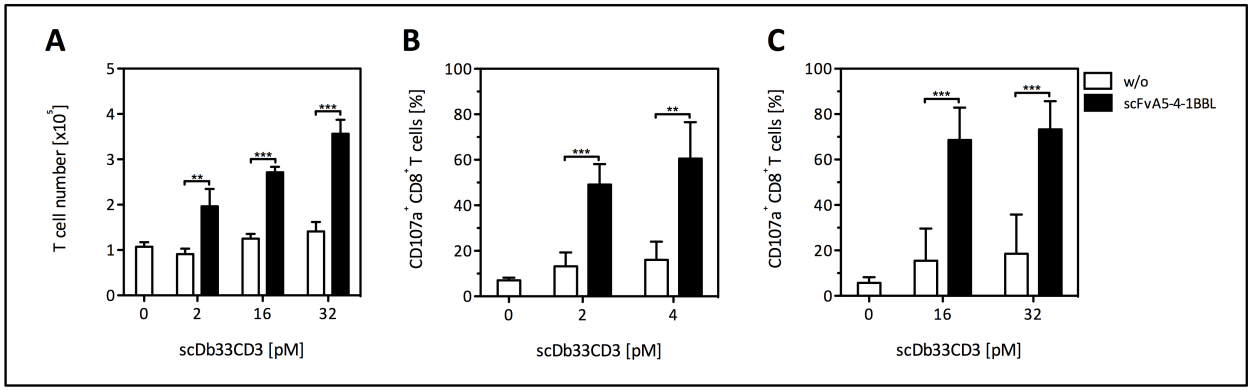

Fig. 26: Expansion and cytotoxic potential of prestimulated naïve CD8$^+$ T cells was analyzed by cell count and degranulation assay. HT1080 #33 were incubated for 1 h with either the scDb alone (2, 4, 16, 32 pM) or in combination with 10 nM scFv-4-1BBL before addition of isolated naïve CD8$^+$ T cells. After 7 days of prestimulation, T cells were collected, counted and analyzed for their expansion (A) and cytotoxic potential (B, C). For the latter, degranulation of T cells was triggered by 1 nM scDb for 6 hours and then measured via flow cytometry (anti-CD3-PE, anti-CD107a-FITC). [n=3-4, mean ± SD, One-way ANOVA, Tukey post test, ** p < 0.01, *** p < 0.001]

Furthermore, also the potential of naïve CD8$^+$ T cells to differentiate into a memory phenotype upon activation was analyzed following the same setting. Memory T cells can be broadly divided into central memory and effector memory T cell subsets based on the expression of cell surface markers, that are related to their different capacities to home to lymphoid or non-lymphoid tissue and to perform effector functions. Therefore, three different cell surface markers were used (CD45RA, CD27, CD62L), allowing the discrimination between naïve T cells ($T_{naïve}$: CD27$^+$, CD62L$^+$, CD45RA$^+$) and a central memory (T_{CM}: CD27$^+$, CD62L$^+$, CD45RA$^-$)- and an effector memory (T_{EM}: CD27$^+$, CD62L$^-$, CD45RA$^-$)-like T cell phenotype[144]. Costimulation with scFv-4-1BBL promoted the differentiation of naïve CD8$^+$ T cells into a memory phenotype with preference for T_{CM} than T_{EM}. This effect was especially evident at higher scDb concentrations (32 pM), where 63 % of the CD8$^+$ T cells showed a central memory- and 19 % an effector memory-like phenotype (Fig. 27). For low scDb concentrations (2 pM), the majority of the cells remained within the naïve phenotype. Thus, upon CD3-induced activation costimulation with scFv-4-1BBL contributed essentially to the stimulation of naïve CD8$^+$ T cells, leading to proliferation, acquisition of cytotoxic potential and differentiation into a central memory-like phenotype.

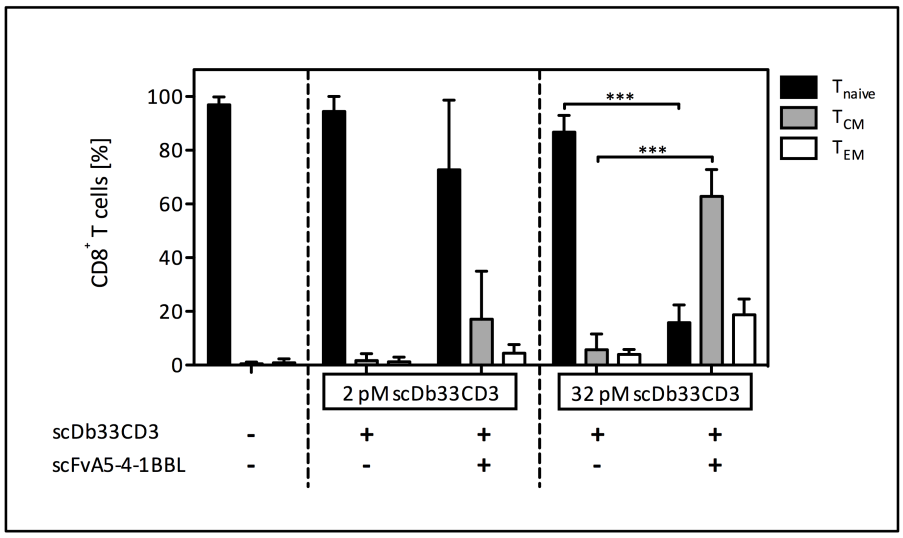

Fig. 27: Costimulation-induced differentiation of naïve CD8$^+$ T cells into a memory phenotype was analyzed by flow cytometry. HT1080 #33 were incubated for 1 h with the scDb (2, 32 pM) alone or in combination with scFvA5-4-1BBL (10 nM) before addition of isolated naïve CD8$^+$ T cells. After 7 days of stimulation, T cells were collected and their phenotype was analyzed by flow cytometry using T cell memory phenotype specific staining ($T_{naïve}$: CD27$^+$, CD62L$^+$, CD45RA$^+$; T_{CM}: CD27$^+$, CD62L$^+$, CD45RA$^-$; T_{EM}: CD27$^+$, CD62L$^-$, CD45RA$^-$). ($T_{naïve}$: naïve T cells, T_{CM}: central memory T cells, T_{EM}: effector memory T cells) [n=3, mean ± SD, One-way ANOVA, Tukey post test, *** $p < 0.001$]

The analysis were also performed with B7.1- and B7.2-Db, but surprisingly no costimulatory activity was observed. Subsequent analysis revealed strong CTLA-4 expression on the isolated naïve CD8$^+$ T cells, that was not observed when analyzing the overall PBMC population. This finding suggests that the isolation procedure of the naïve T cell population might account for the upregulation of this inhibitory receptor, suppressing B7-mediated costimulatory signals.

3.2 - Time-shift application of B7- and 4-1BBL-antibody fusion proteins

3.2.1 - The experimental setting

Throughout the previous experiments, costimulation was analyzed for its effect on unstimulated T cells. Hence, the costimulatory fusion proteins were applied in combination with the bispecific antibody on day 0 and after 2 to 7 days, costimulatory effects were measured. Here, the model system ought to be further expanded in order to analyze the costimulatory influence on the T cell response in a restimulation context. Therefore, T cells were stimulated with the scDb (33 pM, + washing) on day 0 for initial stimulation and on day 3 for restimulation (33 pM + washing), and costimulation with B7.1-Db and scFv-4-1BBL (10 nM) was applied either together with initial or late scDb stimulation. Alternatively, considering that CD28 is constitutively expressed on naïve T cells, while 4-1BB becomes upregulated upon T cell stimulation, peaking at 72 h[14,16], B7.1-Db was concomitantly applied with initial stimulation, while scFv-4-1BBL was applied later on in combination with scDb-mediated restimulation. On day 7, the T cell response was analyzed in terms of proliferation, cytotoxic potential (GrB) and expression of the inhibitory receptors PD-1 and CTLA-4. In Fig. 28, the assay conditions of the combinatorial time-shift setting are summarized.

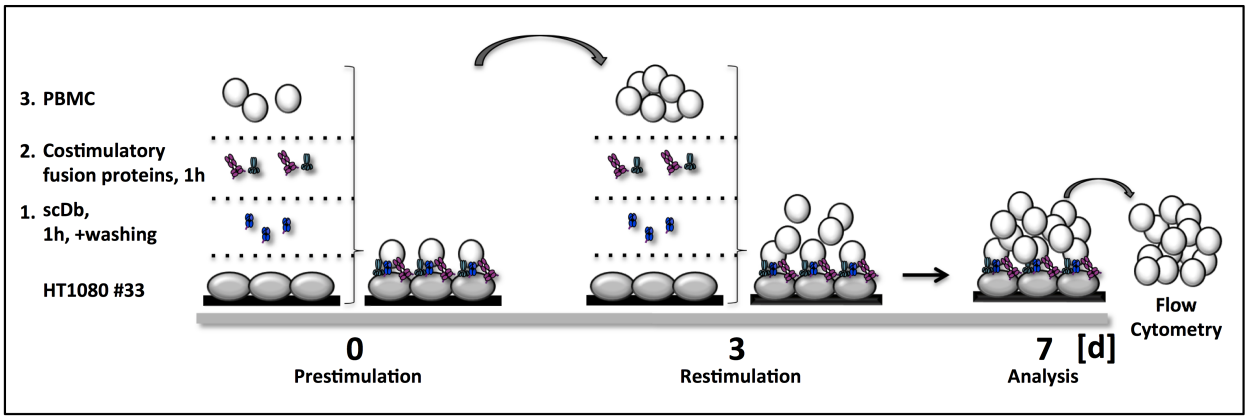

Fig. 28: Schema for the time-shift combinatorial assay setting. T cells were stimulated with scDb on day 0 for initial stimulation and on day 3 for restimulation. Costimulation by B7.1-Db and scFv-4-1BBL was provided either with initial stimulation, with restimulation or in a consecutive manner following the costimulatory receptor expression pattern (B7.1-Db with initial scDb-stimulation and scFv-4-1BBL with scDb-mediated restimulation). Experimental setting: On day 0, scDb (33 pM) was incubated on HT1080 #33 cells for 1 h before non-bound protein was washed away. Afterwards, costimulatory antibody-ligand fusion proteins (10 nM) were applied and incubated for 1 h before addition of PBMC. After 3 days, prestimulated PBMC were transferred to new HT1080 #33 cells previously incubated with scDb (33 pM + washing) followed by the costimulatory constructs. On day 7, PBMC were collected and analyzed for their proliferative and cytotoxic (granzyme B expression) potential and expression of the inhibitory receptors PD-1 and CTLA-4 using flow cytometry.

3.2.2 - Comparative analysis of time-shift versus simultaneous costimulation

3.2.2.1 - Proliferation assays

Initial combined costimulation resulted in a similar percentage of proliferating T cells compared to the effect mediated by restimulation with the scDb alone, whereas both consecutive and simultaneous costimulation during restimulation could further enhance the signal and induced maximal proliferation of T cells (Fig. 29A). For both $CD8^+$ and $CD8^-$ T cells subsets, a similar proliferation pattern could be observed, where the $CD8^+$ T cell subset showed to be slightly more responsive than the $CD8^-$ T cell subset (Fig. 29B, C).

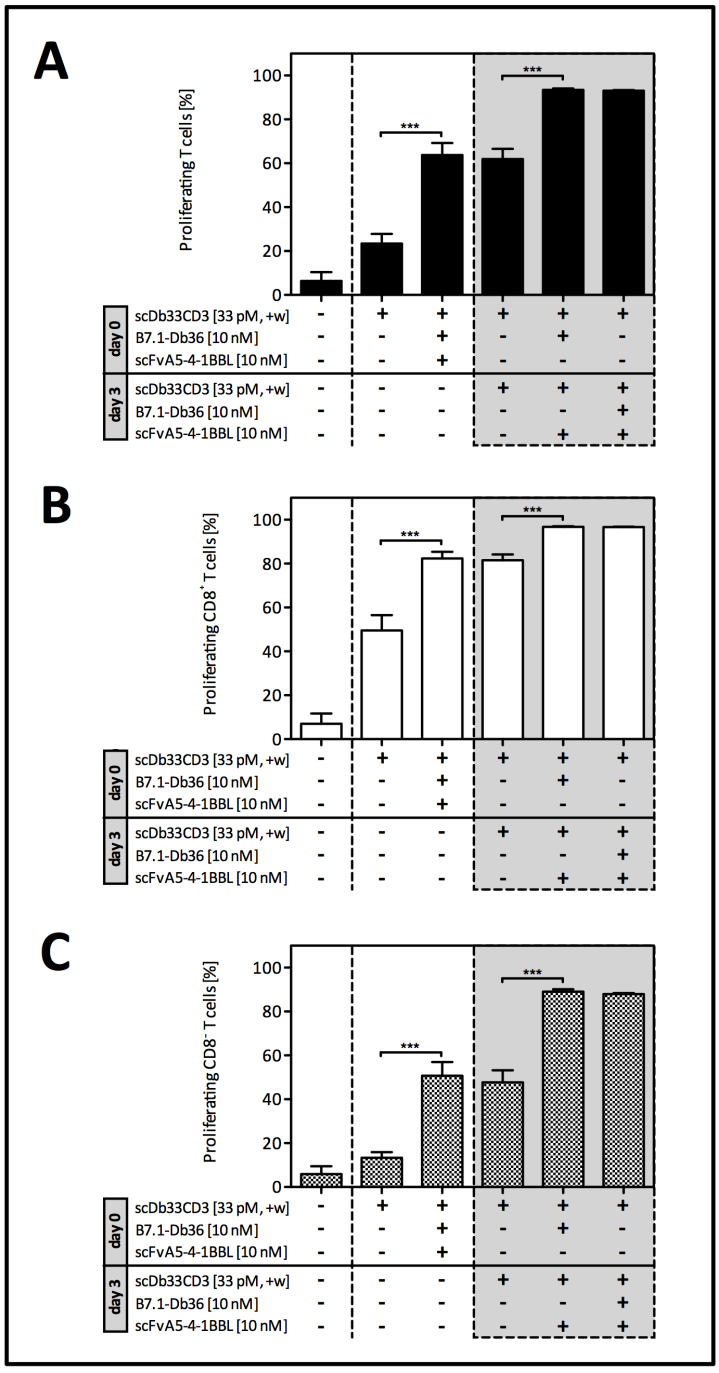

Fig. 29: Combinatorial costimulation by B7.1-Db and scFv-4-1BBL in a time-shift setting analyzed for proliferation of T cells by flow cytometry. ScDb33CD3 (33 pM) was incubated on HT1080 #33 cells for 1h before washing and the addition of PBMC. At day 3, PBMC were collected, washed and transferred to new HT1080 #33 and were then either left untreated or restimulated with scDb as indicated above. Costimulation was applied by the addition of B7.1-Db and scFv-4-1BBL (10 nM each) either during initial scDb stimulation or during scDb-mediated restimulation (consecutively or simultaneously with restimulation). On day 7, proliferation of T cells (A) or $CD8^+$ (B) and $CD8^-$ (C) T cell subsets was analyzed by flow cytometry (anti-CD3-PerCP, anti-CD8-PE). [n=3, block shift correction, mean ± SD, One-way ANOVA, Tukey post test, *** $p < 0.001$]

3.2.2.2 - Expression of Granzyme B

Analyzing unstimulated T cells only a low percentage of GrB expression (approx. 20 %) was detected, which could not be enhanced by stimulation with the scDb (Fig. 30A). Although the combined costimulation with B7.1-Db and scFv-4-1BBL enhanced the amount of GrB expressing T cells up to 40 %, it was still less effective than scDb-mediated restimulation (approx. 60 %). However, in analogy to the results obtained for T cell proliferation, both consecutive and simultaneous costimulation during restimulation further enhanced the signal to maximal percentages of GrB expressing T cells (97-98 %). Furthermore, the pattern of the effect observed for GrB^+ T cells was similar for both $CD8^+$ and $CD8^-$ subsets besides minor differences in the signal level (Fig. 30B, C).

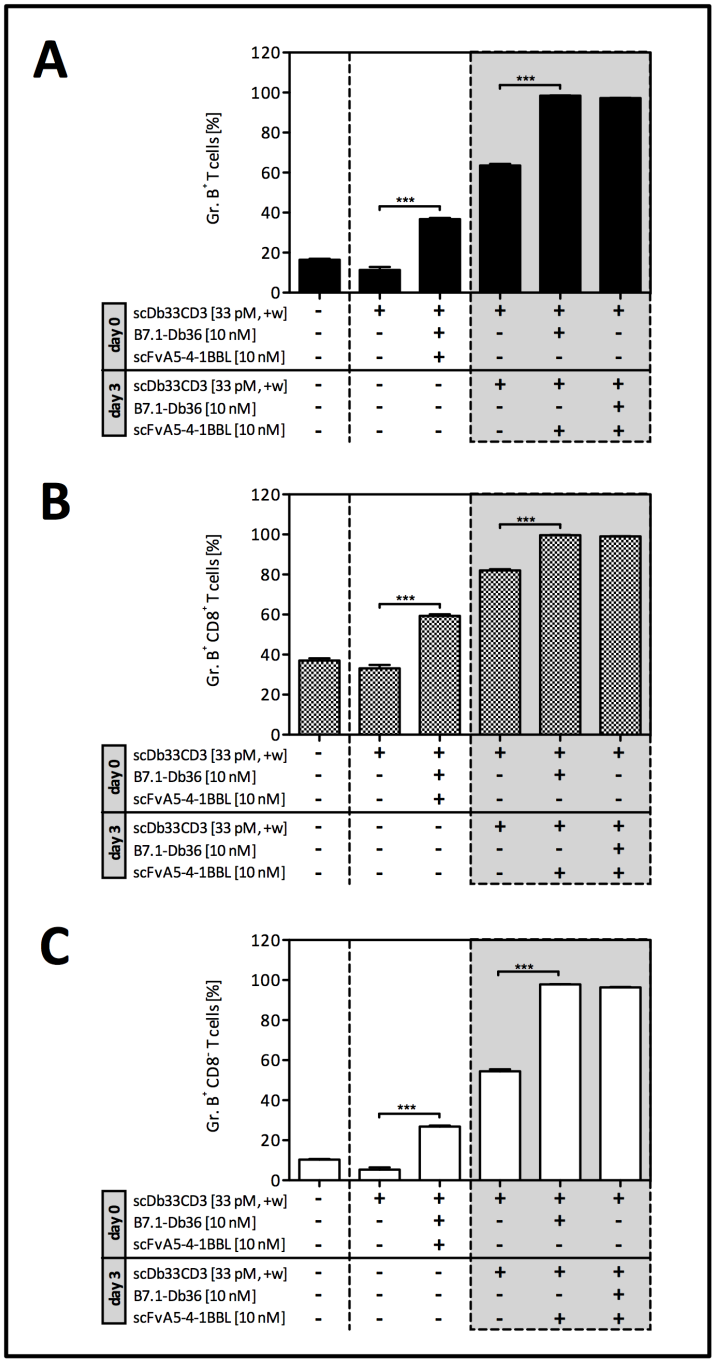

Fig. 30: Combinatorial costimulation by B7.1-Db and scFv-4-1BBL in a time-shift setting analyzed for intracellular granzyme B (GrB) expression on T cells by flow cytometry. ScDb33CD3 (33 pM) was incubated on HT1080 #33 cells for 1h before washing and the addition of PBMC. At day 3, PBMC were collected, washed and transferred to new HT1080 #33 and were then either left untreated or restimulated with scDb as indicated above. Costimulation was applied by the addition of B7.1-Db and scFv-4-1BBL (10 nM each) either during initial scDb stimulation or during scDb-mediated restimulation (consecutively or simultaneously with restimulation). On day 7, PBMC were fixed and permeabilized, stained for intracellular GrB expression of T cells (A) or $CD8^+$ (B) and $CD8^-$ (C) T cell subsets and were analyzed by flow cytometry (anti-CD3-FITC, anti-CD8-PerCP, anti-GrB-PE). [n=3, block shift correction, mean ± SD, One-way ANOVA, Tukey post test, *** $p < 0.001$]

Analysis of the mean fluorescence intensity (MFI) revealed similar patterns for the expression of GrB for both $CD8^+$ and $CD8^-$ T cells, but a more than two-fold higher signal level was observed

for the $CD8^+$ T cell subset (Fig. 31). Surprisingly, the observed pattern for the amount of GrB expression did not correlate with the pattern of the percentage of GrB positive $CD8^+$ T cells, since highest levels were detected for consecutive costimulation (MFI = 94) but not for combined late costimulation (MFI = 47). The latter showed a MFI value comparable to early combined costimulation (MFI = 43). Furthermore, scDb-mediated restimulation (MFI = 33) did not lead to an enhanced GrB expression but enhanced the percentage of GrB^+ $CD8^+$ T cells.

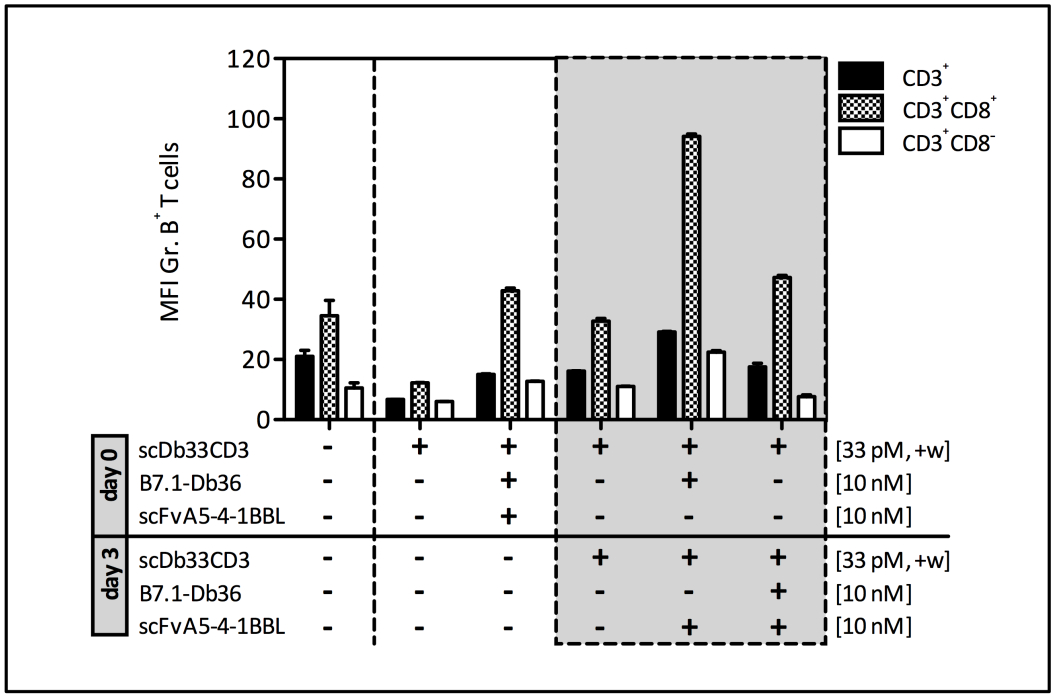

Fig. 31: Combinatorial costimulation by B7.1-Db and scFv-4-1BBL in a time-shift setting analyzed for mean fluorescence intensity (MFI) of intracellular Granzyme B (GrB) expression on T cells by flow cytometry. ScDb33CD3 (33 pM) was incubated on HT1080 #33 cells for 1h before washing and the addition of PBMC. At day 3, PBMC were collected, washed and transferred to new HT1080 #33 and were then either left untreated or restimulated with scDb as indicated above. Costimulation was applied by the addition of B7.1-Db and scFv-4-1BBL (10 nM each) either during initial scDb stimulation or during scDb-mediated restimulation (consecutively or simultaneously with restimulation). On day 7, PBMC were fixed and permeabilized and stained for intracellular GrB expression (anti-CD3-FITC, anti-CD8-PerCP, anti-GrB-PE). MFI of GrB^+ T cells or $CD8^+$ and $CD8^-$ T cell subsets was analyzed by flow cytometry. [n=3, block shift correction, mean ± SD]

3.2.2.3 - Expression of inhibitory receptors

In order to analyze whether time-shift costimulation might have an effect on the duration of the T cell response, expression of CTLA-4 and PD-1 was measured. Since the two inhibitory receptors become upregulated on the T cell surface after T cell activation and are involved in the inhibition of the immune response, a lower expression rate could be considered an indicator for T cell disposition to remain activated. CTLA-4, which is predominately localized in

intracellular perforin-containing secretory granules, is expressed at very low levels on naïve T cells and is rapidly induced after T cell activation (both via new transcription and through regulated trafficking to the cell surface)[22]. Since it was shown to bind B7.1 with a higher affinity than the costimulatory receptor CD28[23], it rapidly attenuates the T cell response. PD-1, which has two known ligands, PD-L1 and PD-L2, is constitutively expressed at low levels by naïve T cells as well, presumably to modulate activating stimuli that might result in autoreactivity[145]. Upon T cell activation, its expression is strongly upregulated. Since it could be shown that CTLA-4 and PD-1 signal through different mechanisms and play distinct roles in regulating T cell responses[146], it appears worthwhile to monitor both expression patterns following stimulation.

PD-1 expression

Expression of the inhibitory receptor PD-1 on unstimulated T cells (20 %) was significantly (*** $p < 0.001$) enhanced by initial scDb-mediated stimulation (38 %, Fig. 32A). In the case of T cells and their $CD8^-$ subset, early combined costimulation slightly further enhanced the expression level of PD-1, whereas for $CD8^+$ T cells, the amount of PD-1 positive cells was significantly lowered (Fig. 32). Moreover, a further enhancement in PD-1 expression mediated by restimulation with the scDb alone could significantly be reduced by consecutive and combined late costimulation. Here, the costimulatory effect was most prominent for the $CD8^+$ T cell population, with late combined costimulation leading to a reduction of PD-1 expression to the level of unstimulated cells (Fig. 32B). In addition, the overall level of PD-1 expression was considerably lower for the $CD8^+$ T cell population, than for the $CD8^-$ cells.

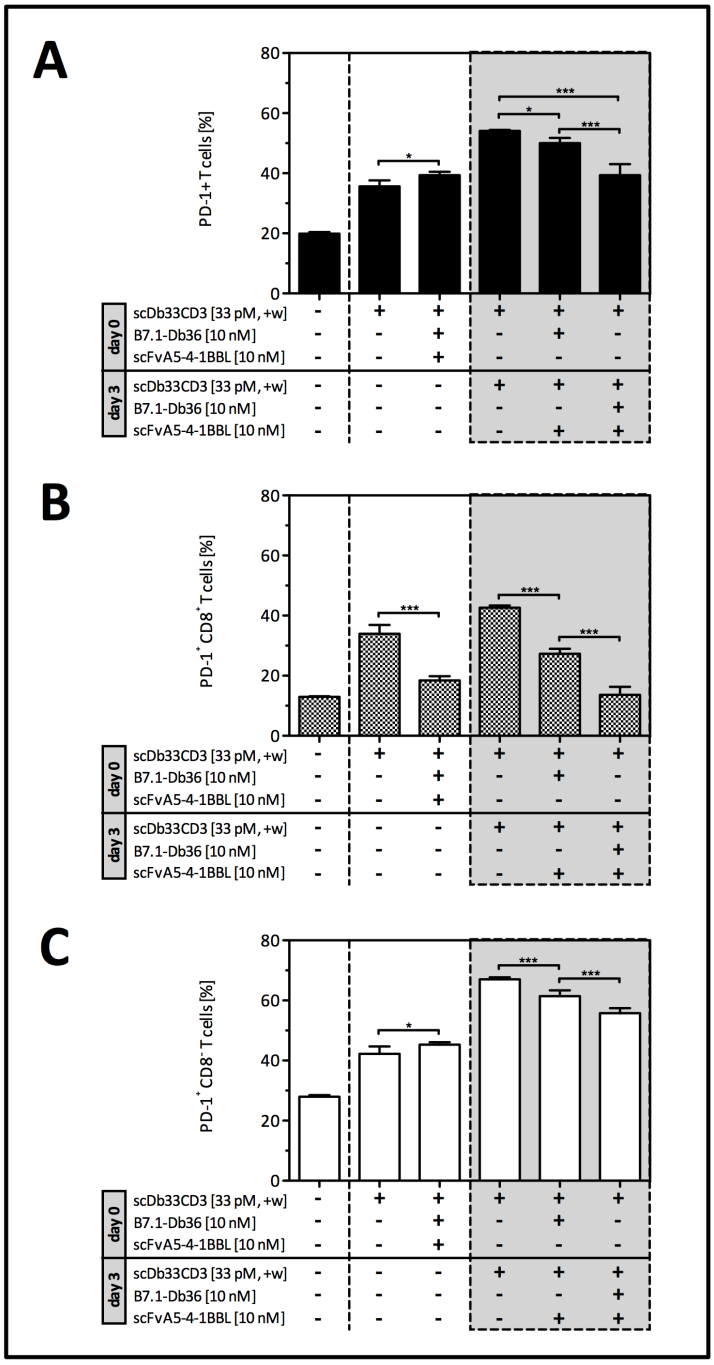

Fig. 32: Combinatorial costimulation by B7.1-Db and scFv-4-1BBL in a time-shift setting analyzed for PD-1 expression on T cells by flow cytometry. ScDb33CD3 (33 pM) was incubated on HT1080 #33 cells for 1h before washing and the addition of PBMC. At day 3, PBMC were collected, washed and transferred to new HT1080 #33 and were then either left untreated or restimulated with scDb as indicated above. Costimulation was applied by the addition of B7.1-Db and scFv-4-1BBL (10 nM each) either during initial scDb stimulation or during scDb-mediated restimulation (consecutively or simultaneously with restimulation). On day 7, PD-1 expression on T cells (A) or $CD8^+$ (B) and $CD8^-$ (C) T cell subsets was analyzed by flow cytometry (anti-CD3-PerCP, anti-CD8-PE, anti-PD-1-FITC). [n=3, block shift correction, mean ± SD, One-way ANOVA, Tukey post test, * $p < 0.05$, *** $p < 0.001$]

The intensity of PD-1 expression (MFI) did not follow the pattern observed for the percentage of PD-1^+ T cells (Fig. 33). In detail, no fundamental MFI changes could be observed for all three

cell populations, despite the finding that unstimulated $CD8^+$ T cells displayed a slightly higher signal than stimulated cells.

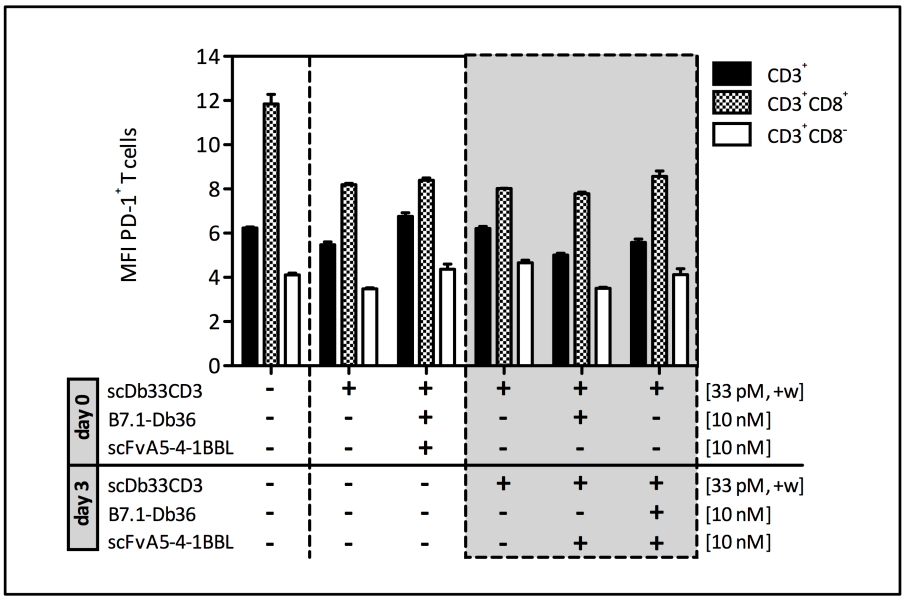

Fig. 33: Combinatorial costimulation by B7.1-Db and scFv-4-1BBL in a time-shift setting analyzed for mean fluorescence intensity (MFI) of PD-1 expression on T cells by flow cytometry. ScDb33CD3 (33 pM) was incubated on HT1080 #33 cells for 1h before washing and the addition of PBMC. At day 3, PBMC were collected, washed and transferred to new HT1080 #33 and were then either left untreated or restimulated with scDb as indicated above. Costimulation was applied by the addition of B7.1-Db and scFv-4-1BBL (10 nM each) either during initial scDb stimulation or during scDb-mediated restimulation (consecutively or simultaneously with restimulation). On day 7, the MFI of PD-1-expressing T cells or $CD8^+$ and $CD8^-$ T cell subsets was analyzed by flow cytometry (anti-CD3-PerCP, anti-CD8-PE, anti-PD-1-FITC). [n=3, mean ± SD]

CTLA-4 expression

The CTLA-4 expression pattern for overall T cells and their $CD8^+$ and $CD8^-$ subpopulations was very similar to the one observed for PD-1, although at a considerably lower expression level (Fig. 34). Here, unstimulated T cells displayed only 2-4 % of CTLA-4 expression which is in accordance with the literature[147], and scDb-mediated restimulation increased the percentage up to a maximum of 13 %.

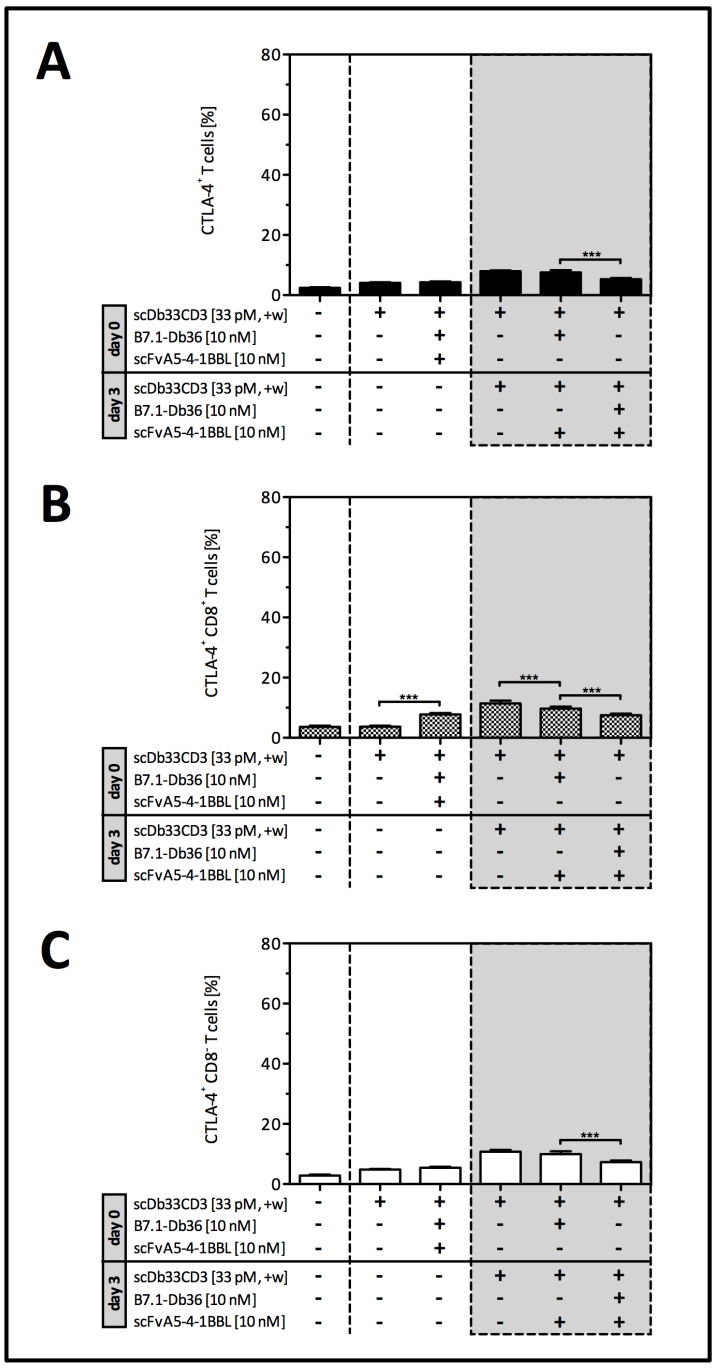

Fig. 34: Combinatorial costimulation by B7.1-Db and scFv-4-1BBL in a time-shift setting analyzed for CTLA-4 expression on T cells by flow cytometry. ScDb33CD3 (33 pM) was incubated on HT1080 #33 cells for 1h before washing and the addition of PBMC. At day 3, PBMC were collected, washed and transferred to new HT1080 #33 and were then either left untreated or restimulated with scDb as indicated above. Costimulation was applied by the addition of B7.1-Db and scFv-4-1BBL (10 nM each) either during initial scDb stimulation or during scDb-mediated restimulation (consecutively or simultaneously with restimulation). On day 7, CTLA-4 expression of T cells (A) or $CD8^+$ (B) and $CD8^-$ (C) T cell subsets was analyzed by flow cytometry (anti-CD3-FITC, anti-CD8-PerCP, anti-CTLA-4-PE). [n=3, block shift correction, mean ± SD, One-way ANOVA, Tukey post test, ** $p < 0.01$, *** $p < 0.001$]

Furthermore, also the intensity of CTLA-4 expression (MFI) was analyzed for all three T cell populations, revealing an almost constant MFI value below 5 throughout the stimulations (Fig. 35).

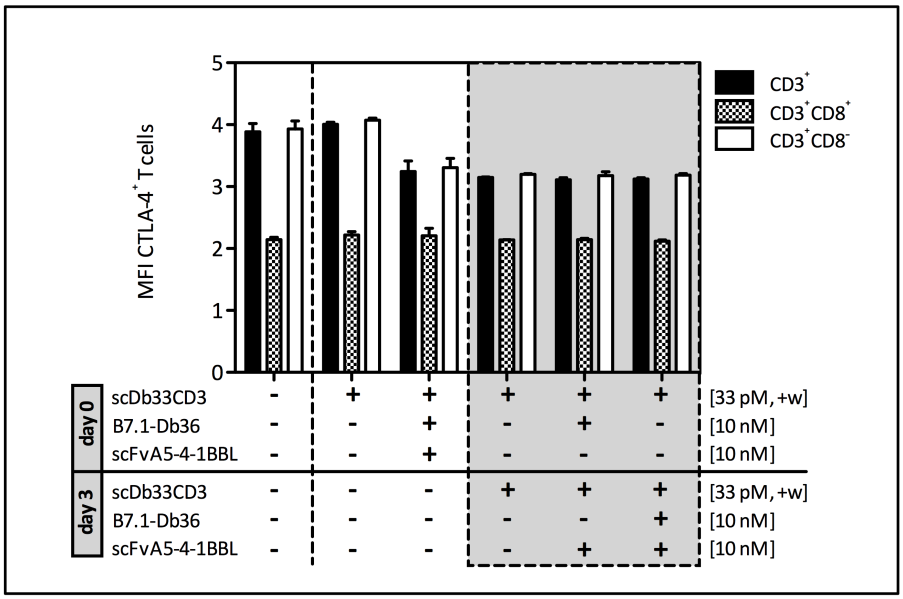

Fig. 35: Combinatorial costimulation by B7.1-Db and scFv-4-1BBL in a time-shift setting analyzed for mean fluorescence intensity (MFI) of CTLA-4 expression on T cells by flow cytometry. ScDb33CD3 (33 pM) was incubated on HT1080 #33 cells for 1h before washing and the addition of PBMC. At day 3, PBMC were collected, washed and transferred to new HT1080 #33 and were then either left untreated or restimulated with scDb as indicated above. Costimulation was applied by the addition of B7.1-Db and scFv-4-1BBL (10 nM each) either during initial scDb stimulation or during scDb-mediated restimulation (consecutively or simultaneously with restimulation). On day 7, the MFI of CTLA-4-expressing T cells or $CD8^+$ and $CD8^-$ T cell subsets was analyzed by flow cytometry (anti-CD3-FITC, anti-CD8-PerCP, anti-CTLA-4-PE). [n=3, block shift correction, mean ± SD]

3.2.3 - Time-shift costimulation in a tumor model

3.2.3.1 - Adapting the combinatorial setting for application to a mouse model

The time-shift costimulatory approach was also analyzed in an in vivo experiment using mice. Therefore, the human in vitro setting had to be adapted to the mouse system: In order to maintain the "two antigen"-strategy originally established with HT1080 #33 ($hFAP^+$, $hEDG^+$), the C57BL/6-derived melanoma cell line B16-FAP was used, which endogenously expresses mouse endoglin (mEDG) and which is transfected with human FAP. Since B7.1-Db36 is directed against human FAP, solely the antibody moiety of scFvA5-4-1BBL targeting human EDG was replaced by a mouse-specific scFv (scFvmE12). Furthermore, the bispecific antibody scDb33CD3 recognizing human CD3 (UCHT-1[117]) and human FAP, was replaced by its mouse analog scDb332C11: The latter is directed against mouse CD3 (2C11[148]) and human FAP and was cloned and

characterized previously in our lab. From literature it is known that B7 is cross-reactive against its mouse counterpart[149] while 4-1BBL shows only a weak interaction with mouse 4-1BB[150]. Based on these findings, a scFvmE12 fusion protein with mouse 4-1BBL (scFvmE12-m4-1BBL) was used[151]. In order to revise cross-reactivity, the binding ability of hB7.1-Db, scFv-h4-1BBL and scFv-m4-1BBL to their respective receptor of human or mouse origin was analyzed in an ELISA. Therefore, the fusion proteins were coated on an ELISA plate, followed by the application of the respective receptors (hCTLA-4-Fc, mCD28-Fc, h4-1BB-Fc or m4-1BB-Fc). Cross-reactivity of the B7.1-fusion protein was confirmed, since it bound to both the human and the murine receptor in a concentration-dependent manner (B7.1-Db, hCTLA-4-Fc: EC_{50} = 7.3 nM, B7.1-Db, mCD28-Fc: EC_{50} = 33.2 nM) (Fig. 36A).

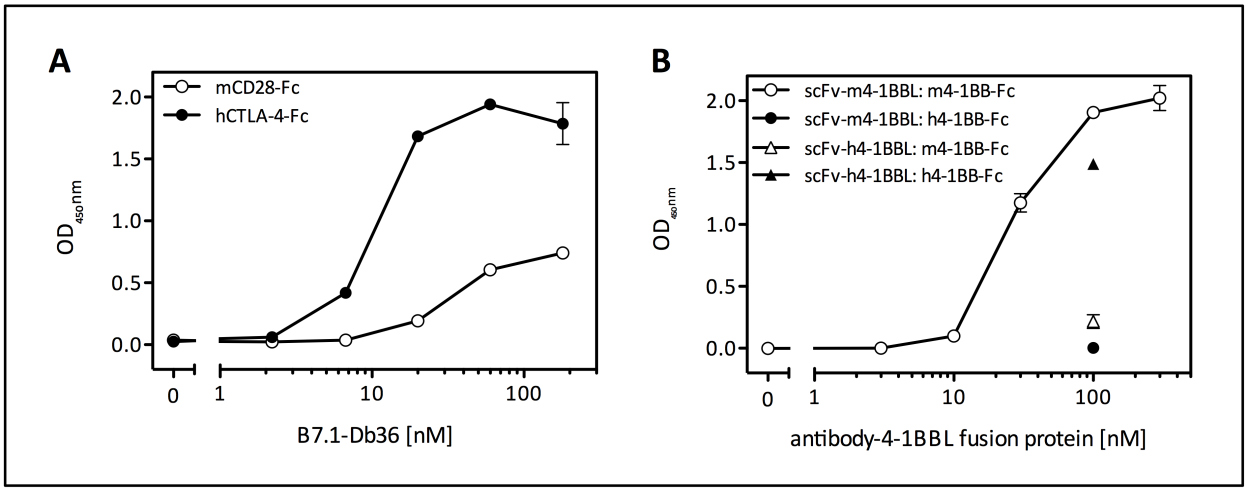

Fig. 36: Cross-reactivity of the ligands hB7.1 (B7.1-Db36), h4-1BBL (scFvA5-h4-1BBL) or m4-1BBL (scFvmE12-m4-1BBL) analyzed via ELISA. Titrating concentrations of hB7.1-Db36 (180-2.1 nM) (A) or scFvmE12-m4-1BBL (300-3 nM) (B) were coated on an ELISA plate. As a control, also 100 nM scFvA5-h4-1BBL was applied (B). Binding to their respective human or murine receptors (B7.1-Db36: hCTLA-4-Fc, mCD28-Fc; scFvmE12-m4-1BBL: h4-1BB-Fc, m4-1BB-Fc) was detected via a Fc-specific HRP-conjugated antibody. [n=1, mean ± SD]

In the case of h4-1BBL, non-cross-reactivity between mouse and human was confirmed since binding was only detected to human 4-1BB but not to mouse 4-1BB. ScFvmE12-m4-1BBL bound to the corresponding mouse receptor and was therefore suitable for the in vivo experiment (Fig. 36B).

In a next step, antigen-specific binding of the antibody moieties was reassessed by incubating 10 µg/ml of the recombinant proteins with B16-FAP ($hFAP^+$, $mEDG^+$) or antigen-negative control cells (HEK293: $hFAP^-$, $mEDG^-$), followed by detection via a PE-conjugated anti-His-tag antibody.

Strong binding of scDb332C11, B7.1-Db36 and scFvmE12-m4-1BBL to B16-FAP cells was detected, while no binding could be observed for antigen-negative HEK293 cells (Fig. 37).

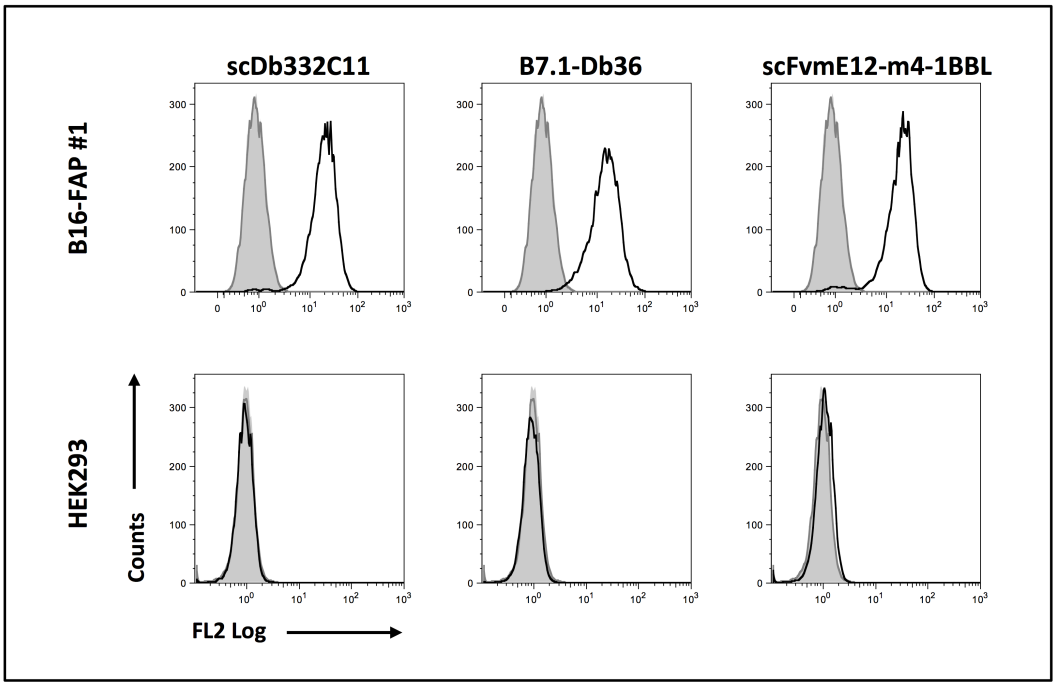

Fig. 37: Specific binding of scDb332C11, B7.1-Db36 and scFvmE12-m4-1BBL to antigen-positive cells analyzed via flow cytometry. Antigen-positive B16-FAP (hFAP$^+$, mEDG$^+$) or antigen-negative HEK293 (hFAP$^-$, mEDG$^-$) cells were incubated with 10 µg/ml scDb332C11, B7.1-Db36 or scFvmE12-m4-1BBL. Bound constructs were detected via a PE-conjugated anti-His-tag antibody (gray filled: cells, dark grey line: detection antibody, black line: construct with detection antibody).

The stimulatory and costimulatory potential of scDb332C11 and scFvmE12-m4-1BBL had been analyzed in B16-FAP coculture assays with mouse splenocytes[151]. In addition, antitumor activity of the scDb332C11 had been shown previously in the lab in a syngeneic subcutan tumor mouse model (B16-FAP cells in C57BL/6) (data not published).

Pharmacokinetic studies

The pharmacokinetic potential of the costimulatory antibody-ligand fusion proteins was analyzed by injecting 0.5 nmol scFvmE12-m4-1BBL or B7.2-Db36 intravenously (i.v.) into the tail vein of C57BL/6 mice. After different time points (3 min, 0.5, 1, 2, 6 and 24 h), blood samples were taken, followed by the determination of the serum concentration of the respective fusion protein via ELISA. Here, both recombinant proteins revealed a biphasic elimination from circulation with a similar initial ($t_{1/2}\alpha$: approx. 24-25 min) and terminal ($t_{1/2}\beta$: approx. 6-7 h) half-

life as well as a comparable bioavailability (area under the curve (AUC): approx. 131-149 h·%) (Fig. 38, Table 2).

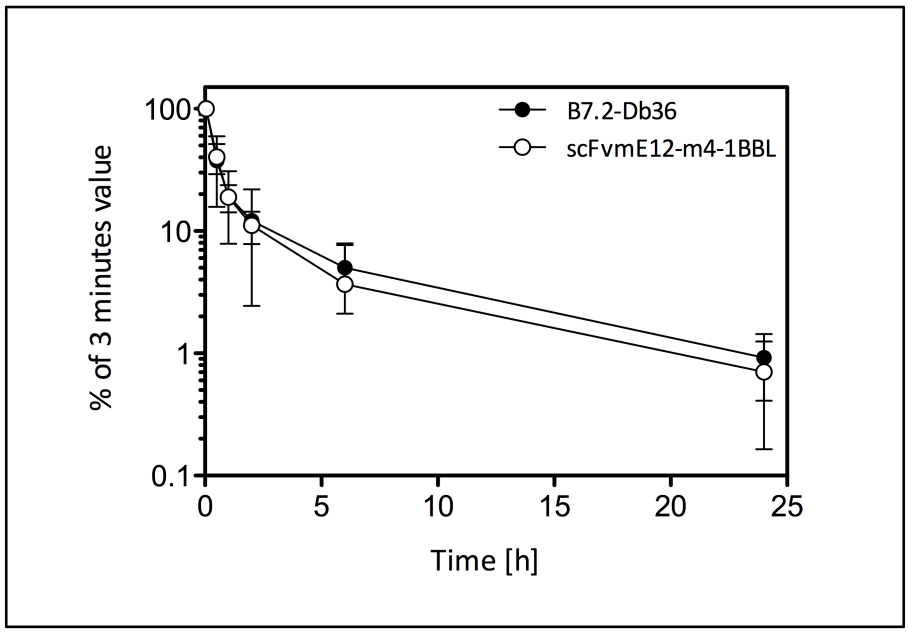

Fig. 38: Pharmacokinetic study of B7.2-Db36 and scFvmE12-m4-1BBL. 0.5 nmol of each fusion protein was injected i.v.into C57BL/6 mice (n= 3–4) and serum concentration was determined at different time points (3 min, 0.5, 1, 2, 6 and 24 h) via an ELISA. Data was normalized considering the first time point (3 min) as 100 %. [mean ± SD]

Table 2: Pharmacokinetic parameters for B7.2-Db36 and scFvmE12-m4-1BBL.

Fusion protein	Molecular mass [kDa]	$t_{1/2}\alpha$ [min]	$t_{1/2}\beta$ [h]	$AUC_{(0\text{-}24h)}$ [h·%]
B7.2-Db36	107.6	24.5 ± 9.2	6.6 ± 1	148.8 ± 76.4
scFvmE12-m4-1BBL	149.4	23.9 ± 3.5	6.0 ± 0.6	130.7 ± 62.9

($t_{1/2}\alpha$: initial half-life, $t_{1/2}\beta$: terminal half-life, AUC: area under the curve)

3.2.3.2 - Therapeutic potential of time-shift costimulation

The therapeutic potential of the combinatorial approach with antibody-ligand fusion proteins was evaluated using a syngeneic pulmonary metastasis mouse model. For this experimental setting, 0.85-1·10^6 B16-FAP cells were injected i.v. in the tail vein of C57BL/6 mice on day 0, followed by treatment (intraperitoneal, i.p.) once a day with the recombinant proteins (scDb: 4 pmol, fusion proteins: 0.2 nmol each) at an early (days 1, 2, 3) and late (days 10, 11, 12) stage. On day 21, mice were sacrificed, their lungs were removed and tumor burden was determined by counting of the pulmonary metastasis.

Based on the in vitro setting, in which best results were obtained for consecutive and late combined costimulation with B7.1-Db and scFv-4-1BBL, these two settings were ought to be translated in vivo. Therefore, in the time-shift costimulation setting, B7.1-Db36 was applied along with the scDb at the early time points (days 1, 2 and 3), while scFvmE1-m4-1BBL was administered together with the scDb at the later time points (days 10, 11 and 12). In contrast, in the second costimulatory setting, B7.1-Db and scFv-4-1BBL were applied simultaneously on day 10, 11 and 12 along with the bispecific antibody, while at the early time points (day 1, 2 and 3) mice were treated solely with the scDb. In order to see whether the antibody-ligand fusion proteins display a therapeutic effect on their own, both costimulatory settings were also applied in the absence of the scDb.

Strongest antitumor effects were observed for treatment with the scDb in combination with both costimulatory fusion proteins, resulting in an average reduction in metastasis formation of 86 % for consecutive and 77 % for late combined costimulation (Fig. 39). On their own, the fusion proteins displayed only a slight therapeutic potential (30 and 34 % average reduction), which was comparable to the effect of the scDb alone (29 % average reduction). Thus, combined costimulation with B7.1-Db and scFv-m4-1BBL led to a considerable improvement of the scDb-induced antitumor effect.

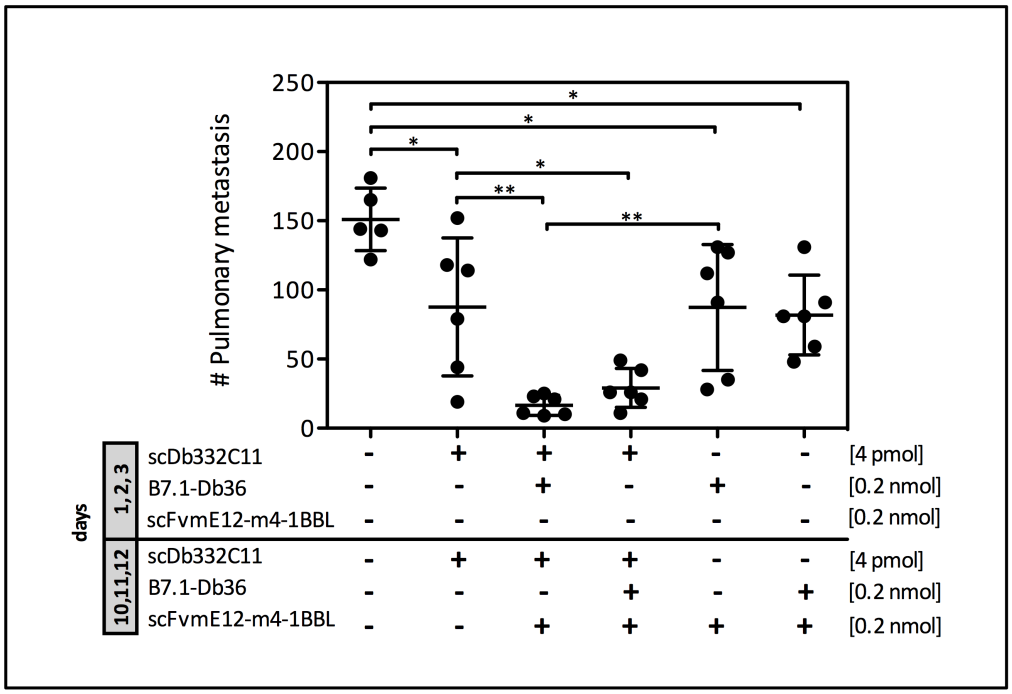

Fig. 39: Therapeutic potential of time-shift costimulation analyzed in a lung metastasis mouse model. C57BL/6 mice were injected i.v. with $0.85 \cdot 10^6$ B16-FAP cells on day 0. Treatment with the indicated antibody combinations and concentrations or control PBS was performed 3-fold at an early time point (days 1, 2, 3) and 3-fold at a later time point (days 10, 11, 12). Mice were sacrificed on day 21, lungs were removed and metastasis counted. [n=5-6 mice/group, One-way ANOVA, * $p < 0.05$, ** $p < 0.01$]

3.3 - Antibody-ligand fusion proteins with other costimulatory members of the TNF-superfamily

3.3.1 - Generation, expression and biochemical characterization

In addition to expanding the costimulatory antibody-ligand fusion protein spectrum with members of the Immunoglobulin-superfamily (3.1.4), also TNF-SF ligand-based fusion proteins were generated. Therefore, the ligands, LIGHT, GITRL and OX40L were chosen based on their high antitumor potential documented in the literature[6]. In order to allow for combinatorial costimulatory approaches with either B7.1-Db36 or scFvA5-4-1BBL and to avoid potential antigen-targeting competition between the antibody moieties, each ligand was fused to a scFv directed against FAP (mo36) or EDG (A5). Additionally, in the case of the GITR ligand, a fusion protein with a tenascin C (TNC) trimerization domain in the linker was generated (scFvA5-/scFv36-TNC-GITRL) in order to enhance the stability of the trimeric protein through disulfide bonds. The successful trimerization based on the TNC-domain could already be shown for several TNF ligand-based constructs, such as Flag-TNC-GITRL, Flag-TNC-CD27L and TNF-Flag-4-1BBL[58]. Furthermore, one of the scFv36-TNF ligand-fusion proteins was already present in our lab, namely scFv36-LIGHT, which was cloned and characterized by a former diploma student[88].

For the generation of the scFv36-TNF-SF ligand fusion proteins, the 4-1BBL domain in the scFv36-4-1BBL sequence was replaced by the sequence coding for the extracellular domain of the respective TNF-SF ligand. The scFv36-TNF-SF ligand fusion proteins were then used as templates for the generation of the analogous scFvA5-TNF-SF ligand fusion proteins by exchanging the antibody moiety scFv36 for scFvA5 (Fig. 40).

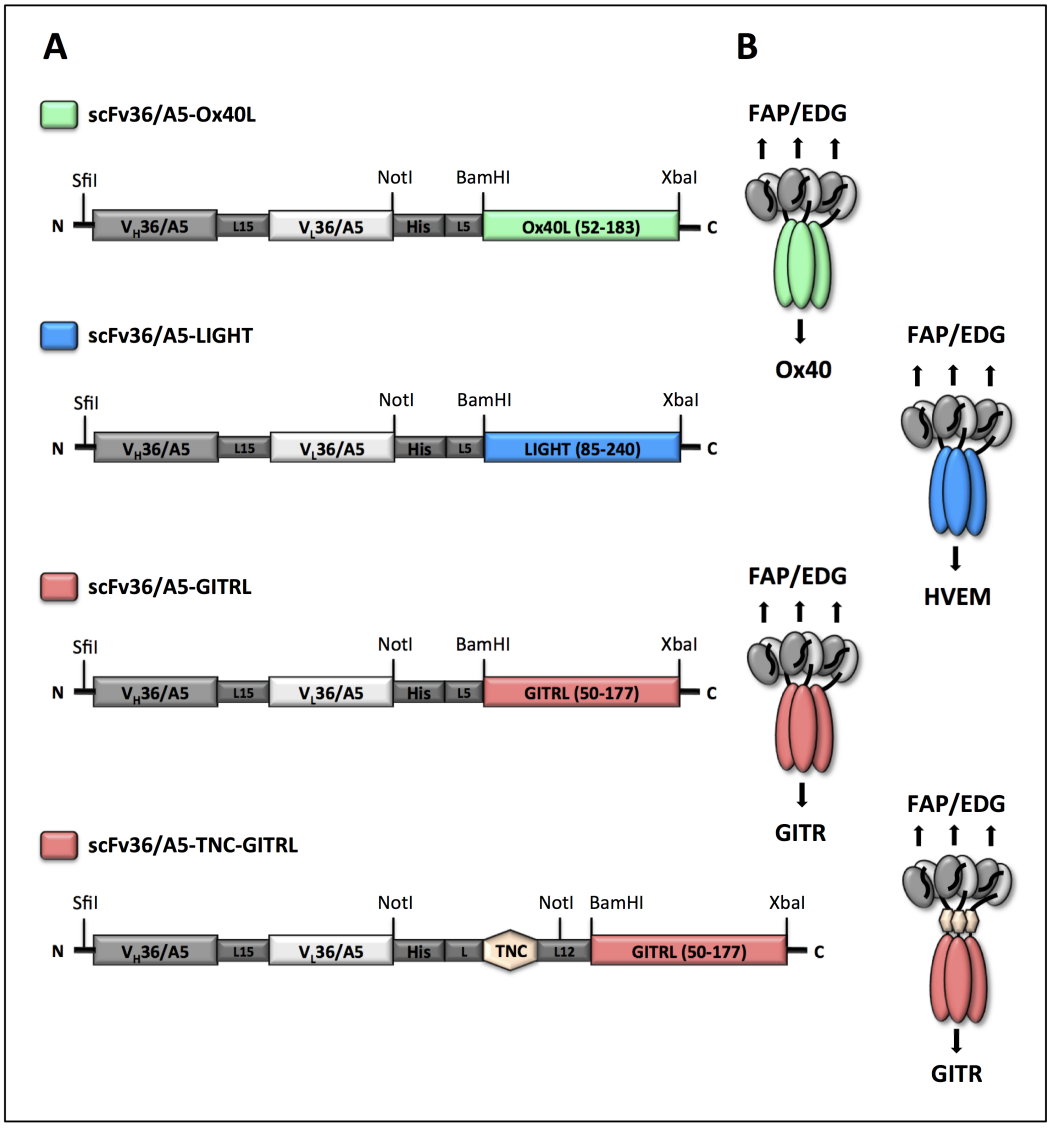

Fig. 40: Schematic representation of scFv36/A5-ligand fusion proteins of the TNF-superfamily. (A) Arrangement of the variable domains of the heavy (V_H) and the light chain (V_L) specific for FAP (mo36) or endoglin (A5) and the extracellular domain of Ox40L, LIGHT or GITRL (L5, L15, L12: linker; His: His-tag; TNC: tenascin C). (B) Structural scheme of the trimerized fusion proteins (linker: black lines). Antigen and receptor binding sites are indicated with arrows.

Expression, purification and biochemical characterization

The scFvA5- and scFv36-ligand fusion proteins of the TNF-superfamily were expressed and produced in HEK293 cells stably transfected with the pSecTagAHis vector encoding the appropriate sequences. In contrast, the scFv36-Ox40L construct could not be expressed, neither in transiently nor in stably transfected HEK293 cells. For purification, the proteins were precipitated from the supernatant and purified via Ni-NTA IMAC with yields ranging from 0.1 to 17.4 mg/l (Table 3).

Table 3: Yields of eukaryotically produced and IMAC-purified scFvA5- and scFv36-TNF-SF ligand fusion proteins

Recombinant protein	Mode of production	Yield [mg/l supernatant]
scFvA5-Ox40L	Eukaryotic (HEK 293)	2.4
scFvA5-LIGHT	Eukaryotic (HEK293)	17.4
scFvA5-TNC-GITRL	Eukaryotic (HEK 293)	8
scFv36-LIGHT	Eukaryotic (HEK 293)	0.9
scFv36-GITRL	Eukaryotic (HEK 293)	0.2
scFv36-TNC-GITRL	Eukaryotic (HEK 293)	0.7

According to Fig. 41, all proteins were obtained with high purity. ScFvA5-TNF-SF ligand fusion proteins showed mostly single bands under reducing or non-reducing conditions, while for scFv36-GITRL and -TNC-GITRL pronounced double bands could be detected. For both scFvA5- and scFv36-TNC-GITRL, bands with higher molecular mass could be observed under non-reducing conditions, which most likely seemed to be TNC-domain linked multimers. Since the exact size of the bands could not be determined from the 12 % PAA-gel, scFvA5-TNC-GITRL was separated under non-reducing conditions in a 4-12 % gradient gel revealing three bands at 127, 178 and 222 kDa (Fig. 41B). Furthermore, for all fusion proteins the bands were diffuse and the calculated molecular masses were higher than expected from their sequence (Table 4). This finding could most likely be attributed to glycosylation, since all three costimulatory ligands comprise potential N-linked glycosylation sites (Ox40L: 4, GITRL: 2, LIGHT: 1) and it might also account for the double bands observed for scFv36-(TNC-)GITRL. In order to revise it, proteins were digested with PNGase F and as indicated in Fig. 42, more distinct bands at lower molecular masses were obtained for scFvA5-LIGHT and -TNC-GITRL. Although a double band was still detectable for scFvA5-Ox40L and scFv36-(TNC-)GITRL, a reduction in the slower migrating band and an increase in the faster migrating band could be observed (Table 4).

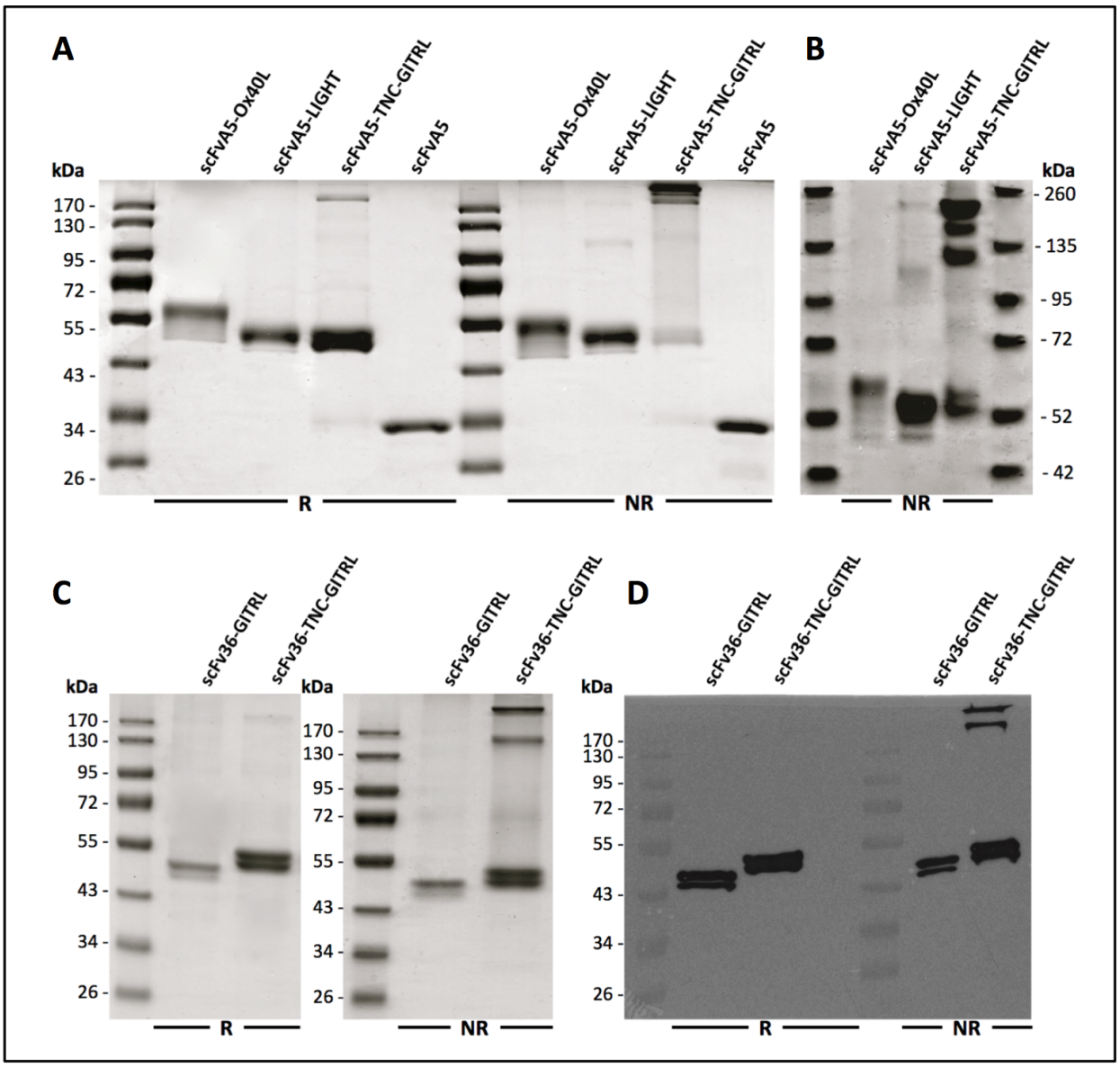

Fig. 41: SDS-PAGE and Western blot of purified scFvA5- and scFv36-TNF-SF ligand fusion proteins. IMAC purified proteins were analyzed via SDS-PAGE (A, C) or Western blot (D) under reducing (R) or non-reducing (NR) conditions (12 %, 3 µg/lane, Coomassie staining). (B) To improve separation of the high molecular mass bands seen for scFvA5-TNC-GITRL under non-reducing conditions, a gradient gel was applied (NuPAGE® 4-12 % Bis-Tris Gel).

Table 4: Overview of molecular masses (M_m) for scFvA5- and scFv36-TNF-SF ligand fusion proteins.

Molecular masses (M_m)	scFvA5-Ox40L	scFvA5-LIGHT	scFvA5-TNC-GITRL	scFv36-GITRL	scFv36-TNC-GITRL
M_m [kDa] calculated from amino acid sequence	42.3	44	45.6	42.9	47
M_m [kDa] determined by SDS-PAGE under nonreducing conditions	53.1	51	127, 178, 222	47,5	50, 53, 155
M_m [kDa] determined by SDS-PAGE under reducing conditions	58	51	51	47,5	50,53
M_m [kDa] of deglycosylated proteins determined by SDS-PAGE under reducing conditions	48,5	48.5	50	45, 48.5	48,52

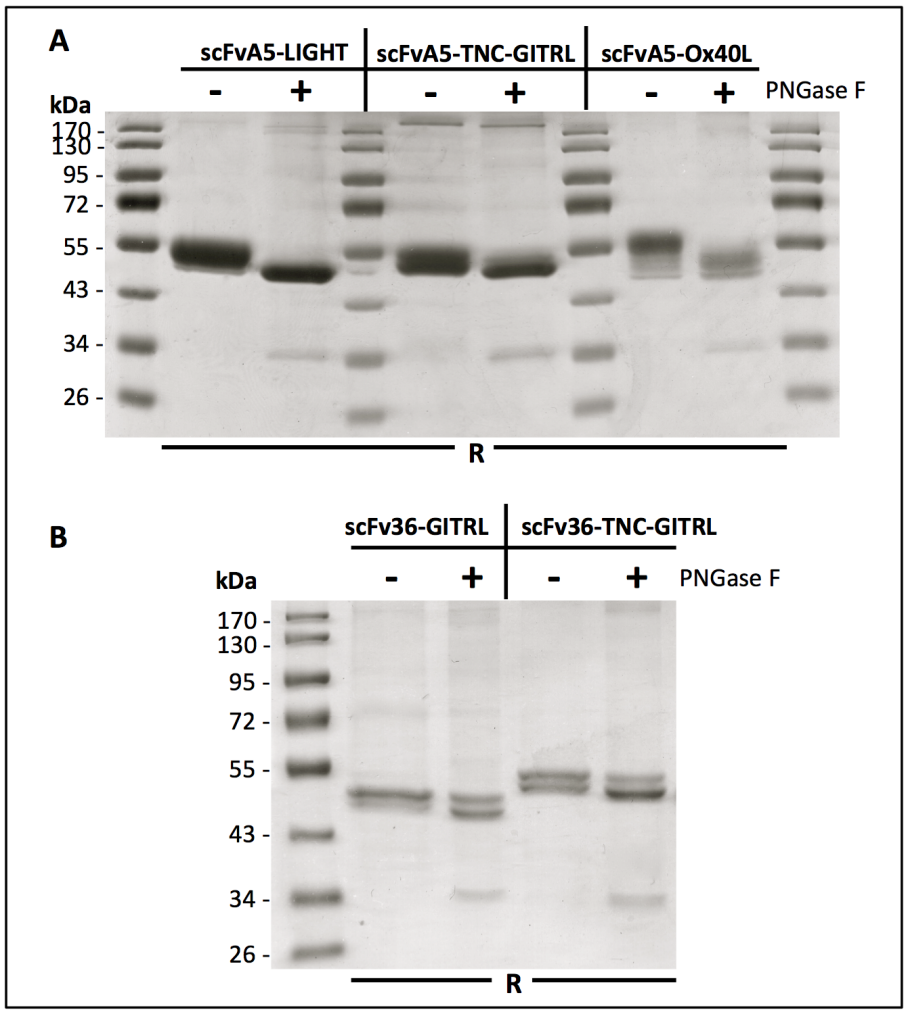

Fig. 42: Deglycosylation of scFvA5- and scFv36-TNF-SF ligand fusion proteins analyzed in SDS-PAGE. 3 µg protein were digested with N-glycosidase PNGase F and were compared to untreated protein under reducing conditions (R) (12 %, 3 µg/lane, Coomassie staining).

Using HPLC analysis, mainly homogenous populations with one major defined peak could be observed for all scFvA5-TNF-SF ligand fusion protein in their native state (Fig. 43).

Determination of the size of the proteins via a set of standard proteins revealed molecular masses correlating with the presence of trimers (scFvA5-Ox40L: 148 kDa, scFvA5-LIGHT: 160 kDa, scFvA5-TNC-GITRL: 174 kDa). Differences between the molecular masses calculated from the protein sequences and the experimentally determined ones are most likely due to glycosylation (Table 4).

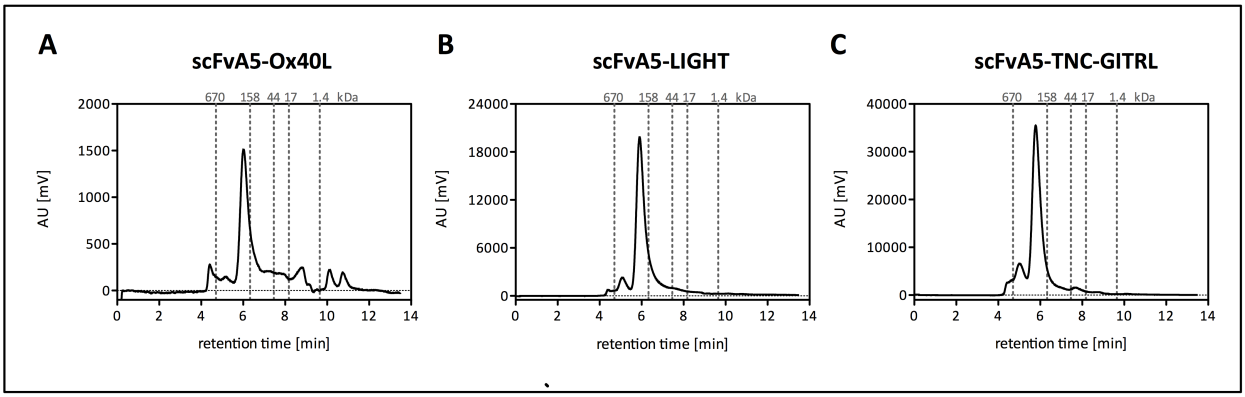

Fig. 43: HPLC analysis of scFvA5-TNF-SF ligand fusion proteins. 2 µg scFvA5-Ox40L (A), 15 µg scFvA5-LIGHT (B) and 15 µg scFvA5-TNC-GITRL (C) were loaded on a TSK-GEL G3000SW$_{XL}$ column with PBS as mobile phase. Peak positions of standard proteins are indicated.

3.3.2 - Binding studies

Target cell-specific binding of the scFvA5- and the scFv36-ligand fusion proteins of the TNF superfamily was analyzed via flow cytometry. Therefore, the recombinant proteins (300 nM each) were incubated on antigen-positive (EDG$^+$, FAP$^+$: HT1080 #33) or antigen-negative (EDG$^-$: HEK293; FAP$^-$: HT1080 wt) cells and were detected via their His-tag. As expected, specific binding of each fusion protein was solely observed to antigen-positive cells, whereas in the absence of the respective antigen, no binding could be detected (Fig. 44).

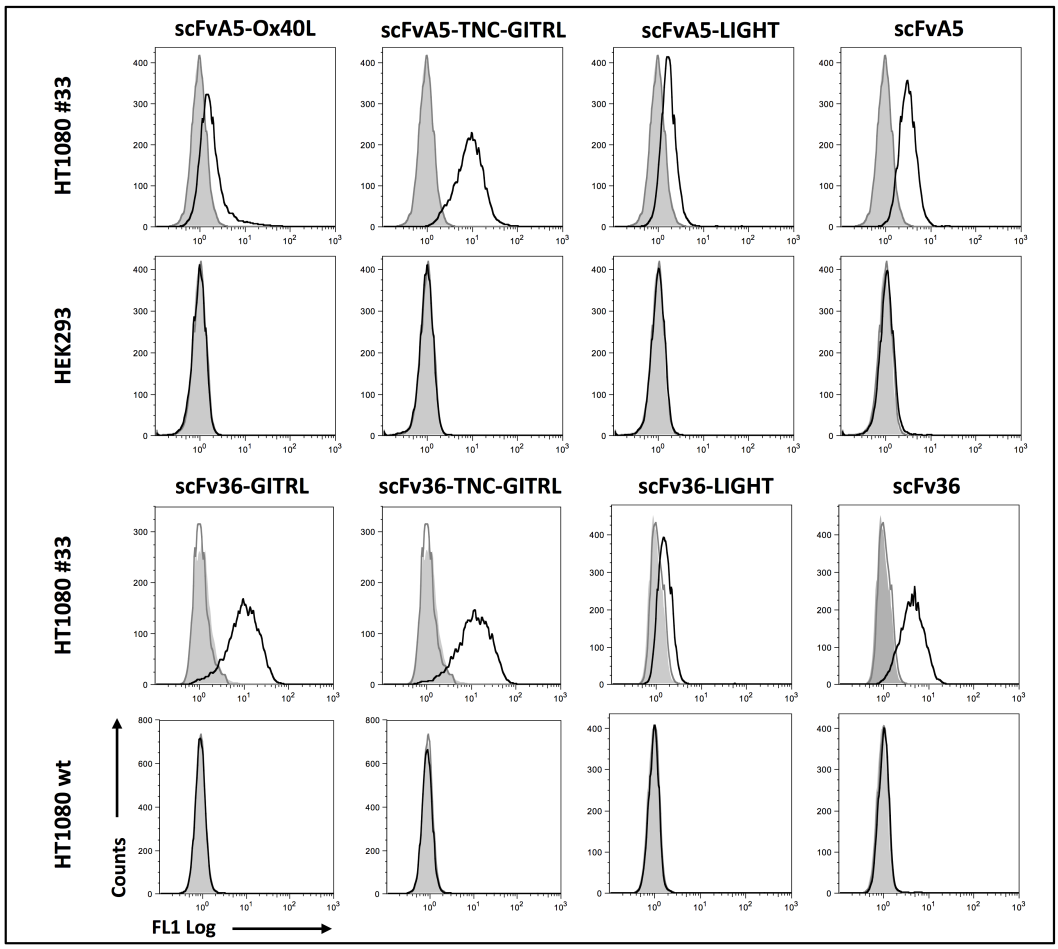

Fig. 44: Specific binding of scFvA5- and scFv36-TNF-SF ligand fusion proteins to FAP-positive cells analyzed via flow cytometry. HT1080 #33 (FAP^+, EDG^+), HT1080 wt (FAP^-, EDG^+) or HEK293 (FAP^-, EDG^-) were incubated with scFvA5-Ox40L, scFvA5-TNC-GITRL, scFvA5-LIGHT, control scFvA5, scFv36-GITRL, scFv36-TNC-GITRL, scFv36-LIGHT or control scFv36 (300 nM each). Bound constructs were detected via a FITC-conjugated anti-His-tag antibody (gray filled: cells, dark grey line: detection antibody, black line: construct with detection antibody).

In the following, scFv36-TNC-GITRL was applied instead of scFv36-GITRL, since the latter showed a tendency to precipitate during the thawing process resulting in very low concentrations.

3.3.3 - Costimulatory activity of the fusion proteins

In order to verify the costimulatory potential of the TNF-SF ligands independent of their antibody moiety, they were analyzed in an immobilized form, thus mimicking a cross-linked state. Therefore, the scDb was titrated (1, 3, 10 nM) and coated in an ELISA plate in the presence or absence of scFvA5- or scFv36-ligand fusion proteins of the TNF-superfamily (50 nM each) in either coated or soluble from.

Costimulation with all antibody-ligand fusion proteins in a cross-linked, i.e. coated form, significantly enhanced scDb-induced PBMC proliferation at all three tested scDb concentrations, while their soluble form remained mainly inactive (Fig. 45A, C-F). Strongest effects were obtained for either 3 nM (scFv36-TNC-GITRL and -LIGHT) or 10 nM scDb (scFvA5-Ox40L, -TNC-GITRL and -LIGHT) with the signals ranging from 7- to 10.8-fold costimulatory enhancement. As expected, the control (scFvA5) did not interfere with the proliferation of scDb-stimulated PBMC (Fig. 45B).

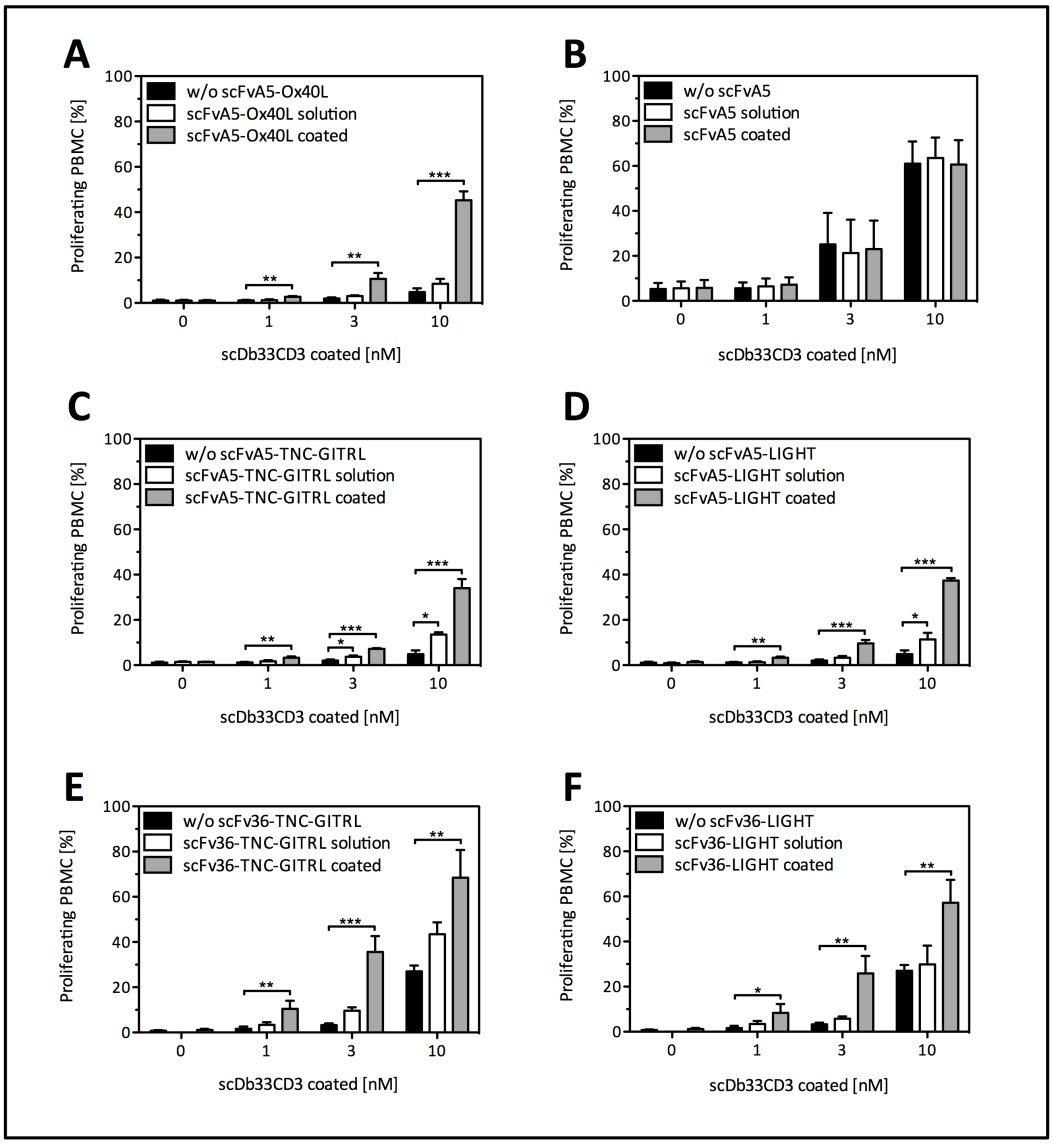

Fig. 45: Costimulatory activity of scFvA5- and scFv36-TNF-SF ligand fusion proteins in coated or soluble form analyzed by proliferation of PBMC via flow cytometry. ScDb33CD3 was titrated and coated in an ELISA plate in the presence or absence of 50 nM scFvA5-Ox40L (A), control scFvA5 (B), scFvA5-TNC-GITRL (C), scFvA5-LIGHT (D), scFv36-TNC-GITRL (E) or scFv36-LIGHT (F) in coated or soluble form. Proliferation of CFSE-labeled PBMC was measured after 4 days by flow cytometry. [n=3, mean ± SD, One-way ANOVA, Tukey post test, * $p < 0.05$, ** $p < 0.01$, *** $p < 0.0001$]

To assess the costimulatory potential of the TNF-SF ligand fusion proteins in the presence of target cells, the fusion proteins were titrated (90-0.3 nM) and incubated together with a constant concentration of scDb (16 pM). After four days, proliferation of PBMC was analyzed.

Under these conditions, no costimulation-mediated enhancement of the scDb-induced signal could be observed for the fusion proteins with the scFv36 (data not shown). A possible explanation could be a competitive effect between scDb33CD3 and the scFv36 moiety for FAP binding, although under equal conditions, a costimulatory effect for B7-Db36 fusion proteins

could be detected. In contrast, scFvA5-LIGHT, scFvA5-TNC-GITRL and scFvA5-Ox40L targeting a different antigen than the scDb (EDG), enhanced scDb-mediated PBMC proliferation in a concentration-dependent manner, with strongest effect (scFvA5-LIGHT: 2.6-, scFvA5-TNC-GITRL: 1.8-, scFvA5-Ox40L: 2.2-fold increase) at lower concentrations (1-3 nM) (Fig. 46). Even at 0.3 nM, a significant enhancement of the scDb-induced signal could be observed for the LIGHT-, GITRL- and Ox40L-based constructs, whereas scFvA5-4-1BBL showed its strongest costimulatory effect at 10 nM (1.8-fold increase). Since in the absence of scDb, no signal could be detected for the fusion proteins, the costimulatory nature of their activity was confirmed.

Thus, although both the scFvA5- and the scFv36-TNF-SF ligand fusion proteins were shown to be functional in terms of antibody-mediated tumor targeting and in displaying a costimulatory activity in a cross-linked, i.e. coated form, only the former ones were shown to be suitable for the incorporation into the target cell-based combinatorial setting established above (3.1.3).

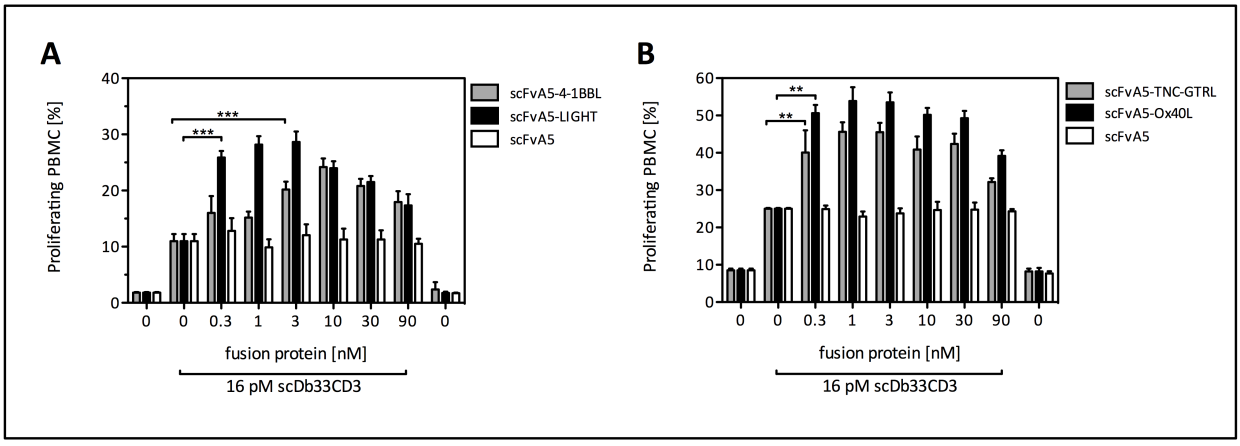

Fig. 46: Costimulatory activity of scFvA5-TNF-SF ligand fusion proteins analyzed by PBMC proliferation. ScFvA5-4-1BBL (A), scFvA5-LIGHT (A), scFvA5-TNC-GITRL (B), scFvA5-Ox40L (B) or control scFvA5 (A, B) were titrated and incubated on HT1080 #33 (FAP^+, EDG^+) in the presence of 16 pM scDb33CD3 for 1 hour before addition of CFSE-labeled PBMC. After 4 days, PBMC proliferation was measured by flow cytometry. [n=3, mean ± SD, block shift correction, One-way ANOVA, Tukey post test, ** $p < 0.01$, *** $p < 0.0001$]

3.3.4 - Combined costimulation of scFvA5-TNF-SF ligand fusion proteins with scFv-4-1BBL or B7.1-Db

ScFvA5-Ox40L, -LIGHT and -TNC-GITRL were combined with either a member of the Ig (B7.1-Db36)- or another member of the TNF (scFvA5-4-1BBL)-superfamily and their combined costimulatory potential in the presence of the scDb33CD3 was analyzed and compared. For the combinatory approach with B7.1-Db36, the setting was in analogy to the experiments shown

earlier (3.1.3), with both fusion proteins targeting separate antigens (B7.1-Db36: FAP, scFvA5-TNF-SF ligand fusion proteins: EDG) (Fig. 47, Setting I).

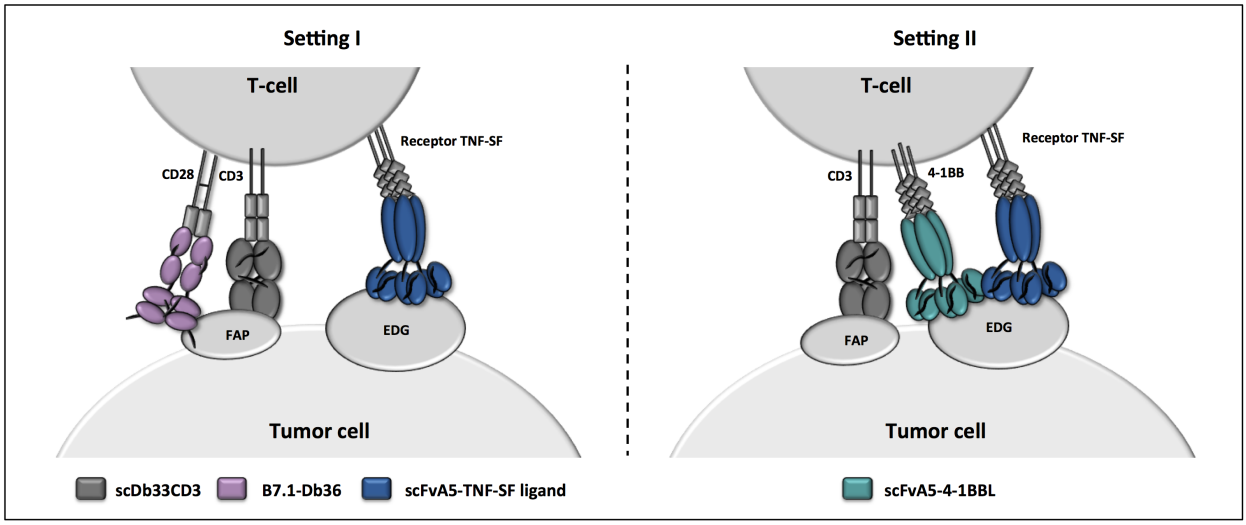

Fig. 47: Schematic representation of 2 different settings for combined T cell stimulation with a scDb and costimulatory antibody-ligand fusion proteins. In setting I, costimulation was provided by a member of the Ig- and a member of the TNF superfamily targeting different antigens (FAP and EDG), while in setting II, 2 TNF-ligand fusion proteins targeting the same antigen (EDG) were combined. In both settings, the first stimulus was provided by the scDb targeting FAP and CD3.

In contrast, for the combination with scFvA5-4-1BBL, both fusion proteins targeted the same antigen (EDG) (Fig. 47, Setting II). Therefore, scFvA5-4-1BBL was applied at a concentration (10 nM), at which an equal concentration of scFvA5 did not interfere with its costimulatory signal and the two-fold concentration led to a further signal enhancement. Accordingly, in order to exclude unequal conditions for EDG-binding, the second scFvA5-TNF-SF ligand fusion protein was applied at the same concentration.

For the analysis, the costimulatory antibody-ligand fusion proteins (10 nM) were incubated together with the scDb (16 pM) on HT1080 #33 cells before addition of PBMC. Cytokine release was analyzed after 4 days, while proliferation and intracellular GrB expression by T cells and $CD8^+$ and $CD8^-$ T cell subsets was measured after 7 days.

3.3.4.1 - Cytokine release assays

Analysis of IFN-γ levels in the supernatant revealed that all 5 costimulatory antibody-ligand fusion proteins significantly (*** $p < 0.0001$) enhanced scDb-induced T cell activation to a similar extent (2.3 to 3.3-fold) (Fig. 51). For the combination of scFvA5-4-1BBL with the scFvA5-

TNF-SF ligand fusion proteins it could be shown that each fusion protein significantly (*** $p < 0.0001$) enhanced IFN-γ release compared to the effect of scFvA5-4-1BBL-mediated costimulation alone (1.9-2.1-fold increase), while also the two-fold concentration of scFvA5-4-1BBL enhanced cytokine release to a similar level. Due to the control scFvA5, which did not decrease the signal of scFvA5-4-1BBL-mediated costimulation, a competition for EDG binding could be excluded for the concentration range used in this assay.

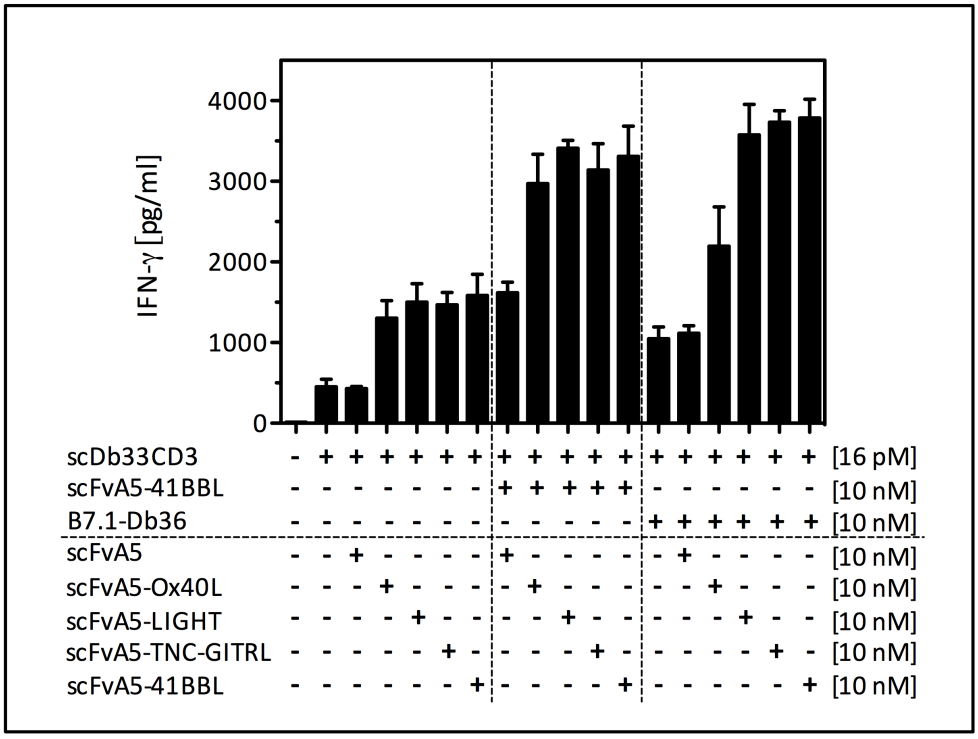

Fig. 48: Combined costimulation of scFvA5-TNF-SF ligand fusion proteins with either scFvA5-4-1BBL or B7.1-Db36 analyzed by cytokine release. HT1080 #33 (FAP^+, EDG^+) were incubated for 1 h with the indicated construct combinations before addition of PBMC. After 4 days, IFN-γ levels were determined via sandwich ELISA [n=3, block shift correction, mean ± SD, One-way ANOVA, Tukey post test]

The combinatorial approach with B7.1-Db36 revealed a significant (*** $p < 0.0001$) enhancement of B7.1-mediated costimulation for all scFvA5-fusion proteins. ScFvA5-4-1BBL, -LIGHT and -TNC-GITRL displayed a similar effect which was significantly (*** $p < 0.0001$) stronger (3.4-3.6-fold increase) compared to scFvA5-Ox40L (2.1-fold increase). Furthermore, the comparative analysis of both combinatorial settings revealed that for scFvA5-LIGHT and scFvA5-TNC-GITRL similar cytokine release levels were achieved for either the combination with scFvA5-4-1BBL or B7.1-Db36, whereas for scFvA5-Ox40L significantly higher signals (*** $p < 0.0001$) were obtained for the combination with scFvA5-4-1BBL.

3.3.4.2 - Proliferation assays

Each costimulatory antibody-ligand fusion protein significantly (*** $p < 0.0001$) enhanced scDb-mediated T cell proliferation (Fig. 49A). The observed signal enhancements were comparable, ranging from 1.6- 1.8-fold of the scDb signal. The costimulatory potential of scFvA5-4-1BBL could be significantly (*** $p < 0.0001$) enhanced by the concomitant addition of either scFvA5-Ox40L, -LIGHT, -TNC-GITRL or by its two-fold concentration resulting in a 2.3 – 2.4-fold enhancement of scDb-mediated T cell proliferation. A similar behaviour was observed for the combinatorial approach with B7.1-Db36, where all combinations with the TNF-SF ligand fusion proteins resulted in comparable percentages of proliferating T cells (2.1-2.2-fold enhancement of the scDb signal). A comparison between the combinatorial settings for all three T cell populations revealed similar proliferation patterns, but subset-specific differences in their proliferation levels ($CD8^+$ T cells displayed a higher proliferative capacity than $CD8^-$ T cells) (Fig. 49). Thus, emphasizing proliferation as a hallmark of T cell activation, a maximal effect was achieved to a similar extent by all combinations of costimulatory fusion proteins.

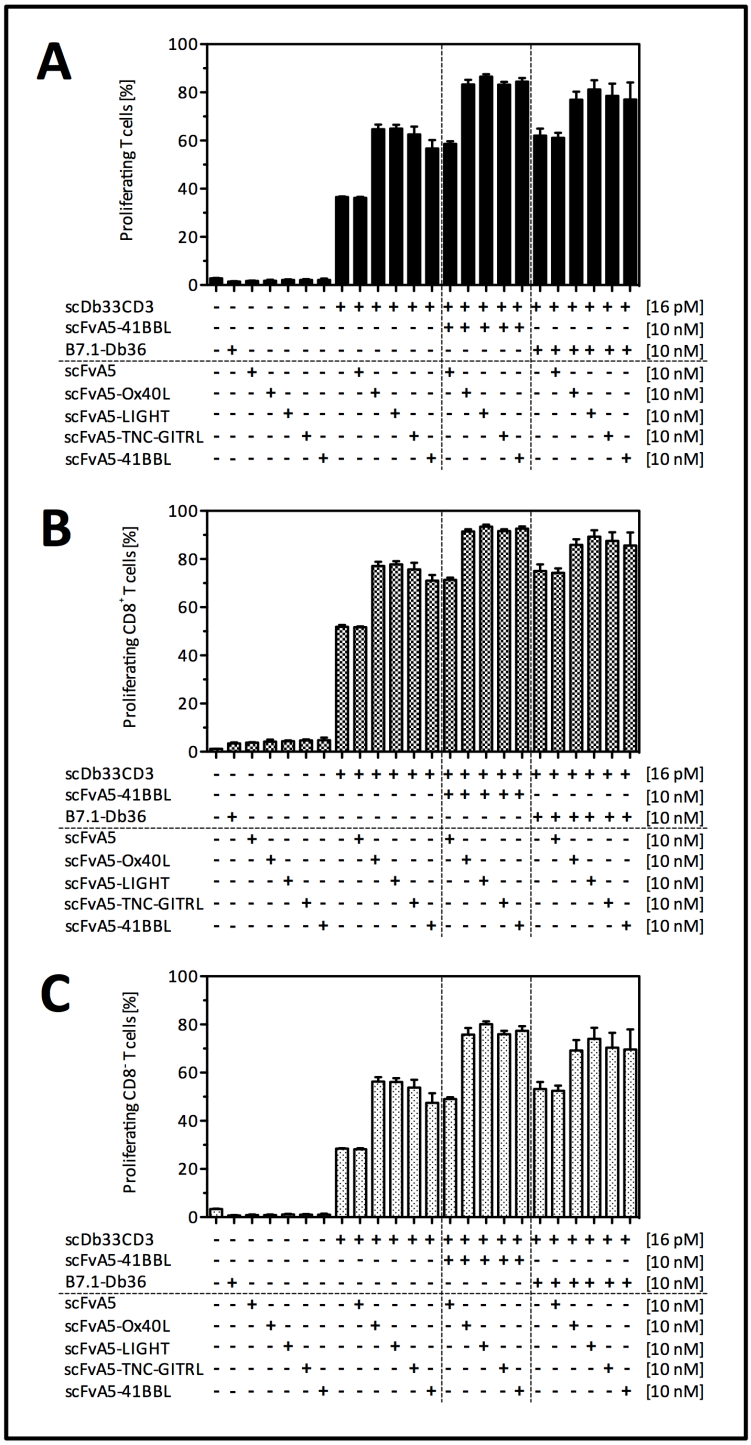

Fig. 49: Combined costimulation of scFvA5-TNF-SF ligand fusion proteins with either scFvA5-4-1BBL or B7.1-Db36 analyzed for T cell proliferation by flow cytometry. HT1080 #33 (FAP^+, EDG^+) were incubated for 1 h with the indicated construct combinations before addition of CFSE-labeled PBMC. After 7 days, proliferation of T cells (A) or $CD8^+$ (B) and $CD8^-$ (C) T cell subsets was assessed via flow cytometry (anti-CD3-PerCP, anti-CD8-PE). [n=3, block shift correction, mean ± SD, One-way ANOVA, Tukey post test]

3.3.4.3 - Expression of Granzyme B

For each costimulatory antibody-ligand fusion protein a significant (*** $p < 0.0001$) enhancement of scDb-induced T cell GrB expression could be observed (Fig. 50A). In detail, strongest effects were shown by scFvA5-Ox40L,-4-1BBL and B7.1-Db36 (1.6 – 1.8-fold increase), whereas the cytotoxic potential of scFvA5-LIGHT and scFvA5-TNC-GITRL was significantly lower (1.4-fold increase). In combination, highest GrB levels were obtained by B7.1-Db together with either scFvA5-4-1BBL, scFvA5-Ox40L or scFvA5-LIGHT (2.1- to 2.3-fold increase of the scDb signal). For the combinatorial setting with scFvA5-4-1BBL, only scFvA5-Ox40L could further increase the cytotoxic potential (1.9-fold), while scFvA5-LIGHT did not. In the case of scFvA5-TNC-GITRL, no further improvement for none of the two combinatorial settings was observed. The costimulatory pattern obtained for GrB^+ T cells was similar for the $CD8^+$ and $CD8^-$ T cell subsets (Fig. 50B, C), differing mostly in the level of the signal: Here, $CD8^+$ displayed the highest amount of GrB^+ T cells, $CD8^-$ T cells the lowest and overall T cells a medium signal (stimulation with scDb: $CD8^+$: 58.9 %, $CD8^-$: 27.3 %, CD3: 37.8 %).

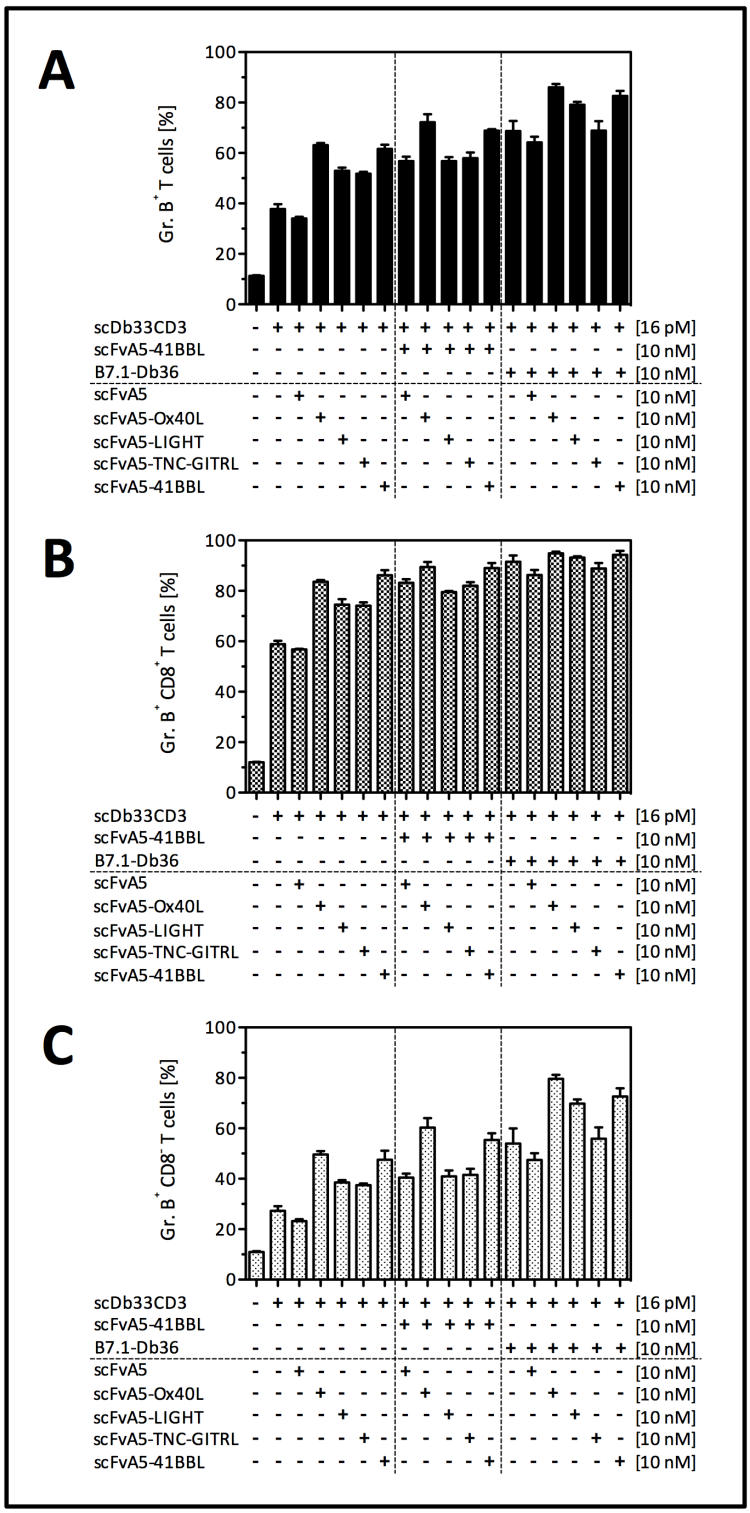

Fig. 50: Combined costimulation of scFvA5-TNF-SF ligand fusion proteins with either scFvA5-4-1BBL or B7.1-Db36 analyzed for intracellular granzyme B (GrB) expression of T cells by flow cytometry. HT1080 #33 (FAP^+, EDG^+) were incubated for 1 h with the indicated construct combinations before addition of CFSE-labeled PBMC. After 7 days, PBMC were fixed and permeabilized, stained for intracellular GrB expression of T cells (A) or $CD8^+$ (B) and $CD8^-$ (C) T cell subsets and were analyzed by flow cytometry (anti-CD3-FITC, anti-CD8-PerCP, anti-GrB-PE). [n=3, block shift correction, mean ± SD, One-way ANOVA, Tukey post test]

In addition to the percentage of GrB^+ T cells, also the amount of GrB expression within the cells was analyzed by its mean fluorescence intensity (MFI). As expected, $CD8^+$ T cells showed the highest level of intracellular GrB expression (Fig. 51B). In this population, individual costimulation with scFvA5-Ox40L, scFvA5-4-1BBL and B7.1-Db revealed an enhancement in the intensity of GrB expression, while scFvA5-LIGHT and scFvA5-TNC-GITRL did not. For the combinatorial settings, a cooperative effect could only be observed for B7.1-Db with either scFvA5-Ox40L or scFvA5-4-1BBL as well as for the combination of scFvA5-4-1BBL with scFvA5-Ox40L. Thus, the amount of intracellular GrB expression seemed to correlate with the percentage of GrB-positive T cells within the $CD8^+$ T cell population. In contrast, for $CD8^-$ T cells, no significant changes in the MFI of GrB expression could be observed (Fig. 51C).

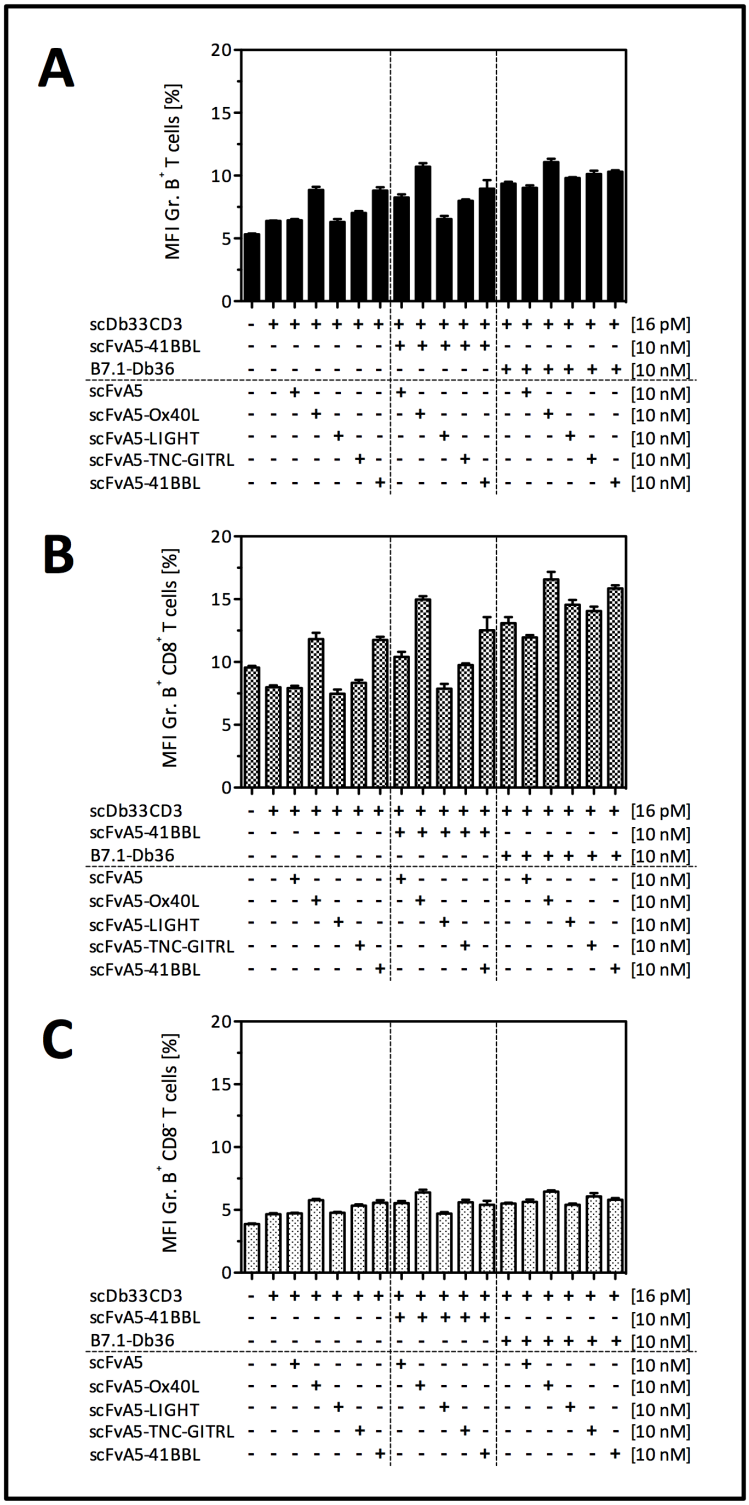

Fig. 51: Combined costimulation of scFvA5-TNF-SF ligand fusion proteins with either scFvA5-4-1BBL or B7.1-Db36 analyzed for mean fluorescence intensity (MFI) of intracellular granzyme B (GrB) expression of T cells by flow cytometry. HT1080 #33(FAP$^+$, EDG$^+$) were incubated for 1 h with the indicated construct combinations before addition of PBMC. After 7 days, PBMC were fixed and permeabilized and stained for intracellular GrB expression (anti-CD3-FITC, anti-CD8-PerCP, anti-GrB-PE). MFI of GrB$^+$ positive T cells (A) or CD8$^+$ (B) and CD8$^-$ (C) T cell subsets was analyzed by flow cytometry. [n=3, block shift correction, mean ± SD]

4 - Discussion

Costimulatory approaches have been successfully employed for cancer immunotherapy. However, within the last years, it has become apparent that combinatorial treatments display a much higher potential. Therefore, several groups started to address multiple costimulatory molecules instead of a single one[7]. Here, a targeted combinatorial setting was established in which two costimulatory antibody-ligand fusion proteins (B7-Db and scFv-4-1BBL) were combined with a bispecific antibody and T cell activation, differentiation and cytotoxic potential was analyzed. Initially, the fusion proteins were applied simultaneously with the bispecific antibody, whereas the approach was also analyzed in terms of a time-shift application of the costimulatory proteins within a restimulation context. Furthermore, the costimulatory ligand spectrum was extended by incorporating other members of the TNFSF into the setting for the combination with either B7.1-Db or scFv-4-1BBL.

4.1 - Simultaneous costimulation of scDb-activated T cells with B7- and 4-1BBL-antibody fusion proteins

In the first part of the work, scFvA5-4-1BBL was applied with either B7.2-Db36 or B7.1-Db36 for the combinatorial setting. Here, the costimulatory activity of the ligands was shown to be restricted to their membrane-bound presentation, by means of antibody binding to the target antigen, since the fusion proteins were able to enhance scDb-mediated T cell proliferation in a coated but not in a soluble form. In this manner, ligand action is confined to the tumor site bringing additional safety to the approach. Accordingly, previous studies have shown that effective costimulatory activity of dimeric B7.1- and B7.2-Fc fusion proteins required coating, additional cross-linking in solution or exposition on the cell surface by binding to Fc receptors[11,152,153]. Furthermore, fusion to diverse Her2-specific recombinant antibody formats, for example B7.1-IgG3[41] and B7.2-scFv[42], restricted their costimulatory activity to the target-bound form on the cell surface remaining inactive in soluble form. For 4-1BBL and most of the TNF ligands in general, it was described as well that they require additional oligomerization by cross-linking or targeting to accomplish their costimulatory activity[58,59,154]. Thus, the ligands B7 and 4-1BBL seem to be suitable for a targeted costimulatory approach.

Since costimulation can only work in the presence of a primary signal, a bispecific antibody, directed against FAP and CD3 was applied, thus achieving a completely targeted approach. It was shown earlier in our group, that the first stimulus and one costimulatory signal can be provided by either targeting two independent antigens or the same one on the surface of tumor cells[88,89]. Here, it could be shown, that it is also feasible to combine the bispecific antibody simultaneously with two fusion proteins, one targeting the same (FAP, B7.2-Db36) and one targeting a second antigen (EDG, scFvA5-4-1BBL). Although binding competition between the bispecific antibody and B7.2-Db could be detected via a control Db lacking the ligand domain, the costimulatory potential of B7.2 overcame the competition leading to a potent enhancement in T cell activation compared to the signal of the scDb alone or in combination with the Db. Thus, a model system was successfully employed allowing the analysis of the impact of individual or combined costimulation on bispecific antibody-induced T cell stimulation. In this manner, it could be shown, that the combination of the bispecific antibody with either B7.2-Db or scFv-4-1BBL significantly enhanced scDb-mediated T cell stimulation, and most importantly, that the combined application of both fusion proteins led to an even further enhancement in terms of cytokine release, proliferation and the expression of the activation marker CD25. The reinforcing effect thereby is most likely due to the synergism between CD28 and 4-1BB, which is described in several in vitro and in vivo studies[54,133,134,155]. Besides the quantitative effects of costimulation via CD28 and 4-1BB, also qualitative effects shaping the T cell population have been observed, namely an increase in T cells displaying an activation-experienced memory phenotype accompanied by a decrease in T cells with a naïve phenotype. This finding correlated with a study for the ex vivo expansion of $CD8^+$ T cells, in which the combination of both costimuli mainly retrieved CTLs of the effector memory subtype[156]. Furthermore, the ligands B7 and 4-1BBL displayed differential effects on T cell subpopulations: While $CD4^+$ T cells responded stronger to costimulation with B7.2, 4-1BBL preferentially addressed $CD8^+$ T cells. This finding could be supported by a study revealing a similar proliferation pattern for $CD4^+$ and $CD8^+$ T cell subsets following costimulation with mAbs directed against CD28 and 4-1BB in mice[157]. Besides the preferential effect of 4-1BB costimulation on $CD8^+$ T cells, Kober and coworkers could also reveal a positive effect of $CD4^+$ T cells on $CD8^+$ T cell proliferation via stimulation of human T cells with a cell line simultaneously expressing a membrane-bound CD3 antibody and 4-1BBL[158]. The differential effects of B7.2 and

4-1BBL could be influenced by the expression profiles of the respective receptors, since flow cytometry analysis revealed that 99% of $CD4^+$ T cells, but only 51% of $CD8^+$ T cells expressed CD28[159]. In addition, kinetic analysis of 4-1BB expression on T cells showed that the $CD8^+$ subset upregulated the receptor to a greater extent and more rapidly than $CD4^+$ T cells[160]. Nevertheless, in the overall T cell response the differential effects of B7.2-Db and scFv-4-1BBL were equalized, showing similar proliferation and activation marker expression for costimulation with either one of them.

Furthermore, also the cytotoxic potential of the combinatorial approach was analyzed: Despite the potency of the bispecific antibody itself to mediate target cell lysis, costimulation with either scFv-4-1BBL or B7.1-Db enhanced the amount of lysed target cells, whereas the effect was much stronger for B7.1-Db. In addition, the combination of both costimulatory fusion proteins led to a slightly further increase. A similar result was shown by Li and coworkers analyzing the cytolytic effect of mouse splenocytes after coincubation with a tumor cell line expressing costimulatory ligands[134]. In this study, the expression of B7.1 and B7.2 led to much higher target cell lysis compared to 4-1BBL, whereas the combined expression of 4-1BBL and both B7 ligands showed a slightly better result as well. A cytotoxic potential of B7.1 was also described by Blanco and coworkers using gene-modified bystander cells simultaneously expressing a bispecific antibody directed against CEA and CD3 and a B7.1-DbCEA fusion protein[13]. Here, the simultaneous expression of both recombinant proteins strongly enhanced target cell lysis compared to the expression of the bispecific antibody alone. In the present work, it was observed, that the increase in the cytotoxic potential of the T cells after treatment with either scDb alone or in combination with the costimulatory fusion proteins was accompanied by an upregulated intracellular GrB expression. As expected, the effect was most profound for the CTLs, namely the $CD8^+$ T cell population, showing not only higher amounts of GrB^+ T cells but also higher levels of intracellular GrB expression. Based on these findings, the costimulatory effect was also analyzed on a defined $CD8^+$ T cell population, namely naïve $CD8^+$ T cells. ScFv-4-1BBL strongly promoted their expansion and their acquisition of cytotoxic potential leading to the generation of a powerful effector T cell population, predominantly of a central memory and to a lesser extent an effector memory phenotype. This is in accordance with published data showing that in cocultures with naïve $CD8^+$ T cells and DCs the addition of 4-

1BBL increased the differentiation into effector and central memory T cell populations[161]. It was long thought that $CD8^+$ T cells with an effector memory phenotype contain the strongest cytolytic capacity, capable of exerting effector functions[162]. However, it was recently observed that $CD8^+$ central memory T cells are superior in inducing antitumor activity compared to the effector memory T cell population[163].

4.2 - Time-shift costimulation of scDb-activated T cells with B7.1- and 4-1BBL-antibody fusion proteins

Due to the promising results obtained for the simultaneous application of the scDb with B7- and 4-1BBL-fusion proteins, the combinatorial approach was also extended in terms of time-shift costimulation in a restimulation context. Therefore, an assay was established, comparing simultaneous costimulation by B7.1 and scFv-4-1BBL on unstimulated or scDb-experienced PBMC or the consecutive application of both. According to the results, the most effective costimulatory strategy was the combined application of both fusion proteins during scDb-mediated restimulation. In this setting, costimulation showed not only the ability to further raise the proliferative and cytotoxic potential of T cells in support of scDb-mediated T cell restimulation, it could also be observed that costimulation could counteract scDb-driven enhancement of T cells expressing the inhibitory receptor PD-1. Since the latter is described to play a key role in T cell exhaustion, a phenomena defined by impaired effector functions[72], and upregulation of its ligand in tumors has been identified as a mechanism of immune evasion[164], low levels of PD-1 are required in order to generate a long-lasting T cell response. This finding is also approached with antagonizing antibodies, several of them being currently investigated in clinical trials[165]. In comparison, the consecutive application of B7.1-Db and scFv-4-1BBL was less effective in down-regulating PD-1, although it revealed similar amounts of proliferating and GrB^+ T cells. A similar expression pattern to PD-1 was observed for the second coinhibitory receptor, CTLA-4, although at a much lower expression level. Furthermore, for all readouts, the overall T cell response as well as its $CD8^+$ and $CD8^-$ subsets were monitored revealing comparable expression patterns for the different stimulations but differences in the expression level. Here, the finding that the $CD8^+$ T cell population showed the highest amount of proliferating and GrB^+ T cells and the lowest amount of $PD\text{-}1^+$ T cells, renders this approach especially suitable for cancer immunotherapeutic approaches.

Due to the promising in vitro results obtained for the two time-shift costimulatory settings, the latter were also tested in vivo in a syngeneic tumor mouse model. Here, both the combined or consecutive application of both costimulatory fusion proteins in the presence of the scDb revealed the strongest reduction in metastasis formation, while neither treatment with the scDb nor the fusion proteins alone were able to reach this effect. A significant reduction in tumor burden could also be observed in two studies using modified tumor cells simultaneously expressing B7.1 and 4-1BBL[54] or B7.1, B7.2 and 4-1BBL[134]. However, since in these studies the ligands were present throughout the entire experiment in the absence of a first signal, the settings differ substantially.

4.3 - Novel antibody-ligand fusion proteins of the TNF-superfamily and their incorporation into the combinatorial setting

Antibody-ligand fusion proteins of the TNF-SF targeting two different antigens (FAP and EDG) were successfully generated and characterized and all of them were shown to be functional in terms of tumor antigen binding. Furthermore, in coated i.e. cross-linked form, all of them strongly enhanced scDb-mediated proliferation of PBMC, whereas their costimulatory activity was almost absent in solution. For Ox40L, this finding could be supported by a study showing that oligomerization (by cross-linking with antibodies or by expression as a hexameric fusion protein) or targeting (via a scFv directed against FAP) of soluble OX40L trimers strongly increased its activity by more than 200-fold[59]. In contrast, human GITRL is described to show only loose trimeric assembly in a dynamic equilibrium with either monomers[166] or dimers[167] due to a smaller intersubunit interface compared to other TNF ligands[168]. Accordingly, for a scFv-GITRL fusion protein a mixed population of monomers and trimers or tetramers was observed displaying a rather low activity for the immobilized, that is targeted GITRL, in comparison to other ligands like e.g. 4-1BBL[15,58]. However, the GITRL fusion protein could be further stabilized by the additional incorporation of a TNC-domain that forces trimerization of soluble TNF ligands by the formation of disulfide bonds[58]. Thus, a mainly homogenous population (only observed for scFvA5-TNC-GITRL) was obtained showing a strong costimulatory capacity in coated form comparable to that of scFv-Ox40L and -LIGHT. In the case of LIGHT, it was shown for the first time in this study, that its costimulatory activity is restricted to a coated form. Thus, all three novel fusion proteins confirmed the underlying concept of antibody-mediated TNF-SF ligand

presentation, i.e. mimicking a membrane-bound state and directing the immune response to the tumor site, thereby reducing the risk of systemic side effects. However, in the coculture assays, only the fusion proteins directed against EDG were shown to display a costimulatory activity when co-applied with the scDb and were therefore chosen for the further studies. In the case of the scFv36-TNF-SF ligand fusion proteins, competitive effects with the bispecific antibody concerning FAP binding seem to most likely account for the lack of costimulatory activity.

All three novel ligand fusion proteins enhanced scDb-mediated stimulation of T cells in terms of proliferation and IFN-γ release. For better comparison, equal concentrations were applied retrieving similar costimulatory effects. In contrast, considerable differences in the costimulatory potential of individual ligands have been described in a setting using transfected cell lines expressing a costimulatory ligand in conjunction with a membrane-bound anti-CD3 antibody, with ligand expression being adjusted to comparable levels[158]. In this study, strongest T cell proliferation could be detected for B7.1, sequentially followed by 4-1BBL, Ox40L and GITRL, whereas LIGHT did not show a costimulatory activity at all. Since other studies could show a costimulatory potential (proliferation and cytokine release) for immobilized human LIGHT[169] or membrane-bound mouse LIGHT[57] in the presence of an antibody against CD3, thus supporting our finding, it is assumed that in the study of Kober et al the strength of the primary signal and ligand presentation appear most likely to account for the differential outcome. Furthermore, other studies also confirmed the costimulatory potential of GITRL and Ox40L: For a scFv-mouse GITRL fusion protein Burckhart and coworkers revealed that its co-administration with an anti-CD3 antibody resulted in enhanced proliferation and IFN-γ secretion of both $CD4^+$ and $CD8^+$ T cells[15]. A study addressing the costimulatory nature of Ox40L could show that its expression on human monocytes led to greater expansion, upregulation of perforin, enhanced cytolytic activity and increased numbers of IFN-γ and TNF-α-producing antiviral memory $CD8^+$ T cells within the T cell culture[170].

The analysis of the cytotoxic potential induced by the costimulatory fusion proteins revealed similar levels of GrB expression for scFv-Ox40L, scFv-4-1BBL and B7.1-Db, while scFv-LIGHT and -TNC-GITRL were less effective. Nevertheless, both ligands are described to have other therapeutically relevant functions: For GITRL, besides the activation of effector cells, the ligand

is also involved in overcoming the suppressive activity of T_{regs}[171]. In the case of LIGHT, it has been described that its expression in the tumor microenvironment mediates the upregulation of chemokines and adhesion molecules and is accompanied by a massive infiltration and activation of naïve T cells subsequently leading to tumor rejection[172].

Besides their individual capacity to costimulate human T cells, Ox40L, LIGHT and GITRL were also analyzed for their cooperative effect in conjunction with either another member of the TNF (4-1BBL)- or a member of the Ig (B7.1)-superfamily. Here, all combinations for both targeting-defined settings were shown to be functional, since each induced a significant costimulatory enhancement compared to the individual effects in at least one of the analyzed readouts. In terms of T cell proliferation, all costimulatory combinations resulted in similar amounts of proliferating T cells, whereas differences could be observed for GrB expression. Here, the combined application of B7.1-Db36 with scFvA5-Ox40L induced the highest effect, followed by the combination of B7.1-Db with scFv-4-1BBL, whereas in the case of scFv-LIGHT and -TNC-GITRL, only the combined application of scFv-LIGHT with B7.1 resulted in a slight increase. So far, besides the well-described interaction of the ligands B7 and 4-1BBL, synergistic or additive effects have been observed for the combination of Ox40L with either B7.1 or 4-1BBL on antiviral $CD8^+$ T cell responses[170]. Furthermore, a reinforcing effect for LIGHT and 4-1BBL could be shown in a study using engineered tumor cells expressing both ligands on their surface[173] and in a setting combining an anti-HVEM antibody expressed on a tumor cell with anti-4-1BB treatment[174]. The synergy of these therapies can partially be explained by the expression patterns of the costimulatory receptors and their non-redundant functions, which have been proven for the TNF receptors Ox40 and 4-1BB[175] and also for GITR and 4-1BB[176]. For CD28 and 4-1BB/Ox40 it is well-described, that CD28 participates in early T cell activation while 4-1BB and Ox40 are subsequently induced following T cell activation[20]. In addition, it is also known, that naïve T cells express high levels of HVEM, whereas the receptor is downregulated after T cell activation and again upregulated in memory T cells, leading to simultaneous expression of HVEM and 4-1BB, which synergistically promote the maintenance of memory T cell population[174]. Furthermore, it seems to be likely, that the differential receptors partly influence the expression of each other: While 4-1BB is able to restore the expression of CD28, GITR was described to lower the threshold for CD28 costimulation in mouse $CD8^+$ T cells[177]. In

contrast, LIGHT and Ox40 were shown to exert their costimulatory activity in a CD28-independent manner[57,178], whereas CD28 can augment the level of OX40 expressed on a T cell[179].

4.4 - A potential translation of the combinatorial approach into the clinic

Due to the promising results obtained for the combinatorial setting with costimulatory antibody-ligand fusion proteins, the latter appear worthwhile for a potential application in cancer immunotherapy. Therefore, the recombinant proteins would have to be produced according to Good Manufacturing Practice (GMP) requirements and would have to pass through an extensive preclinical and clinical drug development process in order to determine their safety, tolerability, toxicity, biological activity, efficacy and dosage, as well as other important parameters (e.g. pharmacokinetic and pharmacodynamic properties)[180]. Furthermore, the recombinant proteins would have to be tested alone and, most importantly, in combination to obtain the optimal drug combination yielding the best therapeutic effect.

Since antibody-ligand fusion proteins have not entered clinical trials yet, adequate therapeutic dosages can only be speculated about. Indications can be found within clinical trials with monoclonal agonist antibodies against the costimulatory receptors 4-1BB and Ox40. Here, a preclinical toxicology study of BMS 663513 (anti-CD137 mAb, fully human IgG4) revealed single high doses (10, 30, 100 mg/kg) or multi-doses of 1, 10 or 100 mg/kg once weekly for 4 weeks to be tolerable in monkeys[181]. Furthermore, in a phase I dose-escalation study, 6 different doses (0.3, 1, 3, 6, 10 or 15 mg/kg) of the mAb were tested via short-term (60 min) infusion (i.v.) once every 3 weeks[181]. Here, clinical activity, by means of partial remission and sustained stable disease, was observed in the 1, 3 and 10 mg/kg groups and biomarker studies indicated that the mAb already elicited biologic activity at the lowest dose tested (0.3 mg/kg). Furthermore, also the adverse events (AEs) (most commonly fatigue, transaminitis, neutropenia, rash, diarrhea) were manageable. On the basis of these results, a multi-dose phase II study of BMS-663513 was designed, consisting of four arms: 0.1 mg/kg every 3 weeks, 1 mg/kg every 3 weeks, 1 mg/kg every 6 weeks, 5 mg/kg every 3 weeks[181]; however, the study was terminated early due to a high incidence of severe liver toxicity that seemed to be dose-dependent. Hence, a clinical trial is currently recruiting patients with advanced or metastatic solid tumors to test lower doses of

the mAb[53]. Another agonist mAb directed against 4-1BB, PF-05082566 (fully human IgG2), is to be tested in a planned phase I trial as either a single agent in patients with solid tumors or in combination with Rituximab in patients with $CD20^+$ B cell Non-Hodgkin's lymphoma (B-NHL)[182]. The antibody was well tolerated in monkeys following either single doses of up to 10 mg/kg or weekly doses of up to 5 mg/kg, while for weekly doses > 5 mg/kg, dose-limiting toxicities have been observed[183].

Besides, the safety and stimulatory activity of a murine Ox40-specific antibody (MEDI-6469) was shown for 3 different doses (0.4, 2.0, and 10 mg/kg) in non-human primates, thus leading to a Phase I dose-escalation trial in patients with advanced solid tumors[184]. Here, dosages of 0.1, 0.4 and 2 mg/kg (administered on days 1, 3 and 5) were tolerable (no toxicity or signs of autoimmunity), revealing increased T cell activation and proliferation and leading to tumor shrinkage in some patients[182]. Currently, two new clinical trials with the anti-Ox40 mAb are recruiting participants: a Phase II trial with an anti-Ox40 mAb monotherapy in metastatic melanoma, and a Phase Ib trial for the combination of the mAb with cyclophosphamide and radiation for the treatment of metastatic prostate cancer[53].

For the remaining costimulatory receptors approached in this study, namely HVEM and GITR, no clinical data with mAb is available yet. However, a Phase I study of a humanized Fc-disabled (aglycosylated), GITR-specific agonist antibody (TRX518) is currently recruiting participants[53]. In the case of CD28, a superagonist mAb (TGN1412) had been tested in a phase I clinical trial, which resulted in severe toxicity involving cytokine release syndrome and multi-organ failure after an initial dose of ~ 7-8 mg[8]. Preclinical data in non-human primates that received 500-fold higher doses did not forecast this adverse event, in spite of the apparent reactivity of primate CD28 with TGN1412[7].

The described application doses for the mAbs provide insights into a potential concentration range for a therapy with costimulatory antibody-ligand fusion proteins. Nevertheless, it has to be kept in mind that mAbs and antibody-ligand fusion proteins are distinct therapeutic agents which, amongst other things, strongly differ in their pharmacokinetic properties: In this study, the observed terminal half-life of the fusion proteins was in the range of 6 h compared with several days for whole IgG molecules. Since both types of molecules have a similar molecular size (mAb (IgG): ~150 kDa; B7-Db: 108 kDa, scFv-4-1BBL: 141 kDa) above the renal clearance

threshold (~ 40-50 kDa), the difference in the serum half-life can most likely be attributed to FcRn-mediated recycling processes which play an important role in the IgG homeostasis[185].

For the bispecific antibody (scDb), first indications of a potential dose range for a cancer immunotherapeutic treatment in humans can be found within clinical trials of BiTE antibodies, where currently three different molecules (MT103 (Blinatumomab, CD19 x CD3), MT110 (EpCAM x CD3) and MT111 (CEA x CD3)) are tested[97]. For Blinatumomab, the dose escalation study in phase I ranged from 0.75 to 13 µg/m^2, whereat the administration form was a short-term i.v. Infusion (2-4 h) once, twice or thrice a week[186]. The most common clinical AEs were flu-like symptoms that were thought to be caused by the initial activation of polyclonal T cells, which led to a transient release of inflammatory cytokines in co-culture experiments. Furthermore, also lymphopenia, leukopenia and increase of C-reactive protein occurred which were most likely be related to B cell depletion and global T cell redistribution. However, some of these first dose reactions could be mitigated using low doses of glucocorticoids as preventive and interventional co-medication at the start of the treatment[186]. Since Blinatumomab has a short serum half-life in humans of ~2 h, its further application was changed towards a continuous i.v. infusion over a period of 4 or 8 weeks[186]. This change did not only seem to improve safety in that AEs associated with an initial polyclonal activation of T cells were limited mainly to the start of infusion, but also allowed for a more sustained activity of T cells through the maintenance of active serum levels of Blinatumomab for an entire treatment cycle. The sustained activity of BiTE-antibody-engaged T cells finally translated into confirmed clinical responses in a variety of CD19$^+$ B cell malignancies. Here, first complete remissions were observed at a dose level of 15 µg/m^2 per day. This dose level led to a sustained serum level of 0.6-1 ng/ml, which is by 4–5 orders of magnitude lower than needed by conventional mAbs to achieve remissions in B-NHL[186].

Since a scDb has a rather short terminal half-life (~1.3 h)[187] comparable to that of the BiTE antibody, strategies to extent its circulation time would be advisable. Here, an increase in the hydrodynamic radius of the protein (e.g. by hyperglycosylation or coupling to polyethylene glycol (PEG) chains) has shown to be suitable[185,188]. Moreover, fusion to the Fc-region of IgG molecules or serum albumin has been proven to additionally prolong the half-life of protein therapeutics via FcRn-mediated recycling, as it could be shown for e.g. growth factors,

hormones, and cytokines and several of these molecules are already approved or are in clinical development[185]. Furthermore, also noncovalent interactions with plasma proteins via the fusion to an albumin-binding domain (ABD) or to an immunoglobulin-binding domain B (IgBDs) have emerged as a half-life extension strategy[187,189,190]. Importantly, it could be shown, that the extended half-life of a bispecific scDb resulted in an improved accumulation in antigen-positive tumors[191]. However, it has to be taken into account, that the modifications might also affect certain scDb-mediated effector functions.

In summary, it is still a long and challenging road to go in order to translate the combinatorial approach into a potential clinical application. Several further modifications (e.g. half-life extensions) and numerous analysis and evaluations are needed to yield a successful cancer immunotherapy.

4.5 - Conclusions and Future Directions

Combinatorial approaches addressing more than one costimulatory molecule become more and more accepted for cancer immunotherapy. Accordingly, in this work, the feasibility of combining two costimulatory antibody-ligand fusion proteins in the presence of a bispecific antibody was demonstrated, and also the relevance of ligand combinations and their spatiotemporal impact was approached. Combined costimulation with B7- and 4-1BBL-fusion proteins led to higher amounts of activated T cells, differentiation into a memory phenotype and a higher target cell killing capacity compared to stimulation with the bispecific antibody alone. For a therapeutic application it would also be important to know, whether costimulation enhances the survival of the T cells. In future studies, this topic could be addressed via e.g. long-term experiments and the detection of the survival marker Bcl-xL[192,193]. The in vitro studies concerning the time-shift costimulation setting look promising. Therefore, it would be worthwhile to further extend the analysis in terms of different time points for the restimulation and to include more readouts such as T cell survival and its target cell lysis capacity. Accordingly, for a detailed and precise analysis, also the individual impact of each costimulatory fusion protein should be determined. Furthermore, since treatment with B7.1 and 4-1BBL also revealed a strong antitumor response in vivo, future work should test the therapeutic potential of the fusion proteins in other tumor models (e.g. a syngeneic subcutaneous tumor) and also for the treatment of already established tumors. In this manner, the determination of the individual therapeutic potential of each fusion protein should be included as well. The generation of novel fusion proteins of the TNF superfamily allowed for several new combinations within the established system. In future studies, the most promising ones could also be incorporated into the time-shift setting and could be tested for their therapeutic potential in a tumor model. In summary, this model system-based study added a valuable contribution to the field of combinatorial cancer immunotherapy and due to the diversity of antibodies, antigens and ligands, the established setting could also be adapted to other systems of tumor therapeutic relevance.

References

1. Aruffo, A. & Seed, B. Molecular cloning of a CD28 cDNA by a high-efficiency COS cell expression system. *Proceedings of the National Academy of Sciences of the United States of America* **84**, 8573–7 (1987).

2. Linsley, P. S., Clark, E. A. & Ledbetter, J. A. T-cell antigen CD28 mediates adhesion with B cells by interacting with activation antigen B7/BB-1. *Proceedings of the National Academy of Sciences of the United States of America* **87**, 5031–5 (1990).

3. Greenwald, R. J., Freeman, G. J. & Sharpe, A. H. The B7 family revisited. *Annual Review of Immunology* **23**, 515–48 (2005).

4. Aggarwal, B. B., Gupta, S. C. & Kim, J. H. Historical perspectives on tumor necrosis factor and its superfamily: 25 years later, a golden journey. *Blood* **119**, 651–65 (2012).

5. Kirkwood, J. M., Butterfield, L. H., Tarhini, A. A. & Zarour, H. Immunotherapy of Cancer in 2012. *American Cancer Society* **62**, 309–335 (2012).

6. Driessens, G., Kline, J. & Gajewski, T. F. Costimulatory and coinhibitory receptors in anti-tumor immunity. *Immunological Reviews* **229**, 126–44 (2009).

7. Melero, I., Hervas-Stubbs, S., Glennie, M., Pardoll, D. M. & Chen, L. Immunostimulatory monoclonal antibodies for cancer therapy. *Nature Reviews. Cancer* **7**, 95–106 (2007).

8. Suntharalingam, G. *et al.* Cytokine Storm in a Phase 1 Trial of the Anti-CD28 Monoclonal Antibody TGN1412. *The New England Journal of Medicine* (2006).

9. Pardoll, D. & Drake, C. Immunotherapy earns its spot in the ranks of cancer therapy. *The Journal of Experimental Medicine* **209**, 201–9 (2012).

10. Pardee, A. D., Wesa, A. K. & Storkus, W. J. Integrating costimulatory agonists to optimize immune-based cancer therapies. *Immunotherapy* **1**, 249–264 (2009).

11. Notter, M. Targeting of a B7-1 (CD80) immunoglobulin G fusion protein to acute myeloid leukemia blasts increases their costimulatory activity for autologous remission T cells. *Blood* **97**, 3138–3145 (2001).

12. Murphy, K. a *et al.* An In Vivo Immunotherapy Screen of Costimulatory Molecules Identifies Fc-OX40L as a Potent Reagent for the Treatment of Established Murine Gliomas. *Clinical Cancer Research* **18**, 4657–68 (2012).

13. Blanco, B., Holliger, P., Vile, R. G. & Alvarez-Vallina, L. Induction of Human T Lymphocyte Cytotoxicity and Inhibition of Tumor Growth by Tumor-Specific Diabody-Based Molecules Secreted from Gene-Modified Bystander Cells. *Journal of Immunology* **171**, 1070–7 (2003).

14. Müller, D., Frey, K. & Kontermann, R. E. A Novel Antibody–4-1BBL Fusion Protein for Targeted Costimulation in Cancer Immunotherapy. *Journal of Immunotherapy* **31**, 714–722 (2008).

15. Burckhart, T. *et al.* Tumor-specific Crosslinking of GITR as Costimulation for Immunotherapy. *Journal of Immunotherapy* **33**, 925–34 (2010).

16. Sharpe, A. H. & Freeman, G. J. The B7–CD28 superfamily. *Nature Reviews Immunology* **2**, 116–126 (2002).

17. Schwartz, R. H. T Cell Anergy. *Annual Review of Immunology* **21**, 305–34 (2003).

18. Jenkins, M. R. & Griffiths, G. M. The synapse and cytolytic machinery of cytotoxic T cells. *Current Opinion in Immunology* **22**, 308–313 (2010).

19. Chen, L. & Flies, D. B. Molecular mechanisms of T cell co-stimulation and co-inhibition. *Nature Reviews Immunology* **13**, 227–242 (2013).

20. Croft, M. Costimulatory Members of the TNFR Family: Keys to Effective T-Cell Immunity? *Nature Reviews. Immunology* **3**, 609–620 (2003).

21. Greene, J. L. *et al.* Covalent Dimerization of CD28/CTLA-4 and Oligomerization of CD80/CD86 Regulate T Cell Costimulatory Interactions. *The Journal of Biological Chemistry* **271**, 26762–71 (1996).

22. Valk, E., Rudd, C. E. & Schneider, H. CTLA-4 trafficking and surface expression. *Trends in Immunology* **29**, 272–9 (2008).

23. Alegre, M., Frauwirth, K. A. & Thompson, C. B. T-Cell Regulation by CD28 and CTLA-4. *Nature Reviews. Immunology* **1**, 220–228 (2001).

24. Bhatia, S., Edidin, M., Almo, S. C. & Nathenson, S. G. Different cell surface oligomeric states of B7-1 and B7-2: implications for signaling. *Proceedings of the National Academy of Sciences of the United States of America* **102**, 15569–74 (2005).

25. Freeman, G. J. *et al.* B7, a new member of the Ig superfamily with unique expression on activated and neoplastic B cells. *Journal of Immunology* **143**, 2714–22 (1989).

26. Freeman, G. J. *et al.* Cloning of B7-2: A CTLA-4 Counter-Receptor That Costimulates Human T Cell Proliferation. *Science* **262**, 909–911 (1993).

27. Collins, A. V *et al.* The interaction properties of costimulatory molecules revisited. *Immunity* **17**, 201–10 (2002).

28. Bhatia, S., Sun, K., Almo, S. C., Nathenson, G. & Hodes, R. J. Dynamic Equilibrium of B7-1 Dimers and Monomers Differentially Affects Immunological Synapse Formation and T Cell Activation in Response to TCR/CD28 Stimulation. *Journal of Immunology* **184**, 1821–1828 (2010).

29. Wong, S., Tan, A. H. & Lam, K. Functional hierarchy and relative contribution of the CD28/B7 and ICOS/B7-H2 costimulatory pathways to T cell-mediated delayed-type hypersensitivity. *Cellular Immunology* **256**, 64–71 (2009).

30. Yoshinaga, S. K. *et al.* Characterization of a new human B7-related protein: B7RP-1 is the ligand to the co-stimulatory protein ICOS. *International Immunology* **12**, 1439–47 (2000).

31. Chattopadhyay, K., Bhatia, S., Fiser, A., Almo, S. C. & Nathenson, S. G. Structural Basis of Inducible Costimulator Ligand Costimulatory Function: Determination of the Cell Surface

Oligomeric State and Functional Mapping of the Receptor Binding Site of the Protein. *Journal of Immunology* **177**, 3920–3929 (2006).

32. Yao, S. *et al.* B7-H2 Is a Costimulatory Ligand for CD28 in Human. *Immunity* **34**, 1–12 (2011).

33. Coyle, a J. *et al.* The CD28-related molecule ICOS is required for effective T cell-dependent immune responses. *Immunity* **13**, 95–105 (2000).

34. Hutloff, A. *et al.* ICOS is an inducible T-cell co-stimulator structurally and functionally related to CD28. *Nature* **397**, 263–266 (1999).

35. Shilling, R. A. *et al.* CD28 and ICOS play complementary non-overlapping roles in the development of Th2 immunity in vivo. *Cellular Immunology* **259**, 177–184 (2009).

36. Van Berkel, M. E. a T. & Oosterwegel, M. a CD28 and ICOS: Similar or separate costimulators of T cells? *Immunology Letters* **105**, 115–22 (2006).

37. Agata, Y. *et al.* Expression of the PD-1 antigen on the surface of stimulated mouse T and B lymphocytes. *International Immunology* **8**, 765–72 (1996).

38. Blank, C., Gajewski, T. F. & Mackensen, A. Interaction of PD-L1 on tumor cells with PD-1 on tumor-specific T cells as a mechanism of immune evasion: implications for tumor immunotherapy. *Cancer Immunology, Immunotherapy* **54**, 307–14 (2005).

39. Blank, C. & Mackensen, A. Contribution of the PD-L1/PD-1 pathway to T-cell exhaustion: an update on implications for chronic infections and tumor evasion. *Cancer Immunology, Immunotherapy* **56**, 739–45 (2007).

40. Zang, X. & Allison, J. P. The B7 Family and Cancer Therapy: Costimulation and Coinhibition. *Clinical Cancer Research* **13**, 5271–5279 (2007).

41. Challita-Eid, P. M. *et al.* A B7.1-antibody fusion protein retains antibody specificity and ability to activate via the T cell costimulatory pathway. *Journal of Immunology* **160**, 3419–26 (1998).

42. Gerstmayer, B., Hoffmann, M., Altenschmidt, U. & Wels, W. Costimulation of T-cell proliferation by a chimeric B7-antibody fusion protein. *Cancer Immunology, Immunotherapy* **45**, 156–8 (1997).

43. Fu, T., He, Q. & Sharma, P. The ICOS/ICOSL pathway is required for optimal anti-tumor responses mediated by anti-CTLA-4 therapy. *Cancer Research* (2011).doi:10.1158/0008-5472.CAN-11-1138

44. Bodmer, J.-L., Schneider, P. & Tschopp, J. The molecular architecture of the TNF superfamily. *Trends in Biochemical Sciences* **27**, 19–26 (2002).

45. Zhang, G. Tumor necrosis factor family ligand-receptor binding. *Current Opinion in Structural Biology* **14**, 154–60 (2004).

46. Shevach, E. M. & Stephens, G. L. The GITR-GITRL interaction: co-stimulation or contrasuppression of regulatory activity? *Nature Reviews. Immunology* **6**, 613–8 (2006).

47. Morel, Y. *et al.* Reciprocal expression of the TNF family receptor herpes virus entry mediator and its ligand LIGHT on activated T cells: LIGHT down-regulates its own receptor. *Journal of Immunology* **165**, 4397–404 (2000).

48. Melero, I., Shuford, W. W. & SA, N. Monoclonal antibodies against the 4-1BB T-cell activation molecule eradicate established tumors. *Nature Medicine* **3**, 682–685 (1997).

49. Pan, P. OX40 Ligation Enhances Primary and Memory Cytotoxic T Lymphocyte Responses in an Immunotherapy for Hepatic Colon Metastases. *Molecular Therapy* **6**, 528–536 (2002).

50. Weinberg, a D. *et al.* Engagement of the OX-40 receptor in vivo enhances antitumor immunity. *Journal of Immunology* **164**, 2160–9 (2000).

51. Ramirez-Montagut, T. *et al.* Glucocorticoid-Induced TNF Receptor Family Related Gene Activation Overcomes Tolerance/Ignorance to Melanoma Differentiation Antigens and Enhances Antitumor Immunity. *Journal of Immunology* **176**, 6434–42 (2006).

52. Vinay, D. S. & Kwon, B. S. Immunotherapy of Cancer with 4-1BB. *Molecular Cancer Therapeutics* **11**, 1062–1070 (2012).

53. Croft, M., Benedict, C. a & Ware, C. F. Clinical targeting of the TNF and TNFR superfamilies. *Nature Reviews. Drug Discovery* **12**, 147–68 (2013).

54. Melero, I. *et al.* Amplification of tumor immunity by gene transfer of the co-stimulatory 4-1BB ligand: synergy with the CD28 co-stimulatory pathway. *European Journal of Immunology* **28**, 1116–21 (1998).

55. Piao, J. *et al.* Enhancement of T-cell-mediated anti-tumour immunity via the ectopically expressed glucocorticoid-induced tumour necrosis factor receptor-related receptor ligand (GITRL) on tumours. *Immunology* **127**, 489–99 (2009).

56. Nishikawa, H. *et al.* Regulatory T cell-resistant CD8+ T cells induced by glucocorticoid-induced tumor necrosis factor receptor signaling. *Cancer Research* **68**, 5948–54 (2008).

57. Tamada, K. *et al.* Modulation of T-cell-mediated immunity in tumor and graft-versus-host disease models through the LIGHT co-stimulatory pathway. *Nature Medicine* **6**, 283–9 (2000).

58. Wyzgol, A. *et al.* Trimer Stabilization, Oligomerization, and Antibody-Mediated Cell Surface Immobilization Improve the Activity of Soluble Trimers of CD27L, CD40L, 41BBL, and Glucocorticoid-Induced TNF Receptor Ligand. *Journal of Immunology* **183**, 1851–61 (2009).

59. Müller, N., Wyzgol, A., Münkel, S., Pfizenmaier, K. & Wajant, H. Activity of soluble Ox40 ligand is enhanced by oligomerization and cell surface immobilization. *FEBS Journal* **275**, 2296–2304 (2008).

60. Sadun, R. E. *et al.* Fc-mOX40L fusion protein produces complete remission and enhanced survival in 2 murine tumor models. *Journal of Immunotherapy* **31**, 235–45 (2008).

61. Zhang, N. *et al.* Targeted and untargeted CD137L fusion proteins for the immunotherapy of experimental solid tumors. *Clinical Cancer Research* **13**, 2758–67 (2007).

62. Acuto, O. & Michel, F. CD28-Mediated Co-Stimulation: a Quantitative Support for TCR Signalling. *Nature Reviews. Immunology* **3**, 939–951 (2003).

63. Del Rio, M. L., Lucas, C. L., Buhler, L., Rayat, G. & Rodriguez-Barbosa, J. I. HVEM/LIGHT/BTLA/CD160 cosignaling pathways as targets for immune regulation. *Journal of Leukocyte Biology* **87**, 223–35 (2010).

64. Denoeud, J. & Moser, M. Role of CD27/CD70 pathway of activation in immunity and tolerance. *Journal of Leukocyte Biology* **89**, 195–203 (2011).

65. Shahinian, A. *et al.* Differential T cell costimulatory requirements in CD28-deficient mice. *Science* **261**, 609–12 (1993).

66. Green, J. M., Karpitskiy, V., Kimzey, S. L. & Shaw, A. S. Coordinate Regulation of T Cell Activation by CD2 and CD28. *Journal of immunology* **164**, 3591–5 (2000).

67. Nocentini, G. & Riccardi, C. GITR: a modulator of immune response and inflammation. *Advances in Experimental Medicine and Biology* **647**, 156–73 (2009).

68. Burmeister, Y. *et al.* ICOS controls the pool size of effector-memory and regulatory T cells. *Journal of Immunology* **180**, 774–82 (2008).

69. Cai, G. & Freeman, G. J. The CD160, BTLA, LIGHT/HVEM pathway: a bidirectional switch regulating T-cell activation. *Immunological Reviews* **229**, 244–258 (2009).

70. Boesteanu, A. C. & Katsikis, P. D. Memory T cells need CD28 costimulation to remember. *Seminars in Immunology* **21**, 69–77 (2009).

71. Simpson, T. R., Quezada, S. A. & Allison, J. P. Regulation of CD4 T cell activation and effector function by inducible costimulator (ICOS). *Current Opinion in Immunology* **22**, 1–7 (2010).

72. Wherry, E. J. T cell exhaustion. *Nature Immunology* **131**, 492–499 (2011).

73. Wang, C. *et al.* Loss of the signaling adaptor TRAF1 causes CD8+ T cell dysregulation during human and murine chronic infection. *The Journal of Experimental Medicine* **209**, 77–91 (2012).

74. Bour-Jordan, H. & Bluestone, J. a Regulating the regulators: costimulatory signals control the homeostasis and function of regulatory T cells. *Immunological Reviews* **229**, 41–66 (2009).

75. Zhu, Y., Yao, S. & Chen, L. Cell surface signaling molecules in the control of immune responses: a tide model. *Immunity* **34**, 466–78 (2011).

76. Qureshi, O. S. *et al.* Trans-endocytosis of CD80 and CD86: a molecular basis for the cell-extrinsic function of CTLA-4. *Science* **332**, 600–3 (2011).

77. Butte, M. J., Keir, M. E., Phamduy, T. B., Sharpe, A. H. & Freeman, G. J. Programmed death-1 ligand 1 interacts specifically with the B7-1 costimulatory molecule to inhibit T cell responses. *Immunity* **27**, 111–22 (2007).

78. Eissner, G., Kolch, W. & Scheurich, P. Ligands working as receptors: reverse signaling by members of the TNF superfamily enhance the plasticity of the immune system. *Cytokine & Growth Factor Reviews* **15**, 353–66 (2004).

79. Munn, D. H., Sharma, M. D. & Mellor, A. L. Ligation of B7-1/B7-2 by human CD4+ T cells triggers indoleamine 2,3-dioxygenase activity in dendritic cells. *Journal of Immunology* **172**, 4100–10 (2004).

80. Khawli, A. L., Peisheng, H. & Epstein, A. L. Targeted and Untargeted Fusion Proteins: Current Approaches to Cancer Immunotherapy. *Fusion Protein Technologies for Biopharmaceuticals: Applications and Challenges* 295–314 (2013). doi:10.1002/9781118354599.ch19

81. Kontermann, R. E. Antibody-cytokine fusion proteins. *Archives of Biochemistry and Biophysics* **526**, 194–205 (2012).

82. Chames, P., Van Regenmortel, M., Weiss, E. & Baty, D. Therapeutic antibodies: successes, limitations and hopes for the future. *British Journal of Pharmacology* **157**, 220–33 (2009).

83. Kontermann, R. E. Recombinant bispecific antibodies for cancer therapy. *Acta Pharmacologica Sinica* **26**, 1–9 (2005).

84. Holliger, P., Prospero, T. & Winter, G. "Diabodies": small bivalent and bispecific antibody fragments. *Proceedings of the National Academy of Sciences of the United States of America* **90**, 6444–8 (1993).

85. Gruber, M., Schodin, B. A., Wilson, E. R. & Kranz, D. M. Efficient tumor cell lysis mediated by a bispecific single chain antibody expressed in Escherichia coli. *Journal of Immunology* **152**, 5368–74 (1994).

86. Lechner, M. G., Russell, S. M., Bass, R. S. & Epstein, A. L. Chemokines, costimulatory molecules and fusion proteins for the immunotherapy of solid tumors. *Immunotherapy* **3**, 1317–40 (2011).

87. Ortiz-Sánchez, E., Helguera, G., Daniels, T. R. & Penichet, M. L. Antibody-cytokine fusion proteins: applications in cancer therapy. *Expert Opinion on Biological Therapy* **8**, 609–32 (2008).

88. Frey, K. Novel costimulatory antibody fusion proteins for cellular immunotherapy. *Diploma Thesis* (2007).

89. Diebolder, P. J. Retargeting and costimulation of human T-cells using bispecific antibodies and costimulatory fusion proteins of the TNF and B7 family. *Diploma Thesis* (2009).

90. Müller, D., Karle, A., Ho, I., Stork, R. & Kontermann, R. E. Improved Pharmacokinetics of Recombinant Bispecific Antibody Molecules by Fusion to Human Serum Albumin. *Journal of Biological Chemistry* **282**, 12650 –12660 (2007).

91. Janeway, C. A. J., Travers, P., Walport, M. & Shlomchik, M. J. *Immunobiology: The Immune System in Health and Disease*. (Garland Science: 2001).

92. Dixon, J. F., Law, J. L. & Favero, J. J. Activation of Human T Lymphocytes by Crosslinking of Anti-CD3 Monoclonal Antibodies. *Journal of Leukocyte Biology* **46**, 214–20 (1989).

93. Baeuerle, P. A., Kufer, P. & Lutterbüse, R. Bispecific antibodies for polyclonal T-cell engagement. *Current Opinion in Molecular Therapeutics* **5**, 413–419 (2003).

94. Holliger, P. *et al.* Carcinoembryonic Antigen (CEA)-specific T-Cell Activation in Colon Carcinoma Induced by Anti-CD3xAnti-CEA Bispecific Diabodies and B7xAnti-CEA Bispecific Fusion Proteins. *Cancer Research* **59**, 2909–16 (1999).

95. Cochlovius, B. *et al.* Treatment of Human B Cell Lymphoma Xenografts with a CD3 x CD19 Diabody and T Cells. *Journal of Immunology* **165**, 888–95 (2000).

96. Baeuerle, P. A., Kufer, P. & Bargou, R. BiTE: Teaching antibodies to engage T-cells for cancer therapy. *Current Opinion in Molecular Therapeutics* **11**, 22–30 (2009).

97. May, C., Sapra, P. & Gerber, H.-P. Advances in bispecific biotherapeutics for the treatment of cancer. *Biochemical Pharmacology* **84**, 1105–12 (2012).

98. Haas, C. *et al.* Mode of cytotoxic action of T cell-engaging BiTE antibody MT110. *Immunobiology* **214**, 441–53 (2009).

99. Miles, A. K., Matharoo-Ball, B., Li, G., Ahmad, M. & Rees, R. C. The identification of human tumour antigens: Current status and future developments. *Cancer Immunology, Immunotherapy* **55**, 996–1003 (2006).

100. Bhowmick, N. A., Neilson, E. G. & Moses, H. L. Stromal fibroblasts in cancer initiation and progression. *Nature* **432**, 332–337 (2004).

101. Rønnov-Jessen, L., Petersen, O. W. & Bissell, M. J. Cellular changes involved in conversion of normal to malignant breast: importance of the stromal reaction. *Physiological Reviews* **76**, 69–125 (1996).

102. Kalluri, R. & Zeisberg, M. Fibroblasts in cancer. *Nature Reviews. Cancer* **6**, 392–401 (2006).

103. Brennen, W. N., Isaacs, J. T. & Denmeade, S. R. Rationale Behind Targeting Fibroblast Activation Protein–Expressing Carcinoma-Associated Fibroblasts as a Novel Chemotherapeutic Strategy. *Molecular Cancer Therapeutics* **11**, 257–66 (2012).

104. Scanlan, M. J. *et al.* Molecular cloning of fibroblast activation protein alpha, a member of the serine protease family selectively expressed in stromal fibroblasts of epithelial cancers. *Proceedings of the National Academy of Sciences of the United States of America* **91**, 5657–61 (1994).

105. Park, J. E. *et al.* Fibroblast activation protein, a dual specificity serine protease expressed in reactive human tumor stromal fibroblasts. *The Journal of Biological Chemistry* **274**, 36505–12 (1999).

106. Aertgeerts, K. *et al.* Structural and Kinetic Analysis of the Substrate Specificity of Human Fibroblast Activation Protein α. *The Journal of Biological Chemistry* **280**, 19441–4 (2005).

107. Chen, W.-T. & Kelly, T. Seprase complexes in cellular invasiveness. *Cancer Metastasis Reviews* **22**, 259–69 (2003).

108. Scott, A. M. *et al.* A Phase I Dose-Escalation Study of Sibrotuzumab in Patients with Advanced or Metastatic Fibroblast Activation Protein-positive Cancer. *Clinical Cancer Research* **9**, 1639–47 (2003).

109. Hofheinz, R.-D. *et al.* Stromal antigen targeting by a humanised monoclonal antibody: an early phase II trial of sibrotuzumab in patients with metastatic colorectal cancer. *Onkologie* **26**, 44–8 (2003).

110. Cheng, J. D. *et al.* Promotion of Tumor Growth by Murine Fibroblast Activation Protein, a Serine Protease, in an Animal Model. *Cancer Research* **62**, 4767–4772 (2002).

111. Lee, J., Fassnacht, M., Nair, S., Boczkowski, D. & Gilboa, E. Tumor Immunotherapy Targeting Fibroblast Activation Protein, a Product Expressed in Tumor-Associated Fibroblasts. *Cancer Research* **65**, 11156–63 (2005).

112. Brocks, B. *et al.* Species-Crossreactive scFv Against the Tumor Stroma Marker "Fibroblast Activation Protein" Selected by Phage Display From an Immunized FAP-/- Knock-Out Mouse. *Molecular Medicine* **7**, 461–9 (2001).

113. Mersmann, M. *et al.* Human antibody derivatives against the fibroblast activation protein for tumor stroma targeting of carcinomas. *International Journal of Cancer* **92**, 240–8 (2001).

114. Schmidt, a *et al.* Generation of human high-affinity antibodies specific for the fibroblast activation protein by guided selection. *European Journal of Biochemistry* **268**, 1730–8 (2001).

115. Niedermeyer, J. *et al.* Mouse fibroblast activation protein: molecular cloning, alternative splicing and expression in the reactive stroma of epithelial cancers. *International Journal of Cancer* **71**, 383–9 (1997).

116. Wüest, T., Moosmayer, D. & Pfizenmaier, K. Construction of a bispecific single chain antibody for recruitment of cytotoxic T cells to the tumour stroma associated antigen fibroblast activation protein. *Journal of Biotechnology* **92**, 159–68 (2001).

117. Zhu, Z. & Carter, P. Identification of Heavy Chain Residues in a Humanized Anti-CD3 Antibody Important for Efficient Antigen Binding and T Cell Activation. *Journal of Immunology* **155**, 1903–10 (1995).

118. Fonsatti, E., Nicolay, H. J. M., Altomonte, M., Covre, A. & Maio, M. Targeting cancer vasculature via endoglin/CD105: a novel antibody-based diagnostic and therapeutic strategy in solid tumours. *Cardiovascular Research* **86**, 12–9 (2010).

119. Dallas, N. a *et al.* Endoglin (CD105): a marker of tumor vasculature and potential target for therapy. *Clinical Cancer Research* **14**, 1931–7 (2008).

120. Rosen, L. S. *et al.* A phase I first-in-human study of TRC105 (Anti-Endoglin Antibody) in patients with advanced cancer. *Clinical Cancer Research* **18**, 4820–9 (2012).

121. Bernabeu, C., Lopez-Novoa, J. M. & Quintanilla, M. The emerging role of TGF-β superfamily coreceptors in cancer. *Biochimica et biophysica acta* **1792**, 954–73 (2009).

122. Gougos, A. & Letarte, M. Identification of a Human Endothelial Cell Antigen with Monoclonal Antibody 44G4 produced against a Pre-B Leukemic Cell Line. *Journal of Immunology* **141**, 1925–1933 (1988).

123. Gougos, A. & Letarte, M. Primary Structure of Endoglin, an RGD-containing Glycoprotein of Human Endothelial Cells. *Journal of Biological Chemistry* **265**, 8361–8364 (1990).

124. Bellón, T. *et al.* Identification and expression of two forms of the human transforming growth factor-β-binding protein endoglin with distinct cytoplasmic regions. *European Journal of Immunology* **23**, 2340–5 (1993).

125. Nassiri, F. *et al.* Endoglin (CD105): A Review of its Role in Angiogenesis and Tumor Diagnosis, Progression and Therapy. *Anticancer Research* **31**, 2283–90 (2011).

126. Düwel, A. *et al.* Reduced tumor growth and angiogenesis in endoglin-haploinsufficient mice. *Tumour Biology* **28**, 1–8 (2007).

127. Korn, T., Müller, R. & Kontermann, R. E. Bispecific Single-Chain Diabody-Mediated Killing of Endoglin-Positive Endothelial Cells by Cytotoxic T Lymphocytes. *Journal of Immunotherapy* **27**, 99–106 (2004).

128. Völkel, T., Müller, R. & Kontermann, R. E. Isolation of endothelial cell-specific human antibodies from a novel fully synthetic scFv library. *Biochemical and Biophysical Research Communications* **317**, 515–21 (2004).

129. Völkel, T., Hölig, P., Merdan, T., Müller, R. & Kontermann, R. E. Targeting of immunoliposomes to endothelial cells using a single-chain Fv fragment directed against human endoglin (CD105). *Biochimica et Biophysica Acta* **1663**, 158–166 (2004).

130. Müller, D. *et al.* Murine endoglin-specific single-chain Fv fragments for the analysis of vascular targeting strategies in mice. *Journal of Immunological Methods* **339**, 90–8 (2008).

131. Melero, I. *et al.* Palettes of Vaccines and Immunostimulatory Monoclonal Antibodies for Combination. *Clinical Cancer Research* **15**, 1507–9 (2009).

132. Takeda, K. *et al.* Combination Therapy of Established Tumors by Antibodies Targeting Immune Activating and Suppressing Molecules. *Journal of Immunology* **184**, 5493–501 (2010).

133. Guinn, B., DeBenedette, M., Watts, T. H. & Berinstein, N. L. 4-1BBL Cooperates with B7-1 and B7-2 in Converting a B Cell Lymphoma Cell Line into a Long-Lasting Antitumor Vaccine. *Journal of Immunology* **162**, 5003–10 (1999).

134. Li, G. *et al.* Triple expression of B7-1, B7-2 and 4-1BBL enhanced antitumor immune response against mouse H22 hepatocellular carcinoma. *Journal of Cancer Research and Clinical Oncology* (2010).doi:10.1007/s00432-010-0905-9

135. Adler, A. J. & Vella, A. T. Betting on improved cancer immunotherapy by doubling down on CD134 and CD137 co-stimulation. *OncoImmunology* **2**, e22837 (2013).

136. Gray, J. C. *et al.* Optimising anti-tumour CD8 T-cell responses using combinations of immunomodulatory antibodies. *European Journal of Immunology* **38**, 2499–511 (2008).

137. Uno, T. *et al.* Eradication of established tumors in mice by a combination antibody-based therapy. *Nature Medicine* **12**, 693–8 (2006).

138. Kocak, E. *et al.* Combination therapy with anti-CTL antigen-4 and anti-4-1BB antibodies enhances cancer immunity and reduces autoimmunity. *Cancer Research* **66**, 7276–84 (2006).

139. Vezys, V. *et al.* 4-1BB Signaling Synergizes with Programmed Death Ligand 1 Blockade To Augment CD8 T Cell Responses during Chronic Viral Infection. *Journal of Immunology* **187**, 1634–42 (2011).

140. Melero, I., Hirschhorn-Cymerman, D., Morales-Kastresana, A., Sanmamed, M. F. & Wolchok, J. D. Agonist Antibodies to TNFR Molecules That Costimulate T and NK Cells. *Clinical Cancer Research* **19**, 1044–53 (2013).

141. Gajewski, T. F. *et al.* Immune resistance orchestrated by the tumor microenvironment. *Immunological Reviews* **213**, 131–45 (2006).

142. De Saint Basile, G., Ménasché, G. & Fischer, A. Molecular mechanisms of biogenesis and exocytosis of cytotoxic granules. *Nature Reviews Immunology* **11**, 568–579 (2010).

143. Betts, M. R. *et al.* Sensitive and viable identification of antigen-specific CD8 + T cells by a flow cytometric assay for degranulation. *Journal of Immunological Methods* **281**, 65 – 78 (2003).

144. Klebanoff, C. a, Gattinoni, L. & Restifo, N. P. CD8+ T-cell memory in tumor immunology and immunotherapy. *Immunological Reviews* **211**, 214–24 (2006).

145. Fife, B. T. & Bluestone, J. a Control of peripheral T-cell tolerance and autoimmunity via the CTLA-4 and PD-1 pathways. *Immunological Reviews* **224**, 166–82 (2008).

146. Parry, R. V *et al.* CTLA-4 and PD-1 Receptors Inhibit T-Cell Activation by Distinct Mechanisms †. *Molecular and Cellular Biology* **25**, 9543–9553 (2005).

147. Wang, X. B., Zheng, C. Y., Giscombe, R. & Lefvert, a K. Regulation of Surface and Intracellular Expression of CTLA-4 on Human Peripheral T Cells. *Scandinavian Journal of Immunology* **54**, 453–8 (2001).

148. Liao, K. W., Lo, Y. C. & Roffler, S. R. Activation of lymphocytes by anti-CD3 single-chain antibody dimers expressed on the plasma membrane of tumor cells. *Gene Therapy* **7**, 339–47 (2000).

149. Freeman, G. J. *et al.* Murine B7-2, an Alternative CTLA-4 Counter-receptor that Costimulates T Cell Proliferation and Interleukin 2 Production. *The Journal of Experimental Medicine* **178**, 2185–2192 (1993).

150. Bossen, C. *et al.* Interactions of Tumor Necrosis Factor (TNF) and TNF Receptor Family Members in the Mouse and Human. *Journal of Biological Chemistry* **281**, 13964 –13971 (2006).

151. Reinhardt, K. Mouse and Human 4-1BBL Antibody Fusion Proteins for Targeted Cancer Immunotherapy. *Diploma Thesis* (2011).

152. Rennert, P. *et al.* The IgV domain of human B7-2 (CD86) is sufficient to co-stimulate T lymphocytes and induce cytokine secretion. *International Immunology* **9**, 805–13 (1997).

153. Sturmhoefel, K. *et al.* Potent activity of soluble B7-IgG fusion proteins in therapy of established tumors and as vaccine adjuvant. *Cancer Research* **59**, 4964–72 (1999).

154. Rabu, C. *et al.* Production of recombinant human trimeric CD137L (4-1BBL). Cross-linking is essential to its T cell co-stimulation activity. *The Journal of Biological Chemistry* **280**, 41472–81 (2005).

155. Tammana, S. *et al.* 4-1BB and CD28 Signaling Plays a Synergistic Role in Redirecting Umbilical Cord Blood T Cells Against B-Cell Malignancies. *Human Gene Therapy* **21**, 75–86 (2010).56. Rudolf, D. *et al.* Potent costimulation of human CD8 T cells by anti-4-1BB and anti-CD28 on synthetic artificial antigen presenting cells. *Cancer Immunology, Immunotherapy* **57**, 175–83 (2008).

157. Shuford, W. W. *et al.* 4-1BB Costimulatory Signals Preferentially Induce CD8+ T Cell Proliferation and Lead to the Amplification In Vivo of Cytotoxic T Cell Responses. *The Journal of Experimental Medicine* **186**, 47–55 (1997).

158. Kober, J. *et al.* The capacity of the TNF family members 4-1BBL, OX40L, CD70, GITRL, CD30L and LIGHT to costimulate human T cells. *European Journal of Immunology* **38**, 2678–88 (2008).

159. Rajasekaran, K., Xiong, V., Fong, L., Gorski, J. & Malarkannan, S. Functional Dichotomy between NKG2D and CD28- Mediated Co-Stimulation in Human CD8+ T Cells. *PLoS one* **5**, e12635 (2010).

160. Wen, T., Bukczynski, J. & Watts, T. H. 4-1BB Ligand-Mediated Costimulation of Human T Cells Induces CD4 and CD8 T Cell Expansion, Cytokine Production, and the Development of Cytolytic Effector Function. *Journal of immunology* **168**, 4897–906 (2002).

161. Houtenbos, I. *et al.* Leukemia-specific T-cell reactivity induced by leukemic dendritic cells is augmented by 4-1BB targeting. *Clinical Cancer Research* **13**, 307–15 (2007).

162. Sallusto, F., Lenig, D., Förster, R., Lipp, M. & Lanzavecchia, A. Two subsets of memory T lymphocytes with distinct homing potentials and effector functions. *Nature* **401**, 708–12 (1999).

163. Klebanoff, C. a *et al.* Central memory self/tumor-reactive CD8+ T cells confer superior antitumor immunity compared with effector memory T cells. *Proceedings of the National Academy of Sciences of the United States of America* **102**, 9571–6 (2005).

164. Dong, H. *et al.* Tumor-associated B7-H1 promotes T-cell apoptosis: a potential mechanism of immune evasion. *Nature Medicine* **8**, 793–800 (2002).

165. Topalian, S. L., Drake, C. G. & Pardoll, D. M. Targeting the PD-1/B7-H1(PD-L1) pathway to activate anti-tumor immunity. *Current Opinion in Immunology* **24**, 207–12 (2012).

166. Chattopadhyay, K. *et al.* Assembly and structural properties of glucocorticoid-induced TNF receptor ligand: Implications for function. *Proceedings of the National Academy of Sciences of the United States of America* **104**, 19452–7 (2007).

167. Zhou, Z. *et al.* Human glucocorticoid-induced TNF receptor ligand regulates its signaling activity through multiple oligomerization states. *Proceedings of the National Academy of Sciences of the United States of America* **105**, 5465–70 (2008).

168. Chattopadhyay, K. *et al.* Sequence, structure, function, immunity: structural genomics of costimulation. *Immunological Reviews* **229**, 356–86 (2009).

169. Tamada, K. *et al.* LIGHT, a TNF-Like Molecule, Costimulates T Cell Proliferation and Is Required for Dendritic Cell-Mediated Allogeneic T Cell Response. *Journal of immunology* **164**, 4105–10 (2000).

170. Serghides, L. *et al.* Evaluation of OX40 Ligand as a Costimulator of Human Antiviral Memory CD8 T Cell Responses: Comparison with B7.1 and 4-1BBL. *Journal of Immunology* 6368–6377 (2005).

171. Schaer, D. A., Murphy, J. T. & Wolchok, J. D. Modulation of GITR for cancer immunotherapy. *Current Opinion in Immunology* **24**, 217–24 (2012).

172. Yu, P. *et al.* Priming of naive T cells inside tumors leads to eradication of established tumors. *Nature Immunology* **5**, 141–9 (2004).

173. Sharma, R. K., Yolcu, E. S., Elpek, K. G. & Shirwan, H. Tumor cells engineered to codisplay on their surface 4-1BBL and LIGHT costimulatory proteins as a novel vaccine approach for cancer immunotherapy. *Cancer Gene Therapy* **17**, 730–41 (2010).

174. Park, J.-J. *et al.* Expression of anti-HVEM single-chain antibody on tumor cells induces tumor-specific immunity with long-term memory. *Cancer Immunology, Immunotherapy* (2011).doi:10.1007/s00262-011-1101-8

175. Dawicki, W., Bertram, E. M., Sharpe, A. H. & Watts, T. H. 4-1BB and OX40 act independently to facilitate robust CD8 and CD4 recall responses. *Journal of Immunology* **173**, 5944–51 (2004).

176. Snell, L. M., Lin, G. H. Y., McPherson, A. J., Moraes, T. J. & Watts, T. H. T-cell intrinsic effects of GITR and 4-1BB during viral infection and cancer immunotherapy. *Immunological Reviews* **244**, 197–217 (2011).

177. Ronchetti, S. *et al.* Glucocorticoid-induced TNFR-related protein lowers the threshold of CD28 costimulation in CD8+ T cells. *Journal of Immunology* **179**, 5916–26 (2007).

178. Rogers, P. R., Song, J., Gramaglia, I., Killeen, N. & Croft, M. OX40 promotes Bcl-xL and Bcl-2 expression and is essential for long-term survival of CD4 T cells. *Immunity* **15**, 445–55 (2001).

179. Walker, L. S. *et al.* Compromised OX40 Function in CD28-deficient Mice Is Linked with Failure to Develop CXC Chemokine Receptor 5–positive CD4 Cells and Germinal Centers. *The Journal of Experimental Medicine* **190**, 1115–22 (1999).

180. Gad, S. C. *Clinical Trials Handbook*. 1248pp. (John Wiley & Sons: 2009).

181. Ascierto, P. a, Simeone, E., Sznol, M., Fu, Y.-X. & Melero, I. Clinical Experiences With Anti-CD137 and Anti-PD1 Therapeutic Antibodies. *Seminars in Oncology* **37**, 508–16 (2010).

182. Moran, A. E., Kovacsovics-Bankowski, M. & Weinberg, A. D. The TNFRs OX40, 4-1BB, and CD40 as targets for cancer immunotherapy. *Current Opinion in Immunology* **25**, 230–7 (2013).

183. Fisher, T. S. *et al.* Targeting of 4-1BB by monoclonal antibody PF-05082566 enhances T-cell function and promotes anti-tumor activity. *Cancer Immunology, Immunotherapy* **61**, 1721–33 (2012).

184. Weinberg, A. D. *et al.* Anti-OX40 (CD134) Administration to Nonhuman Primates: Immunostimulatory Effects and Toxicokinetic Study. *Journal of Immunotherapy* **29**, 575–85 (2006).

185. Kontermann, R. E. Strategies for extended serum half-life of protein therapeutics. *Current Opinion in Biotechnology* **22**, 868–76 (2011).

186. Nagorsen, D., Kufer, P., Baeuerle, P. a & Bargou, R. Blinatumomab: a historical perspective. *Pharmacology & Therapeutics* **136**, 334–42 (2012).

187. Hutt, M., Färber-Schwarz, A., Unverdorben, F., Richter, F. & Kontermann, R. E. Plasma Half-life Extension of Small Recombinant Antibodies by Fusion to Immunoglobulin-binding Domains. *The Journal of Biological Chemistry* **287**, 4462–9 (2012).

188. Stork, R. *et al.* N-glycosylation as novel strategy to improve pharmacokinetic properties of bispecific single-chain diabodies. *The Journal of Biological Chemistry* **283**, 7804–7812 (2008).

189. Stork, R., Müller, D. & Kontermann, R. E. A novel tri-functional antibody fusion protein with improved pharmacokinetic properties generated by fusing a bispecific single-chain diabody with an albumin-binding domain from streptococcal protein G. *Protein Engineering, Design & Selection* **20**, 569–576 (2007).

190. Unverdorben, F., Färber-Schwarz, A., Richter, F., Hutt, M. & Kontermann, R. E. Half-life extension of a single-chain diabody by fusion to domain B of staphylococcal protein A. *Protein Engineering, Design & Selection* **25**, 81–8 (2012).

191. Stork, R., Campigna, E., Robert, B., Mu, D. & Kontermann, R. E. Biodistribution of a Bispecific Single-chain Diabody and Its Half-life Extended Derivatives. *Journal of Biological Chemistry* **284**, 25612–25619 (2009).

192. Boise, L. H. *et al.* CD28 costimulation Can Promote T Cell Survival by Enhancing the Expression of Bcl-xL. *Journal of Immunology* **3**, 87–98 (1995).

193. Marrack, P. & Kappler, J. Control of T Cell Viability. *Annual Review of Immunology* **22**, 765–87 (2004).

Sequences

pSecTagA

Vector map of pSecTagA.

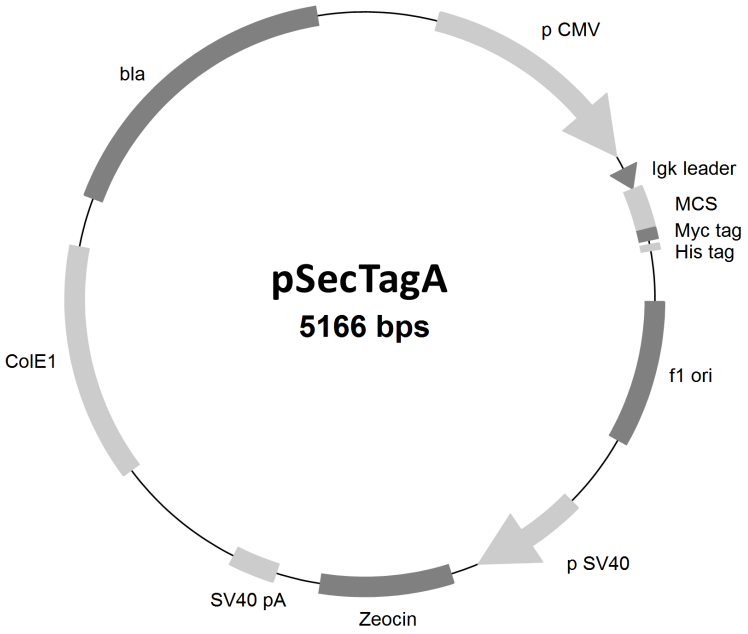

Abbreviations: pCMV: human cytomegalovirus immediate-early promoter, Igκ leader: signal sequence for protein secretion, MCS: multiple cloning site, Myc and His tag: tags for protein purification, f1 ori: phage fi origin of replication, pSV40: simian virus 40 promoter, Zeocin: zeocin resistance gene, SV40 pA: SV40 poly-adenylation site, ColE1: origin of replication for E.coli, bla: β-lactamase (ampicillin resistance).

Section of pSecTagA sequence containing the Igκ leader sequence, Myc- and His-tag, the multiple cloning site and the binding sequences of the primer pET-Seq1 and pSec-Seq2:

```
 871  ctc act ata ggg aga ccc aag ctg gct agc cac cat gga gac aga cac act cct gct atg ggt act gct gct ctg ggt tcc agg ttc
         pET-Seq1
                                                >>.........................Igk leader ............................>
                                                   m   e   t   d   t   l   l   l   w   v   l   l   l   w   v   p   g

                                                                 KpnI
                                                               ------+
                            SfiI                             HindIII                BamHI                        EcoRI
                  ----------+------                          --+-----               -+-----                     --+-----
 958  cac tgg tga cgc ggc cca gcc ggc cag gcg cgc cgt acg aag ctt ggt acc gag ctc gga tcc act agt cca gtg tgg tgg aat tct
      >.........>> Igk leader
      s   t   g   d

           EcoRV                          XhoI           ApaI
         ----+--                       --+-----       -------+
      PstI                        NotI           XbaI
    -----+-                   ---+------       --+-----
1045  gca gat atc cag cac agt ggc ggc cgc tcg agt cta gag ggc ccg aac aaa aac tca tct cag aag agg atc tga ata gcg ccg tcg
                                                           >>..............c-myc tag.............>>
                                                              e   q   k   l   i   s   e   e   d   l   n

1132  acc atc atc atc atc atc att gag ttt aaa ccc gct gat cag cct cga ctg tgc ctt cta gtt gcc agc cat ctg ttg ttt gcc cct
                                                                 pSec-Seq2
        >>......His-tag.......>>
           h   h   h   h   h   h
```

The antibody-ligand fusion protein sequences shown in the following are all a section from a pSecTagA vector.

B7.1-Db36

```
                                                                                SfiI
                                                                          ----------+-----
   1  atg gag aca gac aca ctc ctg cta tgg gta ctg ctg ctc tgg gtt cca ggt tcc act ggt gac gcg gcc cag ccg gcc atg gcc gtg
        m   e   t   d   t   l   l   l   w   v   l   l   l   w   v   p   g   s   t   g   d   a   a   q   p   a   m   a   v
      >>.....................................Igκ leader.....................................>>                  B7.1 >>>

  88  att cac gtg acc aaa gaa gtg aaa gag gtg gcc aca ctg agc tgc ggc cac aac gtg tcc gtg gaa gaa ctg gcc cag acc cgg atc
        i   h   v   t   k   e   v   k   e   v   a   t   l   s   c   g   h   n   v   s   v   e   e   l   a   q   t   r   i
      >.....................................................B7.1.....................................................>

 175  tac tgg cag aaa gaa aag aaa atg gtg ctg acc atg atg agc ggc gac atg aac atc tgg ccc gag tac aag aac cgg acc atc ttc
        y   w   q   k   e   k   k   m   v   l   t   m   m   s   g   d   m   n   i   w   p   e   y   k   n   r   t   i   f
      >.....................................................B7.1.....................................................>

 262  gac atc acc aac aac ctg agc atc gtg atc ctg gcc ctg agg cct tcc gac gag ggc acc tat gag tgc gtg gtg ctg aag tac gag
        d   i   t   n   n   l   s   i   v   i   l   a   l   r   p   s   d   e   g   t   y   e   c   v   v   l   k   y   e
      >.....................................................B7.1.....................................................>

 349  aag gac gcc ttc aag cgc gag cac ctg gcc gaa gtg acc ctg agc gtg aag gcc gac ttc ccc acc ccc agc atc agc gac ttc gag
        k   d   a   f   k   r   e   h   l   a   e   v   t   l   s   v   k   a   d   f   p   t   p   s   i   s   d   f   e
      >.....................................................B7.1.....................................................>

 436  atc ccc acc agc aac atc cgg cgg atc atc tgc agc acc agc ggc ggc ttt cca gag cct cac ctg agc tgg ctg gaa aac ggc gag
        i   p   t   s   n   i   r   r   i   i   c   s   t   s   g   g   f   p   e   p   h   l   s   w   l   e   n   g   e
      >.....................................................B7.1.....................................................>

 523  gaa ctg aac gcc atc aac acc acc gtg tcc cag gac ccc gag aca gag ctg tac gcc gtg tcc agc aag ctg gac ttc aac atg acc
        e   l   n   a   i   n   t   t   v   s   q   d   p   e   t   e   l   y   a   v   s   s   k   l   d   f   n   m   t
      >.....................................................B7.1.....................................................>

 610  acc aac cac agc ttc atg tgc ctg att aag tac ggc cac ctg aga gtg aac cag acc ttc aac tgg aac acc acc aag cag gaa cac
        t   n   h   s   f   m   c   l   i   k   y   g   h   l   r   v   n   q   t   f   n   w   n   t   t   k   q   e   h
      >.....................................................B7.1.....................................................>

                                                                          XhoI
                                                                        --+-----
 697  ttc ccc gac aac ggc gga gga tcc ggg gga gga agt ggc ggc gga tct ggc gga ggc tcg agc gga ggc ggt tca cag gtg cag ctg
        f   p   d   n   g   g   g   s   g   g   g   s   g   g   g   s   g   g   g   s   s   g   g   g   s   q   v   q   l
      >....B7.1....>> >>.....................................Linker.....................................>> >>..VHmo36....>

 784  aag cag tct gga gct gaa ctg gtg aaa ccc ggg gca tca gtg aag ctg tcc tgc aag act tct ggc tac acc ttc act gaa aat att
        k   q   s   g   a   e   l   v   k   p   g   a   s   v   k   l   s   c   k   t   s   g   y   t   f   t   e   n   i
      >.....................................................VHmo36.....................................................>

 871  ata cac tgg gta aag cag agg tct ggg cag ggt ctt gag tgg att ggg tgg ttt cac cct gga agt ggt agt ata aag tac aat gag
        i   h   w   v   k   q   r   s   g   q   g   l   e   w   i   g   w   f   h   p   g   s   g   s   i   k   y   n   e
      >.....................................................VHmo36.....................................................>

 958  aaa ttc aag gac aag gcc aca ttg act gcg gac aaa tcc tcc agc aca gtc tat atg gag ctt agt aga ttg aca tct gaa gac tct
        k   f   k   d   k   a   t   l   t   a   d   k   s   s   s   t   v   y   m   e   l   s   r   l   t   s   e   d   s
      >.....................................................VHmo36.....................................................>

1045  gcg gtc tat ttc tgt gca aga cac gga gga act ggg cga gga gct atg gac tac tgg ggt caa gga acc tca gtc acc gtc tca agt
        a   v   y   f   c   a   r   h   g   g   t   g   r   g   a   m   d   y   w   g   q   g   t   s   v   t   v   s   s
      >.....................................................VHmo36.....................................................>>

1132  ggt gga ggc gga tcc caa att ctg atg acc cag tct cct gct tcc tca gtt gta tct ctg ggg cag agg gcc acc atc tca tgc agg
        g   g   g   g   s   q   i   l   m   t   q   s   p   a   s   s   v   v   s   l   g   q   r   a   t   i   s   c   r
      >>....Linker.....>> >>.....................................VLmo36.....................................................>

1219  gcc agc aaa agt gtc agt aca tct gcc tat agt tat atg cac tgg tac caa cag aaa cca gga cag cca ccc aaa ctc ctc atc tat
        a   s   k   s   v   s   t   s   a   y   s   y   m   h   w   y   q   q   k   p   g   q   p   p   k   l   l   i   y
      >.....................................................VLmo36.....................................................>

1306  ctt gca tcc aac cta gaa tct ggg gtc cct ccc agg ttc agt ggc agt ggg tct ggg aca gac ttc acc ctc aac atc cac cct gtg
        l   a   s   n   l   e   s   g   v   p   p   r   f   s   g   s   g   s   g   t   d   f   t   l   n   i   h   p   v
      >.....................................................VLmo36.....................................................>

1393  gag gag gag gat gct gca acc tat tac tgt cag cac agt agg gag ctt ccg tac acg ttc gga ggg ggg acc aag ctg gaa ata aaa
        e   e   e   d   a   a   t   y   y   c   q   h   s   r   e   l   p   y   t   f   g   g   g   t   k   l   e   i   k
      >.....................................................VLmo36.....................................................>

1480  cgg gcg gcc gcc cac cat cat cac cat cac taa
        r   a   a   a   h   h   h   h   h   h   -
      >>> VLmo36      >>......His tag......>>stop
```

ICOSL-Db36

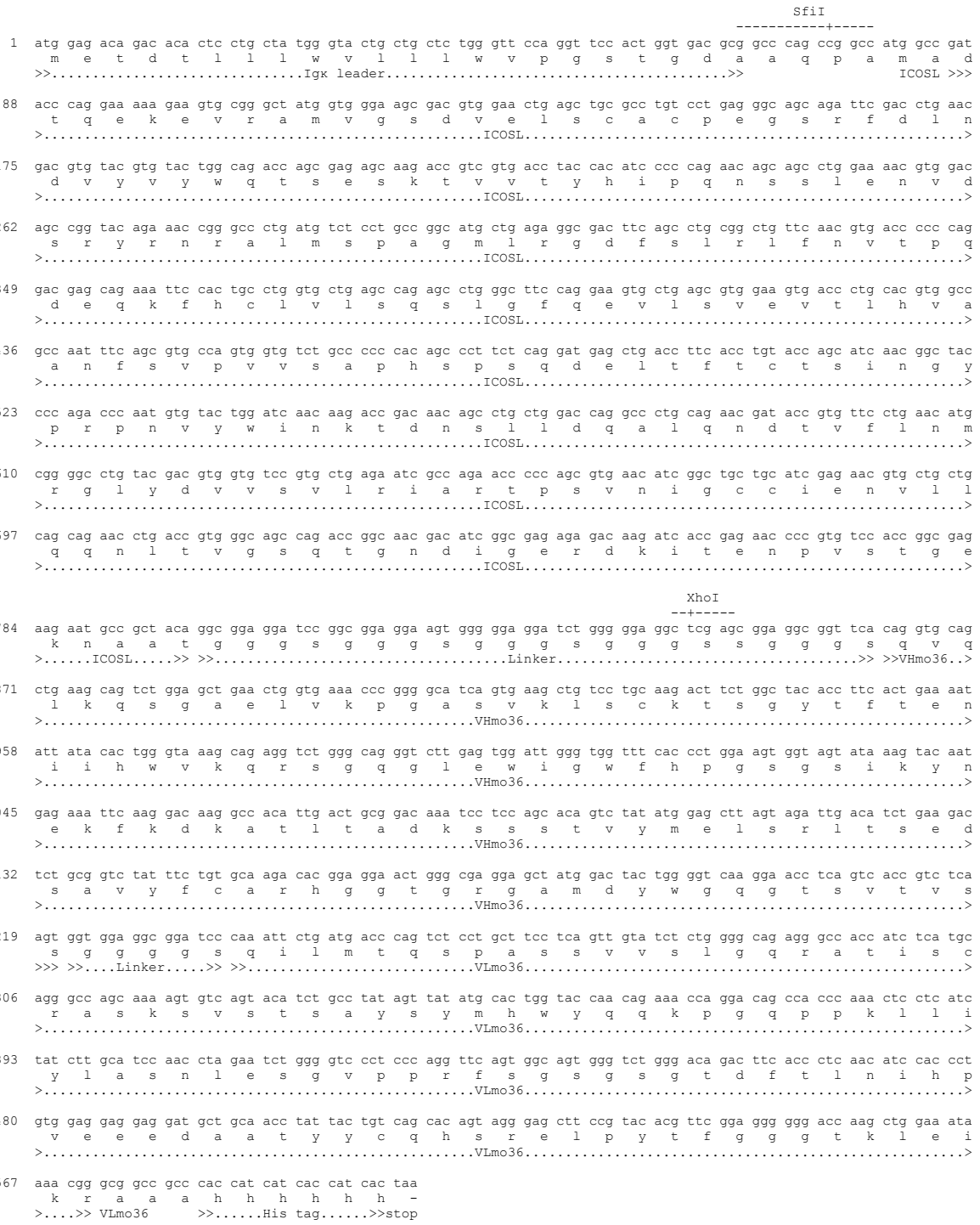
SfiI
1 atg gag aca gac aca ctc ctg cta tgg gta ctg ctg ctc tgg gtt cca ggt tcc act ggt gac gcg gcc cag ccg gcc atg gcc gat
m e t d t l l l w v l l l w v p g s t g d a a q p a m a d
>>.....Igκ leader.....>> ICOSL >>>
88 acc cag gaa aaa gaa gtg cgg gct atg gtg gga agc gac gtg gaa ctg agc tgc gcc tgt cct gag ggc agc aga ttc gac ctg aac
t q e k e v r a m v g s d v e l s c a c p e g s r f d l n
>.....ICOSL.....>
175 gac gtg tac gtg tac tgg cag acc agc gag agc aag acc gtc gtg acc tac cac atc ccc cag aac agc agc ctg gaa aac gtg gac
d v y v y w q t s e s k t v v t y h i p q n s s l e n v d
>.....ICOSL.....>
262 agc cgg tac aga aac cgg gcc ctg atg tct cct gcc ggc atg ctg aga ggc gac ttc agc ctg cgg ctg ttc aac gtg acc ccc cag
s r y r n r a l m s p a g m l r g d f s l r l f n v t p q
>.....ICOSL.....>
349 gac gag cag aaa ttc cac tgc ctg gtg ctg agc cag agc ctg ggc ttc cag gaa gtg ctg agc gtg gaa gtg acc ctg cac gtg gcc
d e q k f h c l v l s q s l g f q e v l s v e v t l h v a
>.....ICOSL.....>
436 gcc aat ttc agc gtg cca gtg gtg tct gcc ccc cac agc cct tct cag gat gag ctg acc ttc acc tgt acc agc atc aac ggc tac
a n f s v p v v s a p h s p s q d e l t f t c t s i n g y
>.....ICOSL.....>
523 ccc aga ccc aat gtg tac tgg atc aac aag acc gac aac agc ctg ctg gac cag gcc ctg cag aac gat acc gtg ttc ctg aac atg
p r p n v y w i n k t d n s l l d q a l q n d t v f l n m
>.....ICOSL.....>
610 cgg ggc ctg tac gac gtg gtg tcc gtg ctg aga atc gcc aga acc ccc agc gtg aac atc ggc tgc tgc atc gag aac gtg ctg ctg
r g l y d v v s v l r i a r t p s v n i g c c i e n v l l
>.....ICOSL.....>
697 cag cag aac ctg acc gtg ggc agc cag acc ggc aac gac atc ggc gag aga gac aag atc acc gag aac ccc gtg tcc acc ggc gag
q q n l t v g s q t g n d i g e r d k i t e n p v s t g e
>.....ICOSL.....>
XhoI
784 aag aat gcc gct aca ggc gga gga tcc ggc gga gga agt ggg gga gga tct ggg gga ggc tcg agc gga ggc ggt tca cag gtg cag
k n a a t g g g s g g g s g g g s g g g g s s g g g s q v q
>.....ICOSL.....>> >>.....Linker.....>> >>VHmo36..>
871 ctg aag cag tct gga gct gaa ctg gtg aaa ccc ggg gca tca gtg aag ctg tcc tgc aag act tct ggc tac acc ttc act gaa aat
l k q s g a e l v k p g a s v k l s c k t s g y t f t e n
>.....VHmo36.....>
958 att ata cac tgg gta aag cag agg tct ggg cag ggt ctt gag tgg att ggg tgg ttt cac cct gga agt ggt agt ata aag tac aat
i i h w v k q r s g q g l e w i g w f h p g s g s i k y n
>.....VHmo36.....>
1045 gag aaa ttc aag gac aag gcc aca ttg act gcg gac aaa tcc tcc agc aca gtc tat atg gag ctt agt aga ttg aca tct gaa gac
e k f k d k a t l t a d k s s s t v y m e l s r l t s e d
>.....VHmo36.....>
1132 tct gcg gtc tat ttc tgt gca aga cac gga gga act ggg cga gga gct atg gac tac tgg ggt caa gga acc tca gtc acc gtc tca
s a v y f c a r h g g t g r g a m d y w g q g t s v t v s
>.....VHmo36.....>
1219 agt ggt gga ggc gga tcc caa att ctg atg acc cag tct cct gct tcc tca gtt gta tct ctg ggg cag agg gcc acc atc tca tgc
s g g g g s q i l m t q s p a s s v v s l g q r a t i s c
>>> >>....Linker.....>> >>.....VLmo36.....>
1306 agg gcc agc aaa agt gtc agt aca tct gcc tat agt tat atg cac tgg tac caa cag aaa cca gga cag cca ccc aaa ctc ctc atc
r a s k s v s t s a y s y m h w y q q k p g q p p k l l i
>.....VLmo36.....>
1393 tat ctt gca tcc aac cta gaa tct ggg gtc cct ccc agg ttc agt ggc agt ggg tct ggg aca gac ttc acc ctc aac atc cac cct
y l a s n l e s g v p p r f s g s g s g t d f t l n i h p
>.....VLmo36.....>
1480 gtg gag gag gag gat gct gca acc tat tac tgt cag cac agt agg gag ctt ccg tac acg ttc gga ggg ggg acc aag ctg gaa ata
v e e e d a a t y y c q h s r e l p y t f g g g t k l e i
>.....VLmo36.....>
1567 aaa cgg gcg gcc gcc cac cat cat cac cat cac taa
k r a a a h h h h h h -
>....>> VLmo36 >>.....His tag.....>>stop

scFvA5-Ox40L

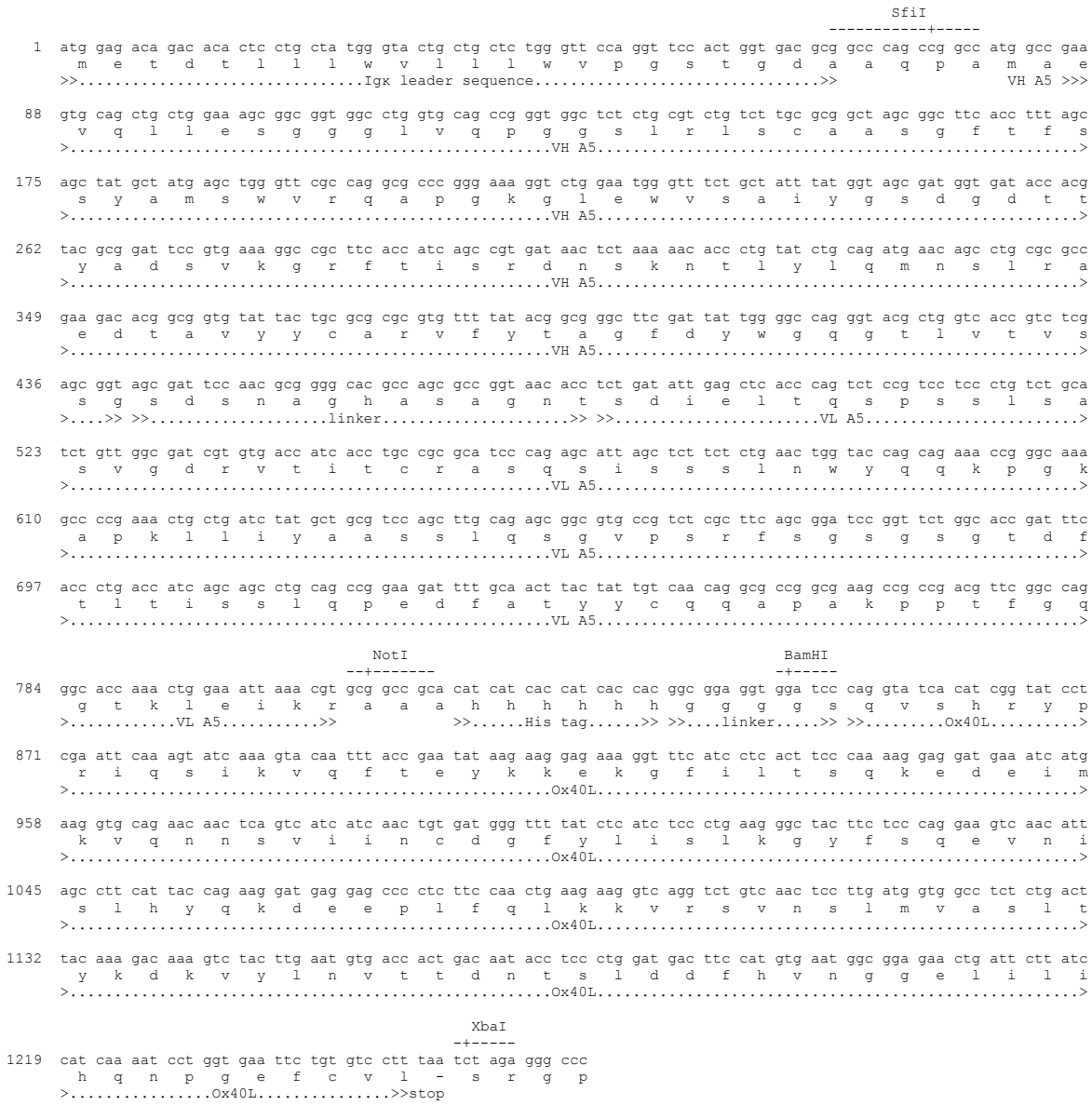

scFvA5-LIGHT

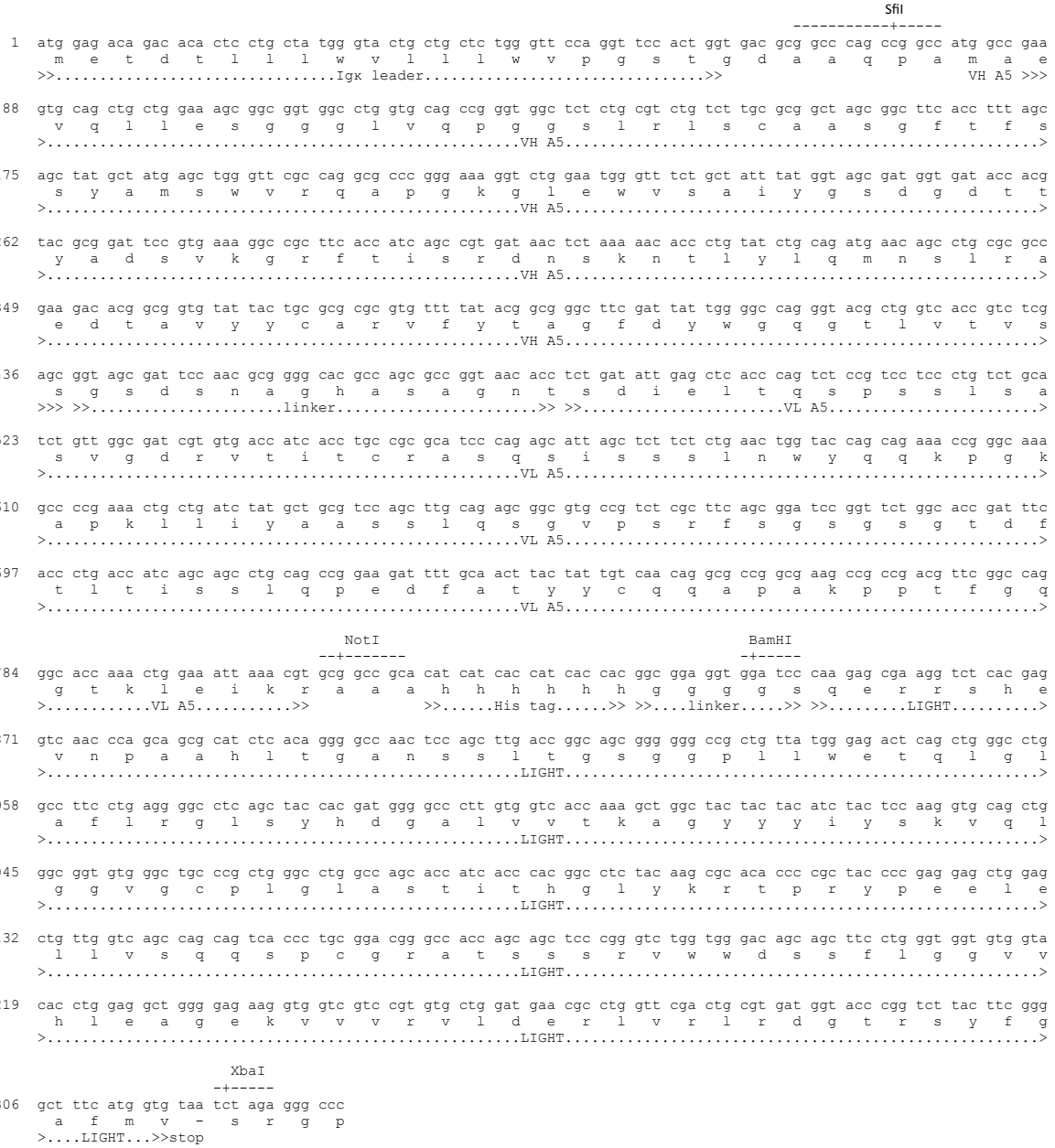

scFvA5-TNC-GITRL

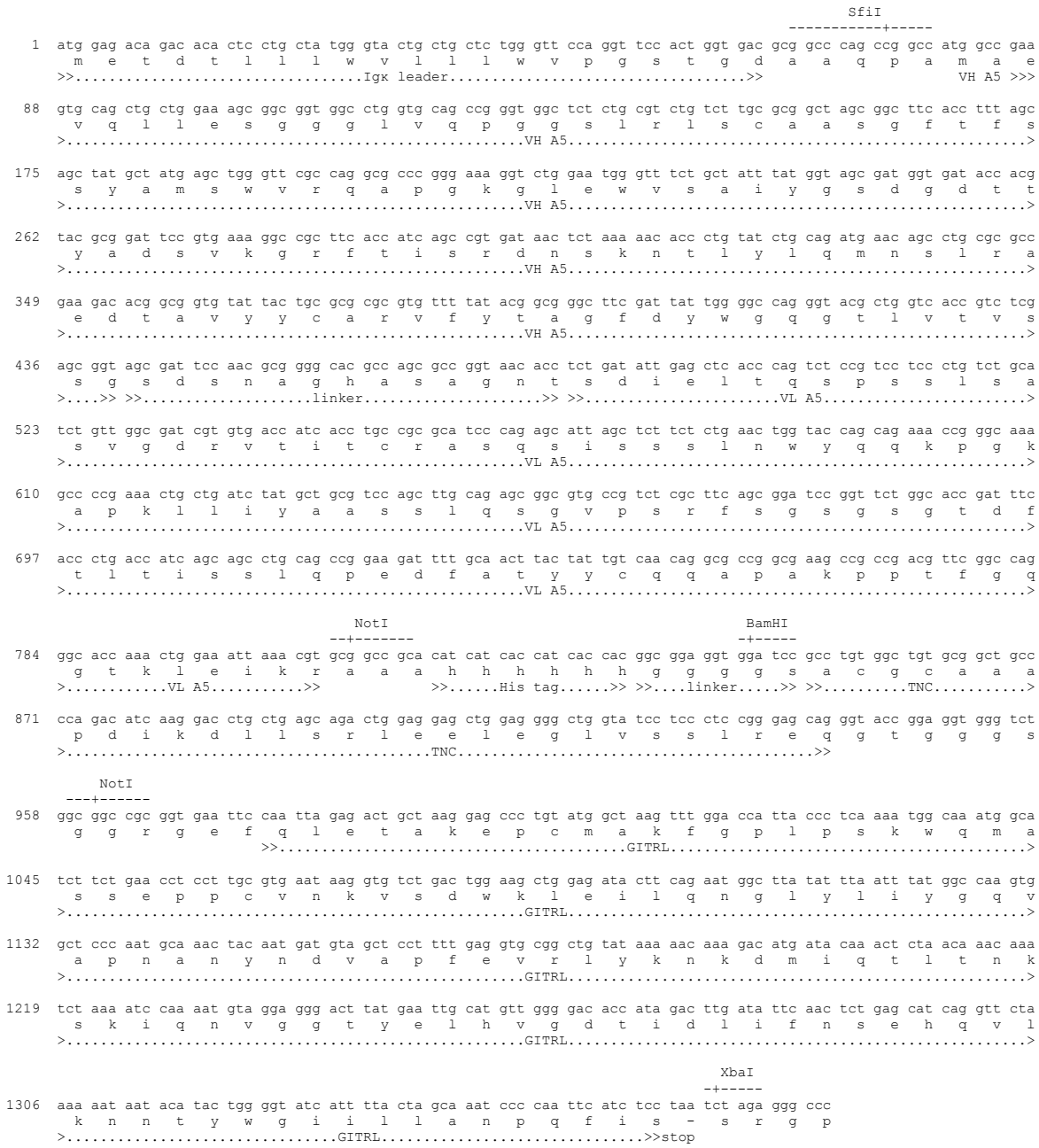

scFv36-Ox40L

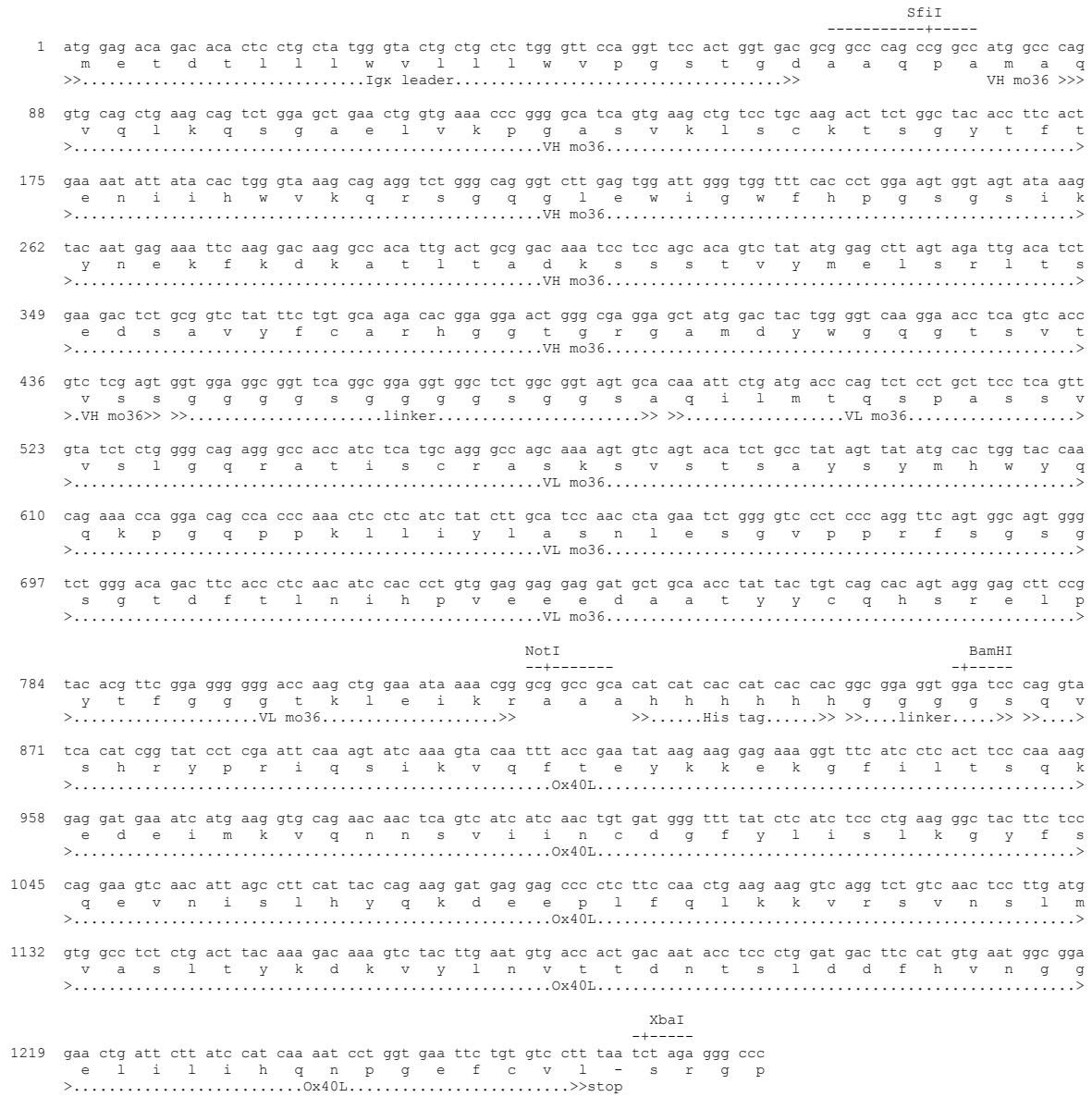

scFv36-GITRL

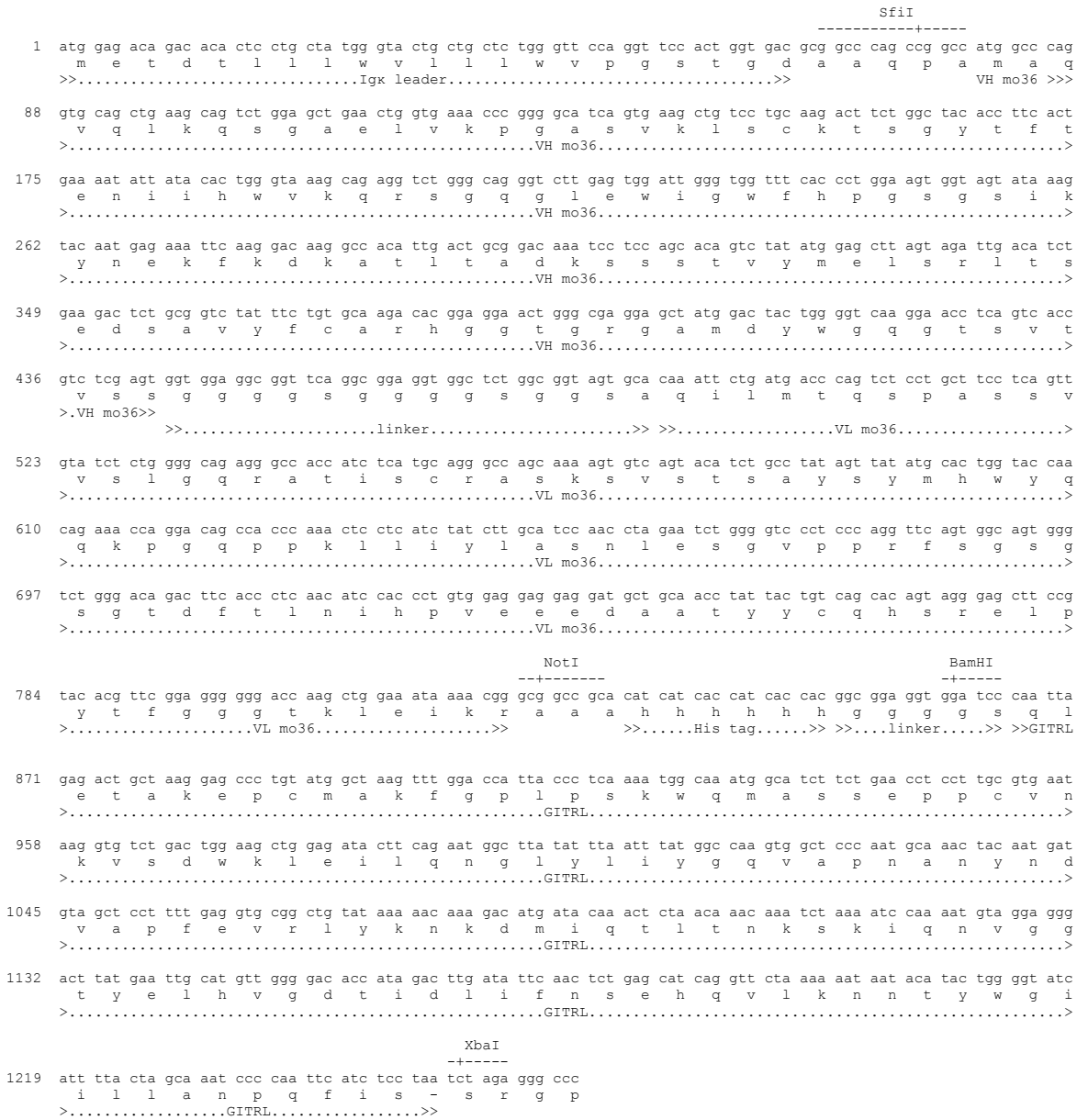

scFv36-TNC-GITRL

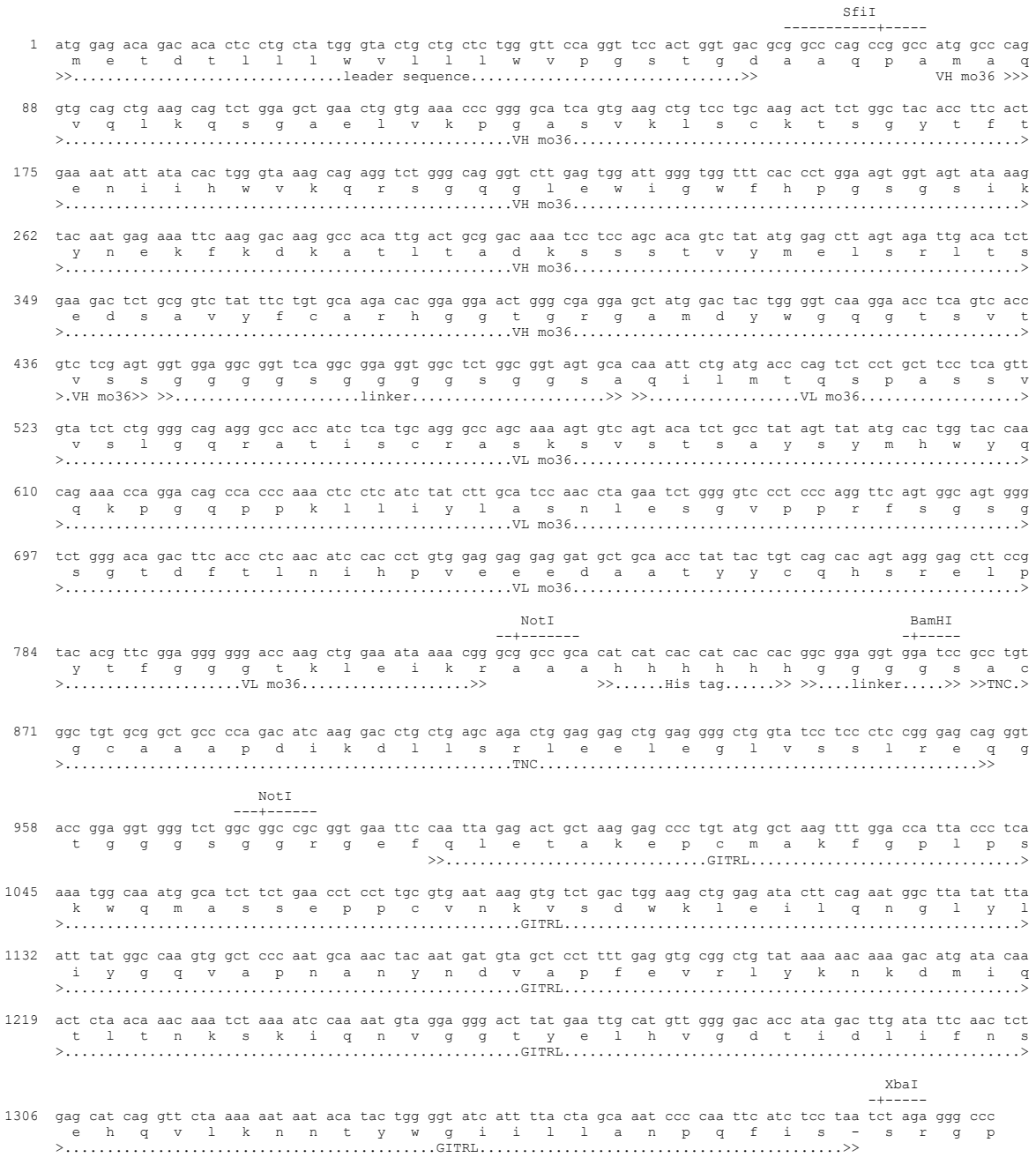

Acknowledgements

Foremost, I wish to express my special gratitude to Prof. Roland Kontermann for providing me with the opportunity to perform my PhD thesis in his lab and to my advisor on the spot, Dr. Dafne Müller for offering me this interesting research project. Both have always been available to advise me and I thank both of them for helpful discussions and for reviewing the manuscript. Moreover, I am very grateful for Dafne's continuous support, guidance, motivation and immense knowledge in Tumor Immunology.

I also would like to thank Prof. Klaus Pfizenmaier for giving me the opportunity to work at the IZI and for being second reviewer of this thesis.

Furthermore, special thanks to all members of the Kontermann lab I was working with during my PhD thesis, in particular Fabi, Oli, Felix, Aline, Sina, Maike, Nadine and Ronny for all the fun activities we had in and outside of the lab. I am very grateful to my dear colleague and friend Vanessa (“Honk”) for spending this intense PhD time together – I couldn`t have asked for a better fellow. In this manner also special thanks to “Mini-Honk” (Steffi). My sincerest thanks to Hanna, Christine and Vanessa for all the after-work and weekend activities – that really helped me through it! Special thanks also to Robert and Gabi. Furthermore, my thanks are also expressed to all colleagues at the IZI for the nice and supportive atmosphere.

My deepest thanks to Hannah N, Hannah F, Steff, Frederick, Astrid, Johannes, Basia, Luisa, Bastian, Jule, Larisa, Yasmin, Babsi, Katharina and Simone for all the nice times we had in the last couple of years and for not giving up on me as someone who never responds to emails. I am especially grateful to Larisa for understanding every thought of me, for answering emergency night calls and for countless wine drinking evenings. I am very grateful to my parents for their support and care throughout my entire life and for always being there for me. Finally and most importantly, I wish to express my sincerest gratitude to Florian, for his love, patience and immense support within the last years and for constantly reminding me that there are much more important things in life...!

Curriculum Vitae

Nora Hornig

PERSONAL DATA

Date of birth:	11.08.1984
Place of birth:	Hanover
Nationality:	German
Marital status:	Single

PROFESSIONAL EXPERIENCE

since 02/2013	EUROIMMUN AG, Lübeck

EDUCATION

07/2009 – 10/2013	**PhD** in Immunology *"Combinations of costimulatory antibody-ligand fusion proteins for targeted cancer immunotherapy"* University of Stuttgart, Stuttgart
10/2005 – 11/2008	**Diploma** in Biochemistry Eberhard-Karls-University, Tuebingen Biological focus: Immunology Chemical focus: Organic chemistry
10/2003 – 09/2005	**Intermediate diploma** in Biochemistry Leibniz-University, Hanover
08/1996 – 06/2003	Secondary school, Neustadt a. Rbge.

RESEARCH AND PROJECT EXPERIENCE

12/2008 – 02/2009	**Research Associate** at the Max Planck Institute for Developmental Biology, Department of Protein Evolution, laboratory of Prof. Andrei Lupas (Tuebingen)
04/2008 – 11/2008	**Diploma student** at the Max Planck Institute for Developmental Biology, Department of Protein Evolution, laboratory of Prof. Andrei Lupas (Tuebingen)
04/2006 – 03/2008	**Research assistant** at the Max Planck Institute for Developmental Biology, Department of Protein Evolution, laboratory of Prof. Andrei Lupas (Tuebingen)

03/2007 – 04/2007	**Visiting scientific researcher** at the University of Chile, Faculty of Medicine, Institute for Biomedical Sciences, laboratory of Prof. Arturo Ferreira, (Santiago, Chile)
08/2006 – 09/2006	**Visiting scientific researcher** at the Friedrich Loeffler Institute, Federal Research Institute for Animal Health, laboratory of Prof. Heiner Niemann (Hanover)
03/2004 – 04/2004	**Internship** at Solvay Pharmaceuticals (Hanover)

PUBLICATIONS, CONFERENCES AND MEMBERSHIPS

Hornig N, Reinhardt K, Kermer V, Kontermann RE & Müller D (2013) *Evaluating combinations of costimulatory antibody-ligand fusion proteins for targeted cancer immunotherapy.* Cancer Immunol Immunother 62 (8), 1369-80.

Kermer V, **Hornig N**, Harder M, Bondarieva A, Kontermann RE & Müller D (2013) *Combining antibody-directed presentation of IL-15 and 4- 1BBL in a trifunctional fusion protein for cancer immunotherapy.* Mol Cancer Ther (accepted for publication).

Hornig N, Kermer V, Frey K, Diebolder P, Kontermann RE & Müller D (2012) *Combination of a Bispecific Antibody and Costimulatory Antibody-Ligand Fusion Proteins for Targeted Cancer Immunotherapy.* J Immunother 35 (5), 418 – 429.

Hornig N and Färber-Schwarz A (2012) *Production of Bispecific Antibodies: Diabodies and Tandem scFv.* Book chapter from: Antibody Engineering: Methods and Protocols, Second Edition, Methods in Molecular Biology, vol. 907, Chames P (ed.), Springer Science+Business Media.

Kermer V, Baum V, **Hornig N**, Kontermann RE & Müller D (2012) *An Antibody Fusion Protein for Cancer Immunotherapy Mimicking IL-15 trans-Presentation at the Tumor Site.* Mol Cancer Ther, 1-10.

Ferris HU, Dunin-Hokawicz S, **Hornig N**, Hulko M, Martin J, Schultz JE, Zeth K & Lupas AN (2012) *Mechanism of regulation of receptor histidine kinases.* Structure 20 (1), 56 – 66.

Hopp J, **Hornig N**, Zettlitz KA, Schwarz A, Fuß N, Müller D & Kontermann RE (2010) *The effects of affinity and valency of an albumin-binding domain (ABD) on the half-life of a single-chain diabody-ABD fusion protein. PEDS 23 (11), 827 – 834.*

Poster presentation:	CIMT conference 2010 in Mainz, Germany CIMIT conference 2011 in Budapest, Hungary ECI conference 2012 in Glasgow, Scotland
Membership	"Deutsche Gesellschaft für Immunologie e.V. (DGfI)"